# EXPERIMENTAL DETERMINATION OF THERMOPHYSICAL PROPERTIES IN SUPERCRITICAL HEAT EXCHANGERS

By

Michael J. Trapani, B.S., EIT

December 2023

Director of Thesis: Dr. Kurabachew Duba
Major Department: Engineering

## ABSTRACT

An ECU team designed, built, and is testing a pilot-scale supercritical water desalination (SWD) system that processed brine discharge from conventional desalination systems. The system completely separates the solid salts from brine wastes. However, SWD is energy intensive. This work presents the design and testing of two heat exchangers (HEXs) used to recover and reuse the waste heat produced during the SWD process to minimize the overall energy requirement. The HEXs have been instrumented with temperature, pressure and flow control components. The collected data is then used to estimate dimensionless numbers (such as Prandtl, Reynolds and Nusselt) using thermophysical properties from the NIST REFPROP database. The dimensionless numbers are useful for HEXs design and are scarce in the literature for supercritical fluids. Brine was also used as a cooling fluid to simulate three different concentrations (3.5%, 7.5% and 14%) of salt which simulate sea water and double the brine waste discharge concentration from conventional desalination processes. The dimensionless numbers are then used to calculate the convective heat transfer coefficients, thermal resistance, and the overall heat transfer coefficient (OHTC). The results show that the Nusselt number for a supercritical HEX in laminar flow conditions is 20 to 30 times greater than that of a conventional counterpart which translates to an order of magnitude higher rate of heat transfer. The heat recovery system saves significant energy with a payback period of around 5 years.

# EXPERIMENTAL DETERMINATION OF THERMOPHYSICAL PROPERTIES IN SUPERCRITICAL HEAT EXCHANGERS

A Thesis

Presented to the Faculty of the Department of Engineering

East Carolina University

In Partial Fulfillment of the Requirements for the Degree

Master of Science in Mechanical Engineering

By

Michael J. Trapani B.S., EIT

December 2023

# EXPERIMENTAL DETERMINATION OF THERMOPHYSICAL PROPERTIES IN SUPERCRITICAL HEAT EXCHANGERS

by

Michael J. Trapani, B.S., EIT

APPROVED BY:

Director of Thesis _____

Dr. Kurabachew Duba, Ph.D.

Committee Member _____

Dr. Tarek Abdel-Salam, Ph.D.

Committee Member _____

Dr. Jinbo Chen, Ph.D.

Chair of the Department of Engineering _____

Dr. Barbara Muller-Borer, Ph.D.

Dean of the Graduate School _____

Dr. Kathleen Cox, Ph.D.

# Acknowledgements

I would like to thank all who assisted me in this endeavor. I would like to thank my parents and family for their love and support. I would also like to thank my grandfather for inspiring me to become an engineer.

I would also like to thank my thesis committee chair Dr. Kurabachew Duba for your guidance, mentorship, and inspiration. Thank you, Dr. Chen and Dr. Abdel-Salem for your support as well.

I would also like to give a special thanks to Danielle Werts, Mina Akhnoukh, and Mason Caroon for your contribution to the lab work that took place for this effort.

I would also like to thank Jon Teboul for his assistance.

I would like to thank Mr. Gene Oakley, Jon Echerd, and Andy Wilson for their fabrication assistance.

# Table of Contents

# List of Tables

# List of Figures

# CHAPTER 1 BACKGROUND AND LITERATURE REVIEW

## BACKGROUND

A team from East Carolina University (ECU) was awarded a $1.4 million grant through the University of North Carolina (UNC) Research Opportunities Initiative (ROI) energy conservation project. A portion of the process diagram and high level project scope is shown in Figure 1. This grant is intended to fund the development of a sustainable desalination system. The project is broken up into different areas of research. One group is developing and designing a wave energy converter and simulations that turns wave motion into energy [1], [2]. Another group is designing a solar collector to power the desalination system [3].

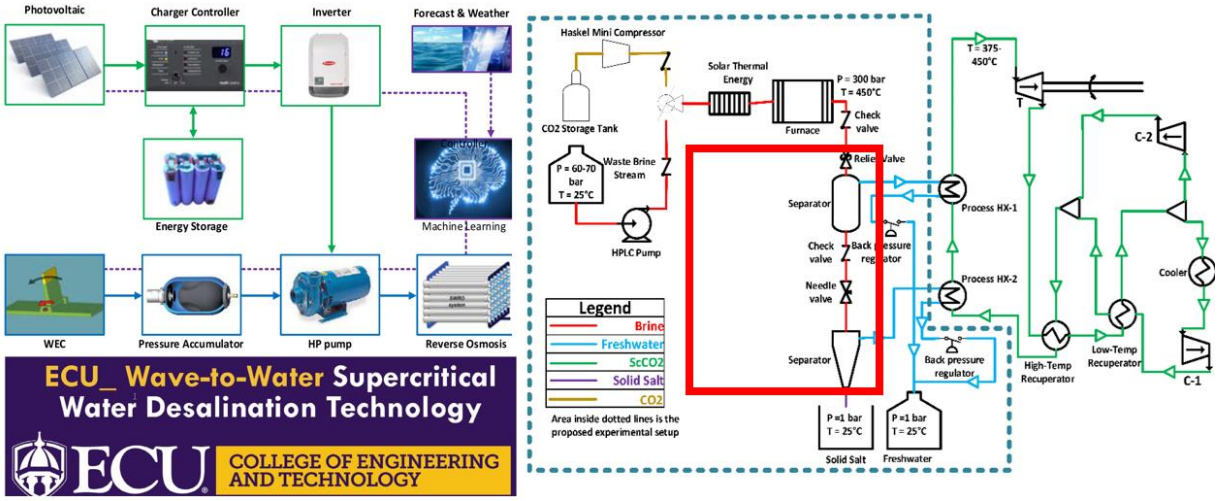


Figure 1: Scope of Wave-to-Water project.

This desalination system operates by feeding brine and saltwater to a reaction vessel of extremely high temperature and pressure. The processed water is then pumped out of the vessel, which still holds heat that

needs to be cooled down for use. The goal is to recover some of the waste heat with a heat exchanger network (HEN); recycling the energy through this process will reduce wasted energy.

To increase the efficiency of the system, lost heat needs to be reduced through heat recovery methods. The first law of thermodynamics is defined as the conservation of energy. It states that the total energy contained in a system can neither be created nor destroyed – only transformed from one form to another [4], [5].

The necessity for the HEN will be determined through thermal calculations and cost effectiveness. Cost-effectiveness will be determined through upscaling size calculations based on the mass flow rate of the system. There are opportunities to add heat exchangers (HEs) to the process to recover heat and increase efficiency. The system is a continuous process, and operating for long periods of time causes the energy losses to add up. Insulated HEs can save money and are traditionally insulated with rock wool, fiberglass and aluminum reflective tapes.

## PROPERTIES OF SUPERCRITICAL FLUIDS

Some materials, gases and elements possess what is known as a critical point. The critical point marks on the phase diagram for this material are where the thermophysical properties of the fluid change. Table 1 shows the critical temperature, critical pressure, and density of the associated material.

Table 1: Critical Pressure, Critical Temperature and Density Example Table

| Molecule | Molecule Name | Critical Temperature, Tc (K) | Critical Temperature, Tc (°C) | Critical Pressure, Pc (MPa) | Critical Pressure, Pc (Bar) | Density, ρ (kg/m$^3$) |
|---|---|---|---|---|---|---|
| $H_2O$ | Water | 647.1 | 409.95 | 22.06 | 220.6 | 322.2 |
| $CO_2$ | Carbon Dioxide | 304.13 | 66.98 | 7.378 | 73.78 | 467.8 |
| $N_2$ | Nitrogen | 126.24 | -110.91 | 3.398 | 33.98 | 313.9 |
| $O_2$ | Oxygen | 154.58 | -82.57 | 5.043 | 50.43 | 436.2 |
| Xe | Xenon | 289.74 | 52.59 | 5.84 | 58.4 | 1113 |
| $SF_6$ | Sulfur Hexaflouride | 318.63 | 81.48 | 3.761 | 37.61 | 742 |
| $H_2$ | Hydrogen | 32.976 | -204.174 | 1.2928 | 12.928 | 31.43 |
| He | Helium | 3.317 | -233.833 | 0.0117 | 0.117 | 41.45 |

The National Aeronautical Space Administration (NASA) directed an experiment that took place on the International Space Station (ISS) where supercritical water was formed in space using one of the ISS

rack mount modular experiment systems. The purpose of this experiment was to see what supercritical water looked like in zero gravity conditions.

Water or $H_2O$ is a bi-polar molecule made of 1 oxygen atom and 2 hydrogen atoms. The hydrogen atoms are angled 104.5 degrees apart. Oxygen is 292 picometers round. The hydrogen is 212 Picometers Round. Sodium chloride is the most common salt found in sea water [6].

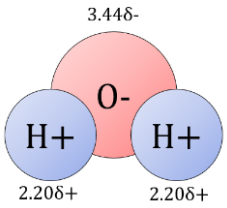

Figure 2: 1 $H_2O$ Molecule

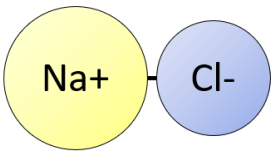

Figure 3: 1 NaCl Molecule

Supercritical $CO_2$ acts as a solvent and can be used to extract oils from grape seeds [7]. A $CO_2$ molecule is straight with 1 carbon atom in the middle and two oxygen atoms on each side. When water is heated and pressurized past the critical temperature and pressure the dielectric constant drops close to the same value of $CO_2$ and other hydrocarbons as shown in National Institute of Standards and Technology Reference Properties Database (NIST-REFPROP or REFPROP). It is at this point where the salt dissolved in the brine desalinates, because the water no longer has the capacity to ionic attract the sodium and chlorine atoms to the water molecule.  A note-to-scale (NTS) phase diagram of $H_2O$ is shown in Figure 4.

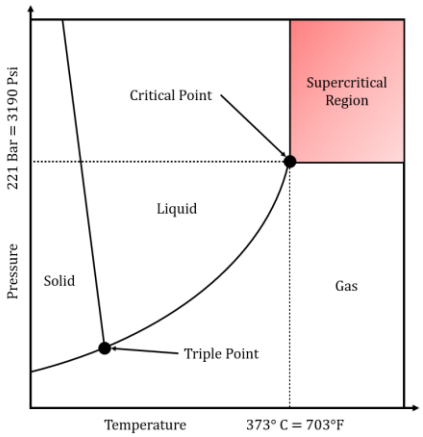

Figure 4: Phase Diagram of water showing super-critical region past the critical point (NTS)

The supercritical region is past the critical point. In the supercritical region the fluid acts as a gas and a liquid, it is a region of mixed properties. The area near the critical point is considered the anomalous zone of some fluids, water is one of those fluids [8]. In this region the properties change which allows the dissolved salt to precipitate out of the fluid, which is what makes supercritical desalination possible.

## RESEARCH QUESTIONS

- Can a simple cost-effective heat exchanger be constructed with commercial off the shelf (COTS) parts and reduce the energy requirement for a supercritical water desalination (SCWD) system?
- Are the values of the dimensionless numbers in the empirical equations that are used to design conventional heat exchangers applicable for supercritical processes?

## SIGNIFICANCE TO THE FIELD

The problem with SCWD-ZLD is that it consumes large quantities of energy to heat up the preheater furnace, power the chiller and power the main reactor [9], [10]. If a system that has a flow rate of 10 ml/min is scaled up to 100 ml/min a second or third reactor is required, and the preheater furnace must increase in size as well as the chiller to accommodate the increase in the required heat to perform the process operation. These added larger pieces of equipment consume even more power to sustain an output of 100 ml/min. The HEX design presented can be scaled in size as well to accommodate larger flow rates. Heat exchangers have been designed and used for SCWD-ZLD in the past using special manufacturing methods. The HEX set produced for this study was designed using commercial off the shelf components, such that the components can be assembled using basic, simple hand tools in a region where electrical power and resources are limited.

SCWD-ZLD technology is relatively new; currently there are very few systems on global records. One system is in the Netherlands and the other is located at East Carolina University. A HE has been fabricated and tested in the system located in the Netherlands. East Carolina University's HEN design is

currently under development. Pinch technology for HEN design has been around since the 1970's and has been applied to many different processes. The Netherlands' team may have applied pinch technology.

## LITERATURE REVIEW

This chapter will discuss the current state of knowledge in the field. The literature review is broken into different sections based on the topic of discussion. The work that comprises this design and experiment can be broken up into different categories. The fields of desalination, heat transfer, and mechanics of materials all need to be considered in HE designs.

## DESALINATION

The water stress is increasing and will affect more than 3.7 billion people. It is expected that this will increase to 5.7 billion by 2050. At the current rate 3.5 million people die annually due to water supply problems. This article is from 2019 Ahmed, et al [11].

This article begins by agreeing with the idea that water scarcity is a challenge that will face the world. It also agrees with assertion that Reverse Osmosis leads the market in desalination technologies is also agreed to.

Different styles of Reverse Osmosis membranes are listed, including plate and frame, tubular, spiral wound, and hollow fiber types [12]. Of the world's water 50% of the water desalinated is produced using RO systems. Different types of RO plants are listed such as brackish water RO (BWRO) and sea water RO (SWRO) plants. The salinity of BWRO is 500 mg/L to 10,000 mg/L and the salinity of SWRO is 30,000 mg/L. The Osmotic pressure section shows Van't Hoff Equation.

Details about RO desalination follows. Retentate is what is retained in the membrane and permeate is the portion of material that passes through the membrane. Energy supplied by the high-pressure pump leaves the RO system in the concentrate stream, this energy can be recovered by rotary devices. Energy can be recovered by devices like the Francis turbine Pelton turbines and turbochargers. Materials used for recovery devise can be made from 316-L stainless steel, 904L duplex SS 245 SMO super Austenitic

stainless steel or SAF 2507 Super Duplex stainless steels. PVC can also be used for low pressure applications. Compared to other desalination methods RO has the lowest energy demand and lowest unit water cost. The cost has decreased from \$2/$m^3$ to \$0.5/$m^3$ from 1998 to 2004. The ability to reject salt has increased reaching as high as 99.8% in commercially available membranes. Energy efficiency of RO systems has also increased. A water cost breakdown graph is provided for BWRO and SWRO systems.

Powering an RO system with renewable energy systems such as solar cells, a solar Rankine cycle, wind energy, and wave energy is discussed.

Able, shows the solubility of various salts at 25 MPa. The salts shown are NaCl, KCl, $CaCl_2$, $CaSo_4$, and $Na_2SO_4$. The dielectric constant of water near the critical point is shown. The critical pressure of NaCl-H2O is shown in a temperature pressure graph. Figure 4 is from Dreisner showing concentration of NaCl, at high pressures and temperatures of 375℃ and 500 ℃. Able, uses ELECNRTL in the ASPEN model. Able included the cost of labor from the Bureau of Labor Statistics for economic analysis. The type of thermocouples used were Type-E from Omega Engineering.

This journal article discusses applying supercritical water desalination processes to hypersaline brines produced by oil and gas wells Chad M. Able. (2018) [9]. This study was conducted in Ohio. Other ions such as Ba2+ and Sr2+ are both naturally occurring radioactive materials that can make desalination difficult and costly. Nanofiltration and Reverse Osmosis (RO) are increasing in interest due to reported high recovery rates, but the concentrations are limited to 50mg/L. Supercritical water desalination (SCWD) is increasingly interesting as it can overcome the difficulties associated with RO such as osmotic pressure problems. SCWD is also good at removing organic wastes, as similar conditions are found in supercritical water oxidation SCWO [9].

A table shows the cations and anions found in the water, this data comes from the USGS database. Hastelloy C-276 was used to build the desalination system in this study because it is highly corrosion resistant. The desalination system was at 230 and 250 bars of pressure. An Inductively Coupled Plasma Optical Emission Spectrometer (ICPOES), model iCAP 6000 manufactured by Thermo Scientific was used to find the cation concentrations.

Able uses Dresner's equation to correlate the binary mix of NaCl-$H_2O$. A table providing pressures, temperatures, flow rates and ppm of NaCl is shown. The method used was Joule-heating which is also known as resistive heating or Ohmic heating. Aspen Plus software was used to model the desalination process using ELECNRTL and Flash 2 models. Results show that the pressures of 230 and 250 bar did not change the composition of what the flash simulation produced.

Chad M. Able. (2020) [13] This paper simulated a SCWD process in Aspen Plus using the ELECNRTL model to estimate the thermodynamic performance of the fluids. The ELECNRTL has an error when used to simulate brines past the water's critical point. Chad then incorporated simulation data from Ogden using FORTRAN. The inlet brine salinity is 176.3 g/L. The composition of the TDS is listed in a table. This process involves chemical pretreatment, sand filtration, and UV systems, these remove bacteria and solids. Hydro cyclones are used to remove $SrSO_4$, $Mg(OH)_2$ and $CaCO_3$, these chemicals cause equipment scaling. One HEX is used in the ZLD case and two are used for heat recovery in the brine concentration case in this journal paper. The HEXs are made from Hastelloy C-276. In the simulation the FORTRAN code was used to calculate the brine heat of vaporization. Non-hazardous salts include chloride and hydroxide. Sodium and potassium salts can also be sold as products once extracted. The brine concentration method costs less than the ZLD process.

Van Wyk, et al, states In Analysis of the energy consumption of supercritical water desalination (SCWD), global desalinated water production is 95.4 million $m^3$/day [14]. Brine production is 141.5 million $m^3$/day, and 50% of brine plants are located near the ocean and dump their waste brine back into the ocean. This threatens marine life and ecosystems. The SCWD process pilot plant developed will process this brine waste. This plant produces a zero liquid discharge (ZLD), or the waste is salt in the solid form. The system has an estimated energy consumption of 0.71 to 0.90 $MJ_{th}$/kg feed. Reference 18 of this paper estimated thermal energy requirement to be 450 $MJ_{th}/m^3$ of drinking water for brine of 3.5wt% NaCl feed. Increasing the NaCl concentration from 0-7% increases performance of the heat exchanger. The energy consumption is a function of NaCl concentrated in the water ranging from 0 to 20%. Increasing the NaCl feed concentration up to 7.5 wt% increases the outlet temperature by 7°C from 390°C. Pre-heating of the feed

for concentrations above 14 wt% before the heat exchanger is recommended because when the wt% increases. (This drives the need for a HEN). Aspen plus was used using the Electrolyte non-random two liquids (eNRTL) model. Supercritical conditions are greater than 374°C and 22.1 MPa. Figure 5 on page 5 shows a Composite Curve Graph (CCG) from pinch analysis. These graphs show the pinch point at 391°C and 397°C from pure water to 7.0 wt% NaCl feed respectively. This group only uses 1 heat exchanger for this. A network of heat exchangers may increase the thermal energy recovered. In section 5.2 it is stated that 14wt% brine is produced by the mining and dairy industry. Pre heating the feed before the heat exchanger shifted the pinch point to a higher temperature region. Increasing the pressure increases the NaCl Concentration of the SCW stream and decreases the SCW recovery. Dr. Andrzej Anderko offered to share his original FORTRAN code to aid in some of these calculations in the paper.

A SCWD pilot plant that feeds 5 kg/h has been produced in Design and results of a first-generation pilot plant for supercritical water desalination (SCWD) [15]. The feed stream is 3.5wt% NaCl. This study was conducted to evaluate the repeatability and stability of the setup [15]. The sides of the heat exchanger can be switched. This study made the annulus the hot side, while the tube core was the cold side. Results for 3.0, 7.0 and 16 wt% were evaluated and shown in a table. Incoloy 825 was selected for the gravity separator, cyclone, cyclone collector and salt collector respectively. Titanium Grade 2 was used for the heat exchanger. The valve is made from a chromium-nickel based alloy, a creep resisting austenitic steel. The HEX design for this pilot plant had hot fluid in the shell and cooling fluid in the center. The temperature was measured with K-type thermocouples and the pressure was measured with sputtered thin film type pressure transducers. The flow rate and runtimes for different saline feed concentrations were reported in Table 2.

Table 2: Brine Salinity table from Van Wyk. Paper with added wt% of water, run time in hours and volume fed [15].

| Water | Concentration | Feed rate | Run Time | | Volume Fed | |
|---|---|---|---|---|---|---|
| wt% H2O | wt% NaCl | kg/hr | min | hr | kg | g |
| 97 | 3 | 5.3 | 64 | 1.07 | 5.65 | 5653.3 |
| 93 | 7 | 5.5 | 23 | 0.38 | 2.11 | 2108.3 |
| 86.7 | 13.3 | 2.2 | 33 | 0.55 | 1.21 | 1210.0 |
| 84 | 16 | 1 | 47 | 0.78 | 0.78 | 783.3 |

HEAT EXCHANGER NETWORK DESIGN

HEX technologies have been around for decades but are used at lower pressures and temperatures with other fluids with less corrosive properties than supercritical saltwater. The HE that is to be designed is unique because of the application.

One of the HEs used in this project will have ; the hot supercritical fluid exiting the reactor will change state from supercritical to a hot vapor and back to liquid. To calculate the latent heat of vaporization and the specific heat of the halite brine solution, the equations in works covering brine properties will be applied [16]–[18]. If calculation precision is an issue, it is not uncommon to overdesign a HE. HEs in the industry are commonly designed to perform when multiple tubes are plugged in the tubes-in-shell type HE [14], [19]–[21]. The papers about the subject of pinch technology are mostly published in chemical engineering journals [21]–[29]. This is no surprise, as Linnhoff, Seligman and Hohmann are all chemical engineers who have contributed to advancements in HE technology.

In the late 1700s, James Watt invented the first steam-based system that can be used to heat a home. Dr. Richard Seligman founded the Aluminum Plant & Vessel Company (APV PLC) in 1910 and was credited for inventing the plate HEX in 1923. APV PLC fabricated equipment for breweries and vegetable oil producers in Wadsworth, South London. Dr. Richard Seligman was an early distinguished member of the Society of Chemical Industry (SCI).

Different types of HEs include but are not limited to, tube-in-shell, plate, spiral, cross/counter flow, and crossflow [30]. HEs can take the form of radiators in vehicles, boilers in trains, and boilers used to heat steam for heating homes. All HEs move heat *via* the three modes of heat transfer: radiation, conduction, and convection [4], [5], [31]. These methods exchange heat between mediums and take different forms on process diagrams to aid engineers, maintenance, and mechanics.

## OVERALL HEAT TRANSFER COEFFICIENT

The overall heat transfer coefficient (OHTC) or *U* $(W/m^2 \cdot °C)$ is a metric found in heat exchanger design that is used to determine the amount of heat that is transferred from one fluid to another. Common OHTCs are shown in Tables 3 and 4 [32].

Table 3 and 4: OHTC Table of Common Fluid Combinations [4]

| Fluid Combination | U ($W/m^2 \cdot °C$) |
|---|---|
| Water to Water | 1140-1700 |
| Water to Brine | 570-1140 |
| Water to Organic Liquids | 570-1140 |
| Water to Condensing Steam | 1420-2270 |
| Water to Gasoline | 340-570 |
| Water to Gas oil | 140-340 |
| Water to Vegetable oil | 110-285 |
| Gas Oil to Gas Oil | 110-285 |
| Steam to Boiling Water | 1420-2270 |
| Water to Air (finned tube) | 110-230 |
| Light Organics to Light Organics | 230-425 |
| Heavy Organics to Heavy Organics | 55-230 |

| Fluid Combination | U ($W/m^2 \cdot °C$) |
|---|---|
| Water-to-Water | 850-1700 |
| Water-to-Oil | 110-350 |
| Steam Condenser | 1000-6000 |
| Ammonia Condenser (water in tubes) | 800-1400 |
| Alcohol Condenser (water in tubes) | 250-700 |
| Finned-tube heat exchanger (water in tubes, air in cross flow) | 25-50 |

## THERMOPHYSICAL PROPERTIES

The Nusselt number, Prandtl number and the Reynolds number are necessary to find to understand the type of heat transfer the fluid inside the heat exchanger is experiencing. If the Reynolds number is less than 2300 the flow is laminar, if the Reynolds number is greater than 2300 the flow is considered turbulent. The Nusselt number is the convective to conductive heat transfer ratio, it describes if the heat is being transferred by conduction or convection or a combination of the two. The Prandtl number describes how the heat is traveling through the fluid vs how well the fluid moves with the heat, it is a thermal boundary layer and velocity boundary layer comparison metric.

## NUSSELT, REYNOLDS AND PRANDTL NUMBERS

The Nusselt numbers supplied in textbooks used at institutions do not apply to a supercritical water heat exchanger [4], [33]. While solving problems in the field of heat transfer, a common problem that engineers face is to find the value of the convective heat transfer coefficient *h* [4], [33]. To find *h* the geometry of the surface is known, and the conductive heat transfer coefficient *k* value is also known at the

pressure and temperature at location. To solve for *h* the *Nu* value is calculated, or a predetermined value is chosen based on the known conditions. For example, if there is uniform surface temperature of a circular surface *Nu* is set to 3.66 and solved for *h* [4], [33]. If there is uniform heat flux *Nu* is set to 4.36 and then the *Nu* equation is solved for *h* [4], [33]. In the scenario presented in this work neither the heat flux nor the temperature from one end of the heat exchanger to the other is uniform or constant. There is no value that can be used to find *h* as easily as a look up table by the method mentioned for a heat exchanger for supercritical water. Pizzarelli discusses the ability for supercritical water to transfer heat and how the thermophysical effects of supercritical conditions cause this ability to deteriorate [34]. Huang X. writes about supercritical water in horizontal double pipe heat exchanger is difficult to predict due to these thermophysical properties problems [35]. There are other Nusselt number equations that relate the Reynolds number and Prandtl number of the fluid [4], [33]. The Prandtl and Reynolds number relations are valid within Prandtl number and Reynolds number ranges which are not what is found in supercritical water heat exchange. These equations do not support the conditions in which the experiment in this work takes place. In Heat Transfer to Supercritical water Dickinson and Welch stated that "as more accurate knowledge of the properties becomes available, data should be correlated by the use of dimensionless parameters" [36]. Cengel cites *Kays and Perkins, 1972* in Chapter 11 in a table like Table 5 [32].

Table 5: Nusselt number for fully developed laminar flow in a circular annulus with 1 surface insulated and the other isothermal [32].

| $D_i/D_o$ | $Nu_i$ | $Nu_o$ |
|---|---|---|
| 0.00 | N/A | 3.66 |
| 0.05 | 17.46 | 4.06 |
| 0.10 | 11.56 | 4.11 |
| 0.25 | 7.37 | 4.23 |
| 0.50 | 5.74 | 4.43 |
| 1.00 | 4.86 | 4.86 |

PRANDTL NUMBER

The Prandtl number is the ratio of momentum diffusivity over thermal diffusivity [4]. Prandtl numbers for fluids are determined experimentally and is a function of the momentum diffusivity and the thermal diffusivity [4]. Prandtl numbers can be found if other properties are known as well.

$$Pr = \frac{v}{\alpha} = \frac{momenum\ diffusivity}{thermal\ diffusivity} = \frac{{}^{\mu}/_{\rho}}{{}^{k}/_{\rho c_p}} = \frac{c_p \mu}{k}$$

v = Momentum Diffusivity = Kinematic Viscosity, α = Thermal Diffusivity, ρ = Density, cp = Specific heat, k = thermal conductivity

REYNOLDS NUMBER

The Reynolds number equation is shown below as well as the equation for hydraulic diameter [4].

$$R_e = \frac{\rho V D}{\mu} = \frac{V D}{v}$$

Re = Reynolds number, ρ = Density of Fluid (kg/m$^3$), V = Velocity of Flow (m/s), D = Diameter of pipe (m), μ = Dynamic viscosity (Pa·s = kg/m·s), ν = Kinematic Viscosity (m$^2$/s)

When the fluid is flowing through a tube that has a ring cross-section as opposed to a circular cross section the hydraulic diameter must be used in place of diameter D in the Reynolds number equation.

$$D_h = \frac{4A_c}{p}$$

Dh = Hydraulic diameter (m), Ac = Area (m$^2$), p = perimeter (m)

The Hydraulic Diameter for the annulus region of the tubing cross section is in this case is 4 times the area over the perimeter [4].

$$p = \pi D$$

$$A_c = \pi \left(\frac{D_o}{2}\right)^2 - \left(\frac{D_i}{2}\right)^2$$

Kinematic viscosity and dynamic viscosity are the same and can be used interchangeably. Kinematic viscosity is the ratio of viscus force over the internal force or in this case density [4].

$$v = \frac{\mu}{\rho}$$

THERMOPHYSICAL PROPERTIES OF $H_2O$

On the following thermophysical properties graphs the red line represents the max temperature the water experiences during the supercritical water desalination process, the black line represents 374℃ the critical temperature of water or the critical pressure of 221 Bar depending on the context of the x-axis, and

the blue line represents the minimum temperature intended for cold exit line of the heat exchanger to be designed. The density curves shown in Figure 5 are all very similar where the density drops rapidly once the fluid temperature passes over the critical point. In the near critical region on the higher side a small change in temperature can cause a rapid change in fluid density. Similar behavior is observed in Figure 6. Figures 5 through 20 all show information gathered from the NIST-REFPROP database for water.

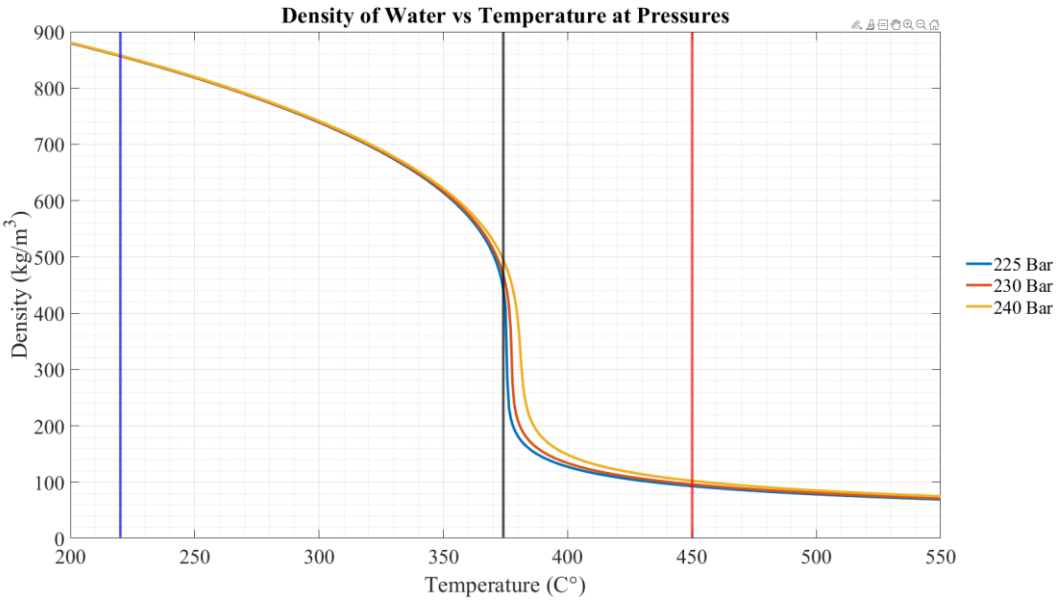


Figure 5: Density of $H_2O$ at temperatures from 200°C to 550°C over pressures of 225, 230, 240 Bar

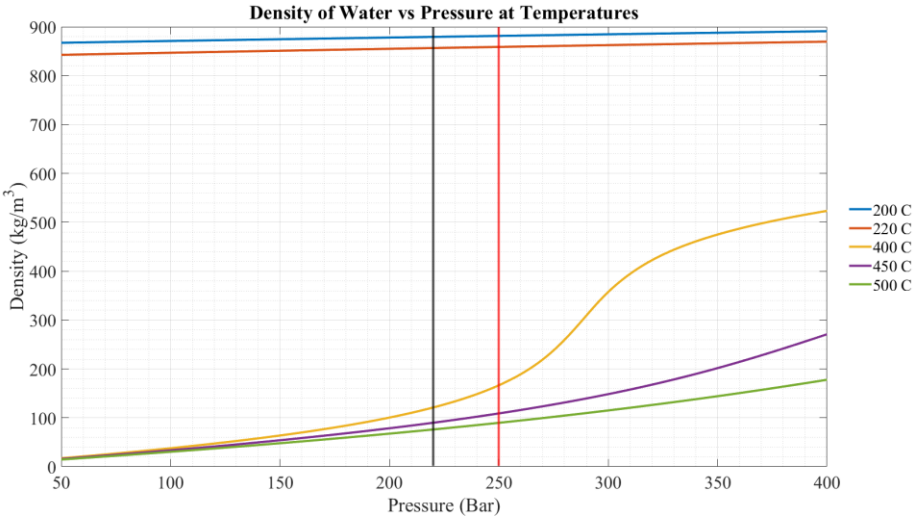


Figure 6: Density of $H_2O$ at pressures from 50 Bar to 400 Bar over a temperature range of 200°C to 500°C

Figure 7 shows the viscosity of water as a function of temperature at pressures of 225, 230, 240 Bar. The viscosity decreases a small amount as the temperature increases until the temperature passes over

the critical temperature, where the viscosity then rapidly increases. Figure 8 shows the viscosity as a function of pressure from 200°C to 500°C.

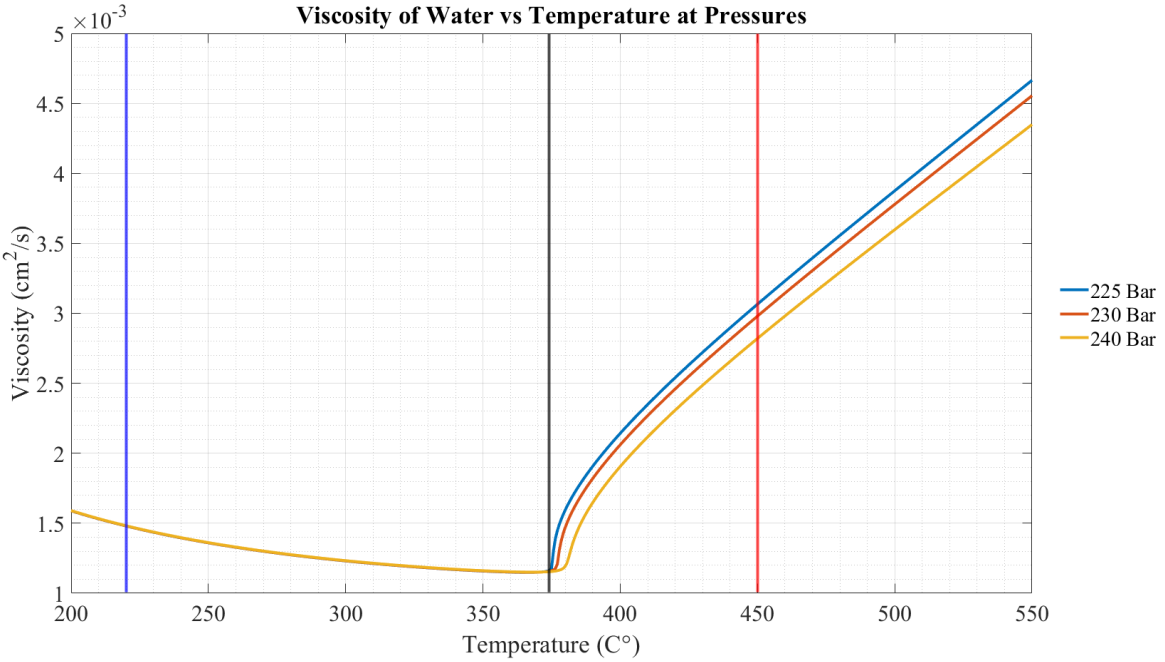


Figure 7: Viscosity of $H_2O$ at temperatures from 200°C to 550°C over pressures of 225, 230, 240 Bar

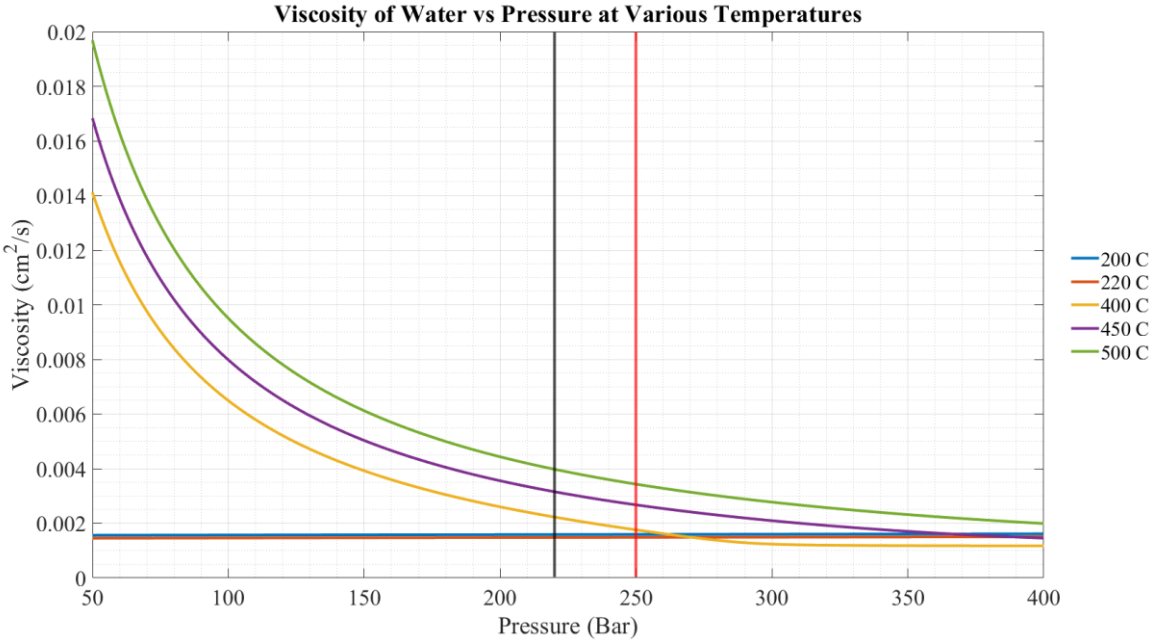


Figure 8: Viscosity of $H_2O$ from 50 Bar to 400 Bar over a temperature range of 200°C to 500°C

The specific heat shown in Figure 9 remains constant until the critical temperature where it then spikes very high then drops back down. The Prandtl number behaves in a similar pattern as shown in Figure 10.

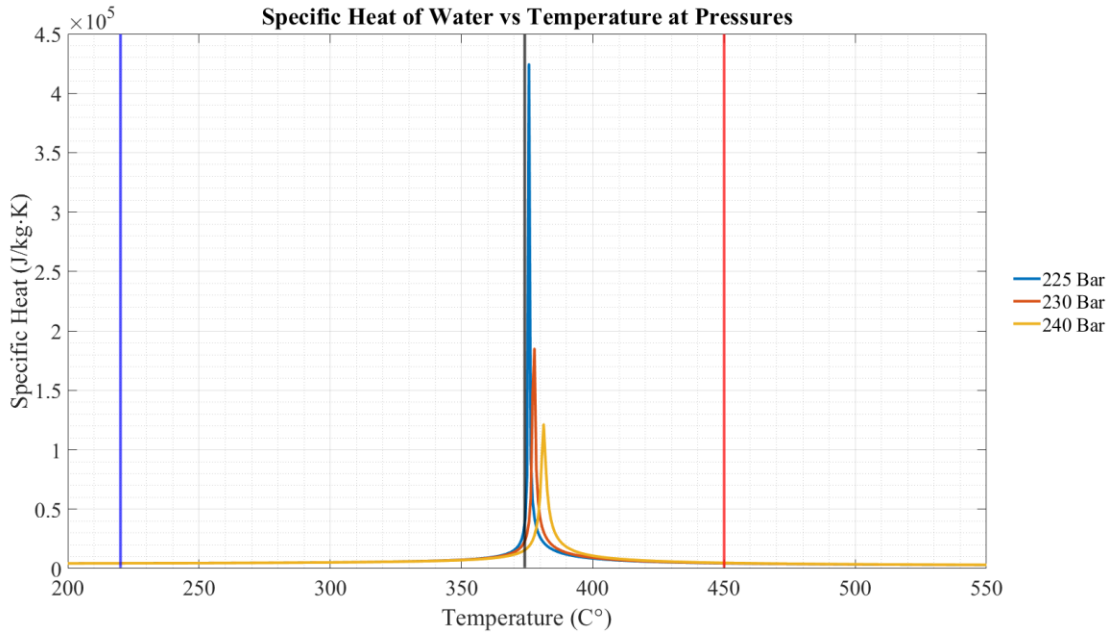


Figure 9: Specific Heat of $H_2O$ at temperatures from 200°C to 550°C over pressures of 225, 230, 240 Bar

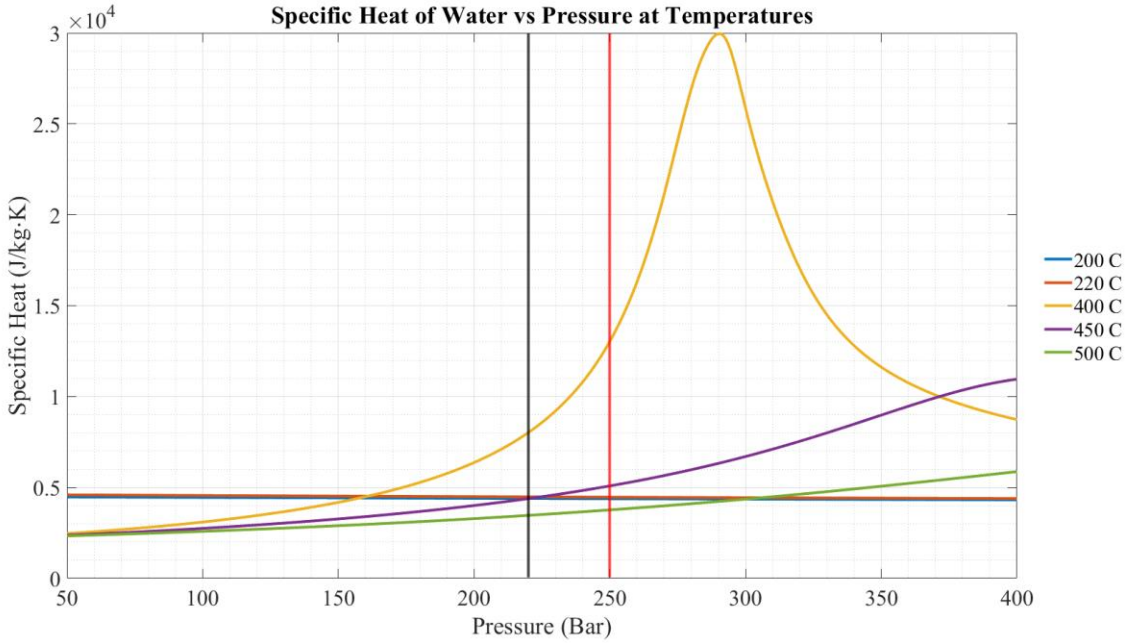


Figure 10: Specific Heat of $H_2O$ from 50 Bar to 400 Bar over a temperature range of 200°C to 500°C

The enthalpy of water shown in Figure 11 increases gradually with temperature as it approaches the critical temperature, once the fluid temperature passes the critical temperature the enthalpy rises rapidly then the slope changes back to a value like the region before the critical temperature. Figure 12 shows enthalpy as S-curve function of pressure within the temperature range of 200℃ to 500℃.

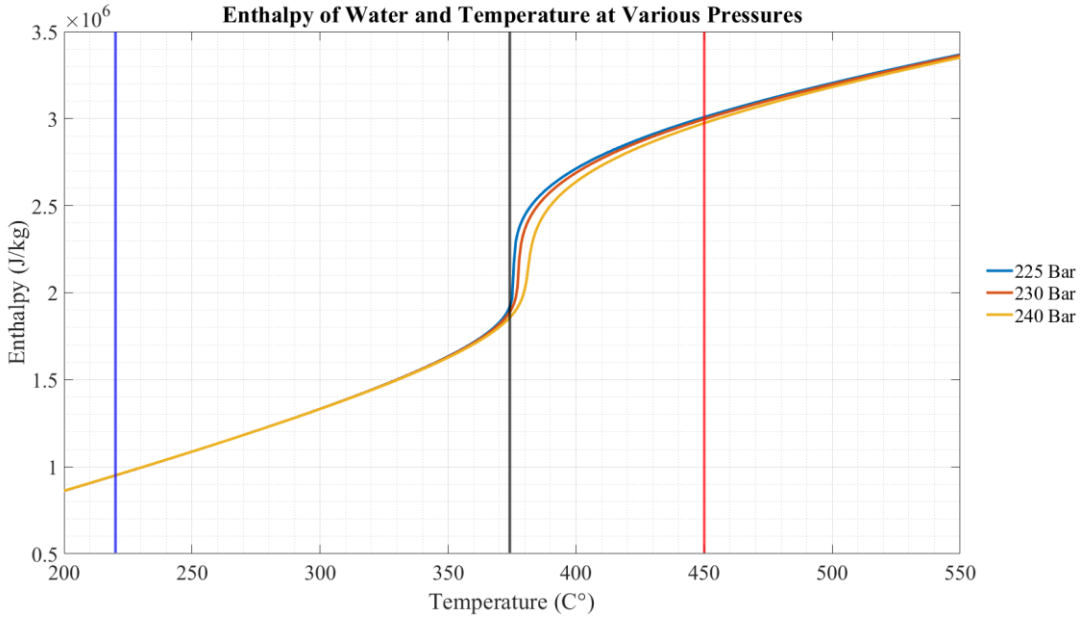


Figure 11: Enthalpy of $H_2O$ at temperatures from 200℃ to 550℃ over pressures of 225, 230, 240 Bar

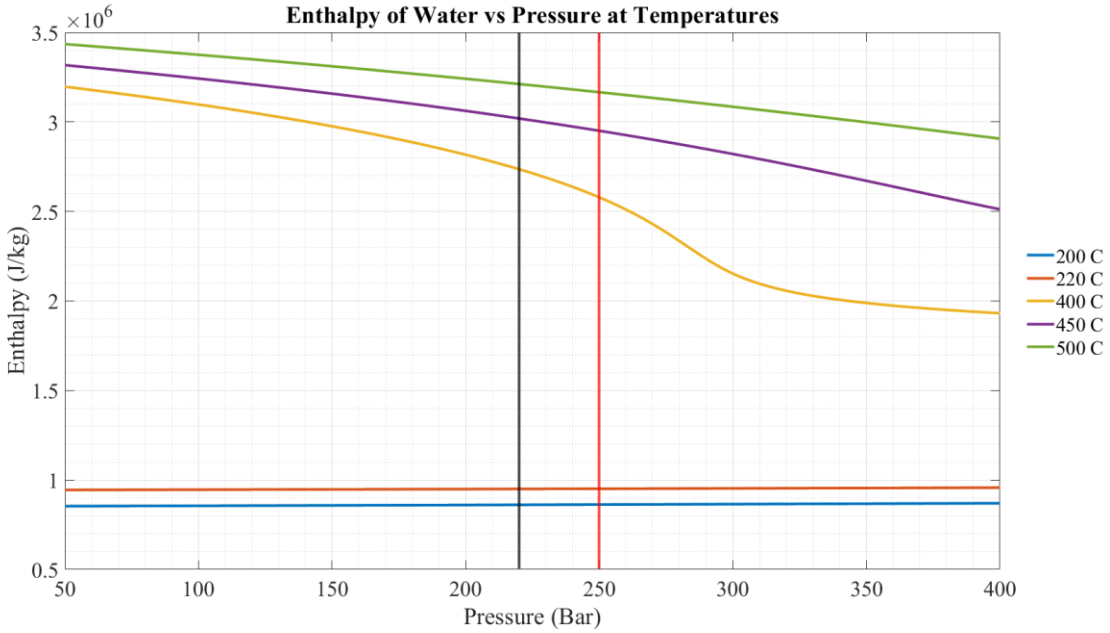


Figure 12: Enthalpy of $H_2O$ from 50 Bar to 400 Bar over a temperature range of 200℃ to 500℃

The dielectric constant of water shown in Figure 13 drops constantly as temperature increases until the fluid temperature reaches the critical temperature where the dielectric constant drops to a similar level as Nitrogen, Octane, Isobutane, Oxygen and Carbon Dioxide. Salt does not dissolve in any of these fluids because they are non-polar. Water is classified as a bi-polar non-covalent molecule until it reaches a critical temperature under supercritical pressures. This is what makes SCWD possible.

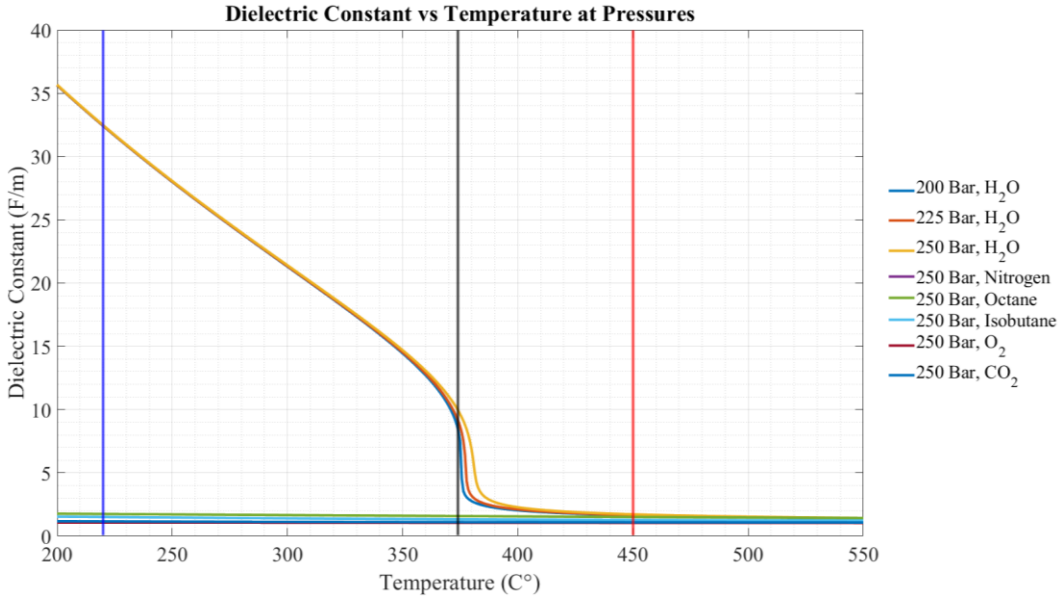


Figure 13: Dielectric Constant of $H_2O$ at temperatures from 200°C to 550°C over pressures of 225, 230, 240 Bar compared to non-polar hydrocarbons and various solvents

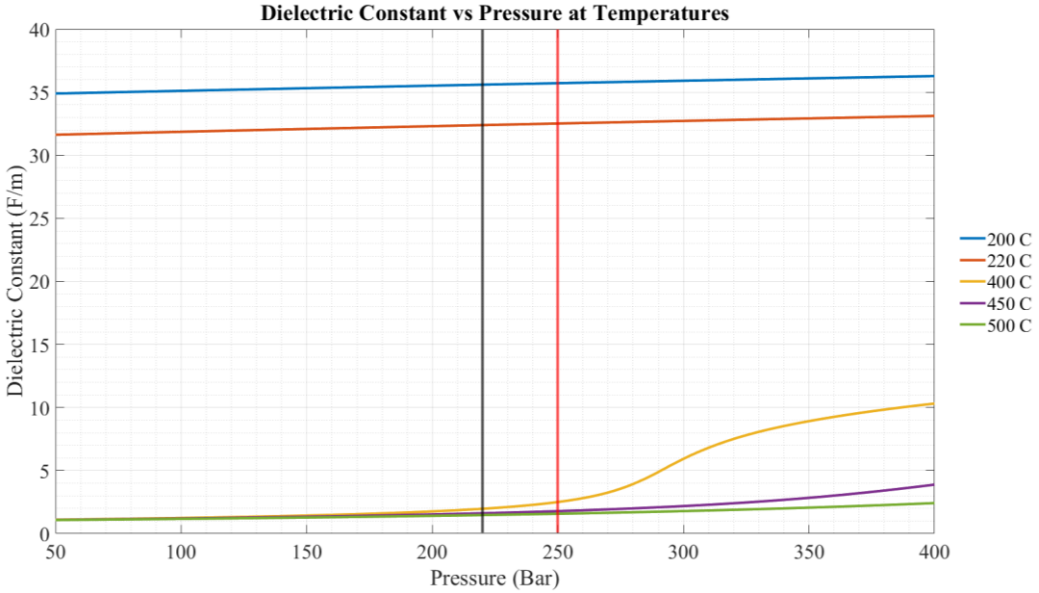


Figure 14: Dielectric Constant of $H_2O$ from 50 Bar to 400 Bar over a temperature range of 200°C to 500°C

The thermal conductivity of water is shown in Figure 15 from 200℃ to 550℃ from 225 to 240 Bar. Figure 15 shows the thermal conductivity of water as a function of pressure from 50 bar to 400 bar across temperature range of 200℃ to 500℃.

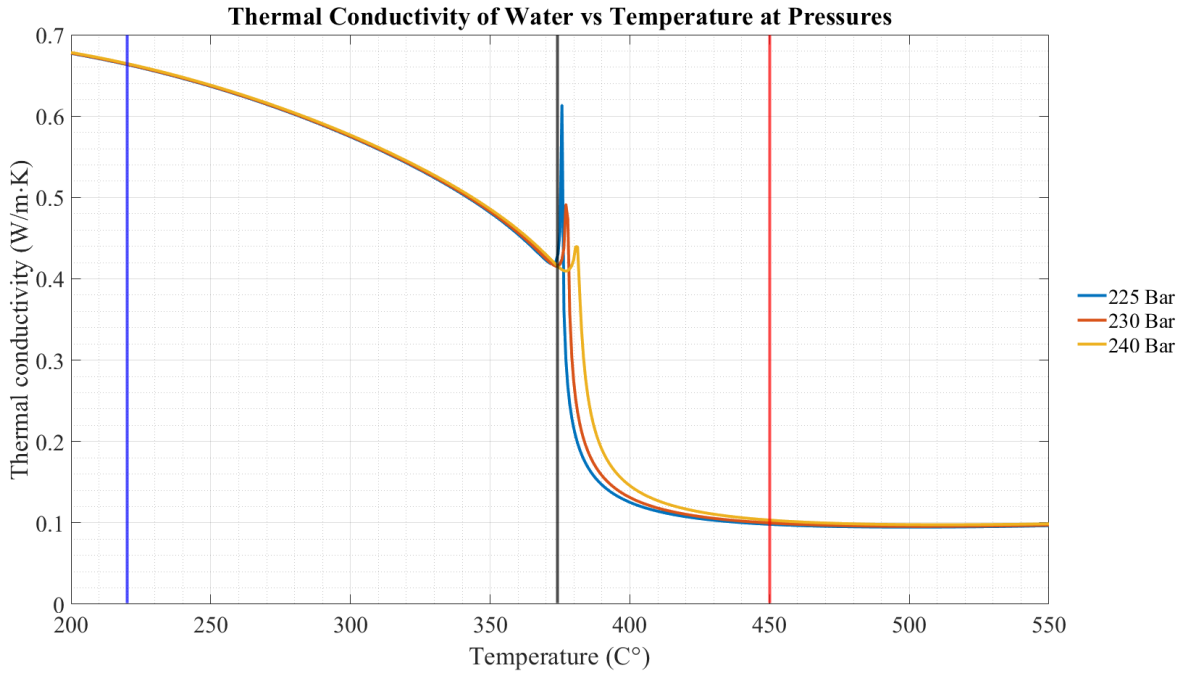


Figure 15: Thermal Conductivity of $H_2O$ at temperatures from 200℃ to 550℃ over pressures of 225, 230, 240 Bar

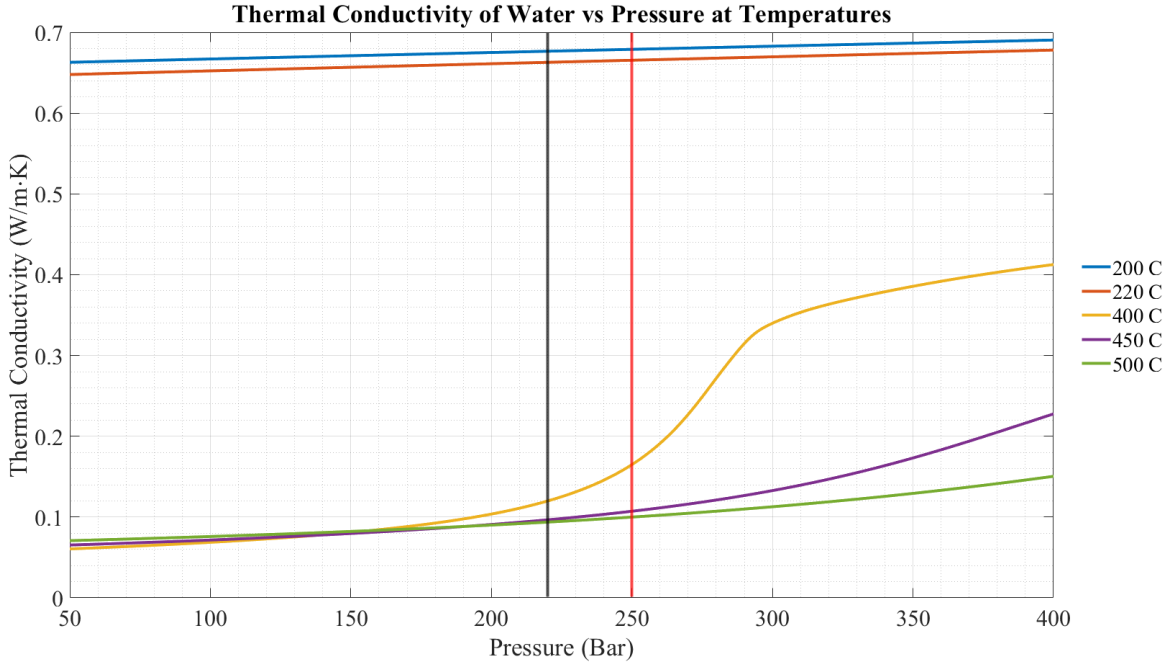


Figure 16: Thermal Conductivity of $H_2O$ from 50 Bar to 400 Bar over a temperature range of 200℃ to 500℃

The Prandtl number curves take a similar shape to the specific heat, where the lower pressure line spikes higher than the higher-pressure curves as shown in Figure 17. Figure 18 shows the Prandtl number of $H_2O$ as a function of pressure from 50 Bar to 400 Bar over the temperature range of 200°C to 500°C.

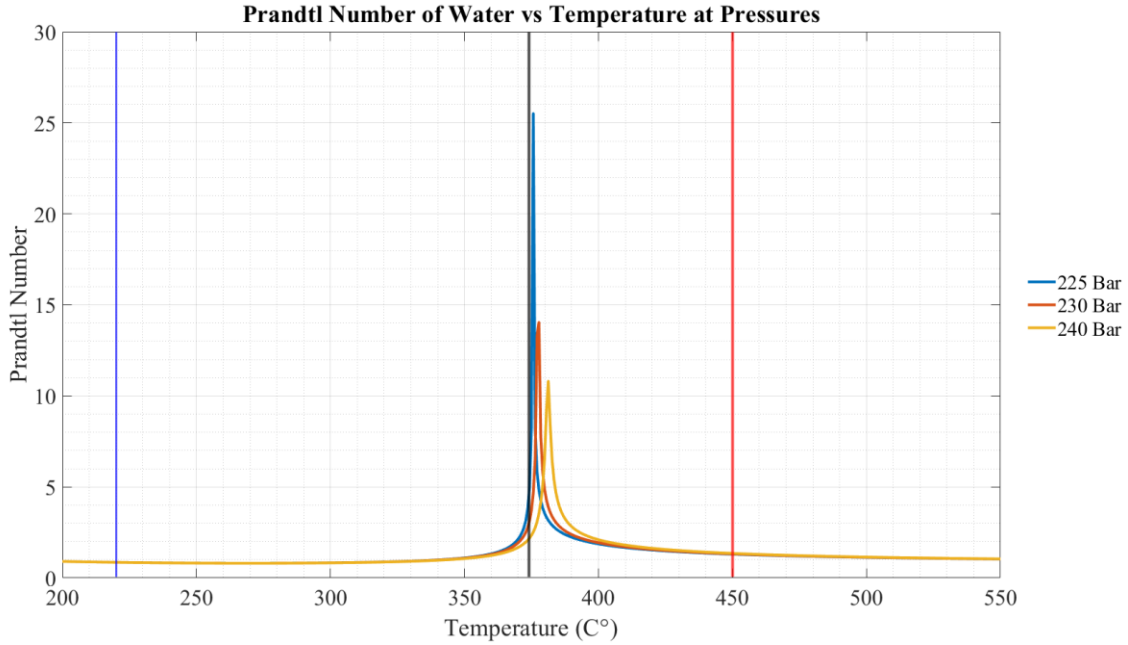


Figure 17: Prandtl Number of $H_2O$ at temperatures from 200°C to 550°C over pressures of 225, 230, 240 Bar

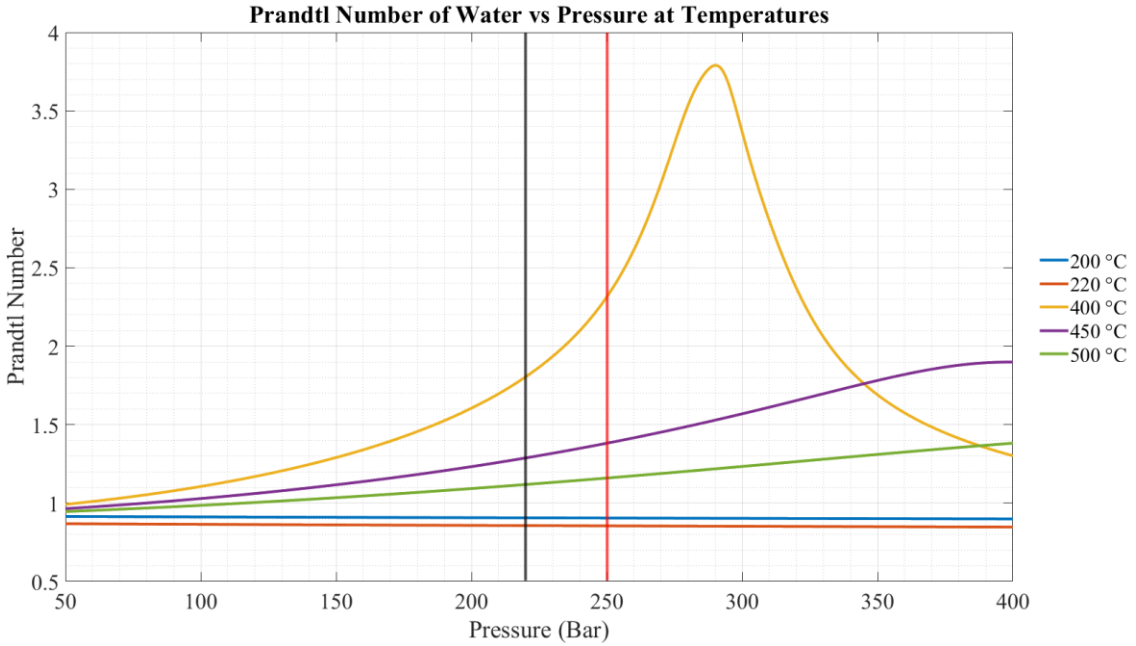


Figure 18: Prandtl Number of $H_2O$ from 50 Bar to 400 Bar over a temperature range of 200°C to 500°C

Figure 19 shows the Entropy of water from 200℃ to 500℃ at pressures of 225, 230 and 240 Bar.

Figure 20 shows entropy increasing with temperature as a function of pressure.

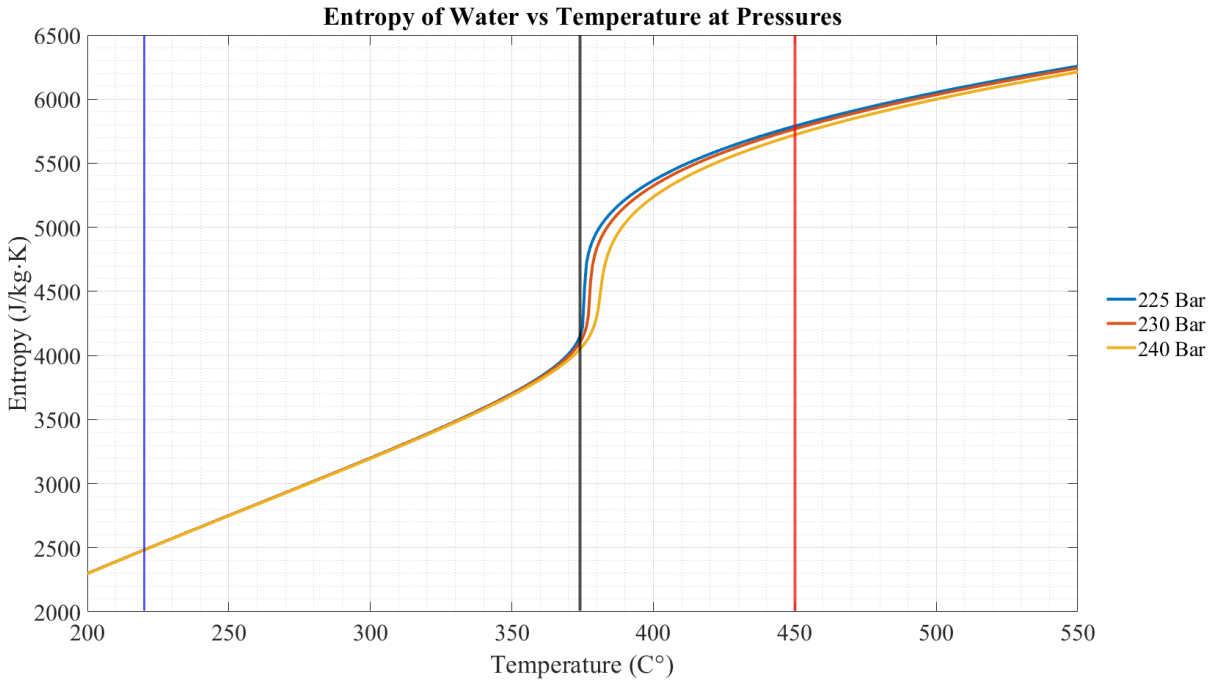


Figure 19: Entropy of $H_2O$ from temperatures from 200℃ to 550℃ over pressures of 225, 230, 240 Bar

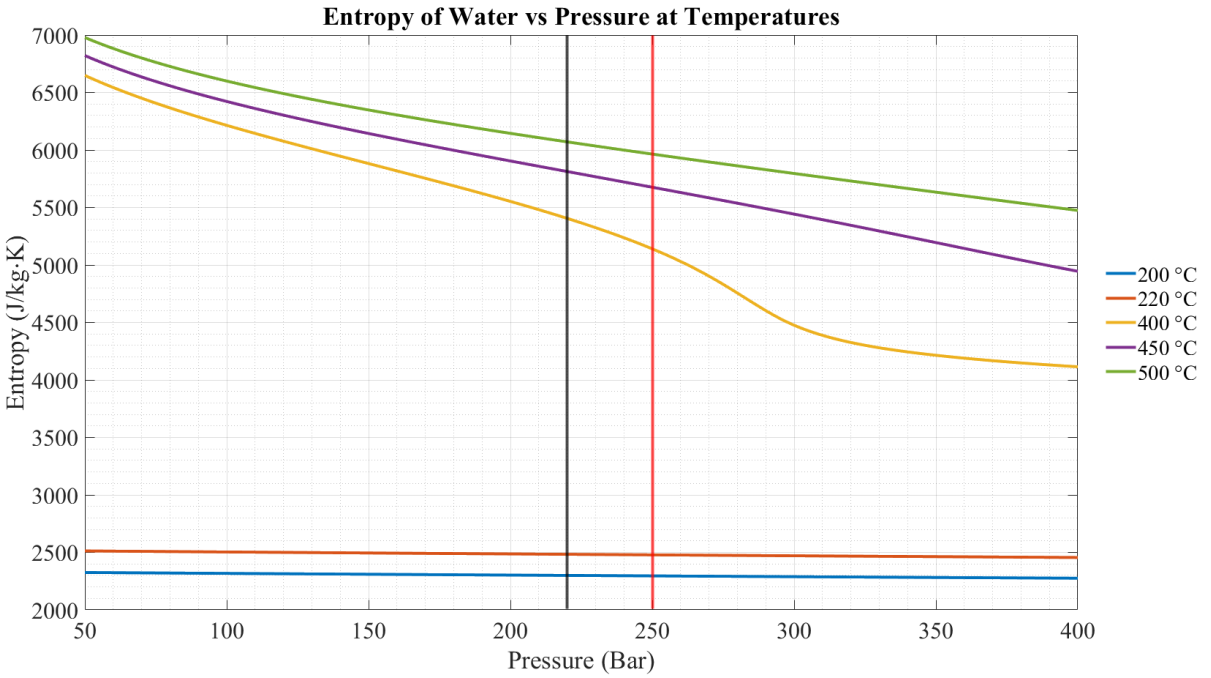


Figure 20: Entropy of $H_2O$ from 50 Bar to 400 Bar over a temperature range of 200℃ to 500℃

The thermophysical properties graphs shown all depict the abrupt changes that occur near the critical temperature of water, these changes make it difficult to produce a reliable mathematical model that can be used to predict the behavior of a supercritical HEX for various applications.

## MATERIALS REVIEW

A short list of materials was considered for the hot and cold tubes of the heat exchanger design presented in this work, as shown in Figure 21. The desired material qualities are strength, corrosion resistance and the ability to transfer heat conductively.

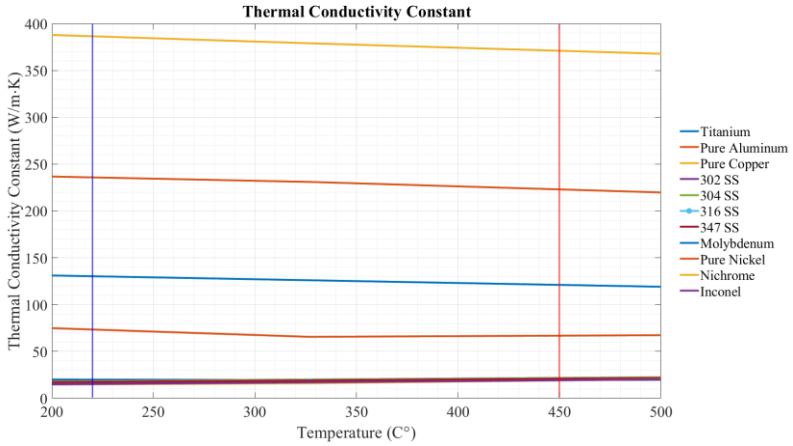


Figure 21: Thermal Conductivity of Various Materials as a Function of Temperature [4]

Considering the specific heat of the material used to fabricate a heat exchange can assist in calculating the amount of heat that is lost to warming up the heat exchanger during system start up. If the mass is to large it will take longer to heat up and cool down.

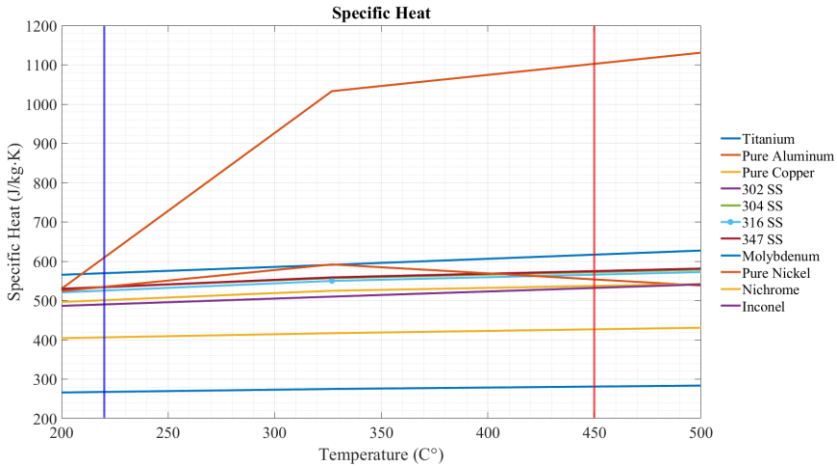


Figure 22: Specific Heat of Various materials as a function of Temperature from 200°C – 500°C [4]

As the temperature of 316 stainless steel increased the yield stress decreases. The yield stress of 316 stainless steel at room temperature is about 42ksi, this value decreases to approximately 1 half of its original value when the 316 stainless steel reaches its maximum operating temperature in supercritical desalination applications.

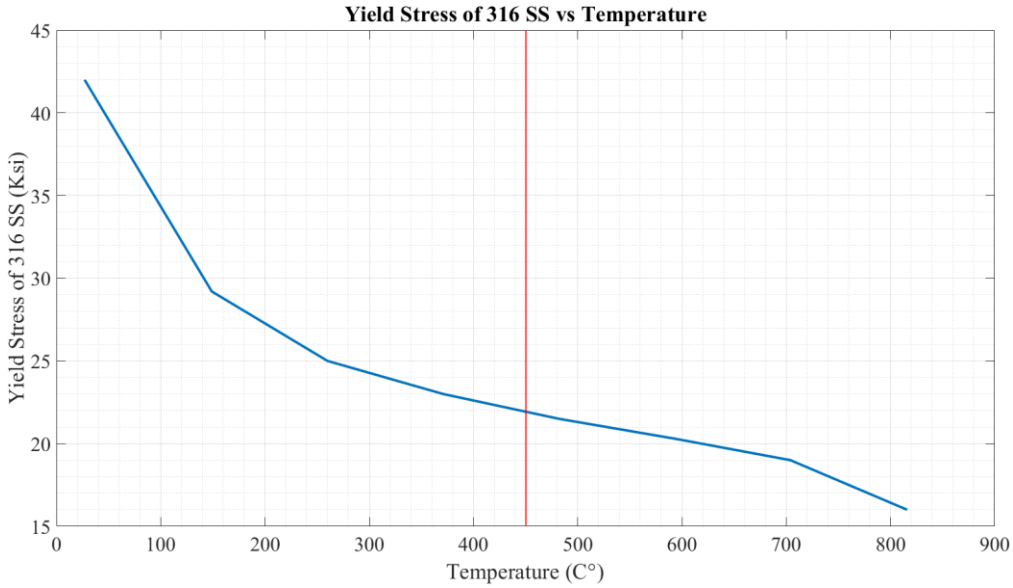


Figure 23: Yield Stress of 316 SS as a Function of Temperature from 0°C to 900°C

The surface tension data is only available for saturated conditions and not available for supercritical conditions because surface tension is a phenomenon that occurs in liquids. The material chosen was 316 stainless steel because it is corrosion resistant enough to last through the experiment at an economic price as well as strong enough to handle the large pressures associated with creating supercritical water.

## BRIEF REVIEW OF CORROSION REDUCTION METHODS

Corrosion is a sizeable enough problem to where it got its own section [15]. Incoloy 825 was selected for the processing component and grade 2 titanium has been chosen for the HEX in van Wyk et al [37]. Van Wyk narrowed down the source of corrosion to Incoloy 825 not titanium. Van Wyk, et al. [15] stated that an in-depth material study needs to be conduct, but a solution using titanium is suggested. The HE in van Wyk's work started to function properly, although corrosion is still an issue. Grade 2 titanium is pure alpha titanium and is the most common. Other titanium types exist that should be considered when

designing a new HEX. The type of corrosion was not stated in this article. Titanium that is resistant to crevice corrosion is TIMETAL 50A Code-12 and 50A Pd wit. Although titanium is corrosion resistant it is still susceptible to corrosion and more advanced corrosion resistant titanium may be needed [38].

Corrosion is a problem with HEXs and is expected as shown in Failures of heat exchangers [39]. Corrosion problems can be solved through the means of surface treatments such as, passivation, ceramic, or other non-reactive coatings [14]. Metal sputtering may also be considered as an application method to apply a solution to the corrosion problem. A sacrificial anode may also be required to reduce titanium corrosion. Corrosion is a design consideration depending on the environment the product will be used in, but it is commonly overlooked and found after an unforeseen situation causes it.

Coating the titanium may cost more but it will allow the HEX constructed of an already expensive material to last longer. Advanced plating technologies may be a possible solution to the anticipated corrosion problem.

If this design does not seem to work and off the shelf, HEX may be needed or outsourced to another vendor. The hot HEX in the HEN could require some additional insulation to reduce heat energy loss to the surrounding environment.

## EXPERIMENT

To find the Nusselt number, Prandtl number and Reynolds number an experiment must take place. During the experiment pressure and temperature will be recorded. The temperatures and pressures recorded will then be used to look up the values of the thermophysical properties needed to find the Nusselt number, Prandtl number and the Reynolds number. This data was looked up using NIST-REFPROP database.

# CHAPTER 2 METHODS

## INTRODUCTION

This chapter will discuss the methods implemented to run the experiments on the desalination system to collect data about the properties of the fluid as if flows though the heat exchangers (HEX) of the heat exchanger network (HEN). The procedures discussed will cover start up, operation and shut down operations and methods. The components of the desalination system and the heat exchanger cart (HEC) will also be covered. The existing system is shown in Figure 24. This system requires a feed water heater also known as a pre-heater and a chiller. The FWH is in the form of the first furnace (F1).

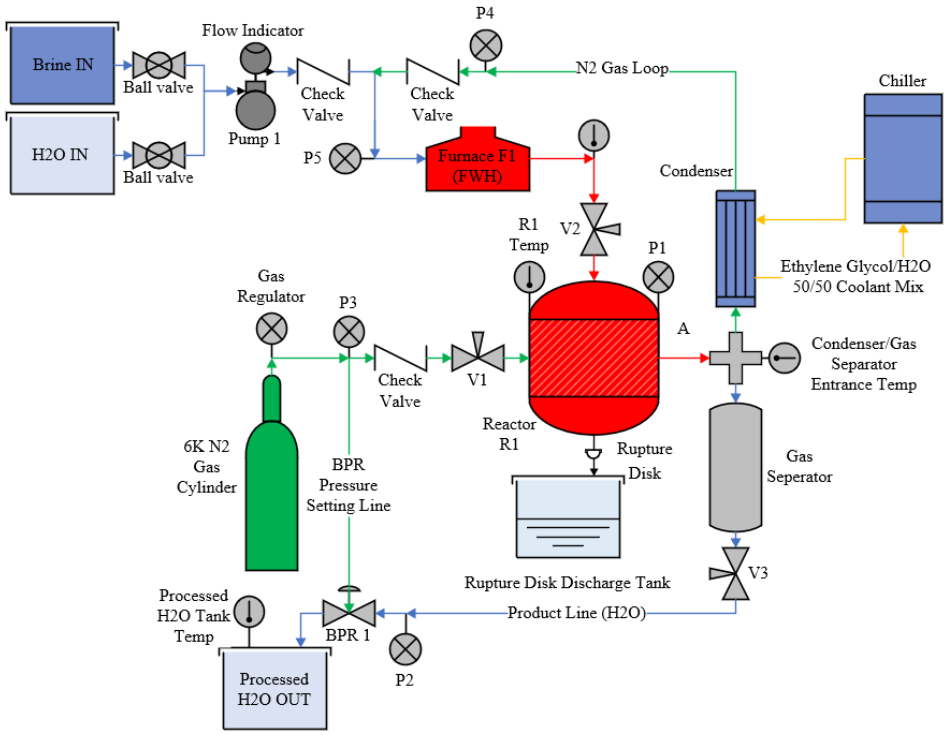


Figure 24: Existing system with 10 mL/min flow rate

The ideal system is shown in Figure 25 where the pre-heater and the chiller have been removed and replaced with a heat exchanger. The heat exchanger is a “passive” element which does not require any outside power to function as a chiller and a furnace do.

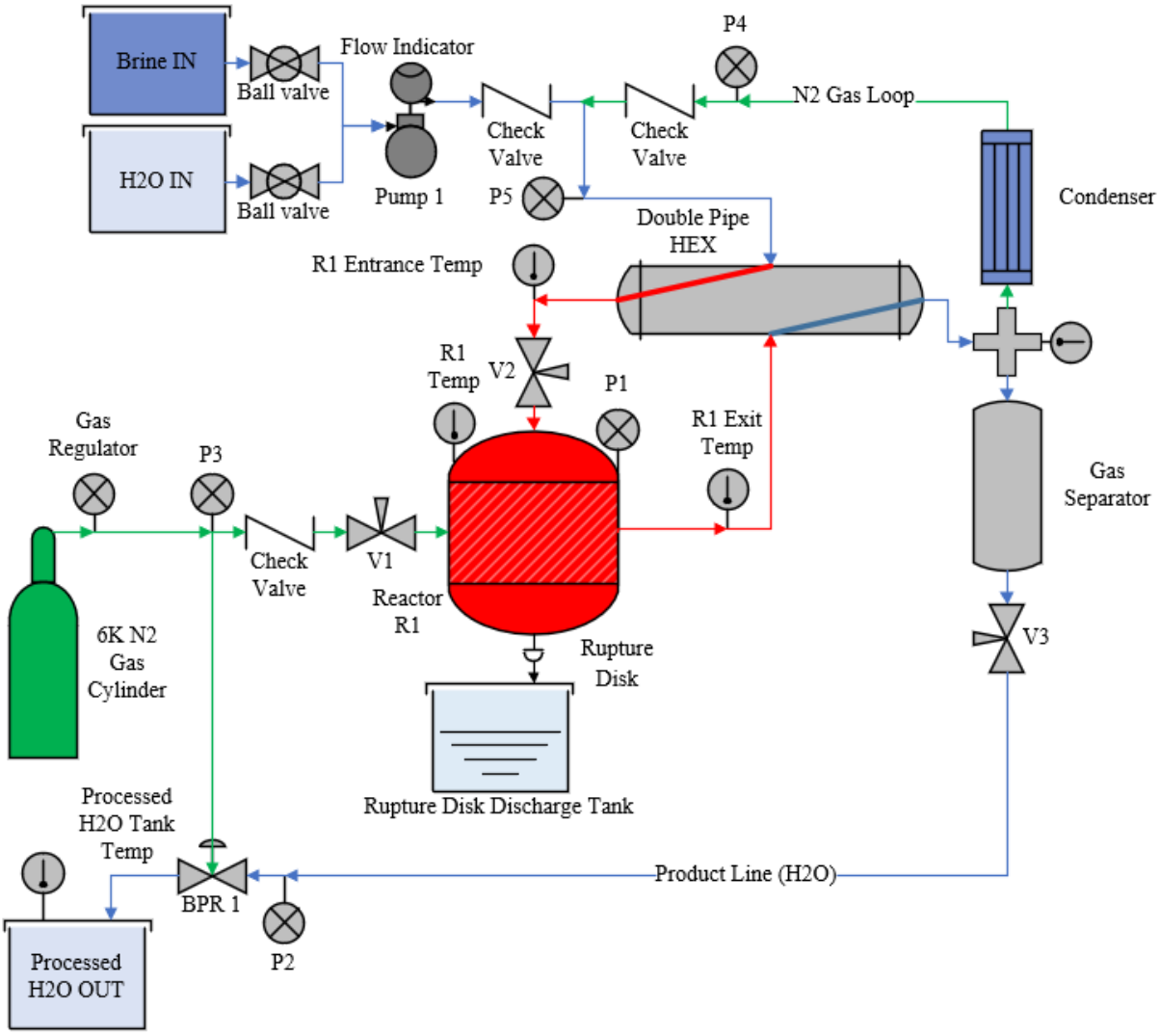


Figure 25: Ideal System

Figure 26 shows the system Process and Instrumentation (PI) diagram that illustrates how the system was set up to collect data on HEX performance at different temperatures and pressures. Furnace 2 (F2) was added between the HEX and the gas separator and condenser assembly. Pump 2 and accompanying water and brine tanks were also added to cool the heat Exchanger. Pump 1 and Pump 2 are linear displacement pumps that are both capable of the same flow rate of 10 mL/min.

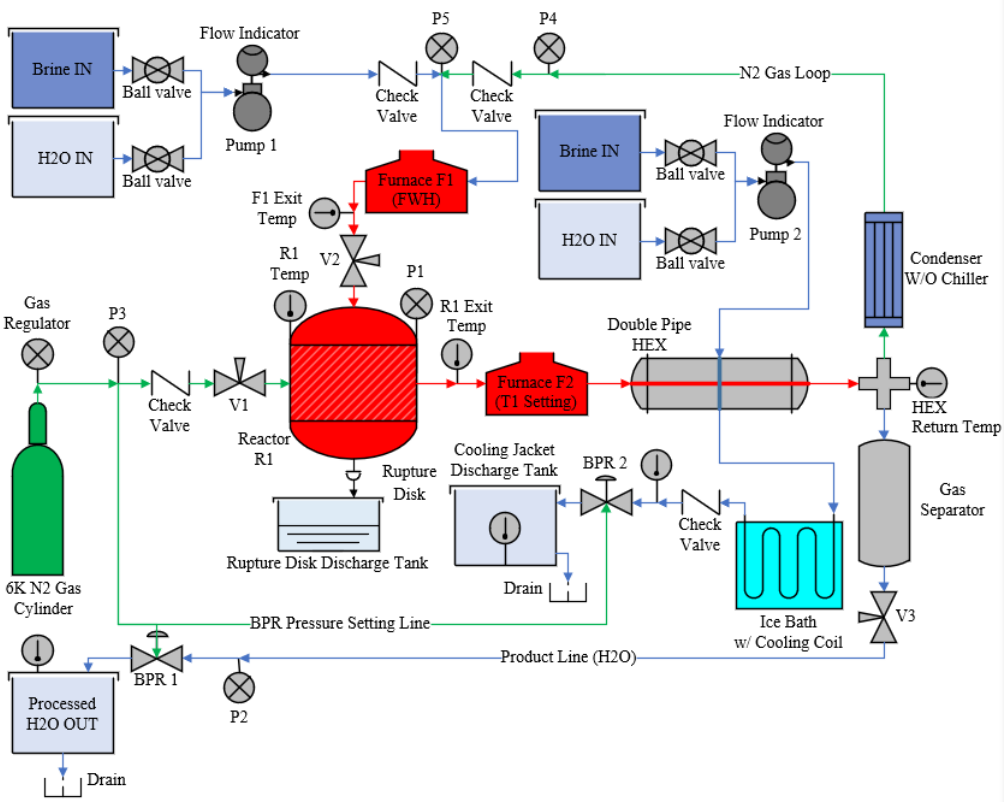


Figure 26: Experiment Setup

There is no added nitrogen gas in the cooling line during experimentation. Pump 2 is running at the beginning of the experiment while the rest of the system is heating up. The nitrogen tank in conjunction with the back pressure regulators (BPR1 and BPR2) set the pressure of the desalination system and the cooling side.

## MATERIALS

The equipment pieces this study applies to are shown in Figure 27 and 28. The smaller 10mL/min system is shown in Figure 27 and the larger supercritical water system that as a flow arete of 100mL/min is shown in Figure 28. HEX1 and HEX2 as mounted to the HEC can provide solutions to the heat exchanger networking needs of the 10mL/min desalination system. HEX2 is designed to work with the 100mL/min system, the data for this scenario was not collected in this study. The intention is to characterize HEX1 and HEX2 on the 10mL/min system then integrate the HEN with the 100mL/min system. The Computer Aided

Design (CAD) model shows the input tanks, pumps, the reactor, gas separator condenser assembly, feed water heater (FWH), and the rupture disc discharge tank.

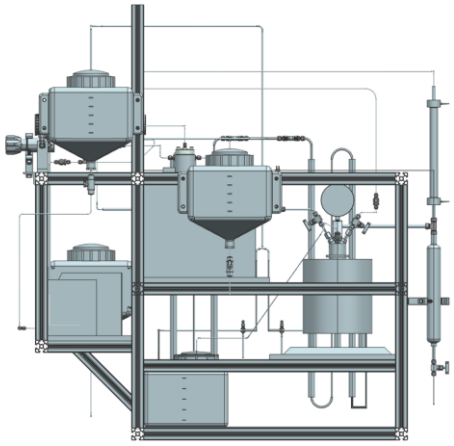

Figure 27: Front view of the 10 mL/min SCWD system SolidWorks CAD model

The 100mL/min system shown in Figure 28 has 2 reactors, a larger FWH and a larger condenser, all larger components to accommodate 10 times increase in flow rate.

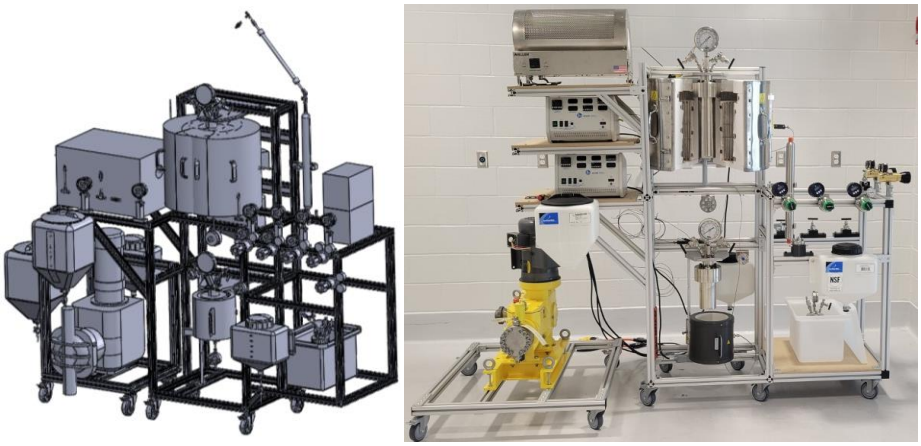

Figure 28: CAD Model (Left) and fabricated system 100mL/min desalination system also known as the 10X system (Right)

The pieces of equipment used for this study include a supercritical water desalination system, the HEC, several pumps, and a nitrogen gas cylinder. The desalination system is not shown in Figure 29. The interventive aspect of this study is the addition of the heat exchanger cart. The parts shown in Figure 29 are the intervening components.

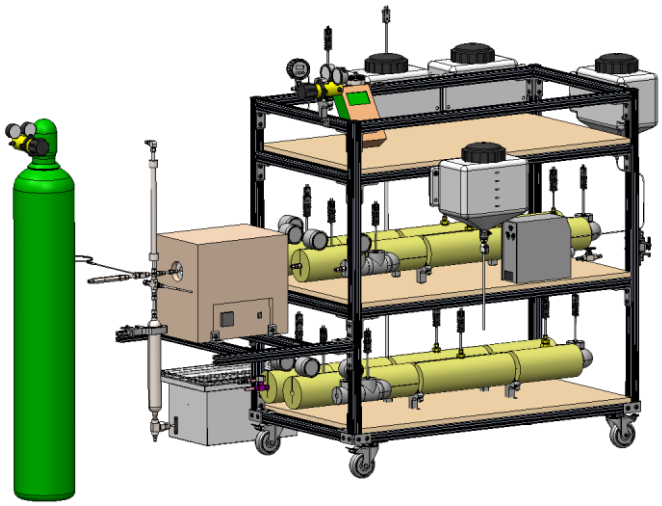

Figure 29: SolidWorks CAD assembly model of the HEC, 2 HEXs, Furnace 2, Pump 2, Ice bath bucket. Desalination system, thermocouple cables and power cables are not shown

The CAD model of HEX1 is shown in Figure 30. HEX1 and HEX2 are similar in design with some minor variations regarding overall length, annulus volume and insulation type. The hot central line is the same material in both HEs.

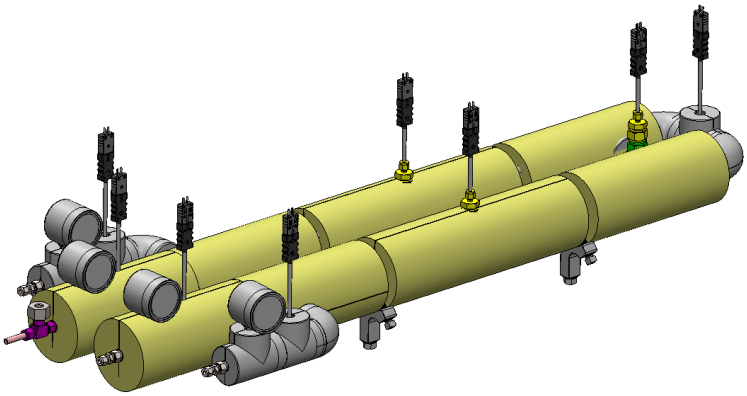

Figure 30: SolidWorks CAD assembly of an individual heat exchanger with rockwool insulation

HEX1 BRINE EXPERIMENT SETUP

The HEC held the tanks which held the water and brine to be pumped into the HEXs that were mounted to the cart. Tank 1 was loaded with deionized water from the ECU Life Sciences building DI-$H_2O$. Tank 2 was loaded with brine for testing. To change the salinity of the solution pumped through the HEX cooling jacket the brine in Tank 2 was drained and replaced with the next brine for testing. Figure 31 shows these tanks mounted to the HEC.

Figure 31: Tank 1 is for H2O, Tank 2 is for 3.5wt%, 7.5wt%, 14wt% NaCl Brine, HEX1 shell output tank

SETTING

The experiments took place at the Life Sciences and Biotechnology Building (LSBB) located on the corner of 10th street and Evans Street in Greenville North Carolina on the campus of East Carolina University. The system was assembled in the High Bay area. The High Bay is equipped with 2 garage doors, a 1 Ton Gantry crane, 2 air snorkels, several tables, a fume hood, a sink, a work area circumferential drain among other common lab items. Figure 32 shows the lab work area.


Figure 32: High Bay of Life Sciences and Biotechnology Building at East Carolina University

A Nitrogen gas cylinder bottle rack was added to the room for the purpose of this project. The LSBB is a newly constructed building and the ribbon cutting ceremony was in the Fall of 2021. The research group the researcher was a part of was one of the first groups in the building. The High Bay was outfitted with a floor drain that encircled the working area. The room next to the High Bay is a bio-processing lab

equipped with a deionized water faucet, which was the source of the working fluid in this experiment. Tap water was not used as the working fluid in the experiments conducted for this study due to its impurity. The reactor is intended to remove salt and other solids from the water. Tap water contains some salts and other elements that may come out of the water during operation. The purpose of using DI-$H_2O$ was to protect the reactor from damage and minimize maintenance throughout the experimentation phase of this work.

Figure 33 shows the 10ml/min SCWD system with the chiller connected to the condenser. The chiller consumes power during normal operation. Adding a heat exchanger will remove the chiller, thus removing the need to power the chiller, reducing the overall power consumed by the desalination system.

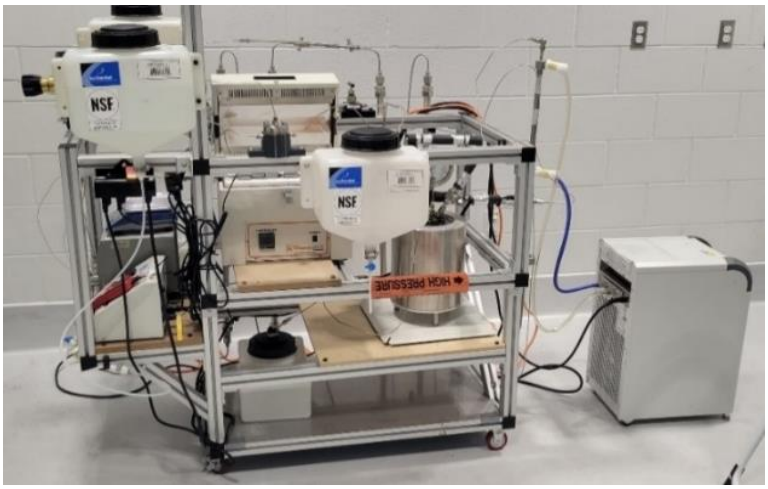


Figure 33: 10mL/min SCWD system with connected chiller and FWH

Figure 34 shows the lab ice machine where the ice for the ice bath was sourced. There are different types of ice that ice machine manufacturers design machines to create, the ice used for the ice bath was classified as the trade name of “nugget” describes. The “nugget” shaped ice resembles ½” to ¾” long cylinders that are ½” to 5/8” round.

Figure 34: Ice Machine – source of ice for ice bath

PARTICIPANTS

The people involved in this study are the authors of this paper. During the earlier phases of testing another graduate student assisted Michael in setting up the system and was to aid on an as needed basis. There were undergraduate students available, but they were not utilized for the data collection portion of the study at hand. There were no populations or people studied in this research effort. This is a project that strictly studies a desalination system and its mechanical and thermal operation.

MATERIALS

The heat exchanger cart (HEC) was constructed with the assistance of 2 other grad students. The cart was modeled in SolidWorks then constructed with Commercial-of-The-Shelf (COTS) components. The metallic compression fittings used were manufactured by Swagelok and Parker Hydraulics. The tubing used to construct the heat exchanger was 316 Stainless Steel tubing sourced from MaxxPro. The HEC is outfitted with 3 shelves total. The top shelf is for data collection equipment and provides a working surface for the operator, the middle and bottom shelves are for HEX1 and HEX2. HEX1 and HEX2 are different in design. HEX1 is shorter and was designed to have a thicker shell wall. HEX1 was also intended for supercritical $CO_2$ ($ScCO_2$) research [3], [40]. $ScCO_2$ research and data is out of scope of the work presented. The HEX set was constructed using the prepared stainless-steel tubing shown in Figure 35.

Figure 35: 316 Stainless-steel tubing prepared for fabrication

The manufacturing and fabrication methods needed to produce the heat exchanger have been limited to simple hand tools because the HEX designed is intended for assembly in a region where power sources are very limited. The HEX designed can be constructed with nothing but 2 sets of wrenches and a hacksaw and some minor gauges and measuring tools such as a tap measure. A de-burring tool is also recommended. Table 6 shows the tubing configurations that were considered for the HEX for experimentation.

Table 6: Heat Exchanger Tubing Dimensions Considered for Design

| Double Pipe Configuration for nominal 1/4" and 3/4" tube HEX | | | | |
|---|---|---|---|---|
| OD (in) | OD (m) | Wall Thickness (m) | ID (m) | Flow Areas ($m^2$) |
| 0.75 | 0.01905 | 0.0042 | 0.0107 | 7.30E-06 |
| 0.25 | 0.00635 | 0.0017 | 0.003 | 8.21E-05 |

| Double Pipe Configuration for Nominal 1/2" and 3/4" Tube HEX | | | | |
|---|---|---|---|---|
| 0.75 | 0.001905 | 0.0042 | 0.0107 | 4.03E-05 |
| 0.5 | 0.0127 | 0.0028 | 0.0072 | 4.91E-05 |

| Double Pipe Configuration for Nominal 3/8" and 3/4" tube HEX | | | | |
|---|---|---|---|---|
| 0.75 | 0.01905 | 0.0042 | 0.0107 | 2.21E-05 |
| 0.375 | 0.009525 | 0.0021 | 0.0021 | 6.72E-05 |

Figure 36 shows a cross section of the hairpin turn at the end of the HEX. The hot fluid flows through the central tube that is shown on the right portion of Figure 36. The cooling fluid flows through the larger diameter section of Figure 36 shown vertically on the left side of Figure 36.

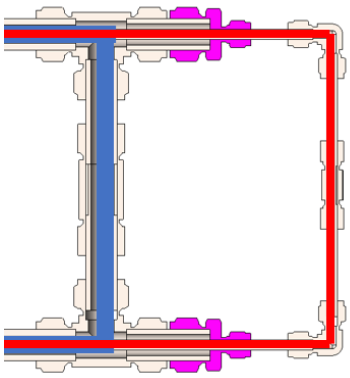

Figure 36: Cross section of internal fluid path of the proposed HEX

Figure 37 shows the metallic compression fittings purchased for the construction of the heat exchanger as received. The fittings for the shell are ¾" and the fittings for the center tube are 3/8" or the SS-2010-X-X series and the SS-600-X-X series from Swagelok.

Figure 37: Metallic compression fittings laid out prior to assembly, connecting tubing is not shown.

INSULATION

Early on the system was uninsulated and through experimentation it was determined that too much heat was lost through convection, conduction, and radiation to the surrounding environment. Rock wool insulation was added to the HEX and the hot lines. The line that is flowing out of Furnace 1 (F1) is insulated as well as the line running out of Furnace 2 (F2) into the HEX on the cart. The rock wool used in HEX1 was 2 in thick 7/8" ID mineral wool pipe insulation purchased from McMaster-Carr. HEX 2 used steam resistant high temperature fiberglass insulation tubes with a 1.5" wall thickness and a 7/8" ID.
Throughout the HEC steam resistant high temperature fiberglass elbows with 1" to 2" wall thickness was used where appropriate. The elbows were comprised of 2 halves held together with wire that was twisted together so secure the insulation where it is needed. Aluminum tape was also used to seal the insulation at the seams and secure insulation where it was needed. The insulation also protects the operator from exposed hot surfaces.

NITROGEN GAS CYLINDER

A nitrogen gas tank from AirGas supplied the nitrogen gas that was used in this experiment. The gas was sold under the trade name (Nitrogen, Compressed, UN1066, CAS# 7727-37-9), it is designated as being 100% Nitrogen. Nitrogen is an asphyxiant and will deprive the body of oxygen if inhaled, if it is

improperly handled death is possible. This gas was used to pressurize the system before the water or brine was pumped through the system. The method for pressurizing the system will be described in greater detail in the procedure. The purpose of the nitrogen is to provide a “gas spring”. Water is an incompressible fluid when it is in the liquid state and pressure spikes can be experienced if it boils. If the system was filled with water first, then heated boiling will occur, therefore the system is first pressurized then filled with water.

An off the shelf brass regulator was purchased, as well as pressure gauges, a 1/8” X 1/4”-NPT metallic compression fitting, and a CGA-677 nipple with the CGA-677 nut for assembly into the regulator that remained on the tank during testing. CGA stands for Compressed Gas Association, this organization has standardized the gas fittings and practices in industry to increase safety. A second regulator was added to the desalination system for the operator to adjust the pressure while the system was pressurized. The line running out of the tank regulator is connected to the “in” port of the regulator mounted to the system. The gas inside a new unused tank is 6000 psi, the maximum limit of the pressure gauge on the reactor is 5000 psi. The regulator that is mounted to the tank sets the pressure of the gas to 4000 psi to protect the pressure gauges on the desalination system. The pressure gauges on the desalination system are oil filled and shock resistant. The pressure gauges mounted on the nitrogen gas cylinder are traditional more economic gauges. The desalination system is equipped with oil filled gauges because they are more precise and hold accuracy over long periods of time when mounted to equipment that is prone to shock and vibration. When the pump is running the desalination cart vibrates from the pump and the pump’s cooling fans, this vibration can cause the gages to drift with system use. The purpose of creating the CAD model shown in Figure 38 is to provide documentation and a visual aid to guide in assembly of the parts used in this experiment.

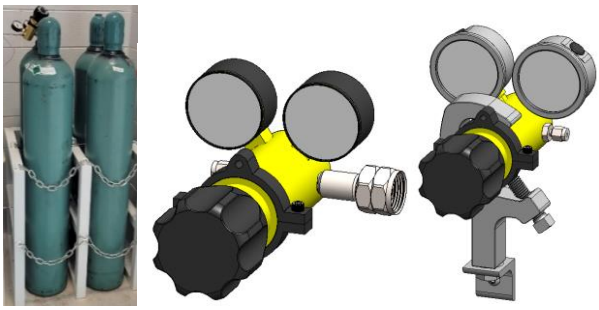

Figure 38: Nitrogen gas cylinders, regulator for the tank and regulator assembly for SCWD Cart and HEC

EXPERIMENTAL SET UP

The following set up method refers to the labeling scheme in the PI diagrams presented. The system was pressurized with Nitrogen gas at a 150 Bar pressure reading. Once pressurized the back pressure regulator was set to the desired experiment pressure of 225, 230 or 240 Bar. The reactor is then turned on and set to 415 ℃. When the Reactor (R1) temperature reads approximately 370-380 ℃ pump 1 is turned on and pumps at a preset flow rate of 10 ml/min. Furnaces 1 and 2 are then turned on. Furnace 1 is set to 350 ℃. Furnace 2 was set to the desired temperature for the experiment. Furnace 2 was added to the system strictly for temperature control to evaluate the performance of the HEXs used in this study and is not necessary for a production level system for commercial use in normal practice.

The Reactor exit temperature was monitored. The reactor exit temperature is recognized as Furnace 2 entrance temperature. T1 is recognized as Furnace 2 Exit temperature. The heat added to the system by Furnace 2 can then be determined through thermodynamic calculations.

The cooling jacket exit temperature was monitored at the heat exchanger cold line exit point, at a point after the cooling ice bath and in the collection tank. The purpose of monitoring this data is so that the HEX cooling jacket exit temperature is known, the ice bath cools the water down so that the hot fluid does not melt the plastic collection tank and the density sample is correct. The diaphragm in Back Pressure Regulator 2 (BPR2) is made from stainless steel as opposed to the Polyether Ether Ketone (PEEK) diaphragms so it can handle high temperatures as a precaution. The temperature of the HEX cooling bath would start off high then drop as water filled the tank. This is because the tank starts empty and mass of water inside the tank increases as water fills the tank. The flow rate was checked incrementally with a beaker and a stopwatch to check if a constant system flowrate of 10 ml/min was maintained. The flow rate did not appear to change throughout the experiment.

The ice machines in the ECU Life Sciences Building were used as an ice source. It was found that adding water to the ice increased the ice's ability to remove heat from the cooling coil, forming a slushy ice water mix. The cooling jacket water was then dumped into a collection tank. Between experiments the heat exchanger cooling water was dumped down the drain with the ice bath water.

BRINE AND WATER

The brine used in the experiments was produced in the lab using a scale, a large 2-liter Erlenmeyer flask, deionized water, and lab grade sodium chloride. Iodized salt commonly found at supermarket establishments was NOT used in this research. Iodine is added to table salt to help regulate hormones that control heart rate and blood pressure among other health benefits and can be absorbed by the 316 stainless steel that the system plumbing is constructed of [41], [42]. This iodine absorption phenomenon is similar to hydrogen-embrittlement which can weaken the 316 stainless steels through a form of corrosion which could cause issues when the system is pressurized. [41]. The lab grade sodium chloride (NaCl) used to create the brine was from ThermoFisher with a CAS # of 7647-14-5 which is >99% NaCl in purity. The brine concentrations created for these experiments are 3.5wt%, 7.5wt% and 14wt% NaCl in batches of 2 liters at a time. This desalination system has already been proven using NaCl and KCl (Potassium Chloride) in previous experiments. It is known that the fluid exiting the reactor is approximately 99% pure water in these experiments where NaCl and KCl are the salts in the brine loaded into the brine for treatment tank. The fluid fed into the desalination system was deionized water mixed with NaCl to form brine for the earlier experiments. The purpose of using deionized water as the hot fluid is to reduce the wear and tear on the desalination system. Tap water is fortified with sodium fluoride, fluorosilicic acid, or sodium fluorosilicate (fluoride), sodium hypochlorite (chlorine) and which are added to drinking water for health benefits, these materials could have negative effects on the stainless steel over the long term.

When using highly concentrated brines the reactor needs to be disassembled periodically for routine maintenance. The objective here is to reduce time and increase experimental run time. There is also the off chance that the rector could be damaged during the O-ring changing procedure. If the fluid is 100% DI water that runs through the desalination side of the system, routine maintenance frequency is greatly decreased. The maintenance procedure includes removing the reactor from the system, placing it in a vise, then removing the bolts and changing the graphite O-ring seal. Before reinstalling the reactor back into the desalination system, the clamps need to be reinstalled and the bolts need to be properly torqued down. If the system needs to have the O-ring changed every 40 hours of run time and 400 hours of experimentation

is needed 10 O-rings need to be consumed and 3 hours of maintenance time is required per O-ring change that is a wasted 30 hours. Therefore, DI water was used as the desalination fluid. This is acceptable based on past system performance.

## MEASUREMENT INSTRUMENTS

The data recorded in this experiment consisted of temperature, pressure, flow rate, conductivity, and density of the operating fluid. The temperature data was collected using J-type thermocouples that were connected to a handheld thermocouple meter. The pressure gauges at the HEX inlets and outlets were analog dial type gauges that were rated for high temperatures and were connected to the T-fittings on the line.

## FLOW MEASUREMENT

The flow rate was periodically checked using a small beaker and a timer. The researcher would place the beaker under the outflow line and catch the water dripping before it entered the product output tank. The timer would begin when the first droplet contacted the bottom of the beaker. Once the 1 minute passed the beaker was removed out of the outflow stream and a measurement is taken. A flow meter could have been installed but the method discussed is more in line with how the flow rate would be measured in the context of and off the grid system. A flow meter would be one more thing that needs to be powered, the flow rate read out on the pump is adequate. The flow rate is shown on a digital display on both Pumps 1 and 2. The 10mL/min system flow rates were set by the control panel on the pump.

## TEMPERATURE MEASUREMENT

All temperatures measured in this study were captured using J-type thermocouples. The thermocouples used to measure the fluid temperature inside the HEX's were ¼" diameter stainless steel probes. The thermocouples used to measure the fluid temperature at different points in the process were 1/8" diameter. The thermocouple cable was shielded with a fiberglass wrap if it contacted a hot surface to protect the wire coating. Each HEX had 3 thermocouples on the hot line, and 5 thermocouples on the cooling

line. The temperature ranges the system experienced during operation was from room temperature to approximately 450℃. Figure 39 is an example of the thermocouple style that was used in these experiments.

Figure 39: Thermocouple used on HEX2 at point T8 pulled for inspection.

The 6-inch long ¼" diameter thermocouples had an accuracy of +/- 0.75% with a readable temperature range of 32°F to 970°F with a 1.3 second response time. The tubular housing is made from 316 stainless steel to resist corrosion. The connection type is round pin. Round pin to flat pin adapters were used to connect the individual thermocouples to the handheld temperature meter during data collection. The temperature meter used to collect the thermocouple temperature data in these experiments is shown in Figure 40.


Figure 40: Proster Thermocouple handheld meter

The meter shown in Figure 40 can receive data from J, K, T, E, N, T, R, and S-type thermocouples. The temperature range of data the meter will display for J-type thermocouples is from -346 F to 2192 F (-210C to 1200C). The accuracy of the meter is +/- 0.1%. Figure 41 shows a 12 channel TM500 manufactured by EXTECH, it was used to monitor the room temperature of the ECU LSBB High Bay while experimental data was being recorded. The room temperature increased and decreased with the rising and setting of the sun by approximately 5℃.

The EXTECH Data logger can stand environmental temperature ranges of -40°F to 482°F. The data logger will accept E, J, K, R, S and T-type flat pin thermocouple and write the data collected to an SD Card and record up to 20,000,000 data points. It can be powered by 8 AA batteries or an AC adapter cable. This meter was left in the on position for the duration of all experiments for data recording.

Figure 41: EXTECH data logger with J-type Probe measuring room temperature.

PRESSURE MEASUREMENT

The pressures of the system were measured using a few different pressure gauges. The room temperature lines were measured using digital high precision pressure gauges that were powered by 9-volt batteries. The hot lines were measured using a high temperature analog pressure gauge. The Reactor pressure gauge (P1) is a large pressure gauge affixed to the top of the reactor that was supplied by the reactor manufacturer PARR Instruments. The nitrogen gas line pressure was measured using analog gauges attached to the regulator. The max pressure the system experienced was close to 260 Bar (3771 psi). 4 pressure gauges were used on each heat exchanger. Pressure gauges used in this study are shown in Figure 42.

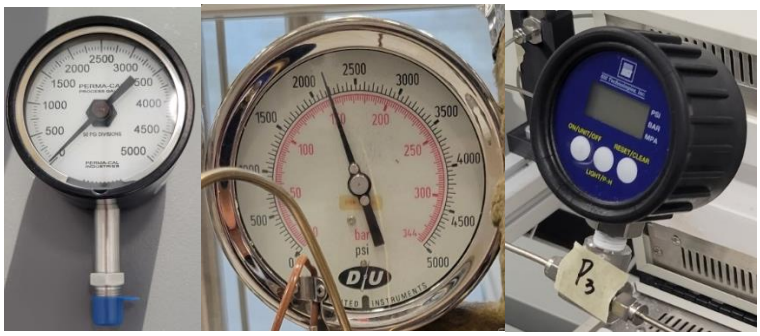


A B C

Figure 42: Pressure gauges

The pressure gauge shown in Figure 42 A, is rated for measuring high temperature fluids and will withstand environmental temperature range from -65° to 400°F (-53° to 204°C) and a process temperature of -65° to 600°F (-53 to 315°C) with an error range of +/-0.5%. The pressure gauge shown in Figure 42B has a large diameter face and maxes out at 5000 Psi. The pressure gauge shown in Figure 42A has an environmental temperature range of 0°F to 185°F and a process temperature range of 15°F to 140°F. The

accuracy is listed to be +/-1%, it is powered by a standard 9V battery and has a resolution of 1 psi (0.0689476 Bar). The pressure range of gauge C in Figure 42 is 0 to 5000 Psi (0-344 Bar). Pressure gauge A in Figure 42 was used in 4 locations on each HE. Gauge B was monitoring the Reactor as P1. Gauge C is used at points P2, P3, P4, and P5 in the Process Diagrams presented in this work.

## ELECTRICAL CONDUCTIVITY MEASUREMENT

The electrical conductivity was measured only during the experiments where a brine solution was pumped through the cooling side of HEX1. The conductivity of the fluid is measured in µS/cm or mS/cm. The conductivity meter is a modular SevenExcellence Multiparameter S400 conductivity, temperature, pH, resistivity meter. The Mettler Toledo InLab Expert Go was the probe used to take these measurements.

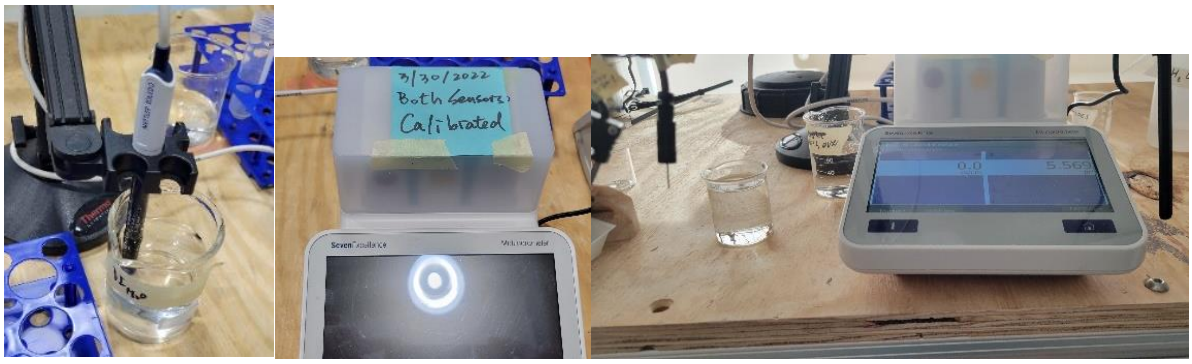


Figure 43: Electrical Conductivity probe and meter

The bench top electrical conductivity meter is capable of measuring a minimum of 0.001 uS/cm and a maximum of 2000 mS/cm with an accuracy of +/-0.5% of the reading.

## DENSITY MEASUREMENT

The density of the output fluid during data collection was measured with a handheld density meter. The plastic sample tube of the density meter was placed in the water collection vial while the vial was filled with the system output water to collect a reading. To operate the density meter the trigger is pulled, and water is pumped into the handheld meter then measured by the electronics housed in the meter. The meter outputs the data on a digital LCD screen. The density meter has an accuracy of +/- 0.001 g/cm$^3$, a

repeatability of 0.0005 g/cm$^3$, and a resolution of 0.0001 g/cm$^3$. The density meter will sample fluids within the temperature range of 0°C to 50°C.

Figure 44: Density Meter

If the sample collected by the density meter is to hot an alarm will sound and the screen will blink to let the operator know that the density shown is incorrect. The alarm trip was avoided by cooling down the water collected to room temperature by cooling the fluid through an ice bath. The density meter was only used to collect density values of the HEX1 salt study. Density measurements were not taken for the water-water studies, where deionized water was used as a hot fluid and a cooling fluid.

## PROCEDURE

This section will discuss the start-up, data collection and shut down procedures for the system produced. The room temperature was monitored during the experiment, it was found to be between 20°C to 27°C depending on the time of day. The room temperature variation had little effect to no effect on the results because it is a small percentage of the range of temperatures HEXs experienced during testing.

## SYSTEM START-UP PROCEDURE

To run an experiment the following procedure was followed:

The nitrogen tank regulator started in a closed position to prevent loss of any nitrogen. Then the nitrogen cylinder valve is opened to the fully open position. Then the nitrogen tank regulator is set to 4000 psi (276 BAR). The regulator on the desalination system is then set to 150 Bar. Valve 1 (V1) is then opened to fill

the system with nitrogen gas to a pressure of 150 Bar. V1 is then closed when the pressure gauge (P1) on top of the Reactor settles at 150 Bar. The regulator on the desalination system is then set to the pressure that is desired for the experiment. The experiments conducted for this research were operation pressures of 225, 230, and 240 Bar. When the system pressure settles to the desired pressure V1 is then closed. When the reactor temperature (R1) reaches 370℃, turn on Furnace 1 (F1), Pump 1, Furnace 2 (F2) and Pump 2, in the order listed. Pump 1 and Pump 2 are both set to 10 mL/min. Adjust pressure as needed to maintain safe pressure levels. The reactor is not to operate above 270 Bar.

## DATA COLLECTION PROCEDURE

The operator is to take the thermocouple meter in hand and insert a thermocouple plug into the thermocouple meter T1 port and then record the temperature in an EXCEL spreadsheet. The pressures shown on the pressure gauges are recorded in the same spreadsheet as well as the electrical conductivity and density of the output water. The flow rate was collected using the flow rate measurement procedure discussed in this chapter. The temperatures were then graphed in EXCEL and used as a readout to see what the system was doing. The generated graph can also be used to make decisions during operation or observe any phenomenon found. Data was collected every in 5, 10, 15-minute increments depending on what was going on. When the system was warming up data was collected at 10 5o 15-minute increments. When the system was at temperature and an experiment was underway data was collected every 5 minutes. A full start up and shut-down cycle could be anywhere from 8 to 24 hours long. 5 minutes is 0.3% of 24 hours or 1% of 8 hours. A LabView data acquisition system was considered but it was determined that it would be too "hands off" for the operator. A data acquisition thermocouple module was considered but not allowed because the thermocouples used in this study were grounded. Thermocouples measure millivolts which are a small change in voltage. All thermocouples would be touching the same ground which would interfere with the measurements taken. Therefore, all measurements were recorded manually. This allowed the operator to be mindful of what was happening inside the system and forced the operator to be more engaged with their surroundings.

SYSTEM SHUT DOWN PROCEDURE

To shut down the system F2 is set to 400°C and stepped down in temperature by 50°C increments every 10 minutes. Once F2 reaches 400°C, Pump1, R1, Furnace 1 (F1), are shut off. Pump 2 is kept running to cool the HEX until R1 reaches 370°C. Once R1 Reaches 370°C Pump 2 is shut off. Data may be recorded to plot the cooling characteristics of the system if desired.

PROCEDURE TO USE BRINE AS A COOLANT

Data for HEX2 is not recorded while data for brine running through the cooling jacket is recorded. There is not enough time available within the 5 minutes between data points to collect data for HEX2 and record the density, conductivity and collect samples. Pump 2 is pumping brine and water through the HEX1 shell. To run brine through the system the following procedure was followed:

Pump DI water through both the Hot Tube and the Cold Shell until both fluid circuits reach steady state. Open the brine feed tank (Tank2) valve then close the DI water feed tank (Tank1) valve. Both valves on the feed tans are never to be left closed at the same time. Measure conductivity at a minimum of every 15-minute increment, every 5 minutes is preferred. Run 3.5wt% NaCl Brine through the HEX shell for 60 minutes. Record 60 minutes of data at 1 point every 5 minutes. Switch back over to pumping DI water by opening the DI water feed line then closing the brine feed line. Run DI water through the system for 15 to 30 minutes, 12 minutes minimum or until the conductivity of the shell output line shows signs of dropping. Change brine in the brine tank from 3.5 wt% NaCl to 7.5 wt% NaCl, disconnecting the feed line over a large beaker, to collect the water. by emptying the tank, closing the valve. Run 7.5 wt% NaCl through the cooling jacket of HEX1 for 60 minutes. Change back to DI water after 60 minutes of data has been recorded by opening DI water feed valve first and closing the Brine feed line valve. Both valves are not to be closed at the same time. Allow the DI water to be pumped for 15 to 30 minutes or until the brine is diluted. Open brine valve first, then close the DI water feed line valve. Run 14 wt% NaCl Brine through the cooling jacket of HEX 1. Allow pump to run for about 15 minutes. Begin collecting data after the electrical conductivity

is showing signs of increasing. Collect 60 minutes of data. After 60 minutes of data is collected open the DI water valve and close the brine feed line valve. Pump DI water through the system util the electrical conductivity cannot go any lower. Follow system shut down procedure but allow Pump 2 to continuously run while the system cools down. This will keep washing out the brine and salt water that may remain inside the cooling shell.

THE PURPOSE OF FURNACE 1 and FURNACE 2

Furnace 1 (F1) is used as a pre-heater also known as a Feed Water Heater (FWH) which increases the temperature of the brine before it enters the reactor. The brine flows through the furnace tube which is held in F1. The exit temperature of F1 at normal operating conditions is around 230℃ to 250℃. The FWH in this application reduces the amount of thermal shock or thermal gradient that the reactor experiences. The FWH also reduces the amount of energy the reactor heater consumes. Furnace information can be found on the Furnace name plate shown in Figure 45.

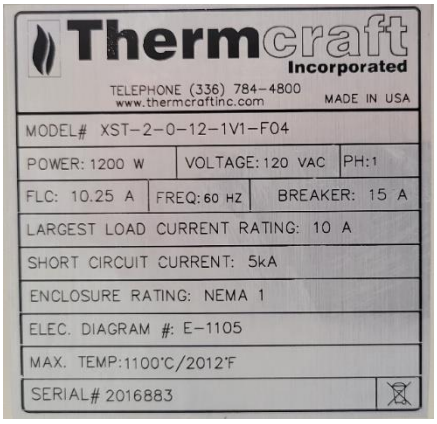

Figure 45: Furnace 1 and Furnace 2 Name plate data

Both F1 and F2 are a Thermcraft Inc. XST-2-0-12-1V1-F04 Portege Tube Furnace with smart control. These furnaces both run off single phase 120 VAC power and produce 1200W of heat. The max load rating is 10 Amps. Furnace 2 as added to the system for the purpose of controlling the temperature of the reactor outlet temperature for data collection. The researchers needed to control the HEX inlet temperature so the following HEX temperatures could be measured. This method allowed for a heat

exchanger performance curve to be generated. Once the data has been collected and the performance metrics of the heat exchangers are understood the furnace can be removed from actual practice. Adding a furnace after the reactor in the process is thermally counterproductive and wasteful in commercial applications. The reactor is capable of higher operational temperatures but was not pushed to high levels for safety reasons, therefore a furnace was added to find thermophysical properties at the maximum operational ranges of the HEXs. Furnace 2 will not be necessary in practice in a production scale system that would be used to treat water in real world applications.

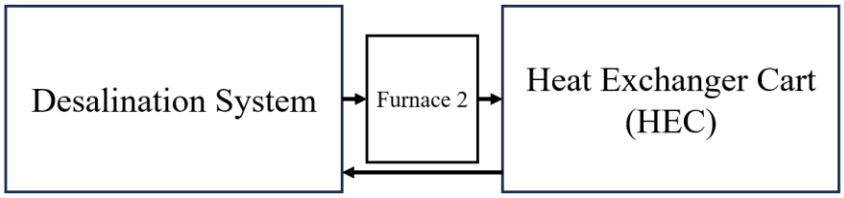


Figure 46: Furnace 2 Location

The exit temperature of the reactor is near the critical temperature of water. Near the critical point of water, the enthalpy needs to be increased substantially to raise the temperature of the fluid by 1 degree. Near the critical point of $H_2O$ the specific heat spikes from about 7.7 kJ/kg·K to about 400 kJ/kg·K. The increase in specific heat means more energy is required to increase the temperature of the fluid by 1 degree, therefore a furnace needed to be added to test the HEXs in this study. The treated supercritical water flows out of the 10mL/min desalination system into Furnace 2 where the temperature is increased to the desired HEX inlet temperature. The fluid then flows into the HEX on the HEC. Once the hot fluid is cooled down the fluid flows back to the condenser and gas separator that is mounted to the desalination system.

FURNACE 1 HEAT ABSORBTION TUBE

The furnace tube in F1 is a thick walled 316 SS 20 in long tube that has added aluminum heat sinks. The aluminum heat sinks help increase the effectiveness of the furnace tube in absorbing heat thus transferring the heat to the water flowing through it. The water temperature will rise, and the fluid enthalpy will increase with temperature. The added enthalpy from the furnace will enter the reactor thus adding heat to the reactor which will reduce the energy the reactor heater needs to add to the reactor to heat the fluid.

Figure 47 shows viable aluminum heat sink patterns that can aid in improving the furnace tube's effectiveness.

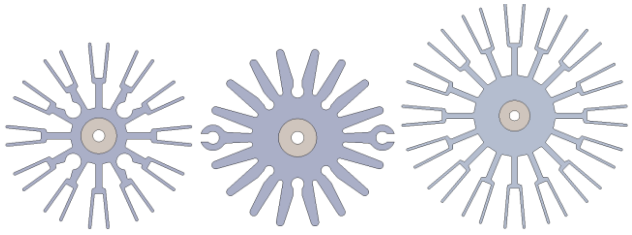

Figure 47: Viable heat sinks cross sections for Furnace 1

Furnace 2 (F2) also serves as a preheater for the HEC like F1 does for the reactor, but its main purpose is to control the temperature so the researchers can characterize the thermophysical properties of the fluid flowing through HEX1 and HEX2. The furnace temperature is used to control T1 at the hot line entrance point. The rest of the heat exchangers' performance is determined by its geometry and the properties of the insulation.

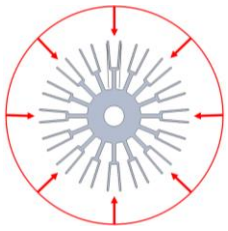

Figure 48: Illustrating the Radiation received from all sides of the heat sink inside the furnace.

Heat was also transferred to the FWH tube by conduction and convection. The fluid surrounding the tube inside of the furnace was hot air. An individual heat sink and stack of heat sinks on the thick-walled FWH tube is shown in Figure 49.

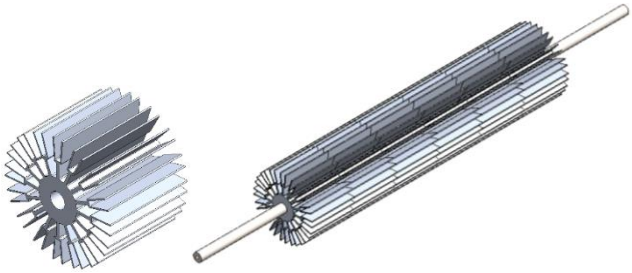

Figure 49: Furnace tube with Installed heat sinks.

The heat sink geometry improvements are shown in Table 7. Thermal paste was added to the furnace tube prior to installing the heat sinks. The thermal past is intended to increase the surface contact between the heat sinks and the 316 stainless steel tubing.

Table 7: Heat Sink Data

| Furnace Tube Heat Sink Comparison | | |
|---|---|---|
| Length | 2 | in |
| Tube OD | 0.375 | in |
| Circumference | 1.18 | in |
| Surface Area Per Length | 2.36 | $in^2$ |
| Total Surface Area of Heat Sink | 103.72 | $in^2$ |
| Hole in Center | 2.36 | $in^2$ |
| Ends | 3.22 | $in^2$ |
| Effective Area of Heat Sink | 98.14 | $in^2$ |
| Tubing equivalent length | 83.31 | in |
| % increase | 42 | % |

By adding a heat sink to the furnace tube for the pre-heater, also known as the FWH, the surface area is increased by 42% per 2 inches of tubing with added heat sink.

## FURNACE COIL CONSTRUCTION FOR FURNACE2

The furnace coil is only intended for F2. The furnace tube or coil was produced by wrapping a 1/8" OD, 0.055" ID, 316 stainless steel tube around the stainless-steel pipe shown in Figure 50. The pipe has an approximately ¼" by 1" notch cut in the end.

Figure 50: 1-inch stainless steel pipe

The tubing was placed against the floor and rolled around the stainless steel pipe. Fittings were added to allow the furnace tube to be attached to the rest of the system. The furnace coils shown in Figure 51 each have 65 turns per foot.

Figure 51: Furnace coil (top), Used furnace tube coil with fittings (Bottom)

Each coil is 12” long and fits in the furnace’s heat effected zone as shown in Figure 52. The ends of the furnace are thermally insulated by the rockwool insulation to maximize the internal temperature of the furnace and reduce heat loss to the ambient environment.

Figure 52: Furnace coil installed in Furnace 2

The inner diameter of the furnace coil is approximately 1.314”, which is the diameter of the pipe used as a core form. The length of the coil is determined by the diameter multiplied by π multiplied by the number of coils. Solving the equation for L yields 22.4 ft of tubing is needed at minimum to create the coiled section of this tubing run for the furnace. Additional tubing is needed on each side for connection. A length of approximately 25 ft was used for the coils shown, which is convenient in size because 1/8” tubing coils are sold in lengths of 50 ft. Purchasing one 50 ft coil is ideal for producing 2 coils.

$$L = \pi dn = \pi \times 1.314" \times 65 = 268.32in/12 = 22.4ft$$

25 ft of tubing will allow the fluid to spend more time in the furnace while the pump is running allowing the fluid to pick up more heat. The CAD model shown in Figure 53 was formulated by modeling the inside of the furnace and calculating how many turns the helix would need to evenly space the 1/8” tubing sections. The distance between each coil from edge to edge is a gap of approximately 0.06”.

Figure 53: SolidWorks model of the Furnace 2 Coil

The purpose of using small diameter tubing is to increase the length of the coil which increases the length of time the fluid spends in the furnace which increases how much heat the fluid absorbs while it is in the furnace. Figure 54 shows the furnace mounted between the HEX cart and the reactor (R1). The chiller is not shown attached to the system because it is no longer needed.

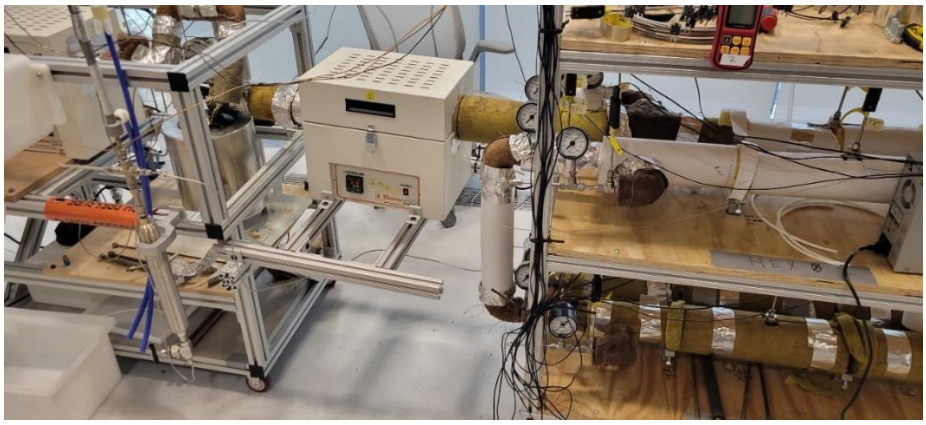

Figure 54: Furnace 2 between the desalination system (Left) and the Heat Exchanger Cart (HEC) (Right).

The furnace is supported by extruded aluminum framing that is mounted to the upright supports on the desalination system. Another experiment could be done with the coil added to Furnace1 for the FWH, which could lower the furnace's operating temperature yielding the same designed exit temperature.

DIGITAL SCALE AND STIRRER

A Mettler Toledo ME4002E precision scale was used to measure the materials for producing the brine used in this study is shown in Figure 55.


Figure 55: Mettler Toledo Scale ME4002E

To produce a brine of 3.5wt% NaCl for experimentation a beaker was placed on the scale then the scale was "Tared", such that the scale reads 0.00g. To create a brine solution that is 3.5wt% NaCl of an

approximately 2000 mL solution 75 grams of NaCl was then poured into the beaker until the scale reads 75.00g. Once the scale reads 75g, water was added until the scale reads 2000 grams. The scale is not "Tared" between measuring out the salt and the water.

The brine mixtures are listed in Table 8. The Brine recipe table shows the grams of NaCl needed to create a brine solution of the corresponding wt%. The density of each solution was measured for reference. The "# of boats of 75g" column shows the number of weigh boats needed to create the corresponding brine of the corresponding wt%.

Table 8: Brine Recipe Table

| wt% NaCl | g/1L | g/2L | # of boats of 75 g/ea. | Density (g/ml) |
|---|---|---|---|---|
| 3.50% | 35 | 70 | 1 | 1.023 |
| 7.50% | 75 | 150 | 2 | 1.05193 |
| 14% | 140 | 280 | 4 | 1.10064 |
| | 250 | 500 | 7 | TOTALS |

The Mettler Toledo digital balance is advertised as having a readability of 0.01g and 0.007g of repeatability. This scale is more than precise enough for the experiments taking place. The brine was mixed using a Corning PC-535 Stirrer shown in Figure 56.


Figure 56: Corning PC-535 Stirrer alone (Left), Stirrer mixing 14wt% NaCl Brine (Right)

The water was mixed at room temperature, and not heated using a hot plate. The NaCl brines were mixed in ~2-liter batches and were pumped through the shell section of the HEX1 using Pump2. Figure 57 shows the finished 2L brine batches for use as a cooling fluid.

Figure 57: Finished mixed brine of 14wt%, 7.5wt% and 3.5wt% NaCl.

DESALINATION SYSTEM

Figure 58 shows the 10ml/min and the 100 ml/min (The 10X System) for a size comparison. The larger 10X system is equipped with 2 reactors and a larger pre-heating furnace. Future work will involve testing the 10X system with the furnace to compare system performance with system operation with a HEX replacing the furnace.

Figure 58: 10 ml/min Cart (Left), 10X 100 ml/min Desalination System (Right)

BACK PRESSURE REGULATOR

Two back pressure regulators, BPR 1 and BPR2 are shown in Figure 59. BPR1 is used to set the pressure of the desalination system. BPR2 was added to the HEC to set the pressure to set the pressure of the cooling jacket of the heat exchanger undergoing testing. The thermocouple shown in the right image of Figure 59 is used to measure the temperature of the fluid before it flows out of BPR 2 into the cooling line discharge tank. The pressure of both back pressure regulators is set by the same regulator to them both at the same pressure. BPR1 has a PEEK plastic diaphragm. BPR2 on the HEC was outfitted with a stainless-steel diaphragm as a precautionary measure to remove the possibility of melting the plastic PEEK diaphragm. PEEK melts at 343°C (649.4°F). The exit temperature of either HEX cooling line can reach as high as 370°C (698°F), which is enough to melt and weaken the diaphragm enough to cause problems. The 316 Stainless Steel that the high temperature diaphragm is made from melts between 1375°C to 1400°C (2507°F - 2552°F) which is well above the fluid exiting the HEX up for testing, therefore this is a safe acceptable option.

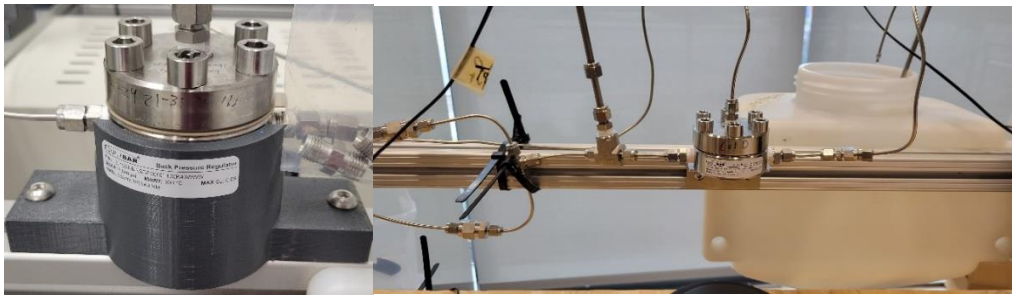

Figure 59: BPR1, located on the desalination cart (Left); BPR2 and Thermocouple, located on the HEC (right)

PUMPS

There are 2 types of pumps found in the supercritical fluid research lab. The pump used during the experiments were ELDEX 2SMP high pressure linear displacement piston pumps, as shown in Figure 60.

Figure 60: HEX cooling jacket pump, Pump CAD model, desalination system pumps

One pump was used for pumping water through the HEX cooling jacket, and another separate pump was used to pump water through the desalination system, both are the same model. There are 2 pumps used for experimentation and HEX characterization but in practice only 1 pump is needed on a SCWD system equipped with a heat recovery system. The ELDEX pump pistons are made of sapphire and seals with black Teflon as shown in Figure 61.

Figure 61: ELDEX sapphire piston (Left) and piston seal (Right)

Figure 62 shows the 10X SCWD system linear displacement diaphragm pump mounted to a cart with attached water and brine tanks.

Figure 62: 10X SCWD system linear displacement pump

The brine and water tanks can be toggled on or off depending on the needs of the system or operator. Milton Roy Model: PK16N610NSSSNNN was mounted to a fabricated cart as shown in Figure 62. The pump weighs approximately 600 lbs. which is why it is on casters with brakes, so it can be easily moved around the lab for maintenance.

## HEAT EXCHANGER CART (HEC) DESIGN

The HEXs are supported by a cart during operation. The heat exchangers need to be held in space horizontally because the density of the working fluid changes drastically as it cools down or heats up. The HEXs are held horizontally on a cart constructed out of extruded aluminum rail and are supported by 4 wheels on casters with locking brakes as shown in Figure 63.

Figure 63: HEC, with Pump 2, Furnace 2 and thermocouple measuring station.

Each shelf is made from plywood. The heat exchanger is connected to the plywood with 4 aluminum clamps per heat exchanger. The clamps when fully closed cannot clamp on to the ¾” shell tube

of the HEX, so a ¾" ID with a 1.5" OD 316 Stainless Steel shaft collar was added to increase the diameter so the clamps could be used. The clamps were radially available in the laboratory as standard equipment for the supercritical desalination systems produced. A custom clamp can be designed later to reduce heat loss from contacting the heat exchanger as the designer sees fit. The thermocouple cables were all attached to the top aluminum bar with reusable zip ties so the cables can be changed out when the pins wear out. The tanks holding the brine and water were mounted to the top rail and the lines were gravity fed into Pump 2 for the HEX cooling shell. The heat exchanger was insulated using rockwool insulation. Fiber glass insulation may be used for this application, but it needs to be rated for temperatures greater than 450°C to 500°C. Traditional residential grade insulation is not recommended for this application. The collection tank for the cooling water is also located on the cart as well as the back pressure regulator. The operator was able to stay within proximity of the system safely though out the experimentation and data gathering portion of this work.

## HEAT EXCHANGER DESIGN

The HEXs designed for this work are both counterflow heat exchangers. Figure 64 shows a standard image of a counterflow heat exchanger and its flow paths. A counterflow heat exchanger is the opposite of a parallel flow heat exchanger, where both fluids flow in the same direction. Higher efficiencies can be achieved with a counterflow heat exchanger [4], [33], [43].

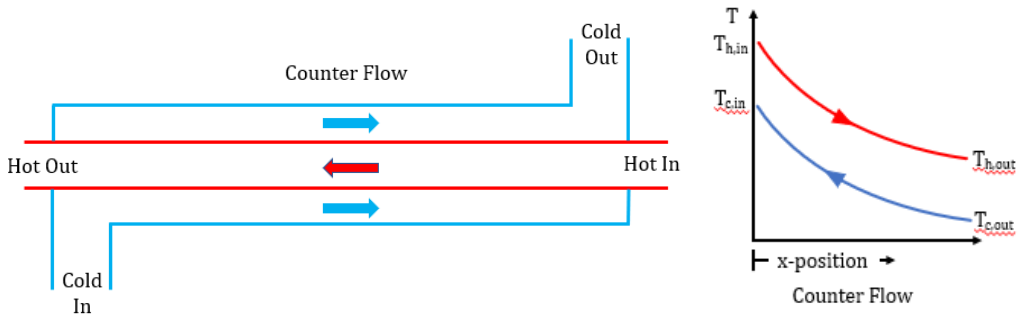


Figure 64: Counterflow Heat Exchanger (HEX)

Each heat exchanger is comprised of thick wall 316 stainless steel tubing and metallic compression fittings. 3/8” OD tubing is used for the hot center tube and ¾” OD tubing is used for the shell or cooling jacket; these terms are used interchangeably. The insulation shown in Figure 65 wrapped around HEX2 is a fiberglass tube wrapped in a white insulating, internally reflective material.

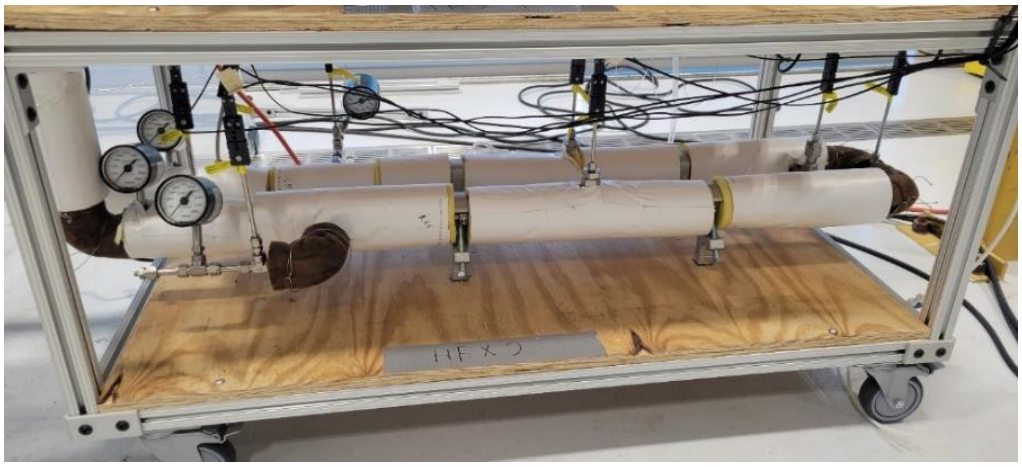

Figure 65: HEX2 wrapped in Fiberglass insulation.

The insulation is received with a longitudinally cut to allow the user to wrap it around a pipe as shown in Figure 66. The white material overlaps the longitudinal cut and is adhered to the other side of the cut to hold the insulation on the pipe insulated.

Figure 66: c

There is also a reflective surface on the inside of the white material that is intended to reflect radiating heat back at the pipe. The adhesive is protected with a paper strip that must be removed before the insulation is sealed. During operation the white surface was warm to the touch when system reached

steady state. The fiberglass changed to a brown color when it was heated. There was no visible smoke or burning. The rockwool and fiberglass insulation methods were the most convenient to install.

## OTHER HEX INSULATION METHODS CONSIDERED

A heat exchanger that experiences temperatures that are vastly different than the surrounding room temperature needs to be insulated to boost efficiency and reduce heat loss to the surrounding environment.

Castable ceramics, rockwool, fiberglass insulation as well as a vacuum evacuated shell were considered for the heat exchanger in this work. Rockwool offered the highest R-value for ease of installation and cost effectiveness. Vacuum fittings and vacuum system assembly methods can be applied to reduce heat loss to the surrounding environment thus increasing the effectiveness of the HEX [44], [45]. Figure 67 shows a cross section of what a vacuum insulated heat exchanger would look like. The 2$^{nd}$ shell would be evacuated of air to reduce loss to the surrounding environment.

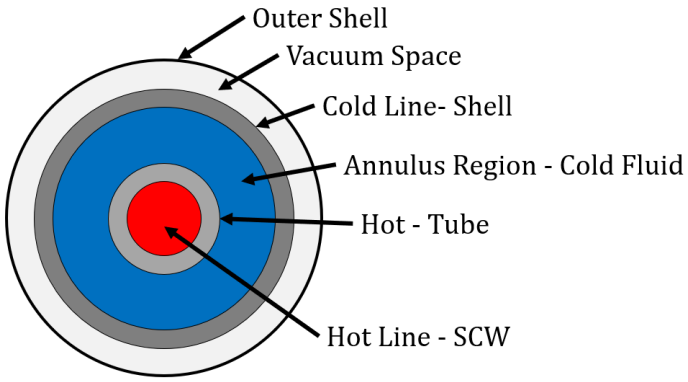


Figure 67: Vacuum insulated double pipe HEX cross section concept

## HEX1 AND HEX2 GEOMETRIC COMPARISON

Table 9 shows the different specifications of HEX1 and HEX2. HEX1 is shorter than HEX2 by 0.2 meters. HEX1 has a smaller cooling shell volume space that could be filled with water. Both HEX1 and HEX2 use the same center tube for the hot line. HEX2 has a thicker shell wall, this is why it was used to test the brine, to preserve the structural integrity of the shell that is expected to occur due to corrosion.

Table 9: HEX1 and HEX2 Geometry and Characteristic Comparison Table

| Metric | Unit | HEX1 | | HEX2 | |
|---|---|---|---|---|---|
| | | HOT | COLD | HOT | COLD |
| MaxPro Part | # | 21TU6M-316 | 21TU12M-316 | 21TU6M-316 | 15TU12M-316 |
| OD | in | 0.375 | 0.75 | 0.375 | 0.75 |
| OD | m | 0.009525 | 0.01905 | 0.009525 | 0.01905 |
| Wall Thickness | m | 0.0021 | 0.0040 | 0.0021 | 0.0030 |
| ID | m | 0.0053 | 0.0111 | 0.0053 | 0.0131 |
| | | Center Tube | Annulus Region | Center Tube | Annulus Region |
| Ratio $D_i/D_o$ | # | 0.56 | 1.17 | 0.56 | 1.38 |
| Flow Areas | $m^2$ | 2.21E-05 | 7.51E-05 | 2.21E-05 | 1.13E-04 |
| | $cm^2$ | 0.22 | 0.75 | 0.22 | 1.13 |
| Hydraulic Diameter | m | 53.086 | 0.0016 | 53.086 | 0.0036 |
| | cm | 0.53086 | 0.0000160 | 0.53086 | 0.00003581 |
| Flow Area Ratio | # | 3.39 | | 5.10 | |
| Length | m | 1.397 | | 1.600 | |
| Aspect Ratios | L/D | 147 | N/A | 168 | N/A |
| | D/L | 0.00682 | N/A | 0.00595 | N/A |
| Heat Transfer Area ($A_o$) | $m^2$ | 0.041803 | N/A | 0.047884 | N/A |
| Hot Tube Inner Surface Area ($A_i$) | $m^2$ | 0.0233 | N/A | 0.0267 | N/A |
| Flow Velocity | cm/sec | 0.75301 | 0.22200 | 0.75301 | 0.14778 |

Table 9 shows the thermal conductivity constant and thermal resistance of the hot tube for both HEX1 and HEX2. The thermal resistance of the stainless-steel changes with temperature changes [4]. As the temperature of the stainless-steel increases, the thermal resistance decreases [4]. Thermal resistance is a function of area, both heat exchangers have different heat transfer areas therefor the thermal resistance is different from HEX1 to HEX2. The thermal resistance equation for a tube is shown as

$$R_{wall} = \frac{\ln\left(\frac{D_o}{D_i}\right)}{2\pi kL}$$

Where $D_o$ is the outer diameter of the tube, $D_i$ is the inner diameter of the tube, $k$ is the thermal conductivity of the tube material, and $L$ is the wall thickness [4], [33]. The total thermal resistance of the tube in a heat exchanger is shown as

$$R_T = R_i + R_{wall} + R_o = \frac{1}{h_i A_i} + \frac{\ln\left(\frac{D_o}{D_i}\right)}{2\pi kL} + \frac{1}{h_o A_o}$$

Where $R_i$ is the thermal resistance of the fluid inside the tube, or the hot fluid, and $R_o$ is the thermal resistance of the fluid surrounding the tube, in the case of the HEX discussed in this work, this is the cooling fluid. The fluid thermal resistances can be calculated if the convective heat transfer coefficient and surface areas are known [4], [33].

Table 10: Thermal Conductivity and Thermal Resistance of HEX1 and HEX2

| Thermal Resistance of Hot Line at Corresponding Temperature for HEX1 and HEX2 | | | |
|---|---|---|---|
| 316SS k (W/m·K) | at temp (°C) | RwallHex1 | RwallHex2 |
| 13.4 | 27 | 0.00497 | 0.00434 |
| 15.2 | 127 | 0.00438 | 0.00383 |
| 18.3 | 327 | 0.00364 | 0.00318 |
| 19.8 | 427 | 0.00336 | 0.00294 |
| Average Thermal Conductivity of 316SS | | Average Rwall | |
| kW/m·K | 0.01601 | 0.00416 | 0.00363 |
| W/m·K | 16.01 | 4.16110 | 3.63270 |

The graph shown in Figure 68 compares the thermal conductivity value as a function of temperature. Titanium is more thermally stable than stainless steel across the same temperature range. Titanium is a more favored material for this application due to its corrosion resistance properties and its ability to remain thermally stable. The problem with using titanium would be the upfront cost.

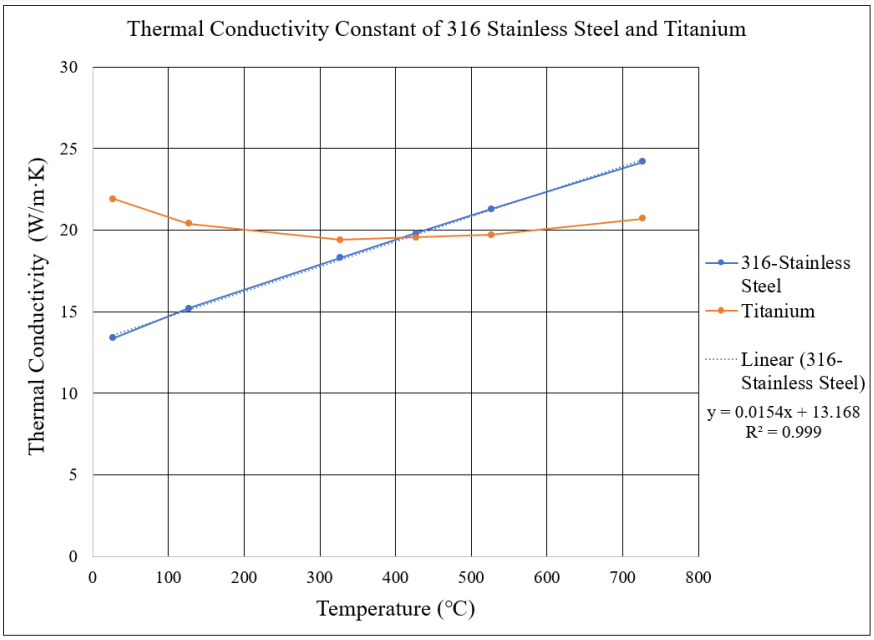


Figure 68: Thermal conductivity of 316 Stainless Steel compared to Titanium.

The thermal conductivity of stainless steel was averaged over the corresponding temperature range yielding a value of 16 W/m·K. To find $h_o$ and $h_i$ the following equation was used.

$$h_{o,i} = \frac{Q(h_1, h_2, \dot{m})}{A_{o,i}\,(T_1 - T_2)}$$

Where Q as a function of changer in enthalpy multiplied by the mass flow rate divided by the product of surface Area of the outer diameter of the hot line and the difference between the hot entrance temperatures $T_1$ and the exit temperature $T_2$. This equation yields the thermal conductivity of the inner fluid as $h_i$ and the outer fluid as $h_o$.

TWISTED TAPE DESIGN FEATURE

Design features such as a wrapped wire, dual wrapped wire and a twisted tape can be applied to the inside bore and annulus region to aid in mixing. The Reynolds numbers found were low, in the 0 to 20 range and showed the flow to be extremely laminar. Turbulent flow is known to increase mixing which is known to increase heat transfer within heat exchangers [46], [47]. If the value of transferred heat is increased a small amount these design features can be useful if the process is running continuously over a long period of time. If the short-term gains are small, they will add up over time. A rupture disk will be added to the design to prevent any damage to the HEX if the pressure spikes to an unsafe level. A rupture disk can also control the venting of excess pressure like a blow off valve should something go wrong. The tubing considered is rated for 103.4 MPa, 1034 Bar, (15,000 psi).

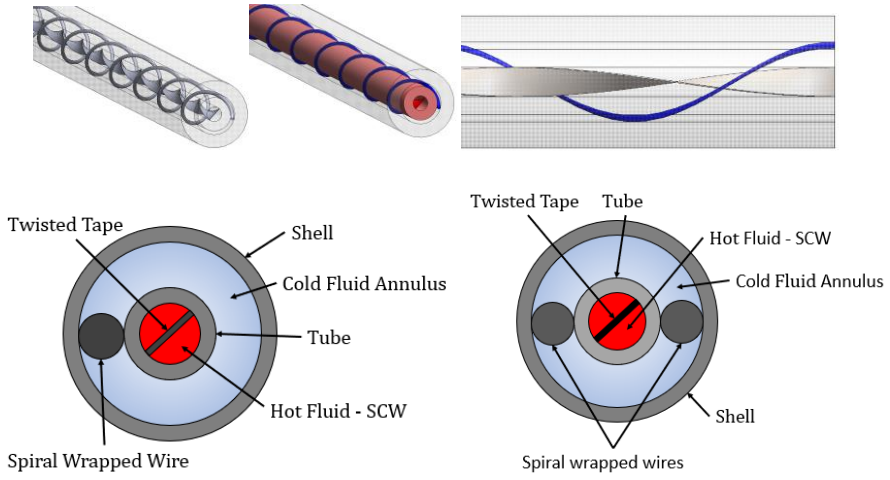


Figure 69: Twisted tape and spiral wrapped wire illustration and cross section views

A custom heat exchanger that was designed for a SWD-ZLD system is presented in, Van Wyk [15]. A wrapped helical wire was added to the heat exchanger to prevent the inner tube from contacting the outer tube. [15], [37]. The twisted wire was added to prevent the center tube from contacting the outer shell tube because the gap was small and close to the thickness of the wire. The twisted wire that was added may have increased mixing and turbulence within the fluid causing a slight increase in the heat transfer coefficient. Recommended materials for tubing and fittings include high corrosion resistance such as 316 Stainless Steel, Titanium, Hastelloy C276, Inconel, Monel, or 254 SMO, another grade of highly corrosion resistant stainless steel.

## FLOW MEASUREMENT

The flow rate is shown on a digital display on both Pumps 1 and 2. The flow rate was periodically checked using a small beaker and a timer. The researcher would place the beaker under the outflow line and catch the water dripping before it entered the product output tank. The timer would begin when the first droplet contacted the bottom of the beaker. Once the A flow meter was purchased but later found to be unnecessary.

## TEMPERATURE MEASUREMENT

All temperatures measured in this study were captured using J-type thermocouples. The thermocouples used to measure the fluid temperature inside the HEX's were ¼" diameter stainless steel probes. The thermocouples used to measure the fluid temperature at different points in the process were 1/8" diameter. The thermocouple cable was shielded with a fiberglass wrap if it contacted a hot surface. The 1/8" diameter thermocouple shown in the left of Figure 70 was used to measure the reactor exit temperature before the fluid entered Furnace 2. All thermocouples used were equipped with a stainless-steel sleeve to protect the weld at the tip where the 2 different metallic wires met.

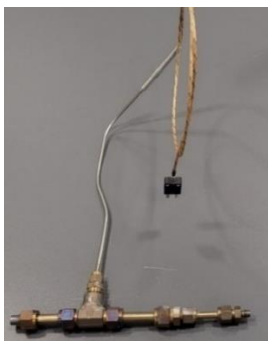


Figure 70: 1/8” X 12” Thermocouple that was used to measure the Reactor exit temperature (Left); ¼” Diameter 6” long Thermocouple with metallic compression fitting (Right)

Figure 70 shows a thermocouple that was removed from a heat exchanger after the experiments were conducted. The ¼” and 1/8” diameter thermocouples were held in the path of the fluid flow within the heat exchanger by metallic compression fittings. The thermocouple cables used were purchased at a specific length such as 10 or 15 feet. For custom systems a custom length thermocouple can be made. Custom length thermocouple wires were not used in this study to save fabrication time. The thermocouple meter shown in Figure 71.

Figure 71: Prostor Thermocouple Meter

The Prostor meter used in this work withstood approximately 120,000 insertion cycles and could read accurate temperature measurements after these points were taken.

CONDENSER

The condenser used in the desalination system is shown in Figure 72. This condenser is a COTS part purchased from a company that specializes in high pressure systems. The condenser is constructed of titanium tubing and machined parts. The design is essentially a tube in shell HEX. The tube ends are metallic compression fittings and the two holes shown in Figure 72 are a 1/16” Pipe thread. The center tube is where the desalination systems working fluid is condensed and the outer shell is where the 50/50 ethylene glycol

coolant mix flows. The condenser coolant can be set up for parallel flow or counterflow. Previous experimentation showed there is little effect of the coolant flow direction on the produced product.

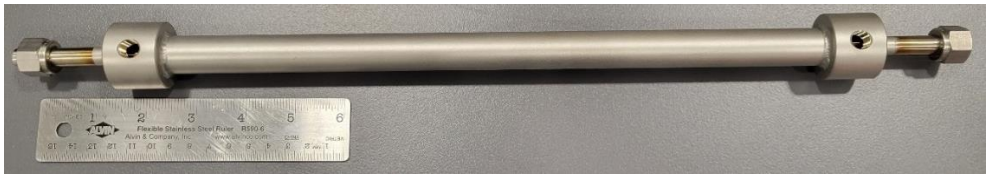

Figure 72: Titanium Condenser

GAS SEPERATOR

The gas separator is a mechanical component that is intended to fill up with water to a level and prevent the nitrogen from flowing out of the system. The gas separator and condenser combination are necessary for the “gas loop” to work. The gas separator could also be called the expansion chamber. By increasing the volume, the gas fills the temperature could decrease by a small amount thus increasing the effectiveness of the assembly that is built for cooling off the fluid exiting the reactor in preparation for collection. The tank used as a gas separator is a Swagelok 316L-50DF4-300, double ended DOT- Compliant Sample Cylinder rate for 5000 psi (344 Bar), this item is shown in Figure 73.

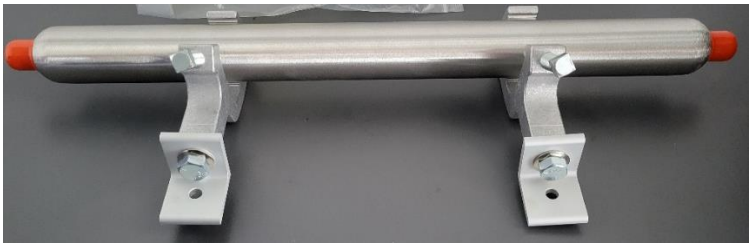

Figure 73: New unused Gas Separator

The gas separator tank was held in place by an aluminum clamp like the clamps shown in Figure 73.

CONDENSER GAS SEPERATOR ASSEMBLY

The condenser and the gas separator are both attached to a “CROSS” or a 4 female port fitting. The fluid exiting the reactor enters the condenser-gas-separator assembly in the middle, where the reactor exit temperature/condenser entrance temperature is measured. Theoretically the reactor exit temperature is higher than the condenser exit temperature, but it can be assumed these temperatures are the same because they are so close in value and proximity. The fluid then travels into the condenser because it is hot because

hot vapors rise. The heat is then removed from the fluid causing it to condense to the inside wall of the center condenser tube. The water droplets then fall to the bottom of the gas separator and then the fluid level rises. The liquid water that accumulates in the bottom acts as a “seal” and prevents the nitrogen from exiting the Back Pressure Regulator flowing into the collection tank at the end of the process as produced water. The valve (V3) at the bottom of the gas separator can be used to regulate the water level inside the gas separator. If the water level gets too low, there will not be enough water to block the nitrogen from exiting the system. The system pressure will push the little amount water that is remaining in the gas separator out of the system causing a pressure drop. If the pressure drops too fast the gas loop is broken and an equivalent amount of nitrogen that was lost needs to be put back into the system. The gas separator assembly shown in Figure 74 does not show the rest of the desalination system or any tubing.

Figure 74: SolidWorks Condenser gas separator assembly (Left) and picture of thermocouple inside (Right)

The clamp holding the gas separator mounts the assembly to the desalination system frame. Valve 3 (V3) is located at the bottom of the gas separator. The A2001HC Reflux/Take-off condenser is modified from original specifications to create what is shown in Figure 74. The 1492HC Helix insert was installed in the condenser center tube during experimentation.

SUPERCRITICAL WATER REACTOR

The reactor is produced by a company that specializes in producing high pressure processing equipment. The reactor is constructed of a thick-walled stainless-steel cylinder, with a flange and a seal at the top side. The reactor is where the action of desalination takes place. The reactor is encased in a heavily insulated heater that is connected to a temperature controller. During startup the first large system element that the nitrogen passes through is the reactor. The first Furnace (F1) out flow line runs over the top of the pressure gauge and into one of the inlet ports atop the reactor as shown in Figure 75. The reactor also contains a thermal well. A thermal well is a tube that a thermocouple rests in while it is recording measurements. The purpose of a thermal well is to allow the operators to change the thermocouple during processing, so the system does not need to be depressurized then emptied just to replace the thermocouple. It saves down time during routine maintenance.

Figure 75: The Reactor (R1) *in situ* (Left), Reactor in vise for routine maintenance (Right)

The reactor also has a rupture-disk module attached to the top of the entry ports which flows into a discharge tank that is on the lower shelf of the cart below the reactor. Figure 76 shows 2 other reactors before installation into a larger system. The Reactor Top that is on the table has an exposed dip tube and an exposed thermal well.

Figure 76: Reactors and accompanying components

The reactor controller is shown in Figure 76. The red thermocouple meter was placed here for early experiments and was used to monitor the temperature of the fluid entering the condenser which is the same as the temperature of the fluid exiting the reactor.

Figure 77: Reactor Controller

The reactor controller acts like a thermostat and adds heat as needed to maintain a set point. This thermal cycling action causes the measured temperatures to oscillate up and down during data collection.

HEX COOLING JACKET RETURN LINE ICE BATH

Figure 78 shows the cooling jacket return line ice bath coil. The coil shown in Figure 78 is submerged in an ice bath to cool the fluid before it flows into the collection tank. Figure 78 also shows the in-floor drain grate that surrounds the working area of the ECU LSBB High Bay. Another reason for cooling the water down was so that the density meter could accurately measure the density of the output fluid. The density meter is equipped with an internal thermocouple that measures the fluid sample temperature. Its temperature resolution is 0.1°C, the temperature accuracy is +/- 0.2°C. Figure 78 shows the lab ice machine where the ice for the ice bath was sourced.


Figure 78: Ice Bath Cooling Coil (Left), Ice Bath (Center), Ice machine (Right)

The ice bath cooling coil is produced with 1/8” OD, 0.059” ID 316 SS high pressure tubing. The coil has a 4-inch ID, ~20 revolutions and is about 1 ft long. A close up of the cooling coil is shown in Figure 79.

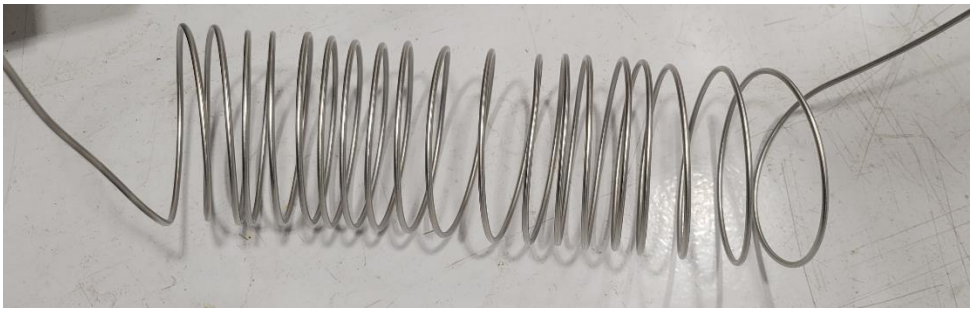

Figure 79: Closer view of the cooling coil.

The cooling coil tube was 26 feet long. The coil began at the midpoint and was offset from the tube length midpoint within 2 feet.

## DATA ANALYSIS METHODS

The data was collected in a spreadsheet and was manually recorded from measurements taken with various types of equipment. The data was later analyzed, and graphs were created. These graphs and analysis are discussed in the Results chapter of this work. Some data that was recorded was removed due to errors found with the equipment. Two of the thermocouples were found to be mounted to close to the hot line within the cooling jacket of the heat exchanger.

# CHAPTER 3 RESULTS

## INTRODUCTION

This chapter will present data and analysis of the data collected during experimentation. These experiments characterized the two fabricated heat exchangers under similar conditions and developed thermophysical properties useful for the design of heat exchangers under supercritical conditions. These properties are either scarce or missing in the scientific literature for supercritical fluids in heat exchanger systems. The purpose of these experiments was to characterize both heat exchangers under conditions that are similar enough to determine how the different geometry effects the heat exchanger performance. The hot lines of the heat exchangers were networked in series, the exit line of the cooling jacket of the HEX being experimented on was ran through a cooling coil. The cooling jacket of the second heat exchanger was not filled with water, only air. The purpose of separating the cooling jackets was to isolate each heat exchanger from the effects of the other heat exchanger to characterize them both individually. This separation also protected the isolated HEX in case anything went wrong during experimentation. HEX1 was tested separately with salt to keep HEX2 clean and ready for testing in the large 10X desalination system which functions at a flow rate of 100 mL/min. It is determined that the heat exchangers can be networked based on the temperatures shown by the results. For example, the temperature of the fluid exiting Furnace 1 or the fluid entering the Reactor of the desalination system is approximately 250℃. The temperature of the cooling jacket exit line of HEX1 under operating conditions is approximately 350℃, therefore HEX1 can be used in place of the Furnace, thus saving energy.

## EXPERIMENTAL RESULTS

Each heat exchanger experienced a range of pressures and temperatures, and brine concentrations as shown in Table 11. Both HEXs were tested at 225, 230 and 240 Bar over a range of temperatures from

380°C to 420°C in increments of 10°. HEX1 was operating at a pressure of 230 Bar and 410°C with brine as a cooling fluid after data for all the other pressure temperature combinations was collected.

Table 11: Experiment Run List

| Line # | HEX (1 or 2) | Pressure (Bar) | Hot Line Inlet Temperature (°C)* | Furnace 2 Temperature Set Point (°C) | Salinity of Fluid in HEX Shell (%wt NaCl) |
|---|---|---|---|---|---|
| 1 | HEX1 | 225 | 380 | 502 | 0 |
| 2 | | | 390 | 584 | |
| 3 | | | 400 | 598-600 | |
| 4 | | | 410 | 606-609 | |
| 5 | | | 420 | 621 | |
| 6 | | 230 | 380 | 475 | 0 |
| 7 | | | 390 | 587 | |
| 8 | | | 400 | 610-615 | |
| 9 | | | 410 | 628-630 | |
| 10 | | | 420 | 655-660 | |
| 11 | | 240 | 380 | 445 | 0 |
| 12 | | | 390 | 520 | |
| 13 | | | 400 | 555 | |
| 14 | | | 410 | 565 | |
| 15 | | | 420 | 570 | |
| 16 | HEX2 | 225 | 380 | 445 | 0 |
| 17 | | | 390 | 603 | |
| 18 | | | 400 | 515 | |
| 19 | | | 410 | 556 | |
| 20 | | | 420 | 570 | |
| 21 | | 230 | 380 | 445 | 0 |
| 22 | | | 390 | 603 | |
| 23 | | 240 | 380 | 440 | 0 |
| 24 | | | 390 | 530 | |
| 25 | | | 400 | 490 | |
| 26 | | | 410 | 517 | |
| 27 | | | 420 | 546 | |
| 28 | HEX 1 | 230 | 410 | 485-495 | 3.5%wt |
| 29 | | | 410 | 485-495 | 7.5%wt |
| 30 | | | 410 | 485-495 | 14%wt |

* Hot Line Inlet Temperature is also defined as T1

The system will begin at ambient temperature, the heat sources will be turned on, the system will heat up, settle at a steady state temperature, and then be allowed to cool down passively by removing the heat added to the system. The data collected during experimentation is expected to have the form shown in Figure 80.

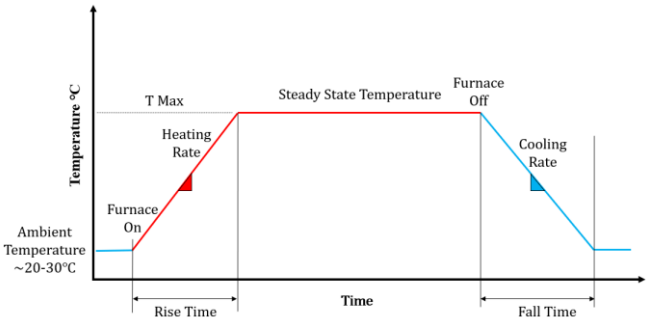


Figure 80: Expected geometry of data collected.

FURNACE VALIDATION STUDY

Furnace 2 with the added furnace coil was tested prior to gathering experimental data. Figure 81 shows how the equipment was set up for this study. Both pumps were pumping DI water. No brine was used to characterize the F2 Coil.

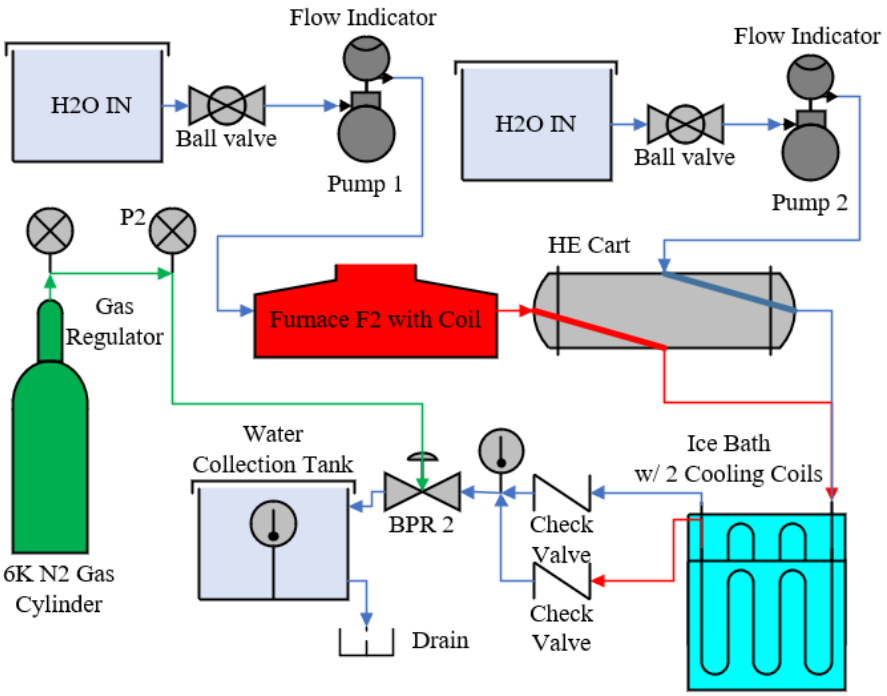


Figure 81: Furnace Coil Validation system setup.

The objective of this validation study was to test to make sure that the furnace coil can reach a measured T1 temperature of 450°C and sustain a steady state for approximately 20 minutes without sustaining any damage to the coil. The purpose of the F2 Coil was to lower the F2 set point. This increases system safety and reduces energy consumption. This test was a success. The F2 coil was used for all experiments expressed in this paper. The F2 coil was changed 1 time to a coil that was produced the exact same way as the first. The timeline of events for the furnace performance test shown in Figure 82 is shown in Table 12. To collect the data shown in Figure 81 the Reactor was by-passed, and a tube was connected to the furnace coil of F2 at the left side and room temperature deionized water of ~20°C (68°F) was pumped at a rate of 10ml/min.

Table 12: Events Timeline of Furnace 2 Coil Test

| Elapsed Time (H:mm) | F2 Set Point Temperature (°C) | F2 Actual Temperature (°C) | F2 Set Point - F2 Actual Temperature (°C Δ) | HEX1 Hot Inlet Temperature (T1) (°C) | HEX1 Inlet Heat Rate (°C/min) | F2 Actual Temperature - HEX1 Inlet Temperature (T1) (°C Δ) | Inlet Temperature Change (t2-t1/time) (°C Δ/minute) | Pump 1 Pressure (Psi) | Pump 2 Pressure (Psi) | BPR setting (Psi) | Events |
|---|---|---|---|---|---|---|---|---|---|---|---|
| 0:00 | 300 | 38 | 262 | 28.8 | N/A | 9.2 | N/A | | | | F2 ON, Pump1 ON, Pump2 ON |
| 0:11 | 300 | 298 | 2 | 119 | -0.3 | 179 | 16 | | | | Increased F2 to 350°C |
| 0:18 | 350 | 349 | 1 | 115.5 | 0.1 | 233.5 | 33 | | | | Increased F2 to 400°C |
| 0:26 | 400 | 401 | -1 | 116.1 | 12.6 | 284.9 | 36 | | | | Increased F2 to 450°C |
| 0:51 | 450 | 452 | -2 | 216.6 | 5.4 | 235.4 | 9 | 106 | 95 | | Increased F2 to 500°C |
| 1:25 | 500 | 500 | 0 | 351.7 | 2.9 | 148.3 | 4 | | | | Incresaed F2 to 550°C |
| 2:44 | 550 | 550 | 0 | 451.9 | -0.1 | 98.1 | 5 | 148 | 95 | | Set BPR to 350 Psi |
| 3:00 | 550 | 550 | 0 | 450.8 | 0.0 | 99.2 | 6 | 225 | 109 | | Audible noise coming from HEX1 |
| 3:03 | 550 | 549 | 1 | 451 | -1.6 | 98 | 33 | 369 | 103 | 311 | Noise persists |
| 3:10 | 550 | 550 | 0 | 446.3 | -0.7 | 103.7 | 15 | 376 | 104 | 308 | Pressure reduced to 100 Psi |
| 3:17 | 550 | 550 | 0 | 441.4 | -4.1 | 108.6 | 16 | 162 | 100 | 79 | Reduced F2 to 500°C |
| 3:29 | 500 | 500 | 0 | 412.6 | -0.5 | 87.4 | 7 | 145 | 106 | 44 | Shut off N2 tank valve |
| 3:37 | 500 | 500 | 0 | 406.6 | -0.1 | 93.4 | 12 | | | | Reduced F2 to 450°C |
| 3:38 | 450 | 487 | -37 | 405.5 | -141.8 | 81.5 | 82 | 141 | 107 | 32 | Reduced BPR setting to 0 psi |
| 4:03 | 450 | 450 | 0 | 263.7 | -0.5 | 186.3 | 7 | 109 | 88 | 2 | N2 connector was removed from regulator |
| 4:11 | 450 | 450 | 0 | 250 | -0.9 | 200 | 25 | 109 | 91 | N/A | Stopped recording BPR setting data |
| 4:19 | 450 | 450 | 0 | 243 | -16.1 | 207 | 26 | 106 | 89 | | Reduced F2 setting to 400°C |
| 4:33 | 400 | 402 | -2 | 114.2 | -0.4 | 287.8 | 21 | | | | Reduced F2 setting to 350°C |
| 4:36 | 350 | 349 | 1 | 108.5 | -1.8 | 240.5 | 80 | | | | F2 OFF |
| 4:45 | 0 | N/A | N/A | 103.2 | -11.5 | | | | | | Pump1 OFF, Pump2 OFF, Test Terminated |

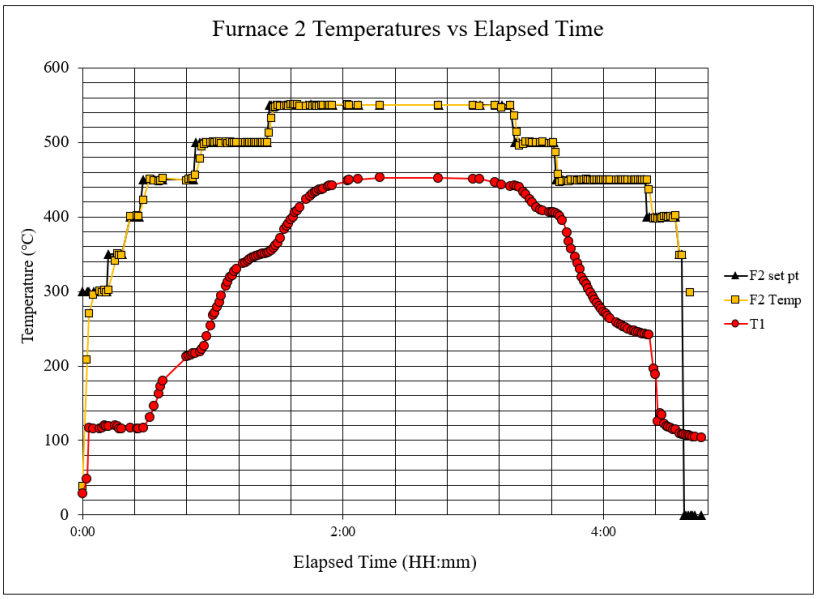


Figure 82: Furnace coil test data

A T1 value of 450°C was exceeded during the test. This test was under low pressure to increase safety and to force the furnace to heat the fluid from room temperature to 450°C. Based on what is known about the thermophysical properties of supercritical water, if the furnace can heat the ~20°C liquid water to 450°C, then the furnace can be used to control the entrance temperature of the HEX so a range of entrance temperatures can be tested. The desalination system was not running during this test and there is no HEX thermocouple data available from this test. The test was focused on the furnace coil performance only. The

missing data was not collected. The timeline of events table shows the F2 Set point, F2 actual temperature and the temperature of T1.

The set point temperature was gradually increased to 500°C (932°F). The set point temperature (F2 Set Pt), the measured internal furnace temperature (F2 Temp) and the furnace coil exit temperature (T1) were all recorded to test if the coil could produce an exit temperature (T1) exceeding 420°C (788°F) while the fluid entering the furnace begins at room temperature. The pressure for the furnace tube test began at 80 Psi (5.5 Bar). The pressure was kept low for safety concerns as this was an initial test. The highest pressure reached during the Furnace Coil test was 376 Psi (26 Bar). The pressure gradually increased until there was a "popping" sound heard inside the heat exchanger, that persisted as the pump kept pumping in new water. This is believed to be boiling. The reason Nitrogen is added to the system first is to pre-pressurize the system to prevent boiling. Boiling can cause sporadic pressure spikes which are not easily controlled which can cause an unsafe condition. When the system volume is low and the fluid is liquid, as the temperature increases past the boiling point boiling may occur if the pressure is low. The raw data can be requested from the author or the institution. The furnace coil test data proves the furnace with the coil is more than capable of providing enough energy to raise the temperature to the points necessary to characterize the heat exchanger and the fluid passing through it.

FURNACE SETTINGS FOR HOT INLET LINE

Figure 83 Shows the furnace set points necessary to achieve the range of hot line entrance temperatures called for by the experiment at different pressure settings. For example, to achieve at T1 value of 400°C while the system is at 240 Bar an F2 set point of 550°C is required. HEX2 has a greater Heat Capacity because the cooling jacket can hold 1.5 times more water than the cooling jacket of HEX1. While HEX2 was being evaluated it was found that the inlet tube was too long. The longer inlet tube increases the tube length from the exit of the furnace to the first temperature measurement probe. The longer the tube is the more heat is lost causing the temperature to drop which would increase the demand from the furnace causing the settings to increase. For the first 2 data points of HEX2 were collected with the longer tube, the

fittings were then changed to a shorter configuration which lowers the demand of the furnace which decreases the furnace set point to achieve the same hot line entrance temperature.

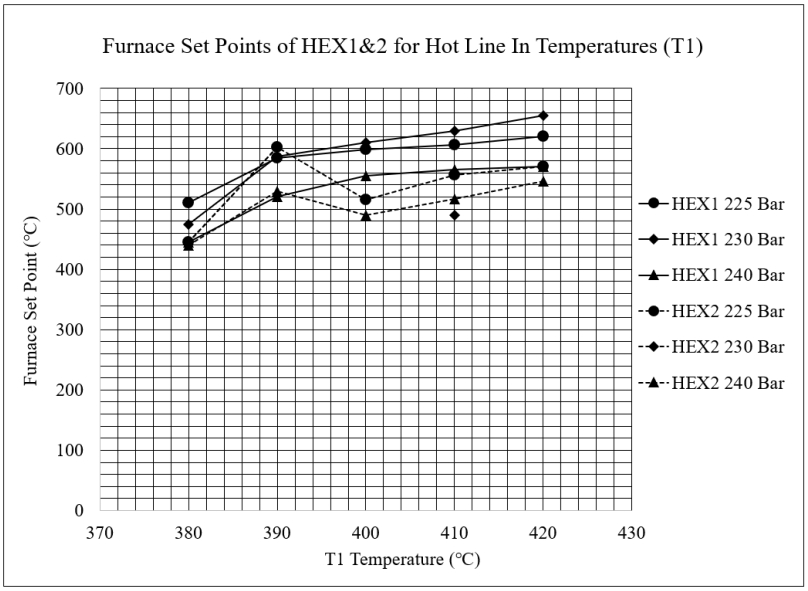


Figure 83: Furnace 2 Set points for HEX1 T1 temperature

Data for hot line entrance temperatures of 400℃, 410℃, and 420℃ were not recorded during the experiments for HEX2 at the pressure of 230 BAR. There may have been problems with the insulation of HEX2. The entrance of HEX2 was too long and the heat capacity of HEX2 is greater than HEX1 by 1.5 times, because HEX2 is longer and has a thinner shell wall tube. This is why at the first 2 temperatures of 380℃ and 390℃ the HEX2 Furnace setting is larger than that of HEX1. After the first set of temperatures for 380℃ and 390℃ entrance temperature were collected at all 3 pressures the fittings connecting Furnace 2 to HEX2 were changed, because using the longer fittings for the higher temperatures of 400℃, 410℃ and 420℃ exit temperatures would demand a higher Furnace 2 setting which is unsafe for the furnace coil. The furnace coil max allowable run temperature was 700℃. If the longer fittings remained the temperature of the furnace setting would have exceeded 700℃. Based on the information this shows that when positioning the HEX on the reactor the tube connecting the heat exchanger to the reactor must be as short as possible.

BRINE SOLUTION VALIDATION

To validate the brine produced for the HEX1 experiments, lines 29-30 in Table 11, a calibration curve was created. The DI-$H_2O$ and NaCl were mixed in solutions of increasing concentrations, from 0 to 15wt% NaCl, then measured with the electrical conductivity meter. Electrical conductivity was chosen as an evaluation metric because it provides a better indication of salt concentration in terms of charge per length rather than pH. The scale of conductivity, 0-∞, is also of much higher resolution then the pH scale, 0-14. The brine was mixed 100 mL at a time then the conductivity was measured. Table 13 shows the values of the graphical data shown in Figure 84, which shows the brine calibration curve. The small batches of brine used to generate the calibration curve were disposed of once the data was collected.

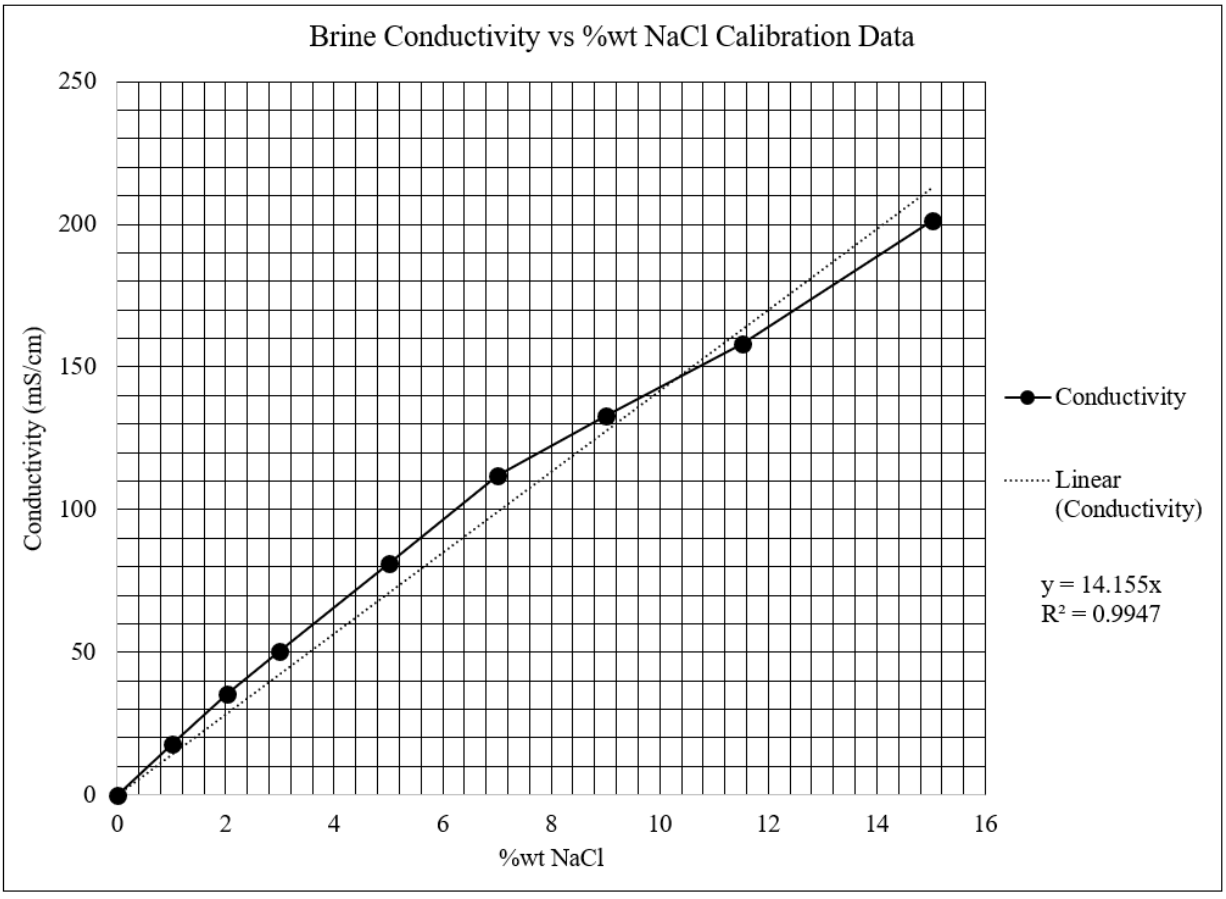


Figure 84: Brine Conductivity Calibration Data

Table 13: Brine Conductivity Calibration Curve Data

| Actual | Theoretical | Conductivity |
|---|---|---|
| g of NaCl /100ml H2O | wt% NaCl | mS/cm |
| 0.00 | 0.00 | 0.0 |
| 1.01 | 1.00 | 17.9 |
| 2.02 | 2.00 | 35.4 |
| 3.00 | 3.00 | 50.2 |
| 5.01 | 5.00 | 81.0 |
| 7.00 | 7.00 | 111.9 |
| 9.01 | 9.00 | 132.9 |
| 11.51 | 11.50 | 158.0 |
| 15.03 | 15.00 | 201.3 |

When the brine was produced in batches of 2 Liters for the HEX1 brine with heat experiment the density and conductivity were measured and recorded as shown in Table 14. The 2 Liter batches were then pumped through the cooling jacket of HEX1 to determine the time necessary to replace the DI-H2O with brine concentrate.

Table 14: 2-Liter Brine Batch Conductivity

| %wt NaCl | Conductivity (mS/cm) |
|---|---|
| 3.5% | 51 |
| 7.5% | 106 |
| 14% | 182 |

Figure 84 shows a linear increasing relationship between brine solution concentration of NaCl and the conductivity of the fluid. This data was collected to provide a reference for the operator to determine the concentration of the fluid inside of the cooling jacket of HEX1. The electrical conductivity of the samples collected was measured to determine if there was any salt lost inside the heat exchanger during experimentation. If too much salt is lost or desalinated inside the cooling jacket of the heat exchanger there could be a buildup of fouling that could cause a drop in pressure and flowrate. A pressure drop that is to large can cause a breakdown of the thermophysical design intention of the heat exchanger leading to a system failure.

HEX1 BRINE CONCENRATION STUDY

The system configuration set up for the HEX1 cooling jacket brine concentration study is shown in Figure 85. The purpose of this study is to determine how long it takes to fill the volume of the cooling side of HEX1 with DI-H2O and Brine of varying concentrations. The equipment not shown in Figure 85 was still set up in preparation for the main experiments but is not shown to show what relevant to the Brine Concentration Study.

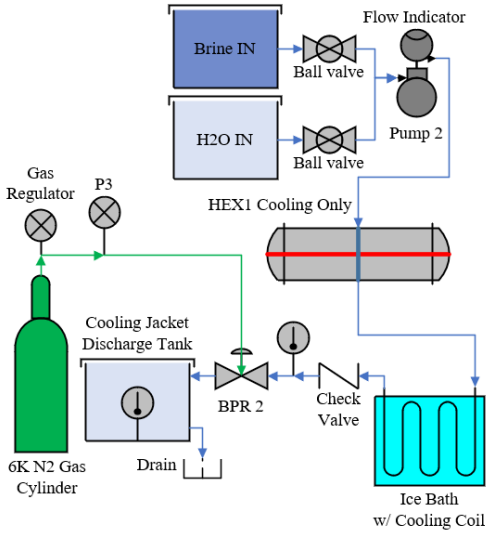


Figure 85: HEX1 Brine Concentration Study Cooling Test Setup

An additional brine validation study was performed using the cooling jacket of HEX1. The purpose of this study was to determine the conductivity level of the brine within the cooling shell as it mixes with the DI-$H_2O$ to eventually determine when the brine replaces the DI-$H_2O$. By determining the conductivity level, the system operator can know when the fluid in the HEX1 cooling shell has reached close to 100 % brine which is when the salinity of the cooling jacket has reached a steady state in preparation for data collection. The following data was collected at low pressure and without heat. Pump 2 was used to pump the DI-$H_2O$ and brine. A measurement was taken approximately every 2 minutes. The BPR was not increased, the pressure of the system was approximately 100 psi during this test. There was no heat applied to the HEX, the purpose of this test was to investigate how long it takes to fill the HEX cooling jacket with

brine while the pump is running. The length of time it takes to push out all the DI-$H_2O$ and replace it with brine was determined to be 10 to 15 minutes. Table 15 shows the concentration study events timeline.

Table 15: HEX1 Brine Concentration Study Timeline of Events

| Elapsed Time (HH:mm) | $H_20$ Tank Flow | Brine Tank Flow | Conductivity of the Fluid Exiting the Shell (mS/cm) | Density of the Fluid Exiting the Shell ($g/cm^3$) | Events |
|---|---|---|---|---|---|
| 0 | ON | OFF | 0.064 | | Pump2 ON, H2O ON |
| 0:06 | ON | ON | 1.921 | | 3.5% wt NaCl Brine ON |
| 0:16 | OFF | ON | 18.647 | | H2O OFF |
| 0:21 | OFF | ON | 51.2518 | | H2O ON |
| 0:32 | ON | OFF | 9.635 | | 3.5%wt NaCl Brine OFF |
| 0:33 | ON | OFF | 0.902 | | Changed Brine Tank to 7.5%wt NaCl |
| 0:45 | ON | OFF | 0.059 | | Recording 3.5% wt NaCl Brine Data Ends |
| 2:50 | ON | OFF | 0.002 | | Recording 7.5% wt NaCl Brine Data Begins |
| 2:58 | ON | OFF | 0.001 | | Brine Tank OFF |
| 3:00 | ON | ON | 0.001 | | Both H2O and 7.5% Brine ON |
| 3:40 | OFF | ON | 94.541 | 1.04562 | H2O OFF |
| 3:50 | OFF | ON | 109.254 | 1.0548 | H2O ON |
| 3:52 | ON | ON | 93.923 | 1.0459 | H2O ON, Brine ON |
| 4:10 | ON | ON | 39.053 | 1.0177 | 7.5% wt NaCl Brine OFF |
| 4:11 | ON | OFF | 39.080 | 1.0177 | Changed Brine Tank to 14%wt NaCl |
| 4:26 | ON | OFF | 0.085 | 1.0009 | Recording 7.5% Brine Data Ends |
| 4:55 | ON | OFF | 0.092 | | Recording 14%wt NaCl Brine Data Ends |
| 6:16 | ON | OFF | 0.033 | 1.0007 | Brine OFF, Begin Wash Out Cycle |
| 6:18 | ON | ON | 0.032 | 1.0005 | H2O ON Brine ON |
| 6:38 | ON | ON | 0.496 | | H2O OFF |
| 6:52 | OFF | ON | 180.221 | 1.1035 | H2O ON |
| 7:09 | ON | ON | 0.580 | 1.0006 | Brine OFF |
| 7:40 | ON | OFF | 0.157 | 1.0007 | Pump OFF, Test Terminatied |

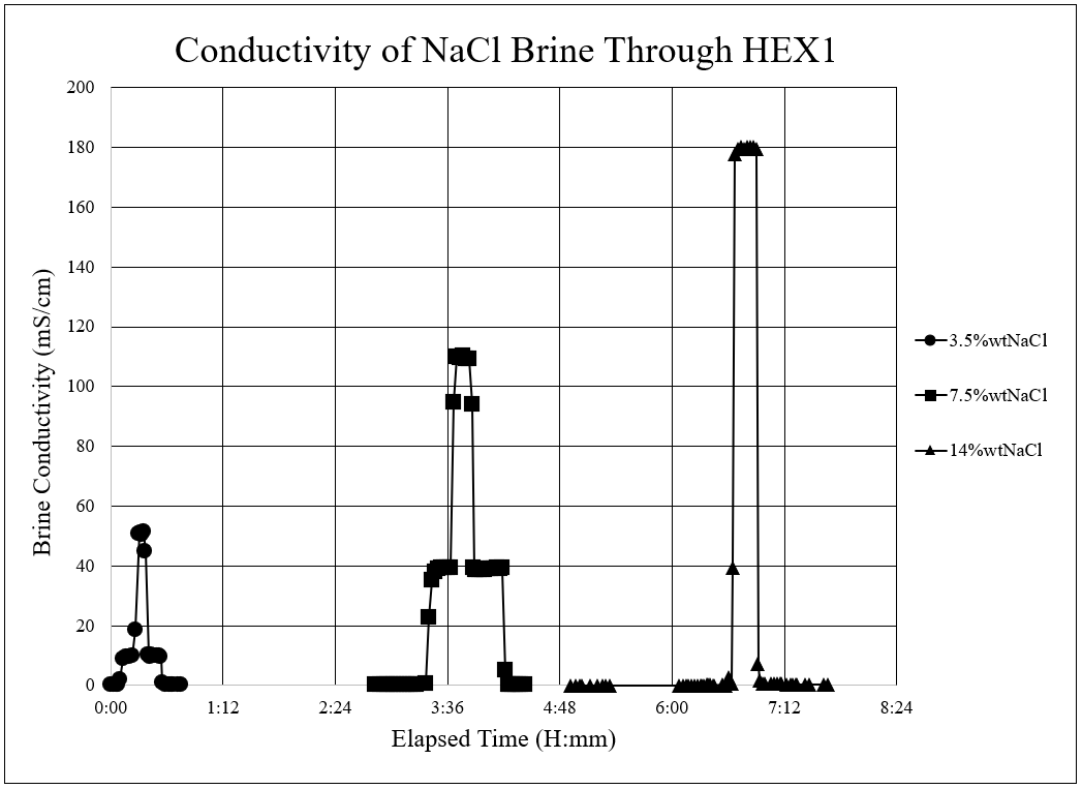


Figure 86: Conductivity of Brine solution experiment results

The three peaks shown in Figure 86 represent the steady state of the brine solution at maximum concentration of 3.5%wt, 7.5%wt and 14%wt NaCl when flowing through the cooling side of HEX1.

## DEIONIZED WATER STABILITY AT STAGNANT CONDITIONS

A 250 mL beaker of DI-$H_2O$ was left in the lab overnight, the conductivity was measured at 0 hours, 3 hours later than 13 hours later. There was a slight increase in conductivity of 0.5 μS, which in comparison to the rest of the conductivity measurements it is concluded that leaving DI-$H_2O$ in the tanks for an extended period has little effect on the conductivity of the liquid. The maximum electrical conductivity measured was 180221 μS/cm, 0.5 μS/cm is 2.77E-5% of the max value which is within the repeatability of the conductivity meter. Therefore, the DI-$H_2O$ used in this study is electrically stable and measuring the conductivity can be used to indicate the salinity of the water. This conclusion substantiates the conductivity data presented.

## LAB EVAPORATION RATE

In another instance a 10mL graduated cylinder was left in the lab for 1 day. It was determined that the evaporation rate of the room is less than 1 mL per day. The purpose of testing the room evaporation rate was to determine if there was any loss of water from the tank over time. If the evaporation rate is high the salt concentration of the brine would change which could possibly invalidate the data collected. If this experiment was not in a controlled environment, the brine could have increased in salt concentration enough to alter the results.

## HEX1

Figure 87 shows the instrumentation added to the heat exchanger to collect pressure and temperature data. The hot line is measured by thermocouples at T1 through T3 and the cold line is measured

by T6 through T10. T4 and T5 measure the temperature of the Feed Water Heater (FWH) and the condenser entrance temperature.

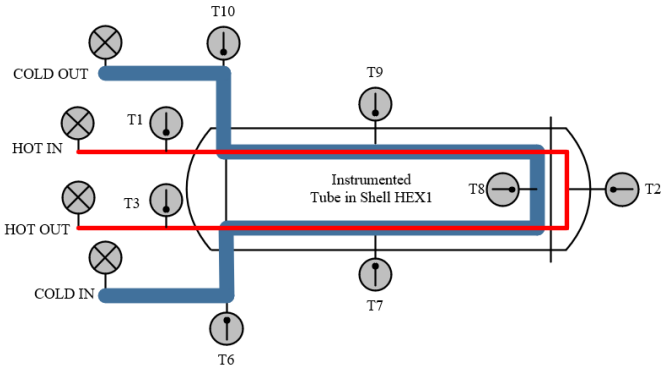


Figure 87: HEX1 Instrument Layout

Figure 88 shows data from an earlier test of HEX 1 while it is connected to the desalination system. T1 is at the exit of F2 therefore it will be the hottest of the 3 temperature readings. T5 and T11 were unused cables at this point of early testing. T12 was the ambient temperature of the room, which is not shown in this example, it remained around 20-22°C. The Reactor (R1) Temperature, Furnace 1 internal temperature, Furnace 2 internal temperature are all shown. The red line at 374°C is the critical temperature of $H_2O$, it is strictly graphed for reference.

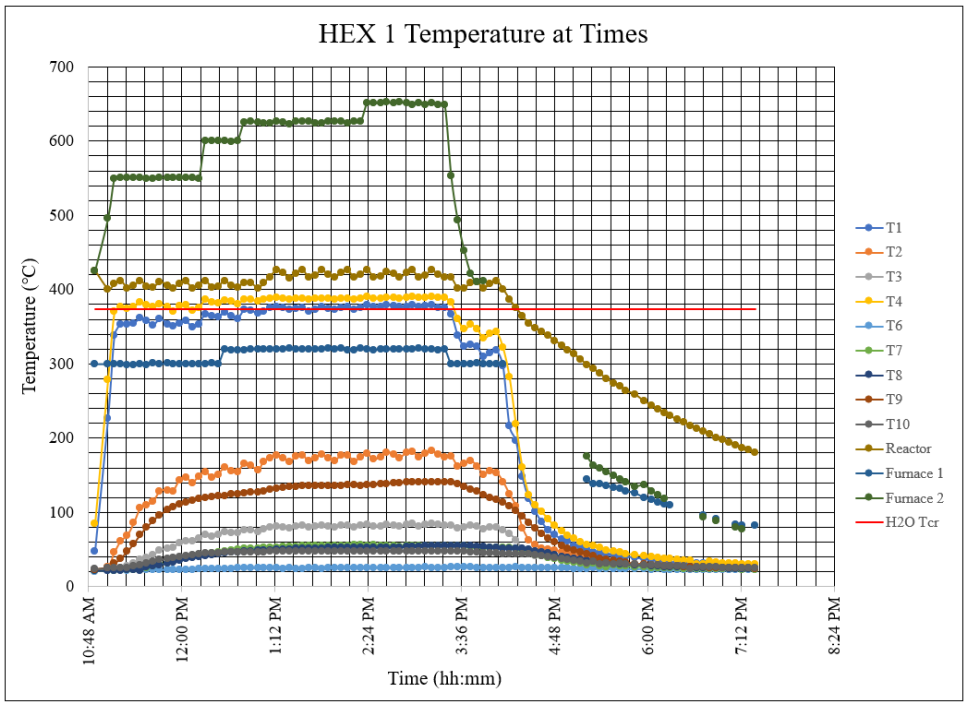


Figure 88: Plotted temperature and time data for HEX1 during early stages of system testing

The event schedule of the plotted data is in accordance with Table 16. Data for HEX 2 was not recorded during this test.

Table 16: Timeline of events for Figure 88

| Line | Elapsed Time | Time | Event |
|---|---|---|---|
| 1 | 0:00 | 10:53:00 AM | Began Start up procedure |
| 18 | 12:13 | 12:13:00 PM | Increased Furnace 2 to 600 |
| 21 | 12:28 | 12:28:00 PM | Increased Furnace 1 to 320 |
| 24 | 12:43 | 12:43:00 PM | Increase Furnace 2 to 625 |
| 26 | 12:53 | 12:53:00 PM | Increased Reactor to 425 |
| 29 | 13:08 | 1:08:00 PM | Broke Critical Temperature |
| 43 | 14:18 | 2:18:00 PM | Increased F2 to 650 |
| 56 | 15:23 | 3:23:00 PM | Decreased R1 to 410, F1 to 300, F2 to 410 |
| 62 | 15:53 | 3:53:00 PM | Shut off F2 |
| 64 | 16:03 | 4:03:00 PM | Shut off R1 |
| 65 | 16:08 | 4:08:00 PM | Shut off F1, and Pump1 |

The purpose of showing the data collected in Figure 88 is to show the response of the heat exchanger under different conditions. Note that the Furnace setting is near 750°C. This data was recorded before the furnace coil was added to F2.

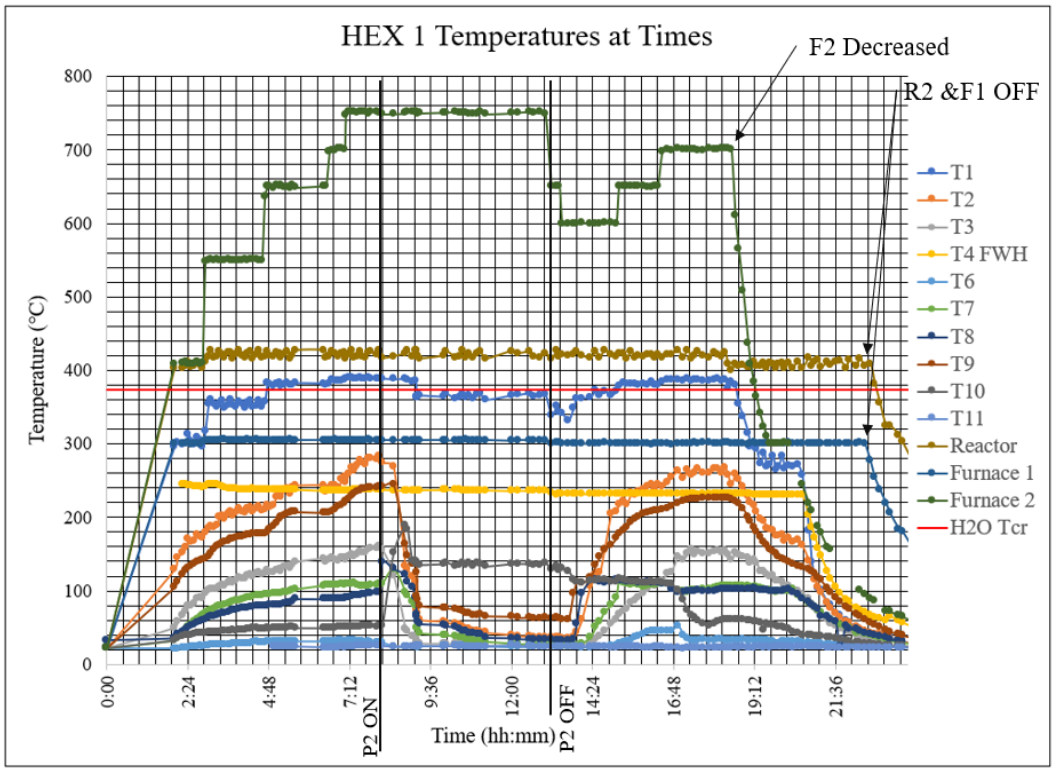


Figure 89: HEX1 Temperatures over time during early system test.

Table 17: Timeline of Events for Figure 89

| Line | t- | Time | Event |
|---|---|---|---|
| 3 | 0 | 10:06:00 AM | System ON |
| 13 | 2:50 | 12:56:00 PM | Increased F2 to 550, F1 to 305, R1 to 425 |
| 34 | 4:36 | 2:42:00 PM | Increased F2 to 650 |
| 48 | 6:30 | 4:36:00 PM | Increased F2 to700 |
| 54 | 7:03 | 5:09:00 PM | Increase F2 to 750 |
| 62 | 7:40 | 5:46:00 PM | Turned on Cooling Jacket Pump2 |
| 82 | 10:38 | 8:44:00 PM | Pressure has risen from atmospheric due to steam |
| 91 | 12:40 | 10:46:00 PM | Added cover back to cold out collection tank, to much steam, causes lost mass, could change humidity of the room. |
| 92 | 12:50 | 10:56:00 PM | Began Shutdown, |
| 93 | 13:00 | 11:06:00 PM | Decreased F2 to 650, F1 to 300 |
| 96 | 13:25 | 11:31:00 PM | Decreased F2 to 600 |
| 98 | 13:41 | 11:47:00 PM | Shut off Pump 2 |
| 101 | 14:05 | 12:11:00 AM | When T9 reaches over 100C and the P2 is off the Hot line cooks the water remaining in the shell and flow is observed at the Cold line outlet into the collection tank |
| 102 | 14:20 | 12:26:00 AM | Needle of Cold line in moved up slightly, due to increased pressure in shell |
| 103 | 14:30 | 12:36:00 AM | video was recorded between this point and last point to show increase in droplet formation rate on cold line collection tank outlet. |
| 107 | 15:06 | 1:12:00 AM | Increased F2 to 650, changed direction on goal, find out how to cook off the remaining water in the shell |
| 108 | 15:11 | 1:17:00 AM | cold line pressure needle increased |
| 118 | 16:20 | 2:26:00 AM | Increased F2 to 700 |
| 119 | 16:28 | 2:34:00 AM | drops are still flowing out of the cold exit line into the collection tank |
| 121 | 16:44 | 2:50:00 AM | opened 7/16" nut on 1/8" fitting at cold in to check fluid, liquid room temp water was still present, approximatly 25-40 mls of water was drained. The driping into the collection take has stopped. |
| 132 | 18:14 | 4:20:00 AM | Decreased R1 to 410C |
| 135 | 18:31 | 4:37:00 AM | Decreased F2 to 565C |
| 137 | 18:44 | 4:50:00 AM | Decreased F2 to 400 |
| 140 | 19:05 | 5:11:00 AM | Decreased F2 to 300 |
| 152 | 20:13 | 6:19:00 AM | F2 Shut off |
| 155 | 20:37 | 6:43:00 AM | P1 was shut off |
| 169 | 22:28 | 8:34:00 AM | Shutoff F1 |
| 170 | 22:38 | 8:44:00 AM | Shutoff R1 |

HEX2

Figure 90 shows the instrument labeling scheme applied to HEX2 during experimentation. The purpose of this image is to provide a reference for the thermocouple locations for the following graphs. The hot line is shown in red, where T1 is the hottest and T3 is the coldest. The cold line is shown in blue where T4 is the coldest and T8 is the hottest.

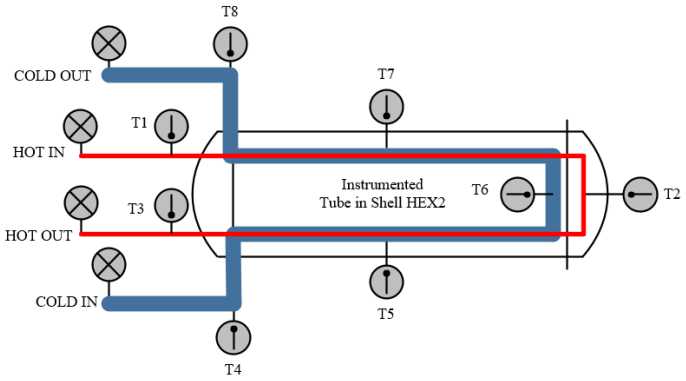


Figure 90: HEX2 Instrument Layout

HEX1 WITH BRINE AS A COOLING FLUID

The salt used to create the brine that was pumped through the system was 99.99% lab grade NaCl. 3 different concentrations of brine were pumped through the cooling jacket of HEX2, 3.5%wt, 7.5%wt and

14%wt NaCl. While the brine was being used as If was found during data collection that the pressure was not as stable as DI-$H_2O$.

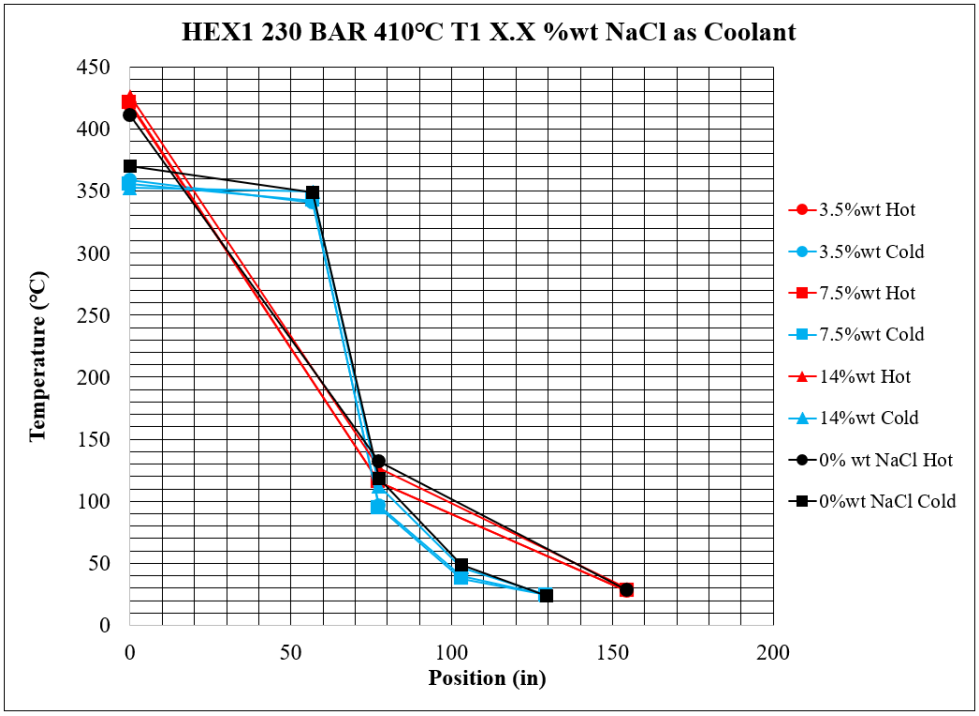


Figure 91: HEX1 at 230 Bar with a hot line entrance temperature of 410°C with NaCl Brine of varying concentrations as a cooling fluid compared to DI-$H_2O$

HEX1 & HEX2 TEMPERATURE COMPARISON

The following graphs and figures show the property listed at the pressures of 225, 230, and 240 Bar at the set hotline inlet temperatures of 380°C, 390°C, 400°C, 410°C and 420°C. The data from T7, and T9 in HEX1 and the data from T5 and T7 in HEX2 were removed on the following graphs to make data comparison and analysis more time efficient. It was found that the thermocouple height within the HEX that collected the data that was removed was inconsistent which made data comparison misleading. The Data collected for the other thermocouples is valid and of good comparison. The data that is shown in a format like Tables 18 and 19 is calculated using 21 different temperature points to collect information from REFPROP. The average temperature in Table 18 and Table 19 is the average temperature of 21 points, each point recorded every 5 minutes. The standard deviations shown in Table18 are also calculated from 21

different temperatures. The standard deviations shown in Tables 18 and 19 are shown as error bars in Figures 97 and 98.

Table 18: Temperature values and Temperature Standard Deviations for HEX1

| Average Temperature Data | | | | | | | | |
|---|---|---|---|---|---|---|---|---|
| HEX1 | | | | | | | | |
| Pressure (Bar) | Hot Line Inlet Set Point | Hot Line | | | Cold Line | | | Salinity of Cold Line (%wt NaCl) |
| | | T1 | T2 | T3 | T6 | T8 | T10 | |
| | | In | Middle | Out | In | Middle | Out | |
| 225 | 380 | 380 | 85 | 27 | 24 | 71 | 353 | 0 |
| | 390 | 390 | 121 | 28 | 24 | 106 | 367 | 0 |
| | 400 | 399 | 140 | 29 | 23 | 126 | 369 | 0 |
| | 410 | 411 | 146 | 29 | 23 | 132 | 370 | 0 |
| | 420 | 421 | 140 | 29 | 24 | 125 | 371 | 0 |
| 230 | 380 | 380 | 65 | 26 | 24 | 54 | 331 | 0 |
| | 390 | 391 | 120 | 28 | 24 | 105 | 367 | 0 |
| | 400 | 402 | 132 | 30 | 25 | 118 | 370 | 0 |
| | 410 | 411 | 132 | 28 | 24 | 118 | 370 | 0 |
| | 420 | 425 | 134 | 28 | 24 | 120 | 369 | 0 |
| 240 | 380 | 381 | 59 | 26 | 24 | 49 | 311 | 0 |
| | 390 | 390 | 115 | 30 | 25 | 102 | 358 | 0 |
| | 400 | 401 | 147 | 32 | 25 | 135 | 366 | 0 |
| | 410 | 413 | 164 | 34 | 24 | 154 | 365 | 0 |
| | 420 | 421 | 180 | 37 | 24 | 171 | 364 | 0 |
| 230 | 410 | 419 | 115 | 28 | 25 | 97 | 359 | 3.5% |
| | 410 | 421 | 115 | 28 | 25 | 95 | 356 | 7.5% |
| | 410 | 426 | 127 | 30 | 24 | 112 | 352 | 14% |

| Standard Deviation of Temperatures | | | | | | | |
|---|---|---|---|---|---|---|---|
| HEX1 | | | | | | | |
| Pressure (Bar) | Hot Line Inlet Set Point | Hot Line | | | Cold Line | | |
| | | T1 | T2 | T3 | T6 | T8 | T10 |
| | | In | Middle | Out | In | Middle | Out |
| 225 | 380 | 0.5 | 3.3 | 0.6 | 0.5 | 3.3 | 1.4 |
| | 390 | 3.5 | 9.4 | 0.5 | 0.3 | 9.8 | 1.0 |
| | 400 | [illegible] | 1.8 | 0.3 | 0.3 | 1.9 | 0.7 |
| | 410 | 14.6 | [illegible] | 1.0 | 0.2 | 1.0 | 0.9 |
| | 420 | 18.2 | [illegible] | 0.9 | 0.3 | 9.5 | 1.0 |
| 230 | 380 | [illegible] | 7.1 | 0.4 | 0.5 | 4.2 | 1.3 |
| | 390 | 4.0 | 6.6 | 0.4 | 0.3 | 7.2 | 4.8 |
| | 400 | [illegible] | 1.4 | 2.2 | 0.3 | 1.1 | 1.1 |
| | 410 | 12.5 | [illegible] | 0.3 | 0.2 | 1.2 | 1.0 |
| | 420 | 22.7 | [illegible] | 0.3 | 0.2 | 2.1 | 1.3 |
| 240 | 380 | [illegible] | 3.4 | 0.3 | 0.2 | 2.4 | 1.4 |
| | 390 | 1.0 | 2.6 | 0.3 | 0.2 | 2.6 | 1.5 |
| | 400 | [illegible] | 1.6 | 0.3 | 0.2 | 1.6 | 1.5 |
| | 410 | 14.5 | [illegible] | 1.0 | 0.3 | 5.0 | 1.9 |
| | 420 | 17.1 | [illegible] | 1.1 | 0.2 | 3.9 | 3.0 |
| 230 | 410 | [illegible] | 5.2 | 0.4 | 0.1 | 8.2 | 1.5 |
| | 410 | 9.8 | 9.4 | 0.6 | 0.2 | 12.6 | 2.7 |
| | 410 | 9.8 | 9.4 | 1.6 | 0.1 | 11.4 | 4.3 |

Table 19: Temperature values and Temperature Standard Deviations for HEX2

| Average Temperature Data | | | | | | | | |
|---|---|---|---|---|---|---|---|---|
| HEX2 | | | | | | | | |
| Pressure (Bar) | Hot Line Inlet Set Point | Hot Line | | | Cold Line | | | Salinity of Cold Line (%wt NaCl) |
| | | T1 | T2 | T3 | T6 | T8 | T10 | |
| | | In | Middle | Out | In | Middle | Out | |
| 225 | 380 | 381 | 123 | 30 | 24 | 124 | 285 | 0 |
| | 390 | 390 | 178 | 39 | 24 | 182 | 337 | 0 |
| | 400 | 401 | 241 | 83 | 26 | 245 | 342 | 0 |
| | 410 | 414 | 260 | 106 | 26 | 266 | 347 | 0 |
| | 420 | 419 | 270 | 120 | 26 | 276 | 347 | 0 |
| 230 | 380 | 382 | 128 | 29 | 24 | 126 | 280 | 0 |
| | 390 | 391 | 209 | 41 | 25 | 211 | 341 | 0 |
| 240 | 380 | 380 | 125 | 30 | 25 | 122 | 272 | 0 |
| | 390 | 390 | 163 | 32 | 25 | 166 | 318 | 0 |
| | 400 | 402 | 193 | 40 | 24 | 195 | 334 | 0 |
| | 410 | 411 | 222 | 60 | 26 | 226 | 345 | 0 |
| | 420 | 420 | 231 | 66 | 26 | 236 | 349 | 0 |

| Standard Deviation of Temperatures | | | | | | | |
|---|---|---|---|---|---|---|---|
| HEX2 | | | | | | | |
| Pressure (Bar) | Hot Line Inlet Set Point | Hot Line | | | Cold Line | | |
| | | T1 | T2 | T3 | T6 | T8 | T10 |
| | | In | Middle | Out | In | Middle | Out |
| 225 | 380 | 1.32 | 12.30 | 0.73 | 0.20 | 10.91 | 7.01 |
| | 390 | 1.88 | 3.25 | 2.21 | 0.78 | 3.50 | 1.43 |
| | 400 | 3.77 | 6.10 | 6.15 | 0.23 | 6.63 | 1.41 |
| | 410 | 3.85 | [illegible] | 6.29 | 0.13 | 4.40 | 1.44 |
| | 420 | 3.65 | [illegible] | 2.16 | 0.23 | 2.24 | 1.48 |
| 230 | 380 | [illegible] | 7.96 | 1.10 | 0.16 | 7.76 | 3.29 |
| | 390 | 1.90 | 1.77 | 1.21 | 0.36 | 2.02 | 1.47 |
| 240 | 380 | 0.90 | 0.86 | 0.39 | 0.25 | 0.89 | 3.16 |
| | 390 | 0.56 | 9.04 | 1.39 | 0.43 | 6.33 | 3.34 |
| | 400 | [illegible] | 5.22 | 3.62 | 0.28 | 5.59 | 1.87 |
| | 410 | 1.88 | [illegible] | 0.91 | 0.29 | 1.76 | 1.77 |
| | 420 | 3.00 | [illegible] | 2.72 | 0.19 | 2.48 | 1.69 |

The graphs shown in Figures 92 and 93 are a visual representation of the data shown in Tables 18 and 19. Figure 92 shows the data of the hot line as the red dots and the data shown for the cold line in blue as well as points of thermal instability encircled in red.

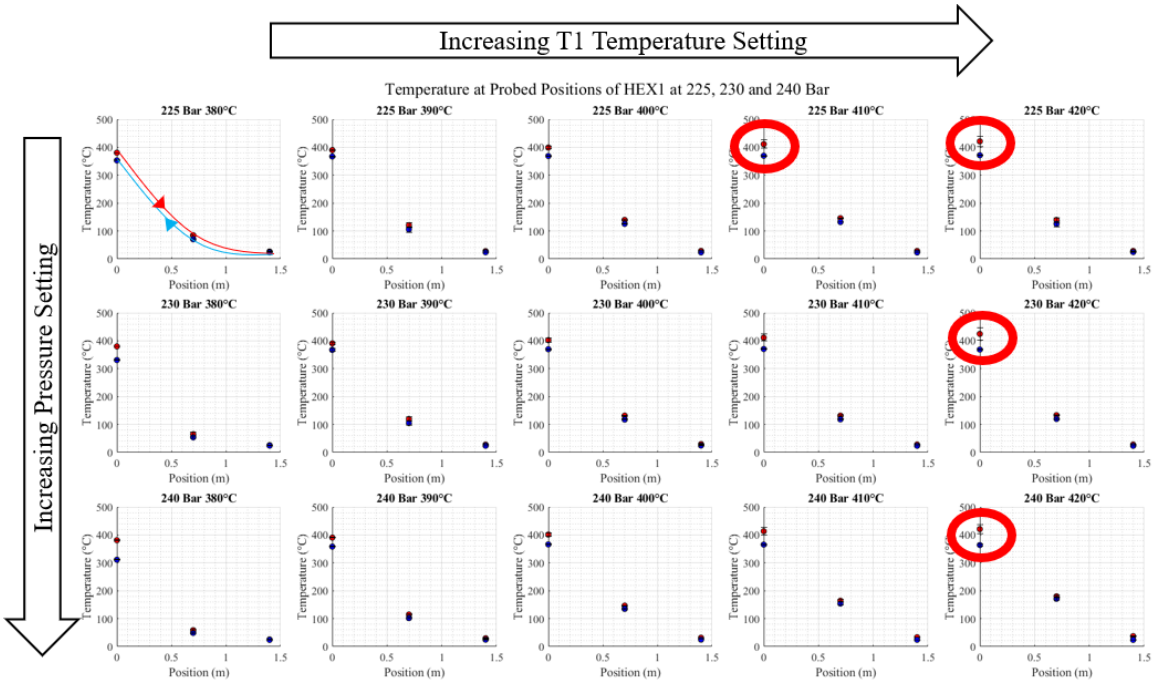


Figure 92: Temperature at Probed Positions of HEX1 at 225, 230 and 240 Bar

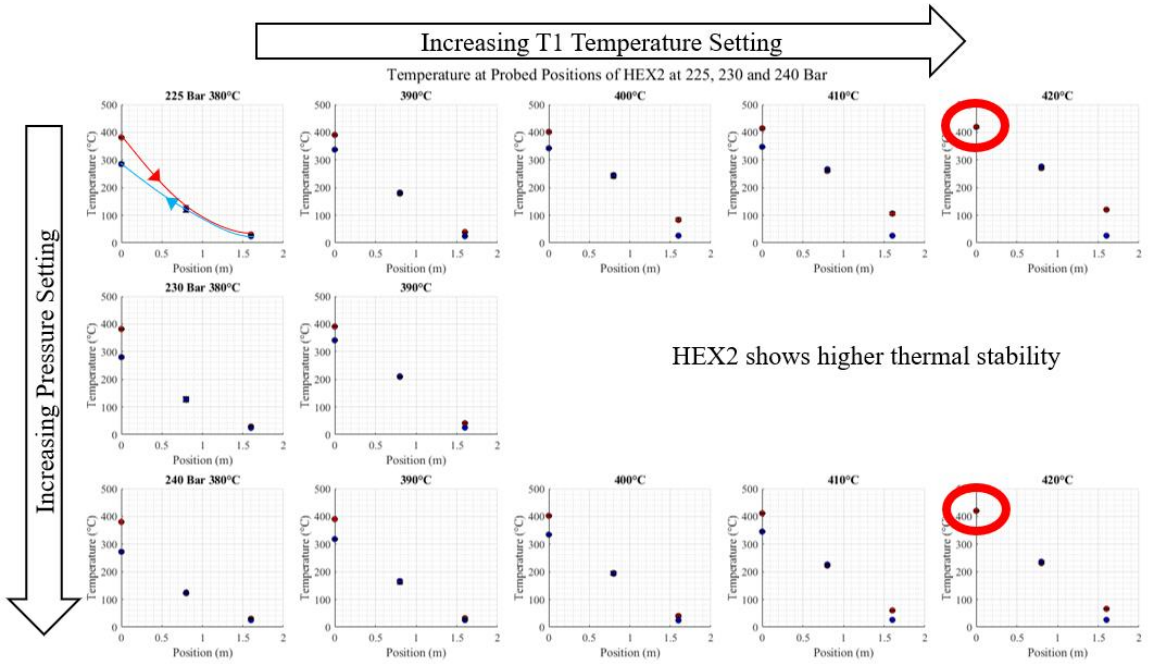


Figure 93: Temperatures at Probed Positions of HEX2 at 225, 230 and 240 Bar

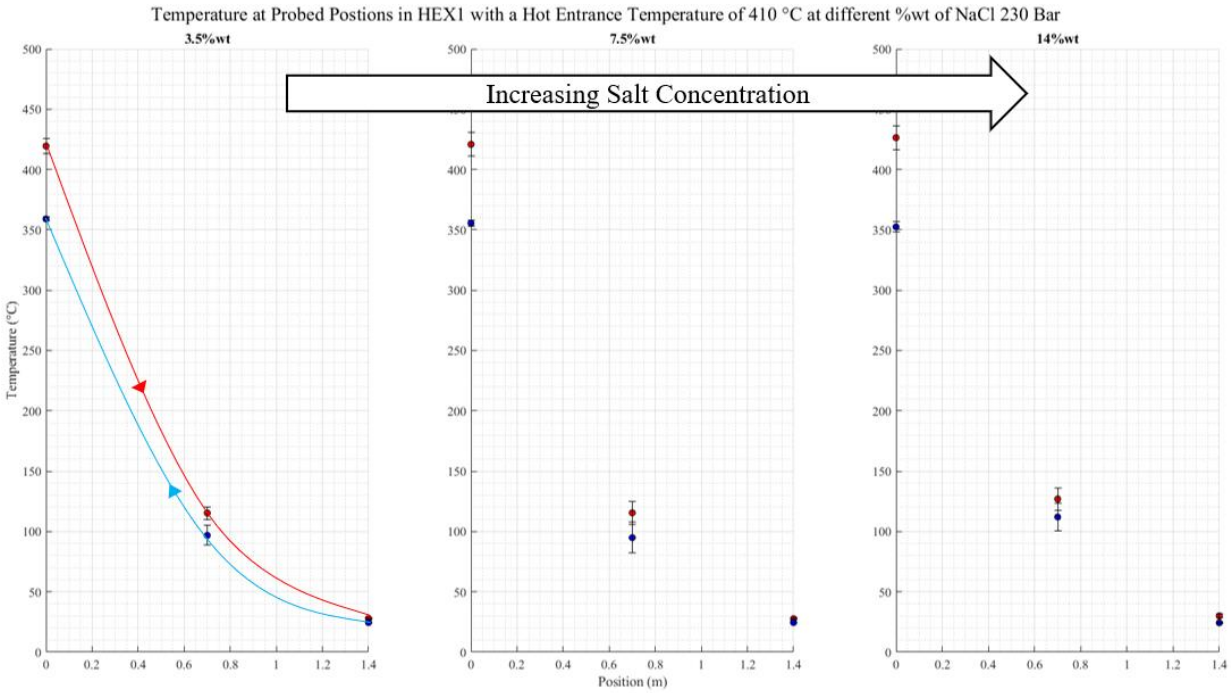


Figure 94: Temperature of Probed Positions in HEX1 with a Hot line entrance temperature of 410°C at 3.5%, 7.5% and 14% NaCl under a pressure of 230 Bar, shows sample standard deviation as error bars.

HEX1 & HEX2 REYNOLDS NUMBER

The Reynolds number calculated is a range because the flow is not constant because the linear displacement pump is pulsing as it pumps the flow is not a constant stream. The flow rate is effectively 10ml/min as indicated by the pumps, but the fluid is not constantly in motion because the pumps are linear displacement pumps. The volumetric flow rate used is average.

If the Reynolds number is greater than 2300 then the flow is considered turbulent. If the Reynolds number is below 2300 then the flow is considered laminar. Turbulent flow occurs at Reynolds numbers above 2300. Flows around 2300 are considered in the transition region [4].

The Reynolds numbers are calculated based off the kinematic viscosity, calculated velocity and known inner diameter of the central tube and the calculated hydraulic diameter of the annulus region surrounding the central tube. The Reynolds numbers calculated for fluid in the hot line are all below 400 and greater than 0. The Reynolds numbers calculated for the fluid in the cooling line are all greater than 0 but less than 1.

***Density***

The densities of the water flowing through both HEX1 and HEX2 are shown in Table 20. These densities were converted to kg/cm$^3$ and used to calculate the flow velocity used to calculate the Reynolds number. The diameters used to calculate the Reynolds number were found by checking the data sheet from tubing manufacturer and checking the physical dimensions of the tubing with digital calipers.

Table 20: Density of H2O that flows through HEX1 and HEX2

| Density of $H_2O$ (kg/m$^3$) | | | | | | | | |
|---|---|---|---|---|---|---|---|---|
| HEX1 | | | | | | | | |
| Pressure (Bar) | Hot Line Inlet Set Point | Hot Line | | | Cold Line | | | Salinity of Cold Line (%wt NaCl) |
| | | T1 In | T2 Middle | T3 Out | T6 In | T8 Middle | T10 Out | |
| 225 | 380 | 181 | 978 | 1006 | 1007 | 987 | 603 | 0 |
| | 390 | 144 | 953 | 1006 | 1007 | 964 | 530 | 0 |
| | 400 | 129 | 938 | 1006 | 1007 | 949 | 514 | 0 |
| | 410 | 115 | 933 | 1006 | 1007 | 944 | 505 | 0 |
| | 420 | 108 | 938 | 1006 | 1007 | 950 | 494 | 0 |
| 230 | 380 | 209 | 990 | 1007 | 1007 | 996 | 673 | 0 |
| | 390 | 151 | 954 | 1006 | 1007 | 965 | 537 | 0 |
| | 400 | 131 | 945 | 1006 | 1007 | 956 | 514 | 0 |
| | 410 | 120 | 945 | 1006 | 1007 | 956 | 514 | 0 |
| | 420 | 109 | 943 | 1006 | 1007 | 954 | 522 | 0 |
| 240 | 380 | 331 | 994 | 1007 | 1008 | 999 | 720 | 0 |
| | 390 | 178 | 958 | 1006 | 1008 | 968 | 591 | 0 |
| | 400 | 147 | 932 | 1005 | 1008 | 943 | 554 | 0 |
| | 410 | 129 | 917 | 1005 | 1008 | 926 | 559 | 0 |
| | 420 | 121 | 902 | 1004 | 1008 | 910 | 564 | 0 |
| 230 | 410 | 113 | 958 | 1006 | N/A | N/A | N/A | 3.5% |
| | 410 | 112 | 958 | 1006 | N/A | N/A | N/A | 7.5% |
| | 410 | 108 | 949 | 1006 | N/A | N/A | N/A | 14% |

| Density of $H_2O$ (kg/m$^3$) | | | | | | | | |
|---|---|---|---|---|---|---|---|---|
| HEX2 | | | | | | | | |
| Pressure (Bar) | Hot Line Inlet Set Point | Hot Line | | | Cold Line | | | Salinity of Cold Line (%wt NaCl) |
| | | T1 In | T2 Middle | T3 Out | T4 In | T6 Middle | T8 Out | |
| 225 | 380 | 175 | 952 | 1005 | 1007 | 951 | 766 | 0 |
| | 390 | 144 | 903 | 1002 | 1007 | 899 | 655 | 0 |
| | 400 | 126 | 831 | 980 | 1007 | 825 | 641 | 0 |
| | 410 | 113 | 804 | 964 | 1007 | 796 | 625 | 0 |
| | 420 | 109 | 790 | 954 | 1007 | 780 | 625 | 0 |
| 230 | 380 | 189 | 948 | 1006 | 1007 | 949 | 774 | 0 |
| | 390 | 151 | 870 | 1002 | 1007 | 868 | 646 | 0 |
| 240 | 380 | 386 | 951 | 1006 | 1008 | 953 | 788 | 0 |
| | 390 | 178 | 918 | 1005 | 1008 | 915 | 706 | 0 |
| | 400 | 145 | 888 | 1002 | 1008 | 886 | 668 | 0 |
| | 410 | 131 | 856 | 993 | 1007 | 851 | 637 | 0 |
| | 420 | 122 | 845 | 990 | 1007 | 838 | 624 | 0 |

The density of the water increases as temperature decreases and the density decreases as the temperature increases. The data collected during experimentation is inline with the thermophysical properties of water that were plotted in preliminary research. The density of water is shown to increase as the fluid cools down as well as increase as the temperature of the fluid increases

***Kinemetic Viscosity***

Data for the kinematic viscosity of the water flowing through HEX1 and HEX2 are shown in Tables 21 and 22. The data in Tables 21 and 22 was produced by entering the temperature and pressure from the data collected during experimentation. The kinematic viscosities were used in calculating the Reynolds number for the probed locations along HEX1 and HEX2.

Table 21: Kinematic Viscosity and Standard Deviations at Positions of HEX1 at 225, 230 and 240 Bar

| Kinematic Viscosity ($cm^2/s$) | | | | | | | | |
|---|---|---|---|---|---|---|---|---|
| HEX1 | | | | | | | | |
| Pressure (Bar) | Hot Line Inlet Set Point | Hot Line | | | Cold Line | | | Salinity of Cold Line (%wt NaCl) |
| | | T1 | T2 | T3 | T6 | T8 | T10 | |
| | | In | Middle | Out | In | Middle | Out | |
| 225 | 380 | 0.00160 | 0.00347 | 0.00844 | 0.009010 | 0.004080 | 0.001160 | 0 |
| | 390 | 0.00191 | 0.00247 | 0.00827 | 0.009010 | 0.002810 | 0.001150 | 0 |
| | 400 | 0.00212 | 0.00216 | 0.00810 | 0.009220 | 0.002380 | 0.001150 | 0 |
| | 410 | 0.00237 | 0.00208 | 0.00810 | 0.009220 | 0.002280 | 0.001150 | 0 |
| | 420 | 0.00256 | 0.00216 | 0.00810 | 0.009010 | 0.002400 | 0.001150 | 0 |
| 230 | 380 | 0.00147 | 0.00443 | 0.00863 | 0.009011 | 0.005190 | 0.001181 | 0 |
| | 390 | 0.00185 | 0.00249 | 0.00827 | 0.009011 | 0.002834 | 0.001150 | 0 |
| | 400 | 0.00210 | 0.00228 | 0.00793 | 0.008814 | 0.002534 | 0.001150 | 0 |
| | 410 | 0.00229 | 0.00228 | 0.00827 | 0.009011 | 0.002534 | 0.001150 | 0 |
| | 420 | 0.00255 | 0.00225 | 0.00827 | 0.009011 | 0.002494 | 0.001150 | 0 |
| 240 | 380 | 0.00124 | 0.00482 | 0.00862 | 0.009006 | 0.005614 | 0.001213 | 0 |
| | 390 | 0.00165 | 0.00260 | 0.00793 | 0.008810 | 0.002915 | 0.001155 | 0 |
| | 400 | 0.00193 | 0.00207 | 0.00761 | 0.008810 | 0.002233 | 0.001151 | 0 |
| | 410 | 0.00218 | 0.00187 | 0.00732 | 0.009006 | 0.001980 | 0.001151 | 0 |
| | 420 | 0.00233 | 0.00173 | 0.00691 | 0.009006 | 0.001807 | 0.001152 | 0 |
| 230 | 410 | 0.00244 | 0.00260 | 0.00827 | N/A | N/A | N/A | 3.5% |
| | 410 | 0.00248 | 0.00260 | 0.00827 | N/A | N/A | N/A | 7.5% |
| | 410 | 0.00257 | 0.00236 | 0.00793 | N/A | N/A | N/A | 14% |

| Standard Deviation of Kinematic Viscosity ($cm^2/s$) | | | | | | | | |
|---|---|---|---|---|---|---|---|---|
| HEX1 | | | | | | | | |
| Pressure (Bar) | Hot Line Inlet Set Point | Hot Line | | | Cold Line | | | Salinity of Cold Line (%wt NaCl) |
| | | T1 | T2 | T3 | T6 | T8 | T10 | |
| | | In | Middle | Out | In | Middle | Out | |
| 225 | 380 | 0.000115 | 0.000216 | 0.000380 | 0.000089 | 0.000117 | 0.000053 | 0 |
| | 390 | 0.000092 | 0.000192 | 0.000078 | 0.000051 | 0.000264 | 0.000001 | 0 |
| | 400 | 0.000114 | 0.000025 | 0.000055 | 0.000062 | 0.000033 | 0.000000 | 0 |
| | 410 | 0.000288 | 0.000018 | 0.000182 | 0.000042 | 0.000016 | 0.000001 | 0 |
| | 420 | 0.000335 | 0.000136 | 0.000153 | 0.000065 | 0.000183 | 0.000002 | 0 |
| 230 | 380 | 0.000028 | 0.000493 | 0.000076 | 0.000093 | 0.000353 | 0.000002 | 0 |
| | 390 | 0.000109 | 0.000139 | 0.000078 | 0.000053 | 0.000199 | 0.000118 | 0 |
| | 400 | 0.000174 | 0.000023 | 0.000135 | 0.000051 | 0.000022 | 0.000001 | 0 |
| | 410 | 0.000244 | 0.000048 | 0.000045 | 0.000045 | 0.000025 | 0.000001 | 0 |
| | 420 | 0.000415 | 0.000034 | 0.000051 | 0.000044 | 0.000041 | 0.000000 | 0 |
| 240 | 380 | 0.000033 | 0.000244 | 0.000055 | 0.000368 | 0.000224 | 0.000025 | 0 |
| | 390 | 0.000030 | 0.000056 | 0.000043 | 0.000030 | 0.000073 | 0.000001 | 0 |
| | 400 | 0.000130 | 0.000021 | 0.000052 | 0.000040 | 0.000024 | 0.000004 | 0 |
| | 410 | 0.000278 | 0.000049 | 0.000141 | 0.000050 | 0.000058 | 0.000001 | 0 |
| | 420 | 0.000314 | 0.000029 | 0.000137 | 0.000039 | 0.000342 | 0.000002 | 0 |
| 230 | 410 | 0.000105 | 0.000115 | 0.004121 | N/A | N/A | N/A | 3.5% |
| | 410 | 0.000166 | 0.000212 | 0.004141 | N/A | N/A | N/A | 7.5% |
| | 410 | 0.000172 | 0.000175 | 0.003931 | N/A | N/A | N/A | 14% |

Table 22: Kinematic Viscosity and Standard Deviations at Positions of HEX2 at 225, 230 and 240 Bar

| Kinematic Viscosity ($cm^2/s$) | | | | | | | | |
|---|---|---|---|---|---|---|---|---|
| HEX2 | | | | | | | | |
| Pressure (Bar) | Hot Line Inlet Set Point | Hot Line | | | Cold Line | | | Salinity of Cold Line (%wt NaCl) |
| | | T1 | T2 | T3 | T4 | T6 | T8 | |
| | | In | Middle | Out | In | Middle | Out | |
| 225 | 380 | 0.001635 | 0.002436 | 0.007931 | 0.00901 | 0.00242 | 0.00126 | 0 |
| | 390 | 0.001907 | 0.001744 | 0.006666 | 0.00901 | 0.00171 | 0.00117 | 0 |
| | 400 | 0.002164 | 0.001392 | 0.003544 | 0.00863 | 0.00138 | 0.00117 | 0 |
| | 410 | 0.002427 | 0.001328 | 0.002808 | 0.00863 | 0.00131 | 0.00116 | 0 |
| | 420 | 0.002521 | 0.001299 | 0.002493 | 0.00863 | 0.00128 | 0.00116 | 0 |
| 230 | 380 | 0.001564 | 0.002346 | 0.008094 | 0.00901 | 0.00238 | 0.00128 | 0 |
| | 390 | 0.001846 | 0.001537 | 0.00643 | 0.00881 | 0.00153 | 0.00117 | 0 |
| 240 | 380 | 0.001193 | 0.002401 | 0.007926 | 0.00881 | 0.00246 | 0.00130 | 0 |
| | 390 | 0.001648 | 0.001883 | 0.007613 | 0.00881 | 0.00185 | 0.00120 | 0 |
| | 400 | 0.001950 | 0.001635 | 0.009006 | 0.00990 | 0.00162 | 0.00118 | 0 |
| | 410 | 0.002137 | 0.001473 | 0.004750 | 0.00862 | 0.00146 | 0.00117 | 0 |
| | 420 | 0.002307 | 0.001433 | 0.004371 | 0.00862 | 0.00141 | 0.00116 | 0 |

| Standard Deviation of Kinematic Viscosity ($cm^2/s$) | | | | | | | | |
|---|---|---|---|---|---|---|---|---|
| HEX2 | | | | | | | | |
| Pressure (Bar) | Hot Line Inlet Set Point | Hot Line | | | Cold Line | | | Salinity of Cold Line (%wt NaCl) |
| | | T1 | T2 | T3 | T4 | T6 | T8 | |
| | | In | Middle | Out | In | Middle | Out | |
| 225 | 380 | 0.000065 | 0.000278 | 0.000127 | 0.000040 | 0.000232 | 0.000018 | 0 |
| | 390 | 0.000049 | 0.000017 | 0.000248 | 0.000153 | 0.000017 | 0.000002 | 0 |
| | 400 | 0.000085 | 0.000022 | 0.000250 | 0.000043 | 0.000023 | 0.000002 | 0 |
| | 410 | 0.000075 | 0.000011 | 0.000168 | 0.000024 | 0.000012 | 0.000001 | 0 |
| | 420 | 0.000069 | 0.000011 | 0.000043 | 0.000043 | 0.000006 | 0.000001 | 0 |
| 230 | 380 | 0.000026 | 0.000147 | 0.000187 | 0.000032 | 0.000149 | 0.000008 | 0 |
| | 390 | 0.000052 | 0.000010 | 0.000140 | 0.000070 | 0.000011 | 0.000002 | 0 |
| 240 | 380 | 0.000041 | 0.000016 | 0.000062 | 0.000047 | 0.000017 | 0.000008 | 0 |
| | 390 | 0.000017 | 0.000097 | 0.000209 | 0.000081 | 0.000063 | 0.000005 | 0 |
| | 400 | 0.000044 | 0.000351 | 0.000427 | 0.000056 | 0.000037 | 0.000002 | 0 |
| | 410 | 0.000037 | 0.000006 | 0.000061 | 0.000055 | 0.000008 | 0.000002 | 0 |
| | 420 | 0.000055 | 0.000010 | 0.000161 | 0.000035 | 0.000010 | 0.000002 | 0 |

Figures 95 and 96 are the graphical representations of Tables 21 and 22. The standard deviations are shown as error bars.

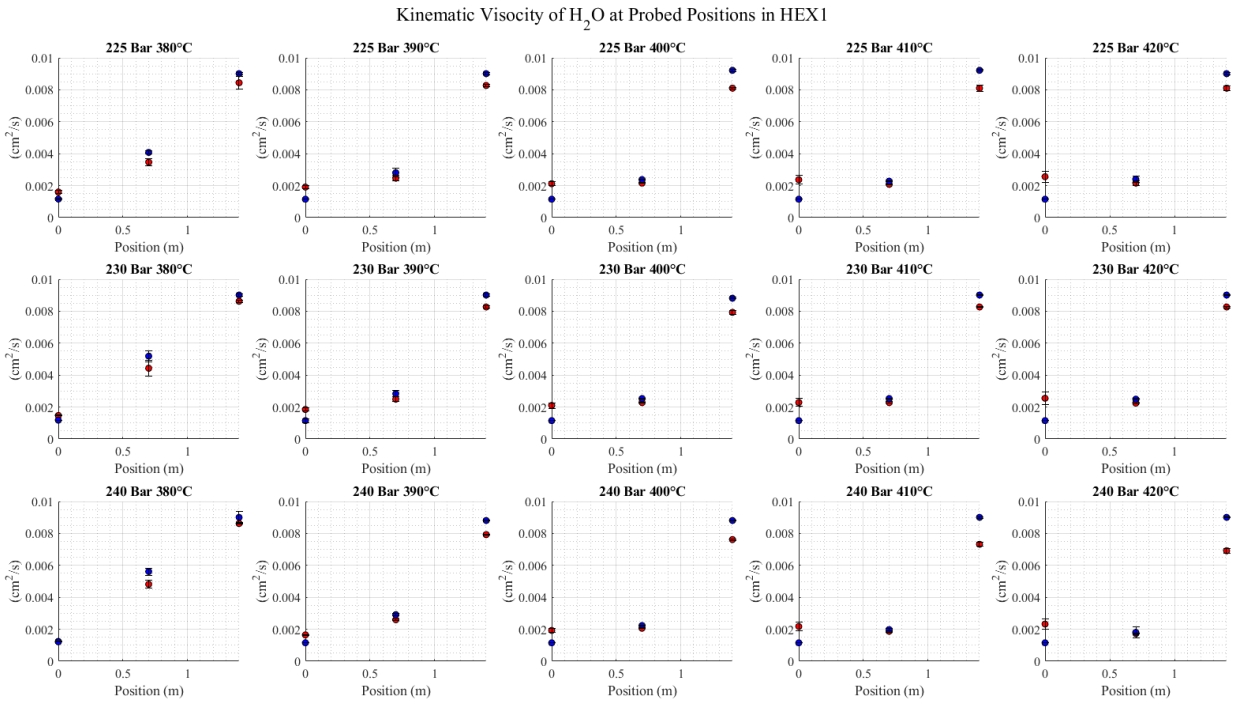


Figure 95: Kinematic Viscosity at Probed Positions of HEX1 at 225, 230 and 240 Bar

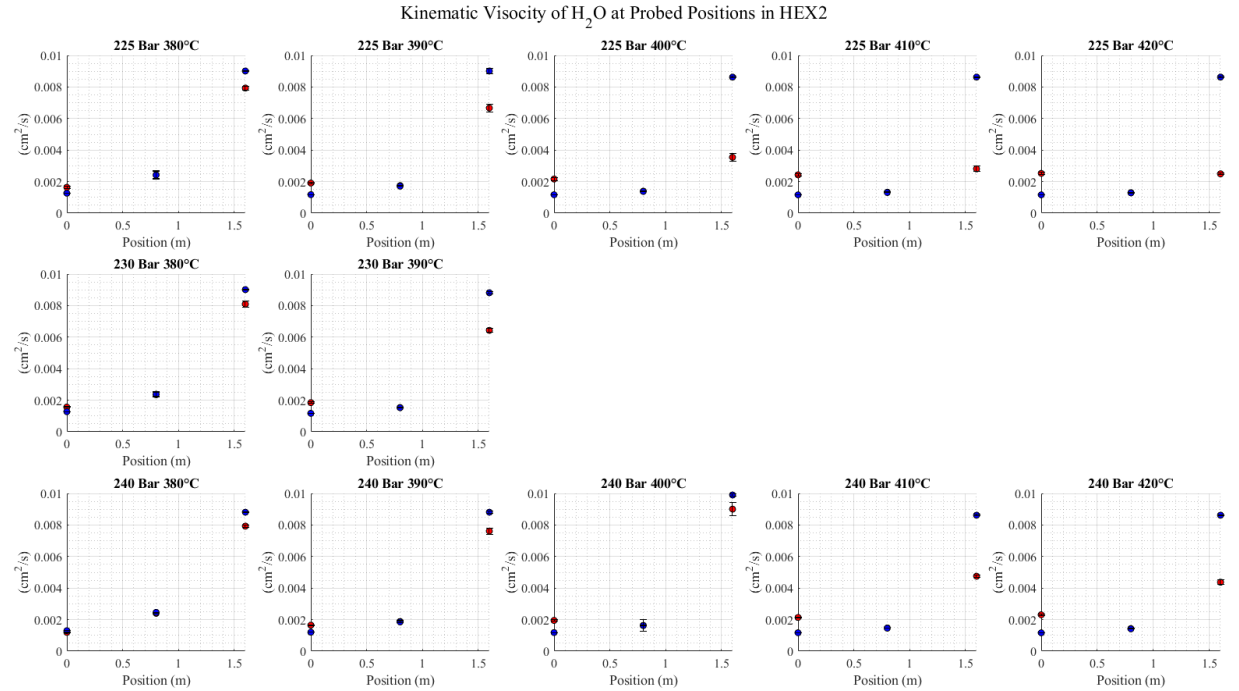


Figure 96: Kinematic Viscosity at Probed Positions of HEX2 at 225, 230 and 240 Bar

The Reynolds number was calculated using the Kinematic viscosity, flow velocity and hydraulic diameter of the fluid flow through the HEXs. The Reynolds Number values are shown in Table 23 and 24.

Table 23: Reynolds Number and Reynolds Number Standard Deviations for HEX1

| Reynolds Number | | | | | | | | |
|---|---|---|---|---|---|---|---|---|
| HEX1 | | | | | | | | |
| Pressure (Bar) | Hot Line Inlet | Hot Line | | | Cold Line | | | Salinity of Cold Line (%wt NaCl) |
| | | T1 In | T2 Middle | T3 Out | T6 In | T8 Middle | T10 Out | |
| 225 | 380 | 250 | 115 | 47 | 0.000394 | 0.0009 | 0.00306 | 0 |
| | 390 | 209 | 162 | 48 | 0.000394 | 0.0013 | 0.00309 | 0 |
| | 400 | 189 | 185 | 49 | 0.000385 | 0.0015 | 0.00309 | 0 |
| | 410 | 169 | 192 | 49 | 0.000385 | 0.0016 | 0.00309 | 0 |
| | 420 | 156 | 185 | 49 | 0.000394 | 0.0015 | 0.00309 | 0 |
| 230 | 380 | 272 | 90 | 46 | 0.000394 | 0.0007 | 0.00301 | 0 |
| | 390 | 216 | 160 | 48 | 0.000394 | 0.0013 | 0.00309 | 0 |
| | 400 | 190 | 175 | 50 | 0.000403 | 0.0014 | 0.00309 | 0 |
| | 410 | 175 | 175 | 48 | 0.000394 | 0.0014 | 0.00309 | 0 |
| | 420 | 157 | 178 | 48 | 0.000394 | 0.0014 | 0.00309 | 0 |
| 240 | 380 | 323 | 83 | 46 | 0.000394 | 0.0006 | 0.00293 | 0 |
| | 390 | 243 | 154 | 50 | 0.000403 | 0.0012 | 0.00308 | 0 |
| | 400 | 207 | 194 | 53 | 0.000403 | 0.0016 | 0.00309 | 0 |
| | 410 | 184 | 213 | 55 | 0.000394 | 0.0018 | 0.00309 | 0 |
| | 420 | 172 | 231 | 58 | 0.000394 | 0.0020 | 0.00308 | 0 |
| 230 | 410 | 164 | 154 | 48 | N/A | N/A | N/A | 3.5% |
| | 410 | 161 | 154 | 48 | N/A | N/A | N/A | 7.5% |
| | 410 | 156 | 169 | 50 | N/A | N/A | N/A | 14% |

| Reynolds Number Standard Deviations | | | | | | | |
|---|---|---|---|---|---|---|---|
| HEX1 | | | | | | | |
| Pressure (Bar) | Hot Line Inlet | Hot Line | | | Cold Line | | |
| | | T1 In | T2 Middle | T3 Out | T6 In | T8 Middle | T10 Out |
| 225 | 380 | 3 | 4 | 1 | 0.000005 | 0.000036 | 0.0000030 |
| | 390 | 10 | 12 | 0 | 0.000002 | 0.000112 | 0.0000004 |
| | 400 | 10 | 2 | 0 | 0.000000 | 0.000021 | 0.0000009 |
| | 410 | 21 | 2 | 1 | 0.000002 | 0.000011 | 0.0000020 |
| | 420 | 21 | 11 | 1 | 0.000003 | 0.000106 | 0.0000048 |
| 230 | 380 | 5 | 9 | 0 | 0.000004 | 0.000044 | 0.0000044 |
| | 390 | 14 | 8 | 0 | 0.000002 | 0.000082 | 0.0002152 |
| | 400 | 15 | 2 | 2 | 0.000002 | 0.000012 | 0.0000016 |
| | 410 | 19 | 4 | 0 | 0.000002 | 0.000014 | 0.0000020 |
| | 420 | 27 | 3 | 0 | 0.000002 | 0.000023 | 0.0000010 |
| 240 | 380 | 8 | 4 | 0 | 0.000002 | 0.000024 | 0.0000060 |
| | 390 | 4 | 3 | 0 | 0.000001 | 0.000030 | 0.0000025 |
| | 400 | 14 | 2 | 0 | 0.000002 | 0.000017 | 0.0000009 |
| | 410 | 23 | 6 | 1 | 0.000002 | 0.000052 | 0.0000013 |
| | 420 | 23 | 4 | 1 | 0.000002 | 0.000038 | 0.0000043 |

Table 24: Reynolds Number and Reynolds Number Standard Deviations for HEX2

| Reynolds Number | | | | | | | | |
|---|---|---|---|---|---|---|---|---|
| HEX2 | | | | | | | | |
| Pressure (Bar) | Hot Line Inlet | Hot Line | | | Cold Line | | | Salinity of Cold Line (%wt NaCl) |
| | | T1 In | T2 Middle | T3 Out | T4 In | T6 Middle | T8 Out | |
| 225 | 380 | 244 | 164 | 50 | 0.000587 | 0.0022 | 0.0042 | 0 |
| | 390 | 210 | 229 | 60 | 0.000587 | 0.0031 | 0.0045 | 0 |
| | 400 | 185 | 287 | 113 | 0.000613 | 0.0038 | 0.0045 | 0 |
| | 410 | 165 | 301 | 142 | 0.000613 | 0.0040 | 0.0046 | 0 |
| | 420 | 159 | 308 | 160 | 0.000613 | 0.0041 | 0.0046 | 0 |
| 230 | 380 | 256 | 170 | 49 | 0.000587 | 0.0022 | 0.0042 | 0 |
| | 390 | 217 | 260 | 62 | 0.000600 | 0.0035 | 0.0045 | 0 |
| 240 | 380 | 335 | 166 | 50 | 0.000601 | 0.0022 | 0.0041 | 0 |
| | 390 | 243 | 212 | 53 | 0.000601 | 0.0029 | 0.0044 | 0 |
| | 400 | 205 | 244 | 44 | 0.000535 | 0.0033 | 0.0045 | 0 |
| | 410 | 187 | 271 | 84 | 0.000614 | 0.0036 | 0.0045 | 0 |
| | 420 | 173 | 279 | 91 | 0.000614 | 0.0037 | 0.0046 | 0 |

| Reynolds Number Standard Deviations | | | | | | | | |
|---|---|---|---|---|---|---|---|---|
| HEX2 | | | | | | | | |
| Pressure (Bar) | Hot Line Inlet | Hot Line | | | Cold Line | | | |
| | | T1 In | T2 Middle | T3 Out | T4 In | T6 Middle | T8 Out | |
| 225 | 380 | 11 | 16 | 1 | 0.000003 | 0.000184 | 0.000058 | |
| | 390 | 5 | 3 | 2 | 0.000010 | 0.000041 | 0.000006 | |
| | 400 | 8 | 5 | 8 | 0.000003 | 0.000065 | 0.000006 | |
| | 410 | 5 | 3 | 8 | 0.000002 | 0.000038 | 0.000006 | |
| | 420 | 4 | 3 | 3 | 0.000003 | 0.000018 | 0.000006 | |
| 230 | 380 | 4 | 10 | 1 | 0.000002 | 0.000130 | 0.000026 | |
| | 390 | 7 | 2 | 1 | 0.000005 | 0.000025 | 0.000006 | |
| 240 | 380 | 11 | 1 | 0 | 0.000003 | 0.000015 | 0.000025 | |
| | 390 | 3 | 10 | 1 | 0.000006 | 0.000095 | 0.000019 | |
| | 400 | 5 | 5 | 4 | 0.000004 | 0.000074 | 0.000009 | |
| | 410 | 3 | 1 | 1 | 0.000004 | 0.000020 | 0.000007 | |
| | 420 | 4 | 2 | 3 | 0.000002 | 0.000026 | 0.000006 | |

The maximum and minimum values of the Reynolds number are shown in Table 25.

Table 25: Reynolds Number Summary Table

| | REYNOLDS NUMBER | | | | | |
|---|---|---|---|---|---|---|
| | HOT | | COLD | | OVERALL | |
| | Max Re | Min Re | Max Re | Min Re | Max Re | Min Re |
| HEX1 | 322.9 | 46.3 | 0.0031 | 0.00039 | 322.9 | 0.00039 |
| HEX2 | 335.1 | 44.4 | 0.0046 | 0.00053 | 335.1 | 0.00053 |

| | REYNOLDS NUMBER STD | | | | | |
|---|---|---|---|---|---|---|
| | HOT | | COLD | | OVERALL | |
| | Max Re | Min Re | Max Re | Min Re | Max Re | Min Re |
| HEX1 | 26.6 | 0.2661 | 0.00022 | 0.00000027 | 26.6 | 0.0000003 |
| HEX2 | 15.7 | 0.3965 | 0.00018 | 0.00000169 | 15.7 | 0.0000017 |

The graphs shown in Figures 95 and 96 are a visual representation of the data shown in Tables 23 and 24. The maximum value of the Reynolds number in HEX2 was close to 335. The minimum Reynolds number values were close to zero and found in the cold side of the HEX, this is because the flow area in

the annulus region is larger than in the central tube. All flows are found to be less than 2300 which means the flow is very laminar.

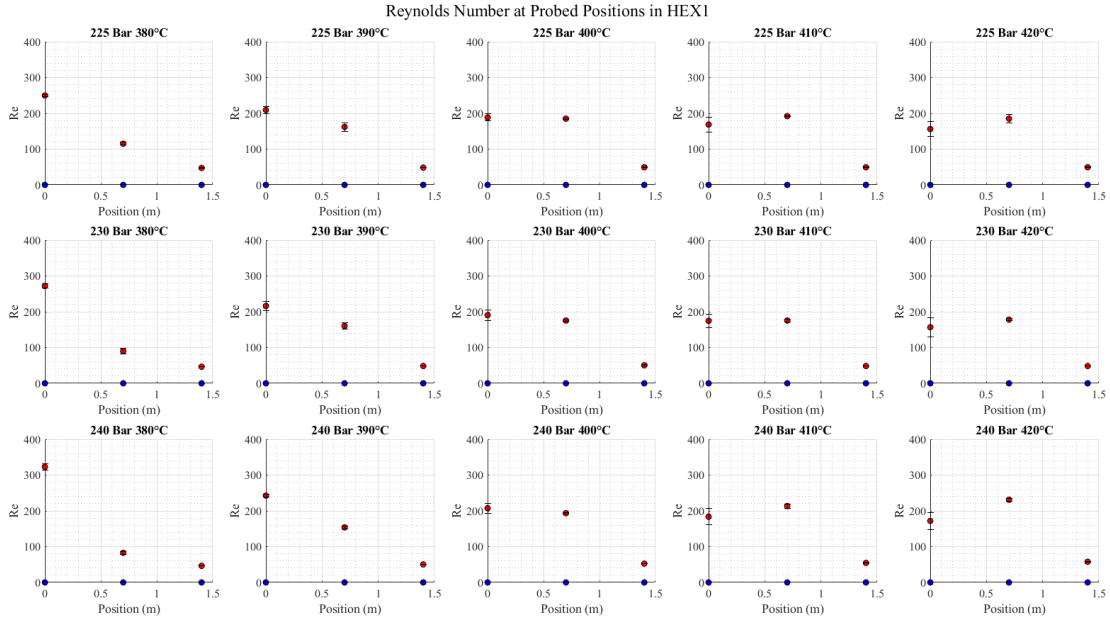


Figure 97: Reynolds Number at Probed Positions in HEX1

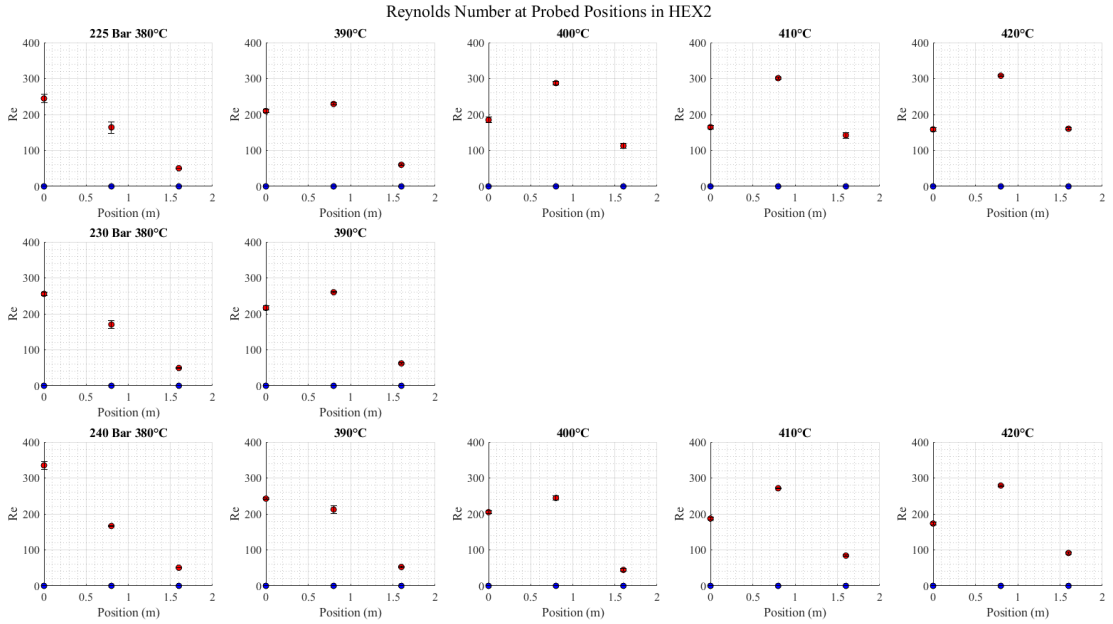


Figure 98: Reynolds Number at Probed Positions in HEX2

HEX1 & HEX2 PRANDTL NUMBER

Figure 26 and Figure 27 show the Prandtl numbers at the probed points along HEX1 and HEX2. The Prandtl number values were found using REFPROP at all the temperatures recorded during an experiment. This list of 21 values was then averaged and standard deviation was also calculated. The standard deviation is shown as the error bars on each point. Table 28 shows the Prandtl number summary for HEX1 and HEX2.

Table 26: Prandtl Number and Prandtl Number Standard Deviations for HEX1

| Prandtl Number | | | | | | | | |
|---|---|---|---|---|---|---|---|---|
| HEX1 | | | | | | | | |
| Pressure (Bar) | Hot Line Inlet Set Point | Hot Line | | | Cold Line | | | Salinity of Cold Line (%wt NaCl) |
| | | T1 In | T2 Middle | T3 Out | T6 In | T8 Middle | T10 Out | |
| 225 | 380 | 3.517 | 2.065 | 5.633 | 6.0614 | 2.4908 | 1.1474 | 0 |
| | 390 | 2.234 | 1.421 | 5.500 | 6.0614 | 1.6247 | 1.7263 | 0 |
| | 400 | 1.893 | 1.226 | 5.373 | 6.2158 | 3.4316 | 1.9604 | 0 |
| | 410 | 1.650 | 1.177 | 5.373 | 6.2158 | 3.3126 | 2.1261 | 0 |
| | 420 | 1.521 | 1.226 | 5.373 | 6.0473 | 1.3737 | 2.3492 | 0 |
| 230 | 380 | 4.764 | 2.722 | 5.766 | 6.0567 | 3.2544 | 0.9231 | 0 |
| | 390 | 2.315 | 1.433 | 5.496 | 6.0567 | 1.6493 | 1.6255 | 0 |
| | 400 | 1.880 | 1.299 | 5.246 | 5.9084 | 1.4581 | 1.9232 | 0 |
| | 410 | 1.691 | 1.299 | 5.496 | 6.0567 | 1.4581 | 1.9232 | 0 |
| | 420 | 1.507 | 1.280 | 5.496 | 6.0567 | 1.4328 | 1.8045 | 0 |
| 240 | 380 | 10.729 | 2.990 | 5.757 | 6.0473 | 3.5530 | 0.8464 | 0 |
| | 390 | 2.816 | 1.498 | 5.239 | 5.8995 | 1.7004 | 1.1865 | 0 |
| | 400 | 2.060 | 1.169 | 5.007 | 5.8995 | 1.2700 | 1.4327 | 0 |
| | 410 | 1.744 | 1.057 | 4.791 | 6.0473 | 1.1187 | 1.3898 | 0 |
| | 420 | 1.615 | 0.978 | 4.493 | 6.0473 | 1.0199 | 1.3514 | 0 |
| 230 | 410 | 1.575 | 1.498 | 5.496 | N/A | N/A | N/A | 3.5% |
| | 410 | 1.551 | 1.498 | 5.496 | N/A | N/A | N/A | 7.5% |
| | 410 | 1.497 | 1.351 | 5.246 | N/A | N/A | N/A | 14% |

| Prandtl Number Standard Deviation | | | | | | | |
|---|---|---|---|---|---|---|---|
| HEX1 | | | | | | | |
| Pressure (Bar) | Hot Line Inlet Set Point | Hot Line | | | Cold Line | | |
| | | T1 In | T2 Middle | T3 Out | T6 In | T8 Middle | T10 Out |
| 225 | 380 | 0.179 | 0.087 | 0.085 | 0.080 | 0.122 | 0.024 |
| | 390 | 0.211 | 0.121 | 0.058 | 0.039 | 0.171 | 0.097 |
| | 400 | 0.142 | 0.015 | 0.015 | 0.047 | 0.021 | 0.101 |
| | 410 | 0.243 | 0.011 | 0.136 | 0.032 | 0.010 | 0.167 |
| | 420 | 0.210 | 0.083 | 0.114 | 0.019 | 0.115 | 0.342 |
| 230 | 380 | 0.605 | 0.346 | 0.057 | 0.070 | 0.251 | 0.007 |
| | 390 | 0.333 | 0.088 | 0.058 | 0.040 | 0.130 | 0.291 |
| | 400 | 0.219 | 0.014 | 0.233 | 0.038 | 0.014 | 0.141 |
| | 410 | 0.221 | 0.030 | 0.034 | 0.034 | 0.016 | 0.153 |
| | 420 | 0.277 | 0.021 | 0.038 | 0.033 | 0.026 | 0.133 |
| 240 | 380 | 1.272 | 0.172 | 0.041 | 0.028 | 0.160 | 0.003 |
| | 390 | 0.134 | 0.036 | 0.032 | 0.022 | 0.047 | 0.031 |
| | 400 | 0.225 | 0.013 | 0.039 | 0.030 | 0.015 | 0.068 |
| | 410 | 0.277 | 0.028 | 0.104 | 0.038 | 0.034 | 0.080 |
| | 420 | 0.260 | 0.015 | 0.100 | 0.029 | 0.019 | 0.084 |

Table 27: Prandtl Number and Prandtl Number Standard Deviations for HEX2

| Prandtl Number | | | | | | | | |
|---|---|---|---|---|---|---|---|---|
| HEX2 | | | | | | | | |
| Pressure (Bar) | Hot Line Inlet Set Point | Hot Line | | | Cold Line | | | Salinity of Cold Line (%wt NaCl) |
| | | T1 In | T2 Middle | T3 Out | T4 In | T6 Middle | T8 Out | |
| 225 | 380 | 3.229 | 1.397 | 5.250 | 6.061 | 1.385 | 0.814 | 0 |
| | 390 | 2.234 | 0.987 | 4.317 | 6.061 | 0.970 | 0.965 | 0 |
| | 400 | 1.842 | 0.824 | 2.118 | 5.770 | 0.820 | 1.006 | 0 |
| | 410 | 1.607 | 0.810 | 1.633 | 5.770 | 0.958 | 1.058 | 0 |
| | 420 | 1.544 | 0.808 | 1.433 | 5.770 | 0.809 | 1.058 | 0 |
| 230 | 380 | 3.602 | 1.341 | 5.369 | 6.057 | 1.362 | 0.810 | 0 |
| | 390 | 2.315 | 0.881 | 4.143 | 5.908 | 0.876 | 0.989 | 0 |
| 240 | 380 | 6.810 | 1.373 | 5.239 | 5.900 | 1.408 | 0.806 | 0 |
| | 390 | 2.816 | 1.063 | 5.007 | 5.900 | 1.046 | 0.865 | 0 |
| | 400 | 2.024 | 0.928 | 4.223 | 6.047 | 0.921 | 0.930 | 0 |
| | 410 | 1.783 | 0.852 | 2.942 | 5.757 | 0.844 | 0.898 | 0 |
| | 420 | 1.629 | 0.836 | 2.679 | 5.757 | 0.829 | 1.049 | 0 |

| Prandtl Number Standard Deviation | | | | | | | | |
|---|---|---|---|---|---|---|---|---|
| HEX2 | | | | | | | | |
| Pressure (Bar) | Hot Line Inlet Set Point | Hot Line | | | Cold Line | | | |
| | | T1 In | T2 Middle | T3 Out | T4 In | T6 Middle | T8 Out | |
| 225 | 380 | 0.256 | 0.071 | 0.094 | 0.034 | 0.054 | 0.039 | |
| | 390 | 0.105 | 0.008 | 0.180 | 0.115 | 0.007 | 0.014 | |
| | 400 | 0.118 | 0.006 | 0.168 | 0.032 | 0.006 | 0.013 | |
| | 410 | 0.055 | 0.002 | 0.109 | 0.018 | 0.001 | 0.017 | |
| | 420 | 0.044 | 0.001 | 0.027 | 0.032 | 0.001 | 0.018 | |
| 230 | 380 | 0.278 | 0.092 | 0.139 | 0.024 | 0.093 | 0.001 | |
| | 390 | 0.155 | 0.004 | 0.101 | 0.053 | 0.005 | 0.012 | |
| 240 | 380 | 2.084 | 0.010 | 0.046 | 0.036 | 0.011 | 0.001 | |
| | 390 | 0.078 | 0.056 | 0.154 | 0.061 | 0.036 | 0.010 | |
| | 400 | 0.073 | 0.180 | 0.310 | 0.042 | 0.019 | 0.010 | |
| | 410 | 0.040 | 0.003 | 0.043 | 0.041 | 0.003 | 0.016 | |
| | 420 | 0.042 | 0.004 | 0.111 | 0.027 | 0.003 | 0.019 | |

Table 28: Prandtl Number Summary Table

| | PRANDTL NUMBER | | | | | |
|---|---|---|---|---|---|---|
| | HOT | | COLD | | OVERALL | |
| | Max Pr | Min Pr | Max Pr | Min Pr | Max Pr | Min Pr |
| HEX1 | 10.73 | 0.98 | 0.85 | 6.22 | 10.73 | 0.85 |
| HEX2 | 6.81 | 0.81 | 0.81 | 6.06 | 6.81 | 0.81 |

| | PRANDTL NUMBER STD | | | | | |
|---|---|---|---|---|---|---|
| | HOT | | COLD | | OVERALL | |
| | Max Pr | Min Pr | Max Pr | Min Pr | Max Pr | Min Pr |
| HEX1 | 1.3 | 0.0107 | 0.3419 | 0.0033 | 1.2717 | 0.0033 |
| HEX2 | 2.1 | 0.0009 | 0.1151 | 0.0006 | 2.0843 | 0.0006 |

The graphs shown in Figures 99 and 100 are representative of the data shown in Tables 26 and 27.

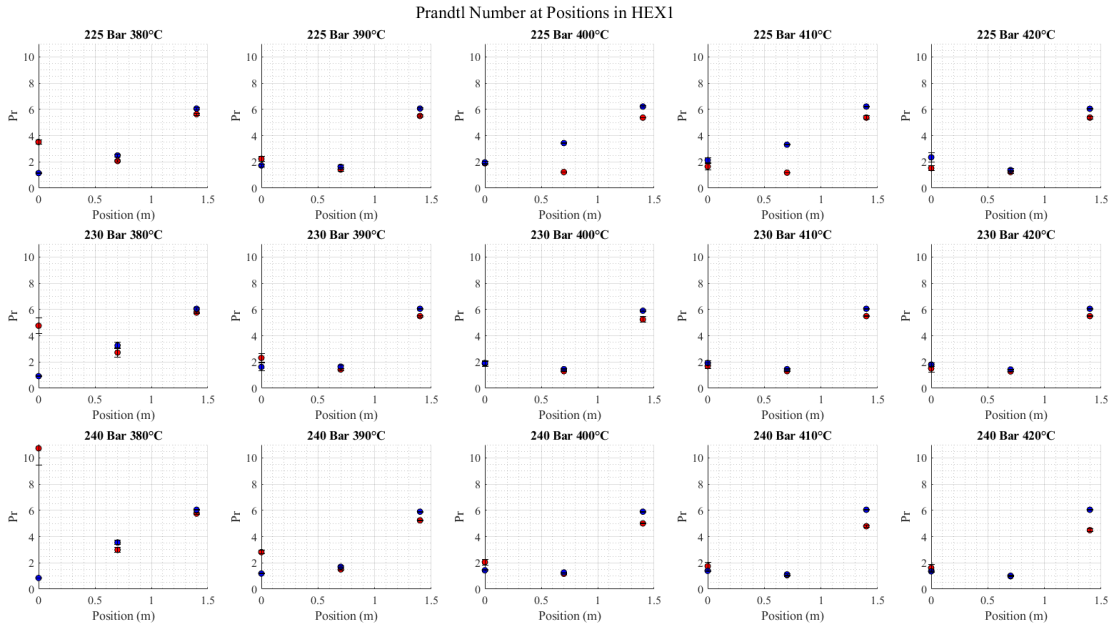


Figure 99: Prandtl Numbers at probed positions in HEX1

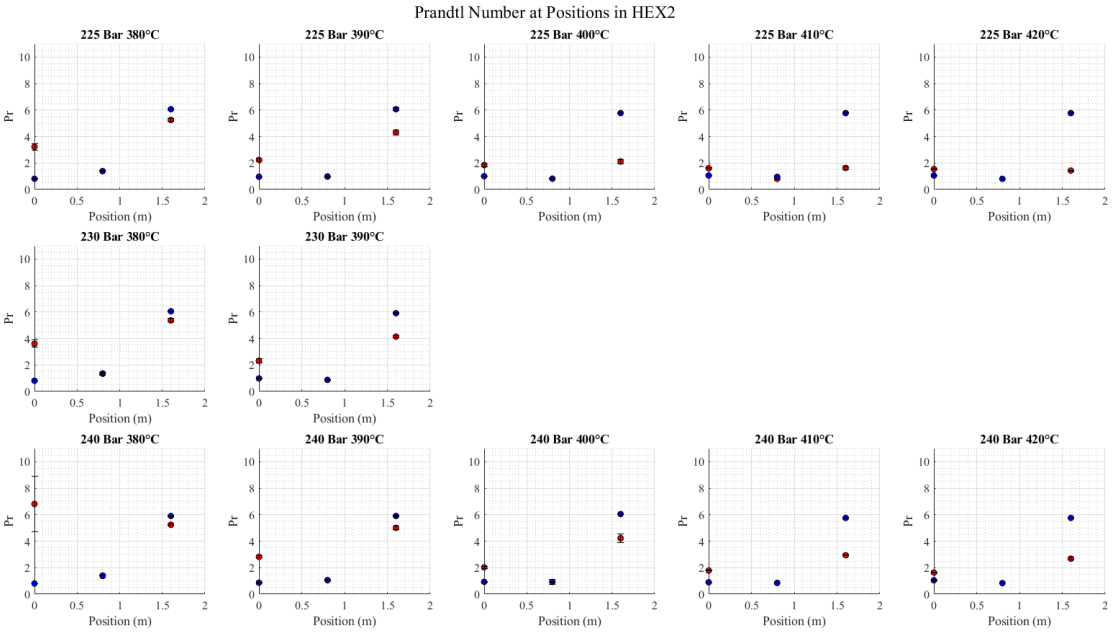


Figure 100: Prandtl Numbers at probed positions in HEX2

HEX1 & HEX2 CONDUCTIVE HEAT TRANSFER COEFFICIENT

The conductive heat transfer coefficient or *k* value describes how well a material transfers heat conductively through physical contact. Liquids, solids, and gases all have a conductive heat transfer

coefficient. The validity of using *k* is to be determined by the Nusselt number. If *Nu* is greater than 1 then there is more convective heat transfer if *Nu* is lower than 1 there is more conductive heat transfer. Tables 29 and 30 show the conductive heat transfer coefficient values for $H_2O$ in HEX1 and HEX2.

Table 29: Conductive Heat Transfer Coefficient and Standard Deviations for HEX1

| Thermal Conductivity of $H_2O$ W/m·K | | | | | | | | |
|---|---|---|---|---|---|---|---|---|
| HEX1 | | | | | | | | |
| Pressure (Bar) | Hot Line Inlet Set Point | Hot Line | | | Cold Line | | | Salinity of Cold Line (%wt NaCl) |
| | | T1 | T2 | T3 | T6 | T8 | T10 | |
| | | In | Middle | Out | In | Middle | Out | |
| 225 | 380 | 0.2150 | 0.6820 | 0.6219 | 0.6172 | 0.6722 | 0.4768 | 0 |
| | 390 | 0.6735 | 0.6957 | 0.6234 | 0.6172 | 0.6920 | 0.4324 | 0 |
| | 400 | 0.1267 | 0.6967 | 0.6249 | 0.6156 | 0.6964 | 0.4258 | 0 |
| | 410 | 0.1134 | 0.6962 | 0.6249 | 0.6156 | 0.6968 | 0.4227 | 0 |
| | 420 | 0.1070 | 0.6967 | 0.6249 | 0.6172 | 0.6963 | 0.4199 | 0 |
| 230 | 380 | 0.2703 | 0.6673 | 0.6206 | 0.6175 | 0.6566 | 0.5234 | 0 |
| | 390 | 0.1542 | 0.6958 | 0.6236 | 0.6175 | 0.6919 | 0.4348 | 0 |
| | 400 | 0.1279 | 0.6971 | 0.6266 | 0.6190 | 0.6955 | 0.4247 | 0 |
| | 410 | 0.1172 | 0.6971 | 0.6236 | 0.6175 | 0.6955 | 0.4247 | 0 |
| | 420 | 0.1078 | 0.6971 | 0.6236 | 0.6175 | 0.6958 | 0.4281 | 0 |
| 240 | 380 | 0.4464 | 0.6622 | 0.6211 | 0.6180 | 0.6516 | 0.5599 | 0 |
| | 390 | 0.1901 | 0.6954 | 0.6271 | 0.6196 | 0.6913 | 0.4657 | 0 |
| | 400 | 0.1432 | 0.6971 | 0.6300 | 0.0620 | 0.6978 | 0.4426 | 0 |
| | 410 | 0.1236 | 0.6936 | 0.6328 | 0.0618 | 0.6960 | 0.4458 | 0 |
| | 420 | 0.1162 | 0.6882 | 0.6369 | 0.0618 | 0.6960 | 0.4488 | 0 |
| 230 | 410 | 0.11110 | 0.69483 | 0.62363 | N/A | N/A | N/A | 3.5% |
| | 410 | 0.10989 | 0.69483 | 0.62363 | N/A | N/A | N/A | 7.5% |
| | 410 | 0.10728 | 0.69677 | 0.62659 | N/A | N/A | N/A | 14% |

| Standard Deviation of Thermal Conductivity of $H_2O$ W/m·K | | | | | | | | |
|---|---|---|---|---|---|---|---|---|
| HEX1 | | | | | | | | |
| Pressure (Bar) | Hot Line Inlet Set Point | Hot Line | | | Cold Line | | | Salinity of Cold Line (%wt NaCl) |
| | | T1 | T2 | T3 | T6 | T8 | T10 | |
| | | In | Middle | Out | In | Middle | Out | |
| 225 | 380 | 0.00820 | 0.00206 | 0.00095 | 0.00083 | 0.00271 | 0.00348 | 0 |
| | 390 | 0.01235 | 0.00182 | 0.00067 | 0.00040 | 0.00367 | 0.00333 | 0 |
| | 400 | 0.00815 | 0.00009 | 0.00048 | 0.00048 | 0.00020 | 0.00233 | 0 |
| | 410 | 0.01292 | 0.00016 | 0.00153 | 0.00032 | 0.00003 | 0.00279 | 0 |
| | 420 | 0.01026 | 0.00033 | 0.00133 | 0.00052 | 0.00149 | 0.00184 | 0 |
| 230 | 380 | 0.01196 | 0.00033 | 0.00133 | 0.00052 | 0.00149 | 0.00304 | 0 |
| | 390 | 0.01921 | 0.00141 | 0.00067 | 0.00042 | 0.00284 | 0.05690 | 0 |
| | 400 | 0.01286 | 0.00005 | 0.00307 | 0.00041 | 0.00021 | 0.00360 | 0 |
| | 410 | 0.01221 | 0.00023 | 0.00039 | 0.00036 | 0.00024 | 0.00327 | 0 |
| | 420 | 0.01418 | 0.00005 | 0.00044 | 0.00034 | 0.00036 | 0.00442 | 0 |
| 240 | 380 | 0.01845 | 0.00338 | 0.00045 | 0.00029 | 0.00276 | 0.00230 | 0 |
| | 390 | 0.00775 | 0.00062 | 0.00039 | 0.00024 | 0.00105 | 0.00391 | 0 |
| | 400 | 0.01423 | 0.00019 | 0.00049 | 0.00032 | 0.00001 | 0.00469 | 0 |
| | 410 | 0.01641 | 0.00144 | 0.00136 | 0.00040 | 0.00098 | 0.00578 | 0 |
| | 420 | 0.01482 | 0.00153 | 0.00143 | 0.00031 | 0.00126 | 0.00828 | 0 |

Table 30: Conductive Heat Transfer Coefficient and Standard Deviations for HEX2

| Thermal Conductivity of $H_2O$ W/m·K | | | | | | | | |
|---|---|---|---|---|---|---|---|---|
| HEX2 | | | | | | | | |
| Pressure (Bar) | Hot Line Inlet Set Point | Hot Line | | | Cold Line | | | Salinity of Cold Line (%wt NaCl) |
| | | T1 | T2 | T3 | T4 | T6 | T8 | |
| | | In | Middle | Out | In | Middle | Out | |
| 225 | 380 | 0.2013 | 0.6960 | 0.6263 | 0.6172 | 0.6961 | 0.5955 | 0 |
| | 390 | 0.1467 | 0.6880 | 0.6387 | 0.6172 | 0.6863 | 0.5104 | 0 |
| | 400 | 0.1238 | 0.6453 | 0.6808 | 0.6203 | 0.6414 | 0.4998 | 0 |
| | 410 | 0.1112 | 0.6259 | 0.6920 | 0.6203 | 0.6191 | 0.4885 | 0 |
| | 420 | 0.1081 | 0.6144 | 0.6955 | 0.6203 | 0.6071 | 0.4885 | 0 |
| 230 | 380 | 0.2223 | 0.6969 | 0.6251 | 0.6175 | 0.6967 | 0.1009 | 0 |
| | 390 | 0.1542 | 0.6716 | 0.6416 | 0.6188 | 0.6703 | 0.5032 | 0 |
| 240 | 380 | 0.4252 | 0.6972 | 0.6271 | 0.6188 | 0.6967 | 0.6137 | 0 |
| | 390 | 0.1901 | 0.6939 | 0.6300 | 0.6196 | 0.6930 | 0.5485 | 0 |
| | 400 | 0.1409 | 0.6821 | 0.6408 | 0.6180 | 0.6810 | 0.5197 | 0 |
| | 410 | 0.1259 | 0.6630 | 0.6632 | 0.6211 | 0.6598 | 0.4970 | 0 |
| | 420 | 0.1170 | 0.6557 | 0.6687 | 0.6211 | 0.6513 | 0.4880 | 0 |

| Standard Deviation of Thermal Conductivity of $H_2O$ W/m·K | | | | | | | | |
|---|---|---|---|---|---|---|---|---|
| HEX2 | | | | | | | | |
| Pressure (Bar) | Hot Line Inlet Set Point | Hot Line | | | Cold Line | | | Salinity of Cold Line (%wt NaCl) |
| | | T1 | T2 | T3 | T4 | T6 | T8 | |
| | | In | Middle | Out | In | Middle | Out | |
| 225 | 380 | 0.03867 | 0.00314 | 0.00110 | 0.00032 | 0.00236 | 0.00853 | 0 |
| | 390 | 0.00621 | 0.00232 | 0.00277 | 0.00123 | 0.00263 | 0.00317 | 0 |
| | 400 | 0.00683 | 0.00583 | 0.00395 | 0.00035 | 0.00658 | 0.00310 | 0 |
| | 410 | 0.00281 | 0.00409 | 0.00233 | 0.00020 | 0.00505 | 0.00334 | 0 |
| | 420 | 0.00216 | 0.00497 | 0.00038 | 0.00035 | 0.00277 | 0.00346 | 0 |
| 230 | 380 | 0.01201 | 0.00103 | 0.00164 | 0.00026 | 0.00119 | 0.00411 | 0 |
| | 390 | 0.01201 | 0.00103 | 0.00164 | 0.00026 | 0.00119 | 0.00411 | 0 |
| 240 | 380 | 0.01309 | 0.00010 | 0.00056 | 0.00038 | 0.00014 | 0.00393 | 0 |
| | 390 | 0.00446 | 0.00220 | 0.00197 | 0.00067 | 0.00178 | 0.00557 | 0 |
| | 400 | 0.00466 | 0.00277 | 0.00463 | 0.00045 | 0.00305 | 0.00362 | 0 |
| | 410 | 0.00239 | 0.00108 | 0.00087 | 0.00045 | 0.00144 | 0.00387 | 0 |
| | 420 | 0.00388 | 0.00195 | 0.00239 | 0.00029 | 0.00221 | 0.00388 | 0 |

The graphs shown in Figures 101 and 102 are a visual representation of the data shown in Tables 29 and 30.

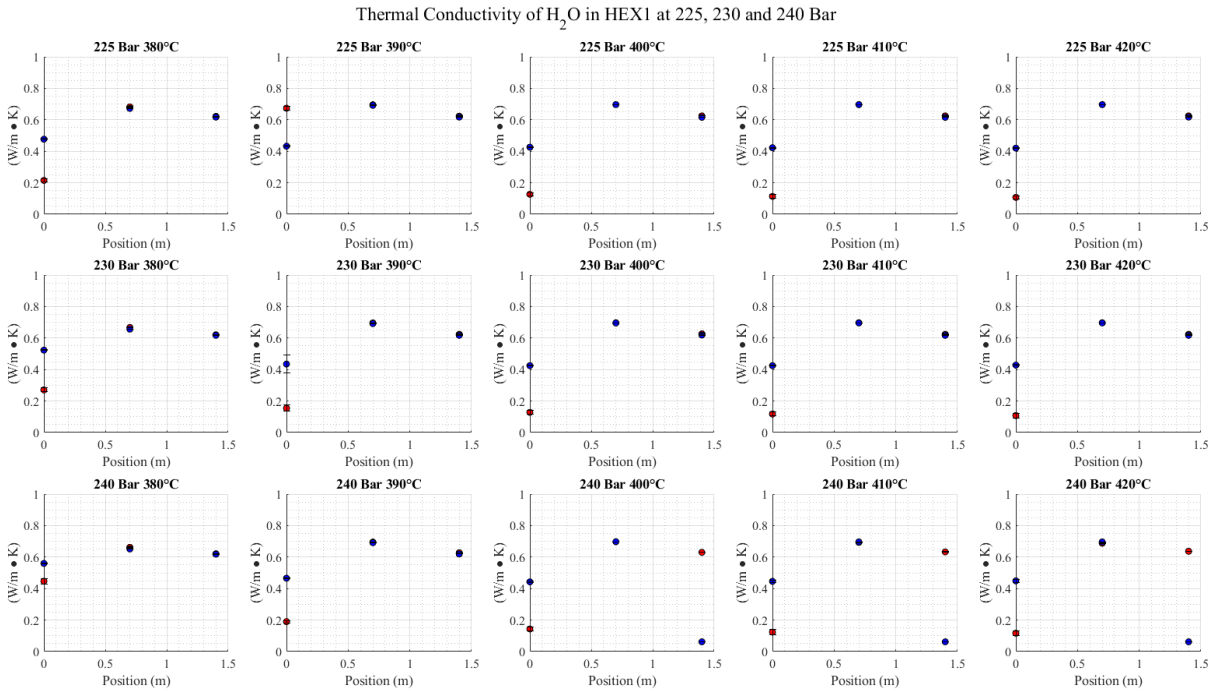


Figure 101: Thermal Conductivity of $H_2O$ in HEX1 at 225, 230 and 240 Bar

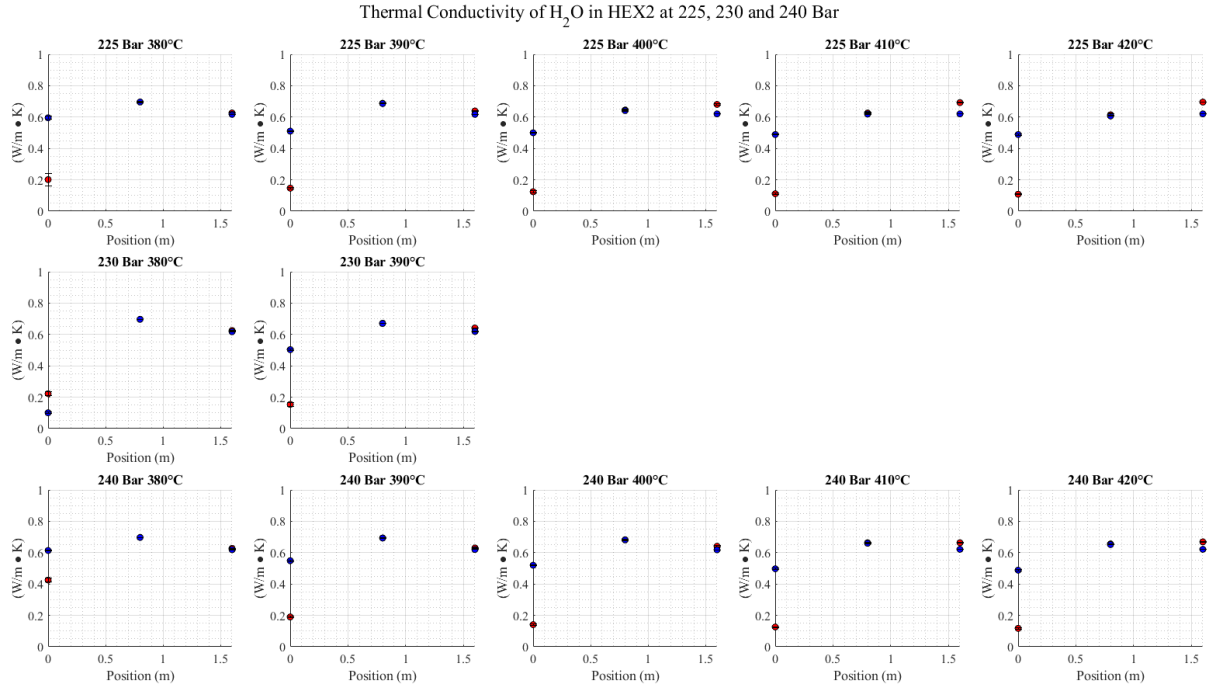


Figure 102: Thermal Conductivity of $H_2O$ in HEX2 at 225, 230 and 240 Bar

HEX1 & HEX2 SPECIFIC HEAT

The specific heat of the hot and cold fluid is shown in Figures 31 and 32. Like the Prandtl number these values were found by entering the recorded temperatures and pressures into REFPROP using 21 different temperatures and pressures collected when the HEX's reached steady state.

Table 31: Specific Heat Capacity and Standard Deviations for HEX1

| Specific Heat Capacity of $H_2O$ (kJ/kg·K) | | | | | | | | |
|---|---|---|---|---|---|---|---|---|
| HEX1 | | | | | | | | |
| Pressure (Bar) | Hot Line Inlet Set Point | Hot Line | | | Cold Line | | | Salinity of Cold Line (%wt NaCl) |
| | | T1 In | T2 Middle | T3 Out | T6 In | T8 Middle | T10 Out | |
| 225 | 380 | 26.134 | 4.154 | 4.122 | 4.121 | 4.145 | 7.802 | 0 |
| | 390 | 11.925 | 4.192 | 4.122 | 4.121 | 4.173 | 12.253 | 0 |
| | 400 | 8.799 | 4.222 | 4.123 | 4.121 | 4.199 | 14.128 | 0 |
| | 410 | 6.842 | 4.234 | 4.123 | 4.121 | 4.208 | 15.484 | 0 |
| | 420 | 5.909 | 4.222 | 4.123 | 4.121 | 4.197 | 17.350 | 0 |
| 230 | 380 | 44.948 | 4.140 | 4.121 | 4.120 | 4.134 | 6.081 | 0 |
| | 390 | 12.794 | 4.189 | 4.121 | 4.120 | 4.171 | 11.454 | 0 |
| | 400 | 8.729 | 4.207 | 4.122 | 4.120 | 4.187 | 13.816 | 0 |
| | 410 | 7.192 | 4.207 | 4.121 | 4.120 | 4.187 | 13.816 | 0 |
| | 420 | 5.835 | 4.210 | 4.121 | 4.120 | 4.189 | 12.864 | 0 |
| 240 | 380 | 116.996 | 4.135 | 4.118 | 4.117 | 4.129 | 5.425 | 0 |
| | 390 | 18.228 | 4.181 | 4.120 | 4.118 | 4.166 | 8.090 | 0 |
| | 400 | 10.437 | 4.232 | 4.121 | 4.118 | 4.210 | 9.952 | 0 |
| | 410 | 7.677 | 4.269 | 4.122 | 4.117 | 4.246 | 9.625 | 0 |
| | 420 | 6.672 | 4.313 | 4.123 | 4.117 | 4.288 | 9.334 | 0 |
| 230 | 410 | 6.320 | 4.183 | 4.121 | N/A | N/A | N/A | 3.5% |
| | 410 | 6.146 | 4.183 | 4.121 | N/A | N/A | N/A | 7.5% |
| | 410 | 5.765 | 4.199 | 4.122 | N/A | N/A | N/A | 14% |

| Specific Heat Capacity Standard Deviations of $H_2O$ (kJ/kg·K) | | | | | | | | |
|---|---|---|---|---|---|---|---|---|
| HEX1 | | | | | | | | |
| Pressure (Bar) | Hot Line Inlet Set Point | Hot Line | | | Cold Line | | | Salinity of Cold Line (%wt NaCl) |
| | | T1 In | T2 Middle | T3 Out | T6 In | T8 Middle | T10 Out | |
| 225 | 380 | 2.161 | 0.002 | 0.000 | 0.00018 | 0.00204 | 0.18221 | 0 |
| | 390 | 2.108 | 0.013 | 0.000 | 0.00009 | 0.01018 | 0.77278 | 0 |
| | 400 | 1.229 | 0.003 | 0.000 | 0.00011 | 0.00276 | 0.81427 | 0 |
| | 410 | 1.922 | 0.003 | 0.000 | 0.00007 | 0.00160 | 1.37898 | 0 |
| | 420 | 1.544 | 0.015 | 0.000 | 0.00012 | 0.01324 | 2.95956 | 0 |
| 230 | 380 | 8.216 | 0.004 | 0.000 | 0.00018 | 0.00222 | 0.05448 | 0 |
| | 390 | 3.516 | 0.008 | 0.000 | 0.00010 | 0.00724 | 1.75368 | 0 |
| | 400 | 1.930 | 0.002 | 0.001 | 0.00010 | 0.00138 | 1.14249 | 0 |
| | 410 | 1.776 | 0.004 | 0.000 | 0.00008 | 0.00164 | 1.25227 | 0 |
| | 420 | 2.091 | 0.004 | 0.000 | 0.00008 | 0.00278 | 1.05523 | 0 |
| 240 | 380 | 18.150 | 0.002 | 0.000 | 0.00007 | 0.00125 | 0.03213 | 0 |
| | 390 | 1.480 | 0.003 | 0.000 | 0.00006 | 0.00259 | 0.23224 | 0 |
| | 400 | 2.124 | 0.003 | 0.000 | 0.00009 | 0.00268 | 0.51561 | 0 |
| | 410 | 2.306 | 0.012 | 0.000 | 0.00010 | 0.01101 | 0.60792 | 0 |
| | 420 | 2.074 | 0.011 | 0.001 | 0.00008 | 0.01064 | 0.63359 | 0 |
| 230 | 410 | 3.176 | 2.082 | 2.051 | N/A | N/A | N/A | 3.5% |
| | 410 | 3.197 | 2.082 | 2.051 | N/A | N/A | N/A | 7.5% |
| | 410 | 2.994 | 2.092 | 2.051 | N/A | N/A | N/A | 14% |

Table 32: Specific Heat Capacity and Standard Deviations for HEX2

| Specific Heat Capacity of $H_2O$ (kJ/kg·K) | | | | | | | | |
|---|---|---|---|---|---|---|---|---|
| HEX2 | | | | | | | | |
| Pressure (Bar) | Hot Line Inlet Set Point | Hot Line | | | Cold Line | | | Salinity of Cold Line (%wt NaCl) |
| | | T1 In | T2 Middle | T3 Out | T4 In | T6 Middle | T8 Out | |
| 225 | 380 | 22.707 | 4.195 | 4.123 | 4.121 | 4.196 | 5.016 | 0 |
| | 390 | 11.925 | 4.313 | 4.127 | 4.121 | 4.325 | 6.413 | 0 |
| | 400 | 8.366 | 4.601 | 4.153 | 4.122 | 4.628 | 6.725 | 0 |
| | 410 | 6.519 | 4.746 | 4.173 | 4.122 | 4.801 | 7.127 | 0 |
| | 420 | 6.066 | 4.840 | 4.190 | 4.122 | 4.905 | 7.127 | 0 |
| 230 | 380 | 27.206 | 4.201 | 4.122 | 4.120 | 4.198 | 4.944 | 0 |
| | 390 | 12.794 | 4.424 | 4.127 | 4.120 | 4.433 | 6.598 | 0 |
| 240 | 380 | 62.967 | 4.194 | 4.120 | 4.118 | 4.190 | 4.841 | 0 |
| | 390 | 18.228 | 4.267 | 4.121 | 4.118 | 4.274 | 5.594 | 0 |
| | 400 | 10.102 | 4.356 | 4.125 | 4.117 | 4.363 | 6.137 | 0 |
| | 410 | 8.000 | 4.480 | 4.135 | 4.118 | 4.501 | 6.743 | 0 |
| | 420 | 6.778 | 4.528 | 4.139 | 4.118 | 4.558 | 7.052 | 0 |

| Specific Heat Capacity Standard Deviations of $H_2O$ (kJ/kg·K) | | | | | | | | |
|---|---|---|---|---|---|---|---|---|
| HEX2 | | | | | | | | |
| Pressure (Bar) | Hot Line Inlet Set Point | Hot Line | | | Cold Line | | | Salinity of Cold Line (%wt NaCl) |
| | | T1 In | T2 Middle | T3 Out | T4 In | T6 Middle | T8 Out | |
| 225 | 380 | 15.8803 | 0.0152 | 0.0003 | 0.000074 | 0.014167 | 0.076104 | 0 |
| | 390 | 1.0316 | 0.0152 | 0.0011 | 0.000287 | 0.017265 | 0.106710 | 0 |
| | 400 | 1.0514 | 0.0416 | 0.0046 | 0.000086 | 0.048155 | 0.100880 | 0 |
| | 410 | 0.4116 | 0.0322 | 0.0065 | 0.000048 | 0.041852 | 0.127637 | 0 |
| | 420 | 0.3183 | 0.0044 | 0.0029 | 0.000085 | 0.025133 | 0.136598 | 0 |
| 230 | 380 | 3.4529 | 0.0116 | 0.0005 | 0.000061 | 0.010911 | 0.037737 | 0 |
| | 390 | 1.6186 | 0.0077 | 0.0006 | 0.000140 | 0.009005 | 0.092885 | 0 |
| 240 | 380 | 28.0798 | 0.0012 | 0.0002 | 0.000101 | 0.001225 | 0.035384 | 0 |
| | 390 | 0.8593 | 0.0213 | 0.0007 | 0.000180 | 0.015781 | 0.087250 | 0 |
| | 400 | 0.6808 | 0.0185 | 0.0018 | 0.000116 | 0.020270 | 0.082017 | 0 |
| | 410 | 0.3299 | 0.0071 | 0.0005 | 0.000124 | 0.009449 | 0.121463 | 0 |
| | 420 | 0.3218 | 0.0130 | 0.0016 | 0.000079 | 0.014936 | 0.141570 | 0 |

The graphs in Figures 108 and 109 are a visual representation of the data shown in Tables 31 and 32 for HEX1 and HEX2.

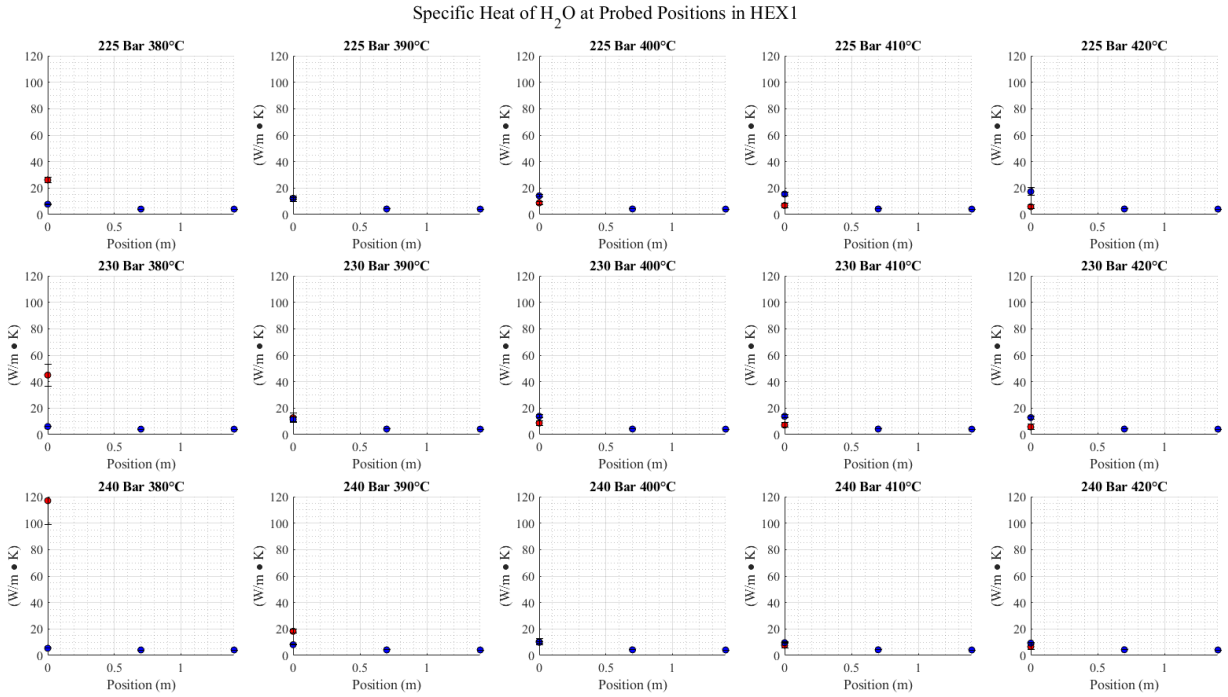


Figure 103: Specific Heat of $H_2O$ at probed positions in HEX1

The highest specific heat occurred at the hot line entrance of the 240 Bar 380°C inlet temperature case of HEX1. The specific heat is increasing as the pressure increases if the inlet temperature is 380°C as shown in both HEX1 and HEX2.

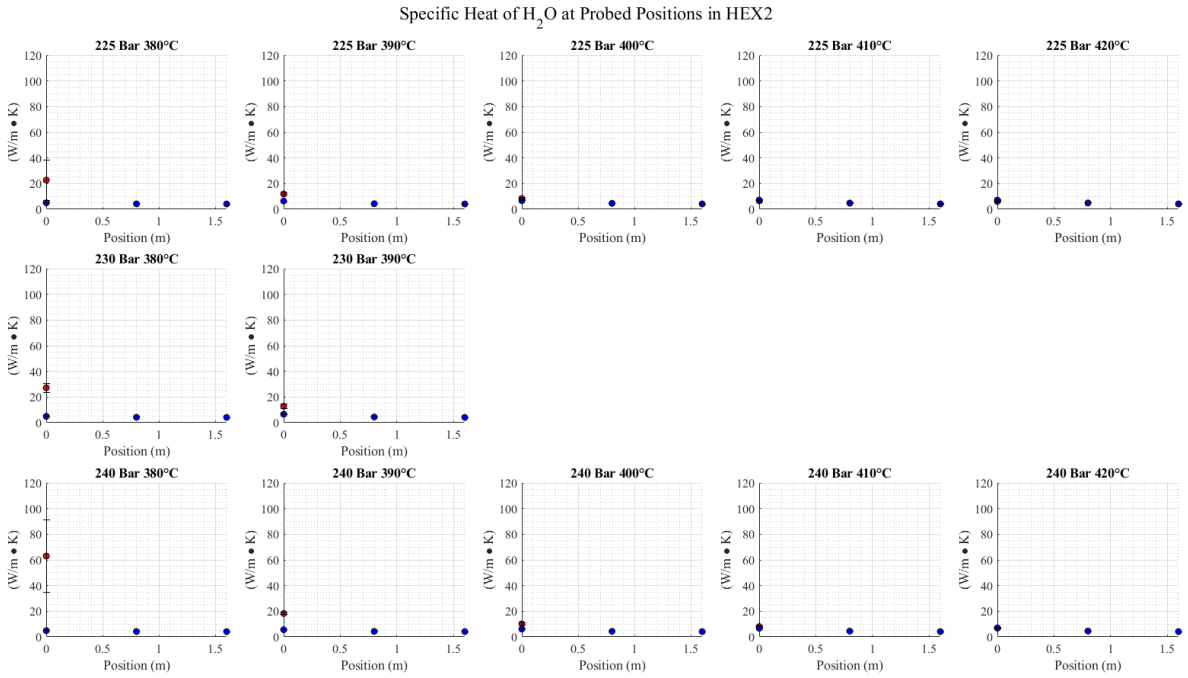


Figure 104: Specific Heat of $H_2O$ at probed positions in HEX2

ENTHALPY

The enthalpy values enthalpy values of $H_2O$ flowing through HEX1 and HEX2 in kJ/kg are shown in Table 33. Enthalpy is used to calculate the heat lost to the ambient environment and the cold fluid.

Table 33: Enthalpy values of $H_2O$ flowing through HEX1 and HEX2 in kJ/kg

| Enthalpy Values of of $H_2O$ (kJ/kg) | | | | | | | | |
|---|---|---|---|---|---|---|---|---|
| HEX1 | | | | | | | | |
| Pressure (Bar) | Hot Line Inlet Set Point | Hot Line | | | Cold Line | | | Salinity of Cold Line (%wt NaCl) |
| | | T1 | T2 | T3 | T6 | T8 | T10 | |
| | | In | Middle | Out | In | Middle | Out | |
| 225 | 380 | 2446 | 374 | 134 | 121 | 316 | 1657 | 0 |
| | 390 | 2613 | 525 | 138 | 121 | 461 | 1788 | 0 |
| | 400 | 2704 | 604 | 142 | 117 | 545 | 1815 | 0 |
| | 410 | 2797 | 629 | 142 | 117 | 570 | 1829 | 0 |
| | 420 | 2860 | 604 | 142 | 121 | 541 | 1846 | 0 |
| 230 | 380 | 2366 | 291 | 130 | 122 | 246 | 1506 | 0 |
| | 390 | 2593 | 520 | 138 | 122 | 457 | 1781 | 0 |
| | 400 | 2707 | 570 | 147 | 126 | 512 | 1819 | 0 |
| | 410 | 2778 | 570 | 138 | 122 | 512 | 1819 | 0 |
| | 420 | 2869 | 579 | 138 | 122 | 520 | 1806 | 0 |
| 240 | 380 | 2110 | 267 | 131 | 123 | 226 | 1390 | 0 |
| | 390 | 2501 | 500 | 148 | 127 | 446 | 1688 | 0 |
| | 400 | 2648 | 634 | 156 | 127 | 584 | 1759 | 0 |
| | 410 | 2755 | 707 | 164 | 123 | 664 | 1750 | 0 |
| | 420 | 2812 | 775 | 176 | 123 | 737 | 1740 | 0 |
| 230 | 410 | 2832 | 499 | 138 | N/A | N/A | N/A | 3.5% |
| | 410 | 2845 | 499 | 138 | N/A | N/A | N/A | 7.5% |
| | 410 | 2874 | 549 | 147 | N/A | N/A | N/A | 14% |

| Enthalpy Values of of $H_2O$ (kJ/kg) | | | | | | | | |
|---|---|---|---|---|---|---|---|---|
| HEX2 | | | | | | | | |
| Pressure (Bar) | Hot Line Inlet Set Point | Hot Line | | | Cold Line | | | Salinity of Cold Line (%wt NaCl) |
| | | T1 | T2 | T3 | T4 | T6 | T8 | |
| | | In | Middle | Out | In | Middle | Out | |
| 225 | 380 | 2471 | 532 | 146 | 121 | 536 | 1255 | 0 |
| | 390 | 2613 | 766 | 183 | 121 | 783 | 1544 | 0 |
| | 400 | 2722 | 1045 | 365 | 130 | 1064 | 1577 | 0 |
| | 410 | 2817 | 1134 | 461 | 130 | 1163 | 1612 | 0 |
| | 420 | 2848 | 1182 | 520 | 130 | 1211 | 1612 | 0 |
| 230 | 380 | 2433 | 554 | 142 | 122 | 545 | 1231 | 0 |
| | 390 | 2593 | 901 | 192 | 126 | 910 | 1569 | 0 |
| 240 | 380 | 2022 | 542 | 147 | 127 | 529 | 1192 | 0 |
| | 390 | 2501 | 702 | 156 | 127 | 715 | 1429 | 0 |
| | 400 | 2658 | 832 | 189 | 123 | 840 | 1522 | 0 |
| | 410 | 2739 | 960 | 271 | 131 | 978 | 1593 | 0 |
| | 420 | 2805 | 1000 | 299 | 131 | 1023 | 1620 | 0 |

HEX1 & HEX2 NUSSELT NUMBER

The Nusselt number is the ratio of convective heat transfer over the conductive heat transfer that is commonly represented by the following equation [4], [33], [43].

$$Nu = \frac{hD}{k}$$

$h$ = Convective heat transfer coefficient of the fluid (W/m$^2$·°C)
$D$ = Diameter of the tube or L as a characteristic length of a plate (m)
$k$ = Conductive heat transfer coefficient of the fluid (W/m·°C)

The Nusselt number for supercritical water within a heat exchanger can be found by measuring the temperatures and pressures along the length of the heat exchanger and finding the values of the thermal conductivity value $k$ and the thermal convective heat transfer coefficient $h$. The values for k can be found with REFPROP. The characteristic dimension $D$ or $L$ is known or measured. The value of h can be calculated

by finding the difference in enthalpy of the fluid at the exit and entrance of the hot line multiplying this difference by the mass flow rate. Q is then divided by the surface area of the inner and outer tube multiplied by the change in temperature. This method yields much higher Nusselt numbers than the literature provides for constant heat flux or constant surface temperature, which are both not valid for the application of a supercritical water heat exchanger. The Nusselt numbers for heat exchange under supercritical water conditions are shown as well as the calculated convective heat transfer values.

Table 34: OHTC, Effectiveness, Total Thermal Resistance, Convective Heat Transfer Coefficient, Nusselt Number for HEX1

| Log Mean Temperature Difference, Heat Transfer Rate, NTU, Effectiveness, Total Thermal Resistance, Convective Heat Transfer Coefficicent, Overall Heat Transfer Coefficient | | | | | | | | | | | | | | | |
|---|---|---|---|---|---|---|---|---|---|---|---|---|---|---|---|
| HEX1 | | | | | | | | | | | | | | | |
| Pressure (Bar) | Hot Line Inlet Set Point | Log Mean Temp | | | HEAT TRANSFER RATE | | | NTU | Effectivenss based on temp | Total Thermal Resistance | Conv. HT Coeff. | | OHTC | | Salinity of Cold Line (%wt NaCl) |
| | | LMTD | | | Q | | | | | $R_T$ | $h_i$ | $h_o$ | $U$ | 1/U | |
| | | ΔT1 | ΔT2 | ΔTlm | Qhot | Qcold | Loss | | ε | $1/h_i A_i + R_{wall} + 1/h_o A_o$ | HOT | COLD | $1/RA$ | $1/U = 1/h_i + L/K$ | |
| | | °C | | | W | | | # | % | °C/W | W/m$^2$·°C | | W/m$^2$·°C | m$^2$·°C/W | |
| 225 | 380 | 27 | 3 | 11 | 2312.6 | 1535.2 | 777.4 | 2.2 | 99.2% | 1.278 | 33.78 | 16.10 | 33.60 | 0.1790 | 0 |
| | 390 | 23 | 4 | 11 | 2475.3 | 1667.0 | 808.3 | 1.8 | 99.0% | 1.259 | 34.28 | 16.15 | 34.10 | 0.1784 | 0 |
| | 400 | 30 | 5 | 14 | 2562.5 | 1697.3 | 865.1 | 1.7 | 98.6% | 1.262 | 34.20 | 16.14 | 34.01 | 0.1785 | 0 |
| | 410 | 41 | 5 | 18 | 2655.0 | 1712.1 | 942.9 | 1.6 | 98.6% | 1.270 | 33.98 | 16.13 | 33.80 | 0.1787 | 0 |
| | 420 | 50 | 4 | 18 | 2718.4 | 1724.3 | 994.0 | 1.4 | 99.0% | 1.275 | 33.85 | 16.19 | 33.67 | 0.1786 | 0 |
| 230 | 380 | 49 | 2 | 14 | 2236.4 | 1384.2 | 852.3 | 2.4 | 99.5% | 1.298 | 33.25 | 16.05 | 33.08 | 0.1797 | 0 |
| | 390 | 23 | 4 | 11 | 2454.3 | 1659.5 | 794.9 | 1.8 | 99.0% | 1.266 | 34.08 | 16.13 | 33.90 | 0.1786 | 0 |
| | 400 | 32 | 5 | 15 | 2560.7 | 1692.9 | 867.8 | 1.7 | 98.7% | 1.264 | 34.13 | 16.15 | 33.95 | 0.1785 | 0 |
| | 410 | 41 | 4 | 16 | 2640.0 | 1697.0 | 942.9 | 1.7 | 98.9% | 1.267 | 34.06 | 16.12 | 33.88 | 0.1787 | 0 |
| | 420 | 56 | 4 | 20 | 2730.2 | 1683.7 | 1046.5 | 1.7 | 98.9% | 1.276 | 33.81 | 16.12 | 33.63 | 0.1789 | 0 |
| 240 | 380 | 70 | 1 | 18 | 1979.5 | 1267.6 | 711.9 | 2.2 | 99.6% | 1.393 | 30.96 | 16.00 | 30.81 | 0.1821 | 0 |
| | 390 | 32 | 5 | 14 | 2353.0 | 1561.3 | 791.7 | 2.1 | 98.7% | 1.294 | 33.33 | 15.98 | 33.16 | 0.1799 | 0 |
| | 400 | 35 | 7 | 17 | 2492.4 | 1632.5 | 859.9 | 2.0 | 98.2% | 1.288 | 33.51 | 15.93 | 33.33 | 0.1799 | 0 |
| | 410 | 48 | 9 | 24 | 2590.6 | 1626.8 | 963.7 | 2.0 | 97.6% | 1.293 | 33.36 | 15.81 | 33.18 | 0.1805 | 0 |
| | 420 | 57 | 13 | 30 | 2635.3 | 1617.4 | 1018.0 | 2.1 | 96.7% | 1.300 | 33.19 | 15.72 | 33.01 | 0.1810 | 0 |
| 230 | 410 | 60 | 3 | 20 | 2693.8 | N/A | N/A | N/A | 99.1% | N/A | 3.33 | N/A | N/A | N/A | 3.5% |
| | 410 | 65 | 3 | 21 | 2706.3 | N/A | N/A | N/A | 99.2% | N/A | 3.26 | N/A | N/A | N/A | 7.5% |
| | 410 | 74 | 6 | 27 | 2727.8 | N/A | N/A | N/A | 98.6% | N/A | 2.97 | N/A | N/A | N/A | 14% |

Table 35: OHTC, Effectiveness, Total Thermal Resistance, Convective Heat Transfer Coefficient, Nusselt Number for HEX2

| Log Mean Temperature Difference, Heat Transfer Rate, Total Thermal Resistance, Convective Heat Transfer Coefficicent, Overall Heat Transfer Coefficient | | | | | | | | | | | | | | | |
|---|---|---|---|---|---|---|---|---|---|---|---|---|---|---|---|
| HEX2 | | | | | | | | | | | | | | | |
| Pressure (Bar) | Hot Line Inlet Set Point | Log Mean Temp | | | HEAT TRANSFER RATE | | | NTU | Effectivenss based on Temp | Total Thermal Resistance | Conv. HT Coeff. | | OHTC | | Salinity of Cold Line (%wt NaCl) |
| | | LMTD | | | Q | | | | | $R_T$ | $h_i$ | $h_o$ | $U$ | 1/U | |
| | | ΔT1 | ΔT2 | ΔTlm | Qhot | Qcold | Loss | | ε | $1/h_i A_i + R_{wall} + 1/h_o A_o$ | HOT | COLD | $1/RA$ | $1/U = 1/h_i + L/K$ | |
| | | °C | | | W | | | # | | °C/W | W/m$^2$·°C | | W/m$^2$·°C | m$^2$·°C/W | |
| 225 | 380 | 96 | 6 | 32.5 | 2325 | 1134 | 1190 | 2.7 | 98.3% | 1.282 | 29.39 | 13.73 | 16.29 | 0.2068 | 0 |
| | 390 | 53 | 15 | 30.1 | 2430 | 1423 | 1007 | 2.5 | 95.9% | 1.276 | 29.53 | 13.51 | 16.36 | 0.2079 | 0 |
| | 400 | 59 | 57 | 58.0 | 2356 | 1448 | 909 | 2.6 | 84.8% | 1.262 | 29.87 | 13.14 | 16.55 | 0.2095 | 0 |
| | 410 | 67 | 80 | 73.3 | 2356 | 1482 | 874 | 2.6 | 79.4% | 1.258 | 29.96 | 13.00 | 16.60 | 0.2103 | 0 |
| | 420 | 72 | 94 | 82.5 | 2329 | 1482 | 846 | 2.6 | 76.1% | 1.255 | 30.04 | 12.92 | 16.64 | 0.2107 | 0 |
| 230 | 380 | 102 | 5 | 31.5 | 2291 | 1109 | 1182 | 2.6 | 98.7% | 1.300 | 28.99 | 13.59 | 16.07 | 0.2080 | 0 |
| | 390 | 50 | 16 | 29.7 | 2401 | 1443 | 957 | 2.4 | 95.6% | 1.303 | 28.92 | 13.13 | 16.03 | 0.2107 | 0 |
| 240 | 380 | 108 | 5 | 34 | 1875 | 1065 | 810 | 2.2 | 98.6% | 1.442 | 26.12 | 13.75 | 14.48 | 0.2110 | 0 |
| | 390 | 72 | 7 | 28 | 2345 | 1302 | 1043 | 2.5 | 98.1% | 1.315 | 28.66 | 13.55 | 15.88 | 0.2087 | 0 |
| | 400 | 68 | 16 | 36 | 2470 | 1400 | 1070 | 2.5 | 95.8% | 1.303 | 28.91 | 13.42 | 16.02 | 0.2091 | 0 |
| | 410 | 66 | 34 | 48 | 2468 | 1462 | 1006 | 2.4 | 91.2% | 1.300 | 28.98 | 13.27 | 16.06 | 0.2099 | 0 |
| | 420 | 71 | 40 | 54 | 2506 | 1490 | 1016 | 2.4 | 89.8% | 1.307 | 28.83 | 13.22 | 15.98 | 0.2103 | 0 |

Table 36 shows the Nusselt number maximum, minimum and average of the calculated Nusselt number values based on the temperatures and pressures that were collected during experimentation. The overall maximum, minimum, and average values include the Nusselt numbers that were found during the brine study that was conducted on HEX1. The Nusselt numbers that were collected for the hot and cold side of both heat exchangers do not include the Nusselt numbers for the brine study.

Table 36: Nusselt Number Summary Table

| Nusselt Number Summary Table (*Nu*) | | | | | | | | | | | | |
|---|---|---|---|---|---|---|---|---|---|---|---|---|
| Heat Exchanger | HOT | | | COLD | | | HOT & COLD | | | OVERALL | | |
| | Min | Average | Max | Min | Average | Max | Min | Average | Max | Min | Average | Max |
| HEX1 | 73.86 | 51.10 | 129.22 | 37.96 | 51.10 | 88.21 | 37.96 | 83.70 | 129.22 | 11.30 | 72.78 | 129.22 |
| HEX2 | 69.34 | 54.00 | 105.03 | 31.17 | 34.31 | 52.86 | 31.17 | 66.71 | 105.03 | | | |

Table 37 and Table 38 show more extensive Nusselt number values for the different pressure and temperature scenarios for HEX1 and HEX2. The summary table is a condensed version of Tables 37 and 38.

Table 37: Nusselt Number Results for HEX1

| Nusselt Number (*Nu*) HEX1 | | | | | |
|---|---|---|---|---|---|
| Pressure (Bar) | Hot Line Inlet Set Point | Salinity of Cold Line (%wt NaCl) | *Nu* ($h_i$) HOT | *Nu* ($h_o$) COLD | *Nu* (t-avg) Temperature Average |
| 225 | 380 | 0 | 113 | 41 | 77 |
| | 390 | 0 | 74 | 43 | 58 |
| | 400 | 0 | 127 | 43 | 85 |
| | 410 | 0 | 129 | 43 | 86 |
| | 420 | 0 | 129 | 44 | 86 |
| | | Average | 114.31 | 42.89 | 78.60 |
| 230 | 380 | 0 | 104 | 39 | 72 |
| | 390 | 0 | 122 | 43 | 83 |
| | 400 | 0 | 126 | 43 | 85 |
| | 410 | 0 | 128 | 43 | 86 |
| | 420 | 0 | 129 | 43 | 86 |
| | | Average | 122.14 | 42.33 | 82.24 |
| 240 | 380 | 0 | 81 | 38 | 59 |
| | 390 | 0 | 114 | 41 | 78 |
| | 400 | 0 | 121 | 88 | 105 |
| | 410 | 0 | 123 | 87 | 105 |
| | 420 | 0 | 123 | 86 | 105 |
| | | Average | 112.49 | 68.07 | 90.28 |
| 230 | 410 | 3.5% | 13 | N/A | |
| | 410 | 7.5% | 12 | N/A | |
| | 410 | 14% | 11 | N/A | |
| | | Average | 12.13 | N/A | |

| Nusselt Number Standard Deviation (*Nu*) HEX1 | | | | | |
|---|---|---|---|---|---|
| Pressure (Bar) | Hot Line Inlet Set Point | Salinity of Cold Line (%wt NaCl) | *Nu* ($h_i$) HOT | *Nu* ($h_o$) COLD | *Nu* (t-avg) Temperature Average |
| 225 | 380 | 0 | 23.61 | 1.01 | 11.93 |
| | 390 | 0 | | | |
| | 400 | 0 | | | |
| | 410 | 0 | | | |
| | 420 | 0 | | | |
| 230 | 380 | 0 | 10.32 | 1.69 | 6.00 |
| | 390 | 0 | | | |
| | 400 | 0 | | | |
| | 410 | 0 | | | |
| | 420 | 0 | | | |
| 240 | 380 | 0 | 17.99 | 26.07 | 20.87 |
| | 390 | 0 | | | |
| | 400 | 0 | | | |
| | 410 | 0 | | | |
| | 420 | 0 | | | |
| 230 | 410 | 3.5% | 0.7 | N/A | N/A |
| | 410 | 7.5% | | | |
| | 410 | 14% | | | |

| | |
|---|---|
| Overall Standard Deviation for HEX1 | 38.32 |
| Average Standard Deviation for HEX1 | 9.34 |

Table 38: Nusselt Number Results for HEX2

| Nusselt Number ($Nu$) HEX2 | | | | | |
|---|---|---|---|---|---|
| Pressure (Bar) | Hot Line Inlet Set Point | Salinity of Cold Line (%wt NaCl) | $Nu\ (h_i)$ HOT | $Nu\ (h_o)$ COLD | $Nu$ (t-avg) Temperature Average |
| 225 | 380 | 0 | 99 | 32 | 65 |
| | 390 | 0 | 105 | 33 | 69 |
| | 400 | 0 | 104 | 33 | 68 |
| | 410 | 0 | 104 | 33 | 68 |
| | 420 | 0 | 104 | 33 | 68 |
| | | Average | 103.33 | 32.64 | 67.98 |
| 230 | 380 | 0 | 96 | 53 | 74 |
| | 390 | 0 | 102 | 33 | 67 |
| | | Average | 98.57 | 42.78 | 70.68 |
| 240 | 380 | 0 | 69 | 31 | 50 |
| | 390 | 0 | 98 | 32 | 65 |
| | 400 | 0 | 103 | 33 | 68 |
| | 410 | 0 | 103 | 33 | 68 |
| | 420 | 0 | 103 | 33 | 68 |
| | | Average | 95.09 | 32.60 | 63.84 |

| Nusselt Number Standard Deviation ($Nu$) HEX1 | | | | | |
|---|---|---|---|---|---|
| Pressure (Bar) | Hot Line Inlet Set Point | Salinity of Cold Line (%wt NaCl) | $Nu\ (h_i)$ HOT | $Nu\ (h_o)$ COLD | $Nu$ (t-avg) Temperature Average |
| 225 | 380 | 0 | 2.34 | 0.66 | 1.48 |
| | 390 | 0 | | | |
| | 400 | 0 | | | |
| | 410 | 0 | | | |
| | 420 | 0 | | | |
| 230 | 380 | 0 | 4.22 | 14.25 | 9.20 |
| | 390 | 0 | | | |
| 240 | 380 | 0 | 14.57 | 0.87 | 2.34 |
| | 390 | 0 | | | |
| | 400 | 0 | | | |
| | 410 | 0 | | | |
| | 420 | 0 | | | |

| | |
|---|---|
| Overall Standard Deviation for HEX2 | 34.02 |
| Average Standard Deviation for HEX2 | 5.65 |

PRESSURE DATA

The pressures were hand recorded while reading off a digital pressure gauge during experimentation. The pressures were consistent enough to consider the temperature values collected during experimentation. The pressure of P2, P3, P4, P5 are shown in Tables 39 and 40, these points correspond to the process diagrams presented in this work. P1 was not included because it was a large analog pressure gauge mounted to the top of the reactor. It has been determined that the pressure reported by the pressure gauge at P1 is inaccurate because the heat from the reactor affects the value shown on the gage. This same phenomenon was observed at the analog pressure gauge near the furnace at the inlet of the HEX being tested. The analog gauges mounted at the HEX hot entrance also showed a 50 psi (3.45 Bar) difference over the length of the heat exchanger when the temperature of the fluid was increased, at low temperatures the pressures at the inlet and outlet read the same value to the precision level of 50 Psi (3.45 Bar). The averages shown in Tables 39 and 40 are from the 21 data points taken at steady state conditions. The pressure effects the thermophysical properties of the fluid as shown in the thermophysical data presented in this work.

Table 39: HEX1 Pressure data summary table

| HEX1 | | | | | Average Pressure in Position (Bar) | | | | Standard Deviation of Pressure at Position (Bar) | | | |
|---|---|---|---|---|---|---|---|---|---|---|---|---|
| Pressure (Bar) | Hot Line Inlet Temperature (°C) | Cold Line Salinity %wt NaCl | Average Pressure (Bar) | Pressure % Error | P2 | P3 | P4 | P5 | P2 | P3 | P4 | P5 |
| 225 | 380 | 0% | 224.7 | 0.13 | 225.6 | 223.4 | 225.0 | 224.8 | 0.25 | 0.04 | 0.12 | 0.19 |
| | 390 | 0% | 224.8 | 0.11 | 225.6 | 223.6 | 224.9 | 224.8 | 0.29 | 0.04 | 0.28 | 0.23 |
| | 400 | 0% | 224.9 | 0.07 | 225.8 | 223.7 | 225.0 | 224.9 | 0.25 | 0.09 | 0.22 | 0.31 |
| | 410 | 0% | 225.0 | 0.00 | 225.9 | 223.8 | 225.2 | 225.1 | 0.25 | 0.07 | 0.19 | 0.22 |
| | 420 | 0% | 225.0 | 0.01 | 225.8 | 224.1 | 225.1 | 225.1 | 0.32 | 0.16 | 0.27 | 0.34 |
| | | Mean | 224.9 | 0.06 | 225.7 | 223.7 | 225.0 | 225.0 | 0.27 | 0.08 | 0.22 | 0.26 |
| 230 | 380 | 0% | 232.0 | 0.86 | 232.9 | 230.7 | 232.3 | 232.2 | 0.16 | 0.07 | 0.16 | 0.01 |
| | 390 | 0% | 232.1 | 0.91 | 233.0 | 230.8 | 232.4 | 232.3 | 0.19 | 0.11 | 0.22 | 0.21 |
| | 400 | 0% | 232.4 | 1.03 | 233.2 | 231.1 | 232.6 | 232.6 | 0.15 | 0.08 | 0.18 | 0.18 |
| | 410 | 0% | 232.7 | 1.16 | 233.6 | 231.3 | 232.9 | 233.0 | 0.08 | 0.05 | 0.09 | 0.09 |
| | 420 | 0% | 231.5 | 0.66 | 232.4 | 230.3 | 231.7 | 231.8 | 0.20 | 0.04 | 0.23 | 0.22 |
| | | Mean | 232.1 | 0.92 | 233.0 | 230.8 | 232.4 | 232.4 | 0.15 | 0.07 | 0.18 | 0.14 |
| 240 | 380 | 0% | 241.9 | 0.77 | 242.8 | 240.4 | 242.2 | 242.1 | 0.30 | 0.04 | 0.14 | 0.14 |
| | 390 | 0% | 242.1 | 0.85 | 242.9 | 240.6 | 242.4 | 242.3 | 0.18 | 0.06 | 0.19 | 0.19 |
| | 400 | 0% | 242.2 | 0.91 | 243.1 | 240.8 | 242.5 | 242.5 | 0.21 | 0.07 | 0.22 | 0.24 |
| | 410 | 0% | 242.3 | 0.94 | 243.2 | 240.9 | 242.5 | 242.6 | 0.16 | 0.08 | 0.22 | 0.18 |
| | 420 | 0% | 242.4 | 0.97 | 243.2 | 241.0 | 242.6 | 242.7 | 0.12 | 0.06 | 0.15 | 0.18 |
| | | Mean | 242.2 | 0.89 | 243.0 | 240.7 | 242.4 | 242.4 | 0.20 | 0.06 | 0.19 | 0.19 |
| 230 | 410 | 3.5% | 231.6 | 0.67 | 232.5 | 229.8 | 232.0 | 231.9 | 1.03 | 1.03 | 1.07 | 1.13 |
| | 410 | 7.5% | 231.8 | 0.77 | 232.8 | 230.1 | 232.2 | 232.1 | 1.36 | 2.26 | 1.41 | 1.37 |
| | 410 | 14% | 232.0 | 0.88 | 232.5 | 231.6 | 232.1 | 231.9 | 3.17 | 1.52 | 2.97 | 2.96 |
| | | Mean | 231.8 | 0.77 | 232.6 | 230.5 | 232.1 | 232.0 | 1.85 | 1.60 | 1.82 | 1.82 |

Table 40: HEX2 Pressure data summary table

| HEX2 | | | | | Average Pressure in Position (Bar) | | | | Standard Deviation of Pressure at Position (Bar) | | | |
|---|---|---|---|---|---|---|---|---|---|---|---|---|
| Pressure (Bar) | Hot Line Inlet Temperature (°C) | Cold Line Salinity %wt NaCl | Average Pressure (Bar) | Pressure % Error | P2 | P3 | P4 | P5 | P2 | P3 | P4 | P5 |
| 225 | 380 | 0% | 224.0 | 0.46 | 225.0 | 222.1 | 224.3 | 224.5 | 0.37 | 0.10 | 0.35 | 0.35 |
| | 390 | 0% | 223.8 | 0.52 | 224.7 | 222.1 | 224.2 | 224.4 | 0.33 | 0.07 | 0.29 | 0.36 |
| | 400 | 0% | 224.1 | 0.40 | 224.1 | 223.8 | 223.5 | 225.0 | 5.02 | 1.89 | 5.03 | 4.94 |
| | 410 | 0% | 223.4 | 0.73 | 223.3 | 223.1 | 222.7 | 224.4 | 1.38 | 1.22 | 1.39 | 1.40 |
| | 420 | 0% | 221.1 | 1.75 | 220.5 | 222.6 | 219.9 | 221.6 | 2.48 | 1.36 | 2.52 | 2.60 |
| | | Mean | 223.3 | 0.77 | 223.5 | 222.7 | 222.9 | 224.0 | 1.91 | 0.93 | 1.92 | 1.93 |
| 230 | 380 | 0% | 228.8 | 0.51 | 229.9 | 226.9 | 229.3 | 229.3 | 0.86 | 0.68 | 0.90 | 0.80 |
| | 390 | 0% | 229.3 | 0.30 | 230.4 | 227.5 | 229.6 | 229.9 | 0.47 | 0.14 | 0.68 | 0.45 |
| | | Mean | 229.1 | 0.41 | 230.2 | 227.2 | 229.4 | 229.6 | 0.66 | 0.41 | 0.79 | 0.62 |
| 240 | 380 | 0% | 239.9 | 0.06 | 240.3 | 239.8 | 239.8 | 239.5 | 1.85 | 1.89 | 1.89 | 1.98 |
| | 390 | 0% | 240.6 | 0.23 | 241.6 | 238.7 | 241.1 | 240.8 | 0.35 | 0.15 | 0.35 | 0.37 |
| | 400 | 0% | 240.1 | 0.06 | 240.9 | 239.0 | 240.3 | 240.4 | 0.95 | 0.99 | 0.97 | 0.99 |
| | 410 | 0% | 238.9 | 0.47 | 239.6 | 237.4 | 238.9 | 239.6 | 2.02 | 2.33 | 2.09 | 3.30 |
| | 420 | 0% | 241.0 | 0.43 | 241.3 | 240.9 | 240.7 | 241.3 | 1.93 | 1.87 | 1.91 | 1.93 |
| | | Mean | 240.1 | 0.25 | 240.7 | 239.2 | 240.2 | 240.3 | 1.42 | 1.44 | 1.44 | 1.71 |

To have confidence in the data collected it is necessary to determine if the data collected is accurate enough to be scientifically valid. The set pressure for the experiment is shown as “Pressure (Bar)”. The Hot

line inlet temperatures for each experiment are broken out. The standard deviations are shown as very small values.

For example, 0.25 Bar is 0.11% of 225 Bar. The precent error of the system set pressure is very low across all experiments that took place. Check valve opening pressure of 5 or 10 psi may have effected pressure readings as well.

The average % error in pressure variation that occurred during data collection during a time of steady state did not exceed 0.77 % in HEX2. The standard deviation did not exceed 3.3 Bar of pressure in HEX2. The digital pressure gauges used to collect the data for P2, P3, P4 and P5 all came with a NIST certification.

CORROSION

The NaCl brine reacted with the 316 Stainless Steel tubing and caused some light rust. The rusty water was collected when it was visually observed during experimentation. The rust color is visible in the output tank as shown in Figure 105.

Figure 105: Rust colored water from corrosion caused by the NaCl brine

The electrical conductivity of the rusty water was 237.8 µS/cm when the rust was settled at the bottom and 245.2 µS/cm when the mixture was mixed with a magnetic chemical stirrer, as shown in Figure 106. The density was also measured to be 0.999 g/cm$^3$ when the rust was settled and 0.9991 g/cm$^3$ when the rust was floating in the water.

Figure 106: Rust mound at beaker wall caused by magnetic stirring bar

The rusty water that was found in the cooling line output tank was sampled with a 250 mL beaker where the rust particulates were allowed to settle to the bottom. A stirring magnet was left next to the beaker wall and the iron oxide was pulled towards the magnet causing a buildup of rust at the beaker wall. If a commercial system was constructed using stainless steel perhaps a magnet could be used to collect iron oxide particles, then cleaned for reuse as opposed to a disposable filter. Titanium is recommended as a heat exchanger material due to its ability to resist corrosion at elevated temperatures [38].

THERMOCOUPLE CORROSION

Some of the thermocouples were tarnished, other thermocouples were not. Figure 107 shows thermocouple T1 from HEX1. T1 is located at the hot tube inlet and is experiencing the maximum temperature the HEX would experience as the fluid running over the thermocouple is coming directly out of Furnace 2 (F2). This thermocouple only encountered $ScH_2O$ and did not contact the brine solution.

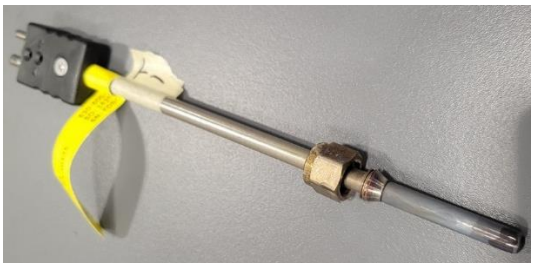
Figure 107: Thermocouple T1 from HEX1 after all experiments were completed.

The 316 SS turned a straw to light brown color at the region close to the hot part of the heat exchanger. The fittings that attached sections of tubing together experienced corrosion and discoloration due to the high heat.

FITTING CORROSION AND DISCOLORATION

The fittings shown in Figure 108 were exposed to high heat, changed from a shiny clean metallic appearance to a dull, dark brown, blue, and straw color as the thermocouple probes did. The insulation was cut to form around the Tee-fitting to form a better seal to hold in the heat, thus increasing the thermal efficiency of the HEX by reducing the thermal energy lost to the ambient air. After heating the fittings are difficult to remove. A wrench was broken when attempting to switch out some of the fittings near Furnace 2.

Figure 108: HEX1 hot line entrance and cooling line exit union

The rock wool changed from a gray to brown color where it contacted the hot tube and the hot outer tube of the HEX as shown in Figure 109. It was found that the rockwool was better held in place by tying it together with soft stainless-steel wire in contrast to aluminum foil tape. The aluminum foil tape would detach from the surface of the insulation over time causing the insulation to open and lose heat during testing. Loose insulation may have caused some drop in heat exchanger effectiveness.

Figure 109: HEX1 hot line entrance and cooling line exit union insulation

The fittings at the cold end of HEX 1 remained clean and reflective as stainless steel naturally looks in appearance as shown in Figure 110. The change in color of the metal is significant as it can show where the hot spots are visually. The temperature the metal experiences affects the tubing strength, therefore if failure were to occur it would be in the area that is the most dull or straw color in appearance. The hottest part of the heat exchanger is the weakest structurally and care should be taken during design.

Figure 110: HEX1 hot fluid exit line exposed for inspection.

The color of the metal is worth noting because there are charts that can be used to determine the temperature a metal has experienced during a heating cooling cycle. Figure 116 shows the natural appearance of stainless steel before it experienced any heating.

Figure 111: Fittings prior to assembly

SAMPLES

Samples were collected in test tubes which were then stored in trays as shown in Figure 117.

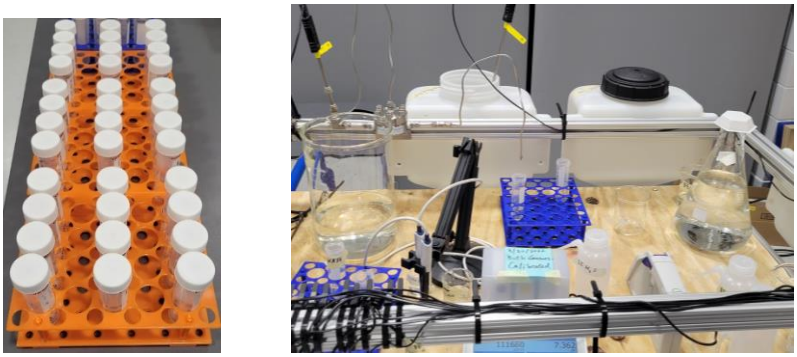

Figure 112: Sample test tubes and sampling method

These samples can be evaluated by a plasma spectrometer to check for salt, iron and any other material that may have found its way out of the heat exchanger material and into the water. Most of the samples are clear like deionized water except for the samples collected when the shell of HEX1 was filled with differing concentrations of brine.

## HEX1 WITH HOT FEED WATER FROM DESALINATION SYSTEM CONDUCTIVITY EXPERIMENT

HEX1 was attached to the 10mL/min desalination system then the system was started up and brought to steady state. The Pump for the cooling side of HEX1 was set up to pump water from the water tank and brine from the brine tank. The conductivity data shown in Figure 113 was recorded while samples of the HEX cooling line output fluid were collected.

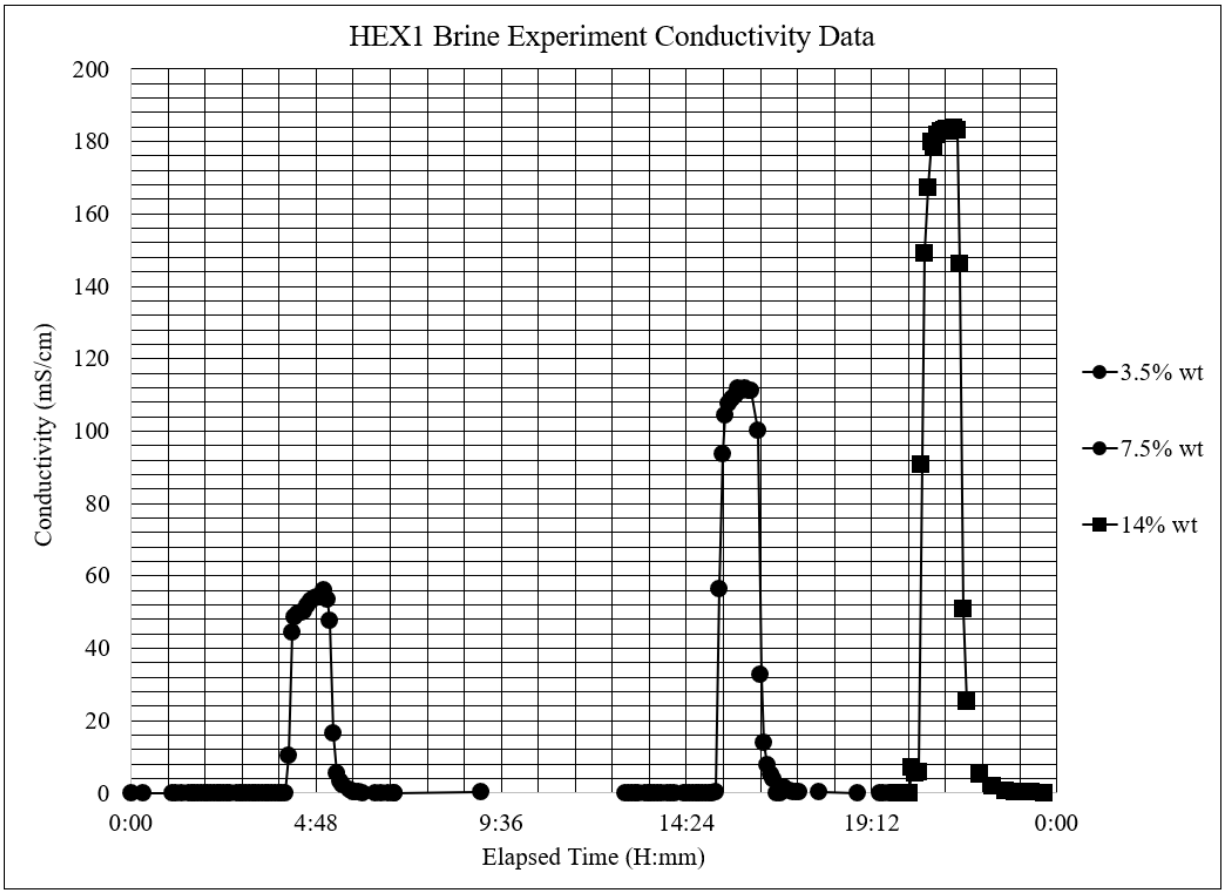


Figure 113: HEX1 With Brine as a Coolant with ScH2O Hot Line, Measured Conductivity

The peaks of the spikes in conductivity at different salinity levels were averaged to yield the following table. Observe that the peaks of the spikes shoot straight up then the slope decreases to a gradual ramp then the conductivity values flatten once the conductivity value reaches a peak. From the beginning of each peak to the end is approximately 65 minutes. Table 41 shows the maximum and average conductivity values recorded during experimentation. The difference table shows how much loss there was in salinity and compares what the conductivity values of the brine were before heat was applied to the desalination system. The loss is low but still present. It is assumed that the lost salt coated the inside walls of the tubing. The negative value in the Average cell for 7.5% of the difference table means that the error was below the expected value by 4%.

Table 41: Conductivity Results Table

| Conductivity | | | | |
|---|---|---|---|---|
| %wt NaCl | HEX1 with Heat | | HEX1 W/O HEAT | |
| | Max | Average | Max | Average |
| 3.5%wt | 54264 | 47337 | 51252 | 44421 |
| 7.5%wt | 111958 | 103430 | 110192 | 107083 |
| 14%wt | 183760 | 177783 | 180221 | 162166 |

| Difference Table | | | Percent Error Table | |
|---|---|---|---|---|
| %wt NaCl | Max | Average | Max | Average |
| 3.5%wt | 3013 | 2917 | 6% | 6% |
| 7.5%wt | 1766 | -3653 | 2% | -4% |
| 14%wt | 3539 | 15617 | 2% | 9% |

The average value of 14%wt NaCl HEX1 with the desalination system off is a little low with an error of 9% but that is because the brine is still mixing with the water that was in the shell side of HEX1. The conductivity of the samples measure below the calibration curve. This means that there is a little less salt in the brine after it exists the heat exchanger, but the temperature appears to have little to no effect. The reduced salt is believed to have reacted with the wall of the heat exchanger chemically. Through the chemical reaction some mass is lost but the conductivity shows that there is a peak point which means the wall reaches a chemical equilibrium and the corrosion eventually stabilizes. It is safe to conclude that a heat exchanger can be added to a $ScH_2O$ system to increase its thermal efficiency without the possibility of desalinating the brine inside the heat exchanger. The solution to the corrosion problem would be to change

the pipe, tubing, and fittings to titanium. The economic feasibility of changing the material needs to be evaluated.

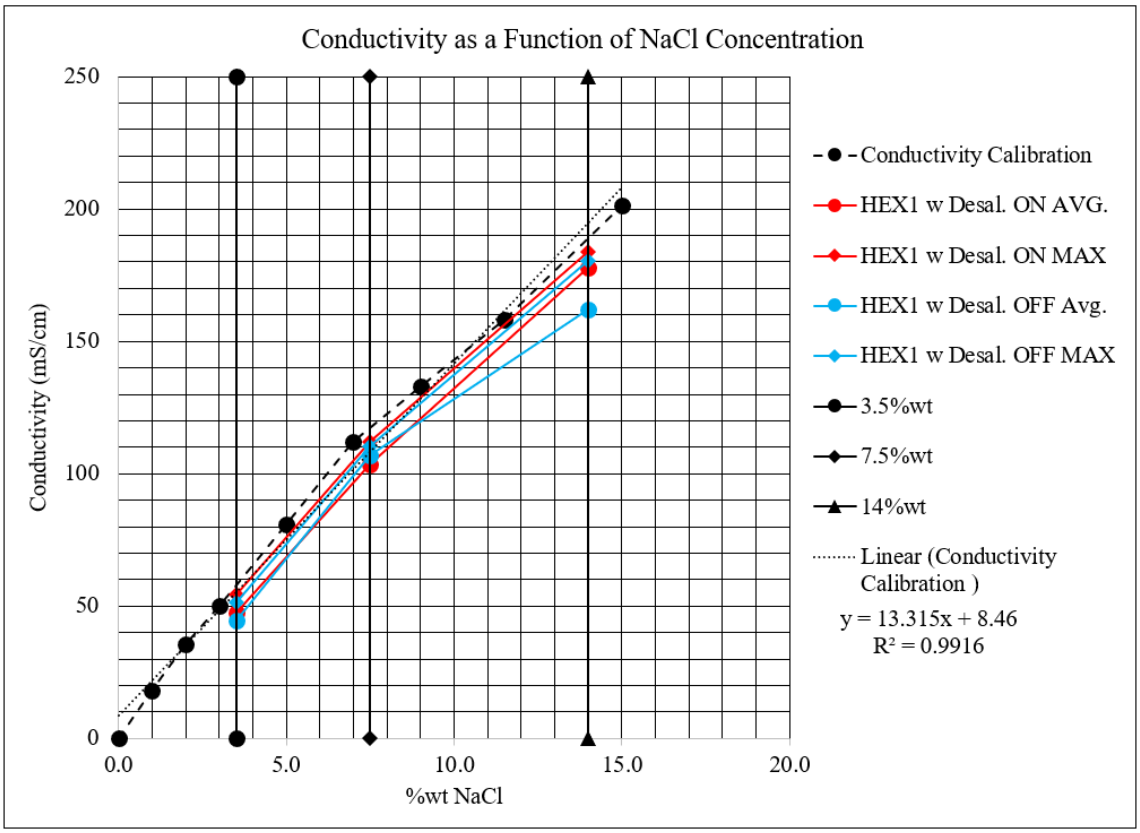


Figure 114: Conductivity Results Comparison

PIN HOLE OBSERVATIONS

Supercritical brine is corrosive and can wear pin holes in the tubing. Regular line inspection is necessary to maintain a safe system. Figure 115 shows a pin hole found in the Reactor entrance line. The image shown in Figure 115 is a freezeframe of a video recording.

Figure 115: Pin hole venting steam shown circled in red.

The pipe section shown in Figure 115 was replaced promptly after it was discovered after the system was shut down, depressurized, and allowed to cool. The data that was collected was collected during the experiment that was taking place and was not used in any of the calculations that took place during data analysis. Figure 116 shows another section of ¼" thick-walled tubing that was to be replaced because of a discovered pin hole leak. The location of the leak is encircled with a black marker. The section of tubing shown in Figure 116 was connecting the FWH tube to the FWH exit line temperature probe.

Figure 116: ¼" diameter thick-walled tubing with pin hole leak

## COLLECTION TANK OBSERVATION OF SUPERCRITICAL WATER

During the early stages of experimentation, it was observed that the water exiting the line out of the system into the collection tank was an opaque white color and contained small bubbles. The "stream" was a slow drip at a rate of 10 ml/min. Once the drop contacted the rest of the water in the collection tank the white coloring from the small bubbles dissipated and the water remained clear as deionized water should be.

During the early stages of experimentation, it was observed that the water exiting the line out of the system into the collection tank was an opaque white color and contained small bubbles. The "stream" was a slow drip at a rate of 10 ml/min. Once the drop contacted the rest of the fluid in the collection tank the bubbles dissipated, and the water returned to its clear appearance. This could provide evidence that slug flow is occurring within the system.

## DISCUSSION

The SCWD system and HEC were running for approximately 210 hours to collect 2261 lines of data which consisted of 53 columns per data set for a total of 199833 data points. 48 hours of the 210 hours

of data were not used due to data collection inconsistencies and other problems that arise. Each average point on the HEX data graphs was averaged from 21 data points. Table 42 shows data points counted.

Table 42: Data counter

| | | H2O used in this study | | | | | | | | | |
|---|---|---|---|---|---|---|---|---|---|---|---|
| | | Flow Rate (ml/min) | | | | | | | | | |
| | | 10 | 53 | columns per set | | | | | | | |
| | | | | | | | | | Pump 1 | Pump2 | |
| Line # | TABNAME | # of Data lines | # of Points Total | TIME | Hours | Minutes | mLs | Liters | Gallons | Gallons | TOTAL GALLONS |
| 1 | EXA HEX1 | 124 | 6572 | 14:56 | 15 | 900 | 9000 | 9 | 2 | 5 | 11.3 |
| 2 | EX1 HEX1 | 252 | 13356 | 14:35 | 14.5 | 870 | 8700 | 8.7 | 2 | 5 | 10.6 |
| 3 | EX2 HEX1 | 334 | 17702 | 19:25 | 19.5 | 1170 | 11700 | 11.7 | 3 | 6 | 19.1 |
| 4 | EX3 HEX1 | 299 | 15847 | 21:50 | 22 | 1320 | 13200 | 13.2 | 3 | 7 | 24.3 |
| 5 | EX4 HEX2 | 288 | 15264 | 12:15 | 12 | 720 | 7200 | 7.2 | 2 | 4 | 7.2 |
| 6 | EX4B HEX2 | 100 | 5300 | 8:55 | 9 | 540 | 5400 | 5.4 | 1 | 3 | 4.1 |
| 7 | EX4C HEX2 | 96 | 5088 | 11:20 | 11.5 | 690 | 6900 | 6.9 | 2 | 4 | 6.6 |
| 8 | EX5 HEX2 | 86 | 4558 | 10:30 | 10.5 | 630 | 6300 | 6.3 | 2 | 3 | 5.5 |
| 9 | EX6 HEX2 | 152 | 8056 | 8:55 | 9 | 540 | 5400 | 5.4 | 1 | 3 | 4.1 |
| 10 | EX7 HEX2 | 135 | 7155 | 15:30 | 16 | 960 | 9600 | 9.6 | 3 | 5 | 12.9 |
| 11 | EX8 HEX2 | 131 | 6943 | 19:30 | 20 | 1200 | 12000 | 12 | 3 | 6 | 20.1 |
| 12 | EX9 HEX1 | 38 | 2014 | 6:45 | 7 | 420 | 4200 | 4.2 | 1 | 2 | 2.5 |
| 13 | EX10 HEX1 | 26 | 1378 | 5:00 | 5 | 300 | 3000 | 3 | 1 | 2 | 1.3 |
| 14 | EX11 HEX1 | 43 | 2279 | 8:30 | 8.5 | 510 | 5100 | 5.1 | 1 | 3 | 3.6 |
| 15 | EX12 HEX1 | 154 | 8162 | 23:40 | 24 | 1440 | 14400 | 14.4 | 4 | 8 | 28.9 |
| | TOTALS | 2258 | 119674 | 36:00.0 | 203.5 | 12210 | 1E+05 | 122 | 32 | 65 | 97 |
| | USEFUL | 1739 | 92167 | 10:00.0 | 156 | 9360 | 93600 | 94 | 25 | 49 | 74 |
| | UNUSED | 519 | 27507 | 26:00.0 | 47.5 | 2850 | 28500 | 29 | 8 | 15 | 23 |

## CONCLUSION

The brine circulated during experimentation was validated as consistent with the expected conductivity values. Furnace 2 added for experimentation was fitted with a coil to allow the experimenter to control the inlet temperature and was proven to provide enough heat to lift the temperature to higher levels. The data that was collected shows that the HEX will not allow the water to desalinate inside the shell because there is little drop is the conductivity of the fluid as it passes through the HEX cooling shell. The reactor allows the water to stagnate which allows the salt to precipitate within the reactor. In the HEX the water is moving and will not desalinate. The slight drop in conductivity could be attributed to the salt sticking to the inner tube wall causing the fluid to lose salinity. At higher concentrations it is believed that there is some slight desalination but not at lower concentrations such as 3.5% and 7.5%.

# CHAPTER 4 DISCUSSION

## INTRODUCTION

All calculations assume that the pump volumetric flow rate remains constant throughout the entire experiment. HEX2 was not as efficient at lower pressure. The heat loss could be attributed to problems with the insulation.

## EFFECTS OF TEMPERATURE

As the temperature of the hot line of the heat exchanger decreases the water in the hot line cools down and the water in the cold line heats up. As the inlet temperature increases the enthalpy of the fluid increases, which is the amount of energy contained in each mass of the fluid. At higher inlet temperatures there is an increase in instability which is reflected in the standard deviations calculated for the temperature data. The change in temperature effects everything related to the thermophysical properties of the supercritical water within the heat exchanger.

## EFFECTS OF PRESSURE

225, 230 and 240 Bar measured by the pressure gauges at P2, P3, P4, and P5, were all held constantly during all experiments. The pressure drifted during experimentation, but it was within the range of 1.4 Bar. 1.4 Bar is 0.62% of 225 Bar the lowest system pressure tested, therefore the pressure data is within an acceptable tolerance range. With the pressure and temperature being high the fluid does not experience boiling. When the pressure increases the thermal stability increases because the specific heat of water is lower at higher pressures.

## EFFECTS OF ASPECT RATIO

Aspect ratio is defined as a ratio of width to length. In the context of heat exchangers there are 2 ratios that can be used to compare the 2 heat exchangers. The center hot tube and the diameter of the heat

exchanger shell is a ratio and the other will be shell area to length. The colors differentiate the manufacturer. Figure 117 shows a visual representation of the tubing combinations considered.

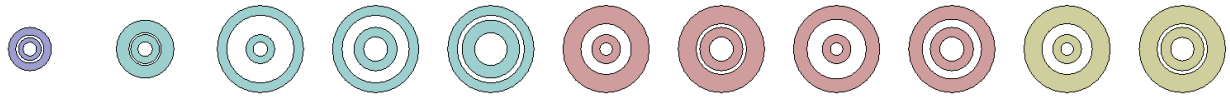

Figure 117: The Various tube in tube combinations considered during design.

HEX1 and HEX2 use 3/8" OD tubing of the same wall thickness and internal diameter. Both HEXs use 3/4". Table 42 shows how aspect ratio can affect the Nusselt number in fully developed laminar flow in a circular annulus with 1 surface insulated and the other is where the temperature is constant. In the HEXs designed in this work the temperature is not constant throughout the fluid or on the surfaces.

Table 43: Nusselt number for fully developed laminar flow in a circular annulus with 1 surface insulated and the other is where the temperature is constant [32]

| $D_i/D_o$ | $Nu_i$ | $Nu_o$ |
|---|---|---|
| 0.00 | N/A | 3.66 |
| 0.05 | 17.46 | 4.06 |
| 0.10 | 11.56 | 4.11 |
| 0.25 | 7.37 | 4.23 |
| 0.50 | 5.74 | 4.43 |
| 1.00 | 4.86 | 4.86 |

The annulus region ratio for HEX1 is 1.17 and is 1.13 for HEX2 which is greater than what the Nu values in Table 43 can support. HEX1 has a smaller annulus region which makes the layer of water thinner.

The aspect ratio of the annulus region affects the efficiency of and thermal stability. HEX1 had good efficiency but it is not as thermally stable as HEX2 witch has a larger space in between the outer diameter of the hot tube and the inner diameter of the cooling tube.

EFFECTS OF SALT CONCENTRATION

By adding salt to the cooling water, the heat capacity of the fluid changes slightly. The salt concentration does not affect the HEX measured temperatures that much when the salt concentration is low or around 3.5%wt NaCl and 7.5%wt NaCl. When the salt concentration increases to 14%wt NaCl heat was

not transferred as well as with pure water. These salt concentrations are what is produced when brine is sent through a reverse osmosis system 2 times.

## EFFECTS OF INSULATION

HEX1 was insulated with rockwool, HEX2 was insulated with fiberglass. The rockwool had a higher R-value but was not as clean to install as the encased fiberglass insulation. The fiberglass insulation of a lower R value allowed heat to be lost to the surrounding environment. T3 or the hot line exit temperature was higher for HEX2 which means less heat was transferred to the cold side than that of HEX1. HEX 1 had a thicker outer tube wall thickness which caused the annulus region to be thinner. Overall, the rockwool performed better than the fiberglass.

## LIMITATIONS

The flow rate could have been a limiting factor in the experiments attempted in this study. The flow rate was checked periodically with a beaker and a stopwatch and timed 1 minute to fill 10ml. This method is acceptable, but a flow meter would have been better. A flow meter that can accurately measure flow rates at the pressures and temperatures the system experienced could give more confidence to the flow rate measurement.

## UNCERTIANTY IN MEASUREMENTS

The thermocouples used have an accuracy of +/- 0.75%. therefore, if the average temperature recorded during the study is 400 degrees and the meter has 0.1% error, and the thermocouple has 0.75% error the temperature of the fluid measured could be between 403.4℃ and 396.6℃ or 400 +/-0.85%.

The low temperature pressure digital gauges used to measure the pressures at points P2, P3, P4, and P5 are certified by NIST to hold +/-1%. For example, when reporting 230 Bar the actual pressure could be within 229.77 to 229.77 Bar.

On a tight temperature measurement such as HEX2 at 225 Bar with a hot line entrance temperature of 380℃ at T6 the with an average value of 24 and a standard deviation is 0.2℃. This shows that the temperature could be 24.2℃ or 23.8℃. Then with the added thermocouple and meter uncertainty the temperature could be within 23.6℃ to 24.4℃. Therefore, the measurement of 24℃ for T6 is 24+/-1.68% accurate. For another example, HEX1 at 230 Bar with a T1 hot entrance temperature of 410℃ the standard deviation is 12.5℃ and the average of 21 data points for 105 minutes is 411℃. 12.5 degrees is 3.55% of 411℃. When including the 0.85% error the actual temperature of the fluid could be between 395.11℃ and 426.99℃. Therefore, the measurement of T1 for HEX1 at 230 Bar is 411 +/-3.89%. The uncertainty of the furnace is taken up by measuring the fluid, therefore the furnace precision could be ignored.

## TWISTED TAPE

The twisted tape method is not needed to increase the thermal efficiency of the HEX. The efficiencies of both heat exchangers are well above the widely accepted 85%. It is believed that the insulation on HEX2 began to detach because of the deteriorating adhesive near the end of the experiment causing heat loss to the surrounding environment. It is believed that if the insulation stayed attached the efficiency of HEX2 would be higher like that of HEX1.

## DESIGN CONCEPT

Based on the data collected during this experiment the design shown in Figure 123 shows a high-pressure desalination reactor with a coil inside. The reactor design can be turned into a heat exchanger. The brine for treatment would flow into the coil inside the reactor causing the brine to be preheated. The brine will flow down into the reactor through the vertical straight tube then it will warm up and the density will go down which will cause it to rise the coil picking up more heat as it rises. The heated brine will then flow up and out back into the main chamber of the reactor where the fluid will desalinate.

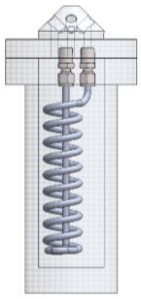

Figure 118: HEX Reactor Concept

In addition to the internal coil another smaller heat exchanger can be added to the inlet and outlet lines of the reactor concept shown.

## CONCLUSION

The engineering, heat transfer and thermodynamic properties of water and brine dictate the design of the HEX which has proven to be valid and functional. The next step is to verify the system and system improvements economically.

# CHAPTER 5 TECHNICAL AND ECONOMIC ANALYSIS

## INTRODUCTION

This chapter will discuss the technical and economic analysis of supercritical water desalination with heat recovery and compare its cost effectiveness to the traditional supercritical water desalination system that includes a chiller and a furnace. The resulting savings in power and maintenance by adding a HEX to the system and removing the chiller and furnace are discussed. Assumptions have been made to simplify the economic problem.

## ASSUMPTIONS

It is assumed that both systems are running for 24/7 or 8760 hours per year. The price of electricity is estimated to be $0.10 and $0.13. Inflation, appreciation, and depreciation are all ignored in this analysis because it is assumed that all components depreciate or appreciate at the same rate, which would cancel each other out anyway. The system will run for 8760 hours at a flow rate of 10ml/min. to calculate the total volume of water consumed. Both systems are estimated to produce the same amount of water at a rate of 5256 Liters (1389 Gallons) per year. The average person needs 100 gallons per day.

## ECONOMIC ANALYSIS

The components evaluated in the economic analysis are the reactor, the chiller, the furnace, and the HEX. These components, and their individual cost are shown in Table 44. Two systems are shown with different configurations. The First system includes the reactor, the chiller, and the furnace. The second system includes only the Reactor and the HEX. The HEX can thermally perform the tasks of the furnace and the chiller. Both systems cost about the same, within $1000 of each other. These values are the initial purchase price.

Table 44: Initial system cost broken out by major components

| Component Cost | | | |
|---|---|---|---|
| Desalination System | | Desal w HEX | |
| Reactor | $20,000 | Reactor | $ 20,000 |
| Chiller | $ 9,600 | HEX | $ 12,000 |
| Furnace | $ 1,500 | - | $ - |
| TOTALS | $31,100 | | $ 32,000 |

The power requirements for each system component are listed below. All components are powered by single phase 120 VAC power sources, except the HEX, which consumes 0W power. The annual energy cost per component if each component was left on individually for 1 year at the cost of $0.13 per kilowatt hour.

Table 45: Individual System Component Energy Consumption Comparison Table

| Individual Componenet Energy Consumption | | | | | | | |
|---|---|---|---|---|---|---|---|
| Component | Power Rating | Current | Voltage | Power | | | Annual Energy Cost Per Component |
| | W | Amps | V | Whrs | kWhrs | Mwhrs | |
| Reactor | 1500 | 11 | 115 | 13140000 | 13140 | 13.1 | $ 1,705.57 |
| Chiller | 1200 | 10 | 115 | 10512000 | 10512 | 10.5 | $ 1,364.46 |
| Furnace | 1200 | 10 | 120 | 10512000 | 10512 | 10.5 | $ 1,364.46 |
| HEX | 0 | 0 | 0 | 0 | 0 | 0 | $ - |

Two systems are represented in the tables below. The first system is comprised of a reactor and a heat exchanger. The second system includes the reactor, the chiller, and the furnace. The total cost of powering each system is listed as the total power cost. The total power consumption is listed as well. Powering the desalination system with waste heat recovery is significantly more cost effective than the system where it uses components where heat is continuously added to the system. Recycling heat costs less than constantly adding heat. A system with waste heat recovery or made from passive heat components costs 1/3 of a system with active heating components.

Tables 46 & 47 System type cost comparison in terms of energy

| | Waste Heat Recovery | | | | |
|---|---|---|---|---|---|
| | MWhrs | kWhrs | Watts | kWatts | Power Cost |
| Reactor | 13.1 | 13140 | 1500 | 1.5 | $ 1,705.57 |
| HEX | 0 | 0 | 0 | 0 | $ - |
| N/A | 0 | 0 | 0 | 0 | $ - |
| Total | 13.1 | 13140 | 1500 | 1.5 | $ 1,706 |

| | Added Heat System | | | | |
|---|---|---|---|---|---|
| | MWhrs | kWhrs | Watts | kWatts | Power Cost |
| Reactor | 13.1 | 13140 | 1500 | 1.5 | $ 1,705.57 |
| Chiller | 10.5 | 10512 | 1200 | 1.2 | $ 1,364.46 |
| Furnace | 10.5 | 10512 | 1200 | 1.2 | $ 1,364.46 |
| Total | 34.2 | 34164 | 3900 | 3.9 | $ 4,434 |

The system with heat recovery costs $1706 for power to run annually. The original unmodified desalination system with the chiller and furnace costs $4334 to power annually. Changing the coolant in the chiller is not included in Tables 45 and 46.

CHILLER MAINTENANCE COST

Removing the chiller will also increase savings in maintenance costs and make the system more environmentally friendly by reducing the need for ethylene glycol. The chiller uses a 50/50 mix of ethylene glycol. The chiller coolant tank capacity is 5.5 L (1.5gallons). If Ethylene glycol costs $51.72 per gallon, the cost per coolant change would be $103.44 annually if the coolant tank is changed quarterly. Any maintenance the furnace requires will also be removed. There are no moving parts on the HEX therefore the chances of something going wrong are reduced.

PAYBACK PERIOD AND PROJECTED ENERGY COST

The HEX will pay for itself in 7 years if the cost of electricity is $0.10/kWhr, if the cost per kilowatt hour increases by 2.9 cents per kWhr to $0.13/ kWhrs the HEX will pay for itself in 5 years in energy savings. If the instrumentation that was added to the heat exchanger for the purpose of this experiment is removed the initial cost of the heat exchanger is reduced to closer to $9K per HEX. This reduction in price will allow the HEX to pay for itself in 3 to 4 years if the price per kWhr remains at $0.13.

Table 48 shows the projected cost and savings out to 50 years assuming the cost of electricity remains the same.

Table 48: Cost Savings Analysis

| Energy Cost Over Time Per System | | | | Savings | | |
|---|---|---|---|---|---|---|
| Years | w HEX | w/o HEX | w/o HEX, Includes Chiller Cost | Energy | Maintenance | Energy and Maintenance |
| 1 | $ 1,706 | $ 4,434 | $ 4,538 | $ 2,729 | $ 103 | $ 2,832 |
| 2 | $ 3,411 | $ 8,869 | $ 9,076 | $ 5,458 | $ 207 | $ 5,665 |
| 3 | $ 5,117 | $ 13,303 | $ 13,614 | $ 8,187 | $ 310 | $ 8,497 |
| 4 | $ 6,822 | $ 17,738 | $ 18,152 | $ 10,916 | $ 414 | $ 11,329 |
| 5 | $ 8,528 | $ 22,172 | $ 22,690 | $ 13,645 | $ 517 | $ 14,162 |
| 7 | $ 11,939 | $ 31,041 | $ 31,765 | $ 19,102 | $ 724 | $ 19,826 |
| 10 | $ 17,056 | $ 44,345 | $ 45,379 | $ 27,289 | $ 1,034 | $ 28,324 |
| 15 | $ 25,584 | $ 66,517 | $ 68,069 | $ 40,934 | $ 1,552 | $ 42,485 |
| 20 | $ 34,111 | $ 88,690 | $ 90,759 | $ 54,578 | $ 2,069 | $ 56,647 |
| 30 | $ 51,167 | $133,035 | $ 136,138 | $ 81,867 | $ 3,103 | $ 84,971 |
| 40 | $ 68,223 | $177,379 | $ 181,517 | $ 109,157 | $ 4,138 | $ 113,294 |
| 50 | $ 85,279 | $221,724 | $ 226,896 | $ 136,446 | $ 5,172 | $ 141,618 |

VALUE OF AN OFF-GRID SYSTEM

If an off-grid system is considered reducing the energy consumption of the desalination system is imperative to system longevity. If the power required is reduced to 1/3 of its original cost the cost of the power generation is reduced by the same amount. By reducing the needed power capacity to power the system the cost of the power generation equipment is reduced. For example, if the reactor heater, furnace, and chiller all need a generator that can output 4 kilowatts and the furnace, and the chiller are removed then replaced with a heat exchanger a generator that can output 4 kilowatts is no longer needed and a less expensive generator that can output 1.5 kilowatts can be used instead. The power capacity of the power equipment needed is reduced.

SCALING UP THE SYSTEM

The first system produced in the laboratory pumped water at a volumetric flow rate of 10ml/min. The next system is intended to increase the water production rate to 100 ml/min, a 10X increase in magnitude. The graph in Figure 119 shows that the amount of water produced at different flow rates increases as the flow rate increases if the system is producing water 24 hours a day for 7 days a week over a year. As expected, the higher flow rate produces more water than lower flow rates. If a system is running at a higher flow rate the cost per gallon produced decreases. If the flow rate is increased the rate of heat lost from the reactor increases which costs the water producer more money which is spent on heating the reactor. If a heat exchanger network is added to the system, the heat can be recirculated.

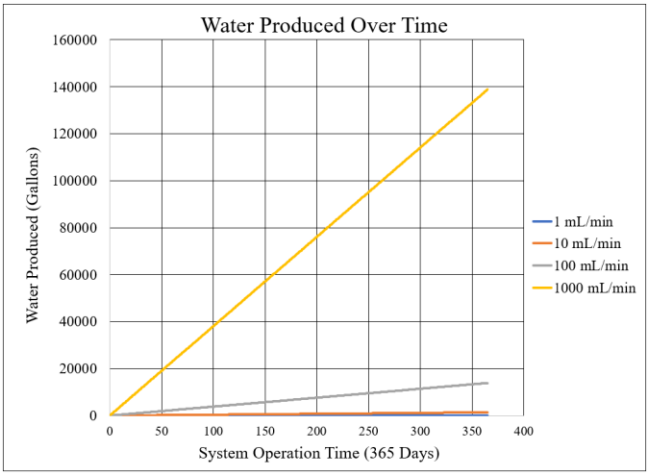


Figure 119: Economies of Scale

If the producing capacity of a SCWD system is increased by an another 10-fold to 1L/min the amount of money available to support the system increases by 10 times, which could also lower the cost of the water produced.

If the average family is 4 people and consumes 300 gallons of water per day how many families can a 210,000 gallon water bladder support for a given number of days. Water can be stored in large rubber bladders that have been designed to hold large amounts of liquid such as brine, oil, water, and fuel.

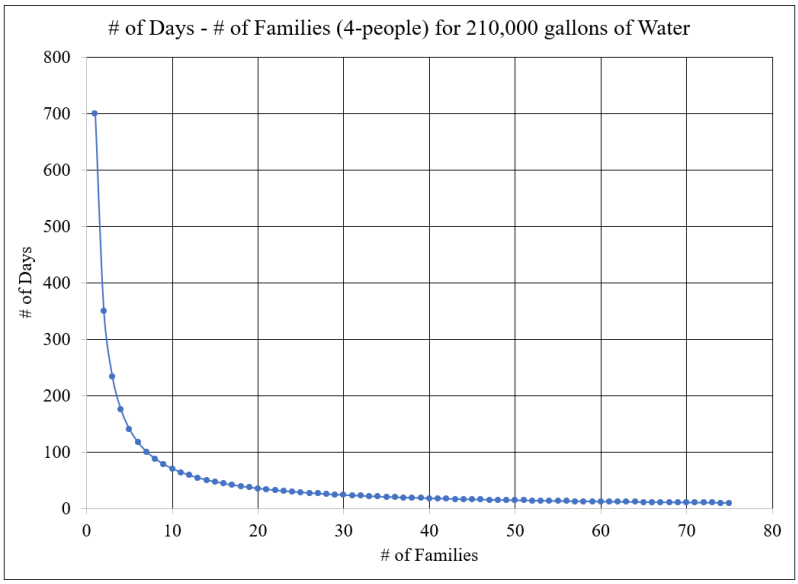


Figure 120: Water supply graph with 210,000 gallons of water available

For example, 7 families can use 300 gallons of water per day for 100 days if a 210,000 water bladder was filled with a desalination system. If a 1000 mL/minute system was produced and ran for 1 year it could not supply 7 families with enough water for 100 days. If the 100mL/min system is running for 1 year and produces 13,885 gallons of water 3 families can get by for about 1 month. Figure # shows the scenario where 13,885 gallons of water are available.

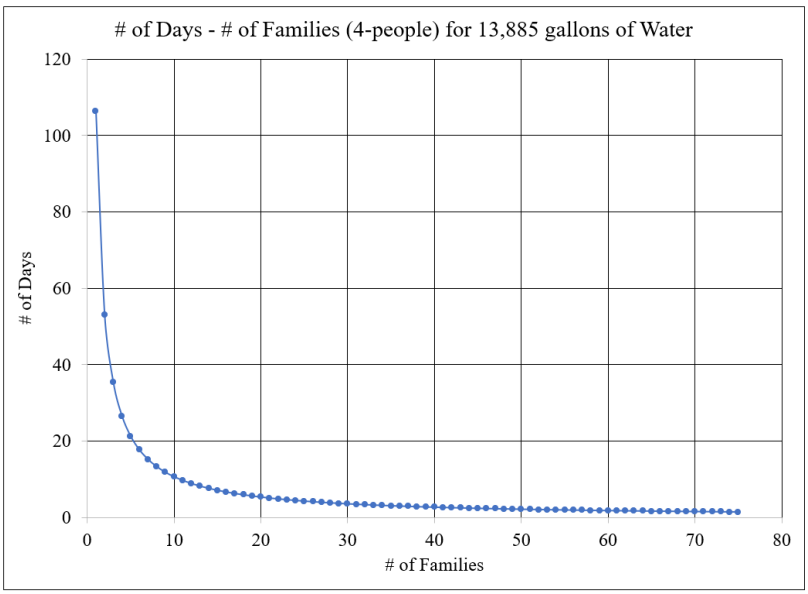

Figure 121: Water supply graph with 13,885 gallons of water available

UNCERTIANTY

It is uncertain of the length of time the HEX will last before the salt corrodes the sidewall of the cooling shell and the hot center tube beyond the safe wall thickness while the system is pressurized. A destructive test is recommended to determine how long 14%wt NaCl brine can be pumped through the system before there are structural integrity issues with the HEX as a pressure vessel. If the HEX can last 10 years before it needs to be replaced, then this is a good safe economically valid solution to the heat recovery problem. If the HEX constructed from 316 stainless steel under the mentioned conditions only lasts 1 year the material needs to be replaced with a more corrosion resistant material like titanium [38], [48].

APPLICATIONS OF SOLID SYSTEM WASTE

The system presented produces solid salt waste. This salt byproduct needs to be studied to find its contents. Once the contents are determined it can be further processed into usable salt. There is concern that heavy metals from the metallic processing equipment may find their way into the solid waste produced. There are salt flats all over the world and these regions could be used as a salt dumping ground. If humanity removes too much salt out of the ocean it can cause salt salinity problems as well. Mankind has proven in

the past to affect climates on a large scale, leading researchers to believe that mankind can also affect ocean salinity on a large scale. The salt waste disposal methods need to be carefully considered to maintain the balance nature desires. Salinity imbalances can have drastic effects on sea life, food chains, ecologies of the ocean. The density of the ocean can change which can affect tides which can alter coastlines. Maintaining balance is key. What is removed from the sea shall be returned to the sea in a consistent manner. If the salt is returned to the sea in a spread out way ill effects can be reduced.

## CONCLUSION

In conclusion, the economic analysis section adding a heat exchanger to a SCWD-ZLD will greatly increase the system's cost effectiveness by reducing the energy cost by 2/3 of the original system cost for the same amount of startup cost.

# CHAPTER 6 CONCLUSION

## INTRODUCTION

This section will discuss the future work and applications of the data that were found in this research study. The questions answered by this research effort are also discussed.

## RESEARCH QUESTIONS ANSWERED

- Can a simple cost-effective heat exchanger be constructed with commercial off the shelf (COTS) parts and reduce the energy requirement for a supercritical water desalination (SCWD) system?

Yes, medium to high pressure tubing and metallic compression fittings can be purchased and assembled using simple hand tools such as a bench vise, hacksaw, and wrench set for assembly in a remote location where power is scarce.

- Are the values of the dimensionless numbers in the empirical equations that are used to design conventional heat exchangers applicable for supercritical processes?

Not really, the values Nusselt number equations for turbulent flow do not apply to the HEXs presented in this work because the range of the Reynolds number values found are from above 0 to 350 which defines the fluid as in a laminar flow condition. The fully developed flow equations for the Nusselt number for constant surface temperature 3.66 and constant heat flux value of 4.36 are too low and do not apply because the heat flux and the surface temperature along the hot tube is not constant due to the thermophysical property variability and the function of the HEX.

The salt that is dissolved in the brine will corrode the wall by a small amount where it coats the boundary layer near the surface. The brine did not appear to desalinate at a pressure of 230 bar and a hot line entrance temperature of 410℃ while passing through HEX1. The temperatures measured throughout HEX1 with brine as the cooling fluid are close in value to the temperatures measured when deionized water

is used as a cooling fluid. This work proves that it is possible to design a heat exchanger out of COTS for a supercritical water desalination system to improve its economic viability.

## SYSTEM CORRECTIONS

It is preferred to use a data logger to collect data over long periods of time. It was attempted to use a data logger to collect data during experimentation, but the grounded thermocouples interfered with each other. The grounded thermocouples that the heat exchanger was constructed with were not compatible with the data logger. If the grounded thermocouples were changed to ungrounded thermocouples the data logger could collect data.

It was unknown at the beginning of the experiments how necessary insulation was. During early desalination experiments the tubing leading to the reactor was lightly insulated. The same light duty insulation was tried during the ramping up phase of experimentation. Both heat exchangers would have been fitted with the same thick-walled rock wool if it were known early on. The effectiveness of the insulation will determine the performance of the heat exchanger and it is necessary to have a thermally efficient system.

## LOGISTICS ISSUES

The logistic problems that caused this work delay were long lead times or indeterminate lead times. Obtaining fittings for the HEX's took months. The pump for the 10X system had a problem upon arrival where the diaphragm had a hole in it. The pump needed to be sent back to the factory for repair, this took approximately 8 months. As a result of the delayed pump the HEC was untested with the larger system. The pump delay delayed the 10X system testing which delayed the 10X HEX test.

## 10X SYSTEM

The 10X system still needs to be tested before introducing the HEXs or the HEC to provide information about its performance parameters with an added heat recovery system. Once the 10X system

is tested with water and salt to form a performance base line various sorts of heat exchangers can be added to increase the overall energy efficiency of the process. Figure 122 shows the 10X system with the large pump.

Figure 122: 10X System with pump

SAMPLES

Samples were collected during the study where brine is the cooling fluid. The Samples were collected after the brine flowed through the cooling jacket of HEX 2. These samples need to be run through a plasma spectrometer to see what materials were pulled out of the stainless-steel tubing through the corrosion processes that took place. It is obvious that the tubing was corroding because of the rust-colored water found in the cooling line collection tank. The best solution to the corrosion problem is to form a maintenance schedule where the heat exchanger is replaced once every “X” hour of run time or replace the 316 stainless steel components with titanium. Titanium equipment will minimize the corrosion that takes place.

FUTURE WORK

The system can be redesigned and produced without a chiller and a feedwater heater. The reduction in the equipment that is powered will reduce the amount of energy consumed by the overall system.

To further advance the technology, steps can be taken to create a heat exchanger network that desalinates the water, reducing the overall need for a reactor or reducing the size of the reactor.

The desalination system used in the experiment is a batch process. The salt needs to be emptied out of the reactor periodically, so the dip tube does not get clogged with salt. If the dip tube gets clogged with salt, there can be pressure to increase rapidly making the conditions unsafe. To stop the process and disassemble the reactor to remove the salt precipitate is time consuming and will be costly at larger scales of production. If the process studied can be continuous it becomes more economical and efficient to operate. Two heat exchangers can be produced and connected in a combination of series and parallel to desalinate some of the brine outside of the reactor. When one heat exchanger is filled with salt the flow can be reversed to clean it out.

Another option could be to have the 2 heat exchanger methods mentioned above and make the reactor smaller to reduce the energy consumed by the system.

This study is focused on heat and thermal engineering, perhaps the energy could be reduced with other methods like vacuum desalination. Vacuum desalination is where the pressure is lowered which lowers the boiling point of the water causing it to evaporate at room temperature. Vacuum desalination may be a more thermally efficient and safer method than SCWD-ZLD. Find Nusselt, Reynolds and Prandtl numbers for turbulent flow of water under supercritical conditions.

Build a supercritical water desalination system with a similar HEX as what is presented here and remove the chiller and FWH from the desalination system and evaluate the system performance.

Different Coatings need to be tested to see if they flake off while the system is functioning.

The 316 Stainless Steel is fine for a less expensive test pilot system, but some corrosion is still present and iron oxide is found in the samples in the form of rust. These particulates can be filtered out with a basic fiber filter yielding good clean drinking water.

It would be beneficial to know if the water molecule deforms under supercritical conditions, does it become flat like $CO_2$ and Nitrogen or does it stay the same shape and the electrons move to a more uniform shape around the molecule causing a charge shift due to the increase in pressure and temperature

that comes with supercritical conditions? Could viewing a water molecule under supercritical conditions be done with a scanning electron microscope?

## APPLICATIONS

As mentioned, the heat exchanger concept can be applied to a SCWD process as shown in this work, but there are other applications where. The Nusselt number found in this work can be applied to Supercritical Water Oxidation (SCWO) systems, or Supercritical Water Reactor (SCWR) [49]. A SCWR is a $4^{th}$ generation concept reactor that is water-cooled high temperature high-pressure light water-cooled reactor that operates above the critical point of water. SCWRs can use supercritical heat exchangers to recover heat or transfer it to a separate fluid to then run a turbine thus turn a generator, generating power for the public.

## CONCLUSION

The technology studied in this paper is still under development and steps must be taken to increase its safety and economic feasibility for larger scale applications. Now that this study is complete the knowledge of supercritical water heat exchangers can be passed on to the next pupil.

# REFERENCES


[1] G. Glosson, “Simulating and Optimizing a Zero-Waste Wave-to-Water Desalination System,” East Carolina University, Greenville, 2023.

[2] J. McMorris, “Oscillating Surge Wave Energy Converter Geometry Optimization for Direct Seawater Desalination,” East Carolina University, Greenville, 2023.

[3] K. Weddle, “Heat Transfer Characteristics of a Heat Exchanger in a Solar-Assisted, Supercritical Brayton Cycle for Power Generation,” East Carolina University, Greenville, 2023.

[4] F. Incropera, D. DeWitt, T. Bergman, and A. Lavine, *Fundamentals of Heat and Mass Transfer*, 6th ed. Hoboken: John Wiley & Sons, 2007.

[5] C. Borgnakke and R. E. Sonntag, *Fundamentals of Thermodynamics*, 7th ed. John Wiley & Sons, 2009.

[6] Y. Zhang *et al.*, “Inorganic salts in sub-/supercritical water—Part A: Behavior characteristics and mechanisms,” *Desalination*, vol. 496, p. 114674, Dec. 2020, doi: 10.1016/j.desal.2020.114674.

[7] K. Duba and L. Fiori, “Supercritical $CO_2$ extraction of grape seeds oil: scale-up and economic analysis,” *Int J Food Sci Technol*, vol. 54, no. 4, pp. 1306–1312, Apr. 2019, doi: 10.1111/ijfs.14104.

[8] S. Han, “Anomalous change in the dynamics of a supercritical fluid,” *Phys Rev E*, vol. 84, no. 5, p. 051204, Nov. 2011, doi: 10.1103/PhysRevE.84.051204.

[9] C. M. Able, D. D. Ogden, and J. P. Trembly, “Sustainable management of hypersaline brine waste: Zero liquid discharge via Joule-heating at supercritical condition,” *Desalination*, vol. 444, pp. 84–93, Oct. 2018, doi: 10.1016/j.desal.2018.07.014.

[10] D. D. Ogden and J. P. Trembly, “Desalination of hypersaline brines via Joule-heating: Experimental investigations and comparison of results to existing models,” *Desalination*, vol. 424, pp. 149–158, Dec. 2017, doi: 10.1016/j.desal.2017.10.006.

[11] F. E. Ahmed, R. Hashaikeh, and N. Hilal, “Solar powered desalination – Technology, energy and future outlook,” *Desalination*, vol. 453, pp. 54–76, Mar. 2019, doi: 10.1016/j.desal.2018.12.002.

[12] M. Qasim, M. Badrelzaman, N. N. Darwish, N. A. Darwish, and N. Hilal, “Reverse osmosis desalination: A state-of-the-art review,” *Desalination*, vol. 459, pp. 59–104, Jun. 2019, doi: 10.1016/j.desal.2019.02.008.

[13] C. M. Able and J. P. Trembly, “Advanced supercritical water-based process concepts for treatment and beneficial reuse of brine in oil/gas production,” *Desalination*, vol. 481, p. 114334, May 2020, doi: 10.1016/j.desal.2020.114334.

[14] S. van Wyk, A. G. J. van der Ham, and S. R. A. Kersten, “Analysis of the energy consumption of supercritical water desalination (SCWD),” *Desalination*, vol. 474, Jan. 2020, doi: 10.1016/j.desal.2019.114189.

[15] S. van Wyk, S. O. Odu, A. G. J. van der Ham, and S. R. A. Kersten, “Design and results of a first generation pilot plant for supercritical water desalination (SCWD),” *Desalination*, vol. 439, pp. 80–92, Aug. 2018, doi: 10.1016/j.desal.2018.03.028.

[16] J. L. Bischoff, R. J. Rosenbauer, and K. S. Pitzer, “The system NaCl-H2O: Relations of vapor-liquid near the critical temperature of water and of vapor-liquid-halite from 300° to 500°C,” *Geochim Cosmochim Acta*, vol. 50, no. 7, Jul. 1986, doi: 10.1016/0016-7037(86)90317-0.

[17] T. Driesner and C. A. Heinrich, “The system H2O–NaCl. Part I: Correlation formulae for phase relations in temperature–pressure–composition space from 0 to 1000°C, 0 to 5000bar, and 0 to 1 XNaCl,” *Geochim Cosmochim Acta*, vol. 71, no. 20, Oct. 2007, doi: 10.1016/j.gca.2006.01.033.

[18] T. Driesner, “The system H2O–NaCl. Part II: Correlations for molar volume, enthalpy, and isobaric heat capacity from 0 to 1000°C, 1 to 5000bar, and 0 to 1 XNaCl,” *Geochim Cosmochim Acta*, vol. 71, no. 20, Oct. 2007, doi: 10.1016/j.gca.2007.05.026.

[19] T. G. Walmsley, N. S. Lal, P. S. Varbanov, and J. J. Klemeš, “Automated retrofit targeting of heat exchanger networks,” *Front Chem Sci Eng*, vol. 12, no. 4, Dec. 2018, doi: 10.1007/s11705-018-1747-2.

[20] M. H. Panjeh Shahi and A. Khoshgard, “Heat Exchanger Networks Targeting and Design with Unequal Heat Transfer Coefficient Regarding Allowable Pressure Drop of Streams,” *Heat Transfer Engineering*, vol. 27, no. 9, Oct. 2006, doi: 10.1080/01457630600845887.

[21] W. Gu, X. Chen, K. Liu, B. Zhang, Q. Chen, and C.-W. Hui, “Retrofitting of the Heat Exchanger Network with Steam Generation in a Crude Oil Distillation Unit,” *Chem Eng Technol*, vol. 38, no. 2, Feb. 2015, doi: 10.1002/ceat.201400232.

[22] N. Jiang, S. Bao, and Z. Gao, “Heat Exchanger Network Integration Using Diverse Pinch Point and Mathematical Programming,” *Chem Eng Technol*, vol. 34, no. 6, Jun. 2011, doi: 10.1002/ceat.201000260.

[23] L. Kang, Y. Liu, and N. Jiang, “Synthesis of large-scale heat exchanger networks using a T-Q diagram method,” *Can J Chem Eng*, vol. 94, no. 10, Oct. 2016, doi: 10.1002/cjce.22556.

[24] A. Isafiade and D. Fraser, “Optimization of combined heat and mass exchanger networks using pinch technology,” *Asia-Pacific Journal of Chemical Engineering*, vol. 2, no. 6, Nov. 2007, doi: 10.1002/apj.100.

[25] R. Nordman and T. Berntsson, “New pinch technology based hen analysis methodologies for cost-effective retrofitting,” *Can J Chem Eng*, vol. 79, no. 4, Aug. 2001, doi: 10.1002/cjce.5450790426.

[26] A. Lazzaretto and F. Segato, “Thermodynamic Optimization of the HAT Cycle Plant Structure—Part II: Structure of the Heat Exchanger Network,” *J Eng Gas Turbine Power*, vol. 123, no. 1, Jan. 2001, doi: 10.1115/1.1339000.

[27] E. M. Al-Mutairi and B. S. Babaqi, “Energy optimization of integrated atmospheric and vacuum crude distillation units in oil refinery with light crude,” *Asia-Pacific Journal of Chemical Engineering*, vol. 9, no. 2, pp. 181–195, Mar. 2014, doi: 10.1002/apj.1758.

[28] J. Zun-long, D. Qi-wu, and L. Min-shan, “Exergoeconomic Analysis of Heat Exchanger Networks for Optimum Minimum Approach Temperature,” *Chem Eng Technol*, vol. 31, no. 2, Feb. 2008, doi: 10.1002/ceat.200700387.

[29] J.-C. Bonhivers, A. Moussavi, R. Hackl, M. Sorin, and P. R. Stuart, “Improving the network pinch approach for heat exchanger network retrofit with bridge analysis,” *Can J Chem Eng*, vol. 97, no. 3, Mar. 2019, doi: 10.1002/cjce.23422.

[30] J. Khorshidi and S. Heidari, “Design and Construction of a Spiral Heat Exchanger,” *Advances in Chemical Engineering and Science*, vol. 06, no. 02, 2016, doi: 10.4236/aces.2016.62021.

[31] Y. A. Cengel, R. H. Turner, and J. M. Cimbala, *Fundamentals of Thermal-Fluid Sciences*, 3rd ed. New York, NY: McGraw-Hill, 2008.

[32] Y. A. Cengel and A. J. Ghajar, *Heat and Mass Transfer Fundamentals & Applications*, Sixth. New York: McGraw-Hill Education, 2020.

[33] R. J. Roselli and K. R. Diller, *Biotransport: Principles and Applications*. New York, NY: Springer New York, 2011. doi: 10.1007/978-1-4419-8119-6.

[34] M. Pizzarelli, “The status of the research on the heat transfer deterioration in supercritical fluids: A review,” *International Communications in Heat and Mass Transfer*, vol. 95, pp. 132–138, Jul. 2018, doi: 10.1016/j.icheatmasstransfer.2018.04.006.

[35] X. Huang, Q. Wang, Z. Song, Y. Yin, and H. Wang, “Heat transfer characteristics of supercritical water in horizontal double-pipe,” *Appl Therm Eng*, vol. 173, p. 115191, Jun. 2020, doi: 10.1016/j.applthermaleng.2020.115191.

[36] N. L. Dickinson and C. P. Welch, “Heat Transfer to Supercritical Water,” 1958. [Online]. Available: http://asmedigitalcollection.asme.org/fluidsengineering/article-pdf/80/3/746/6825089/746_1.pdf

[37] S. O. Odu, A. G. J. van der Ham, S. Metz, and S. R. A. Kersten, “Design of a Process for Supercritical Water Desalination with Zero Liquid Discharge,” *Ind Eng Chem Res*, vol. 54, no. 20, May 2015, doi: 10.1021/acs.iecr.5b00826.

[38] D. Prando *et al.*, “Corrosion of Titanium: Part 1: Aggressive Environments and Main Forms of Degradation,” *J Appl Biomater Funct Mater*, vol. 15, no. 4, Jan. 2017, doi: 10.5301/jabfm.5000387.

[39] R. J. Franco, “Failures of Heat Exchangers,” in *Failure Analysis and Prevention*, vol. 11, ASM International, 2002, pp. 628–642. doi: 10.31399/asm.hb.v11.a0001817.

[40] K. R. Weddle, T. Abdel-Salam, K. Duba, and F. Filho, “NUMERICAL STUDY OF A SOLAR-ASSISTED SCO2 BRAYTON CYCLE FOR POWER GENERATION,” in *Proceeding of 8th Thermal and Fluids Engineering Conference (TFEC)*, Connecticut: Begellhouse, 2023, pp. 599–608. doi: 10.1615/TFEC2023.ens.046408.

[41] C. L. Beck, N. P. Smith, B. J. Riley, and S. B. Clark, “Adsorption of iodine on metal coupons in humid and dry environments,” *Journal of Nuclear Materials*, vol. 556, p. 153204, Dec. 2021, doi: 10.1016/j.jnucmat.2021.153204.

[42] A. M. Leung, L. E. Braverman, and E. N. Pearce, “History of U.S. iodine fortification and supplementation.,” *Nutrients*, vol. 4, no. 11, pp. 1740–6, Nov. 2012, doi: 10.3390/nu4111740.

[43] E. A. Avallone, T. Baumeister III, and A. M. Sadegh, *90th Anniversary Edition Mark’s Standard Handbook for Mechanical Engineers*, 11th ed. New York: McGraw Hill, 2007.

[44] F. Rosebury, *Handbook of Electron Tube and Vacuum Techniques*, 1993rd ed. Woodbury: American Institute of Physics, 1964.

[45] W. H. Kohl, *Handbook of Materials and Techniques for Vacuum Devices*, 1995th ed. Woodbury, NY: American Institute of Physics, 1967.

[46] R. Hosseinnejad, M. Hosseini, and M. Farhadi, “Turbulent heat transfer in tubular heat exchangers with twisted tape,” *J Therm Anal Calorim*, vol. 135, no. 3, Feb. 2019, doi: 10.1007/s10973-018-7400-y.

[47] V. Mokkapati and C.-S. Lin, “Numerical study of an exhaust heat recovery system using corrugated tube heat exchanger with twisted tape inserts,” *International Communications in Heat and Mass Transfer*, vol. 57, pp. 53–64, Oct. 2014, doi: 10.1016/j.icheatmasstransfer.2014.07.002.

[48] R. A, M. S, V. K. Balla, M. Das, and G. Manivasagam, “Current advances in enhancement of wear and corrosion resistance of titanium alloys – a review,” *Materials Technology*, vol. 31, no. 12, Oct. 2016, doi: 10.1080/10667857.2016.1212780.

[49] P. Wu, Y. Ren, M. Feng, J. Shan, Y. Huang, and W. Yang, “A review of existing SuperCritical Water reactor concepts, safety analysis codes and safety characteristics,” *Progress in Nuclear Energy*, vol. 153, p. 104409, Nov. 2022, doi: 10.1016/j.pnucene.2022.104409.

# APPENDIX A: THERMOCOUPLE CALIBRATION

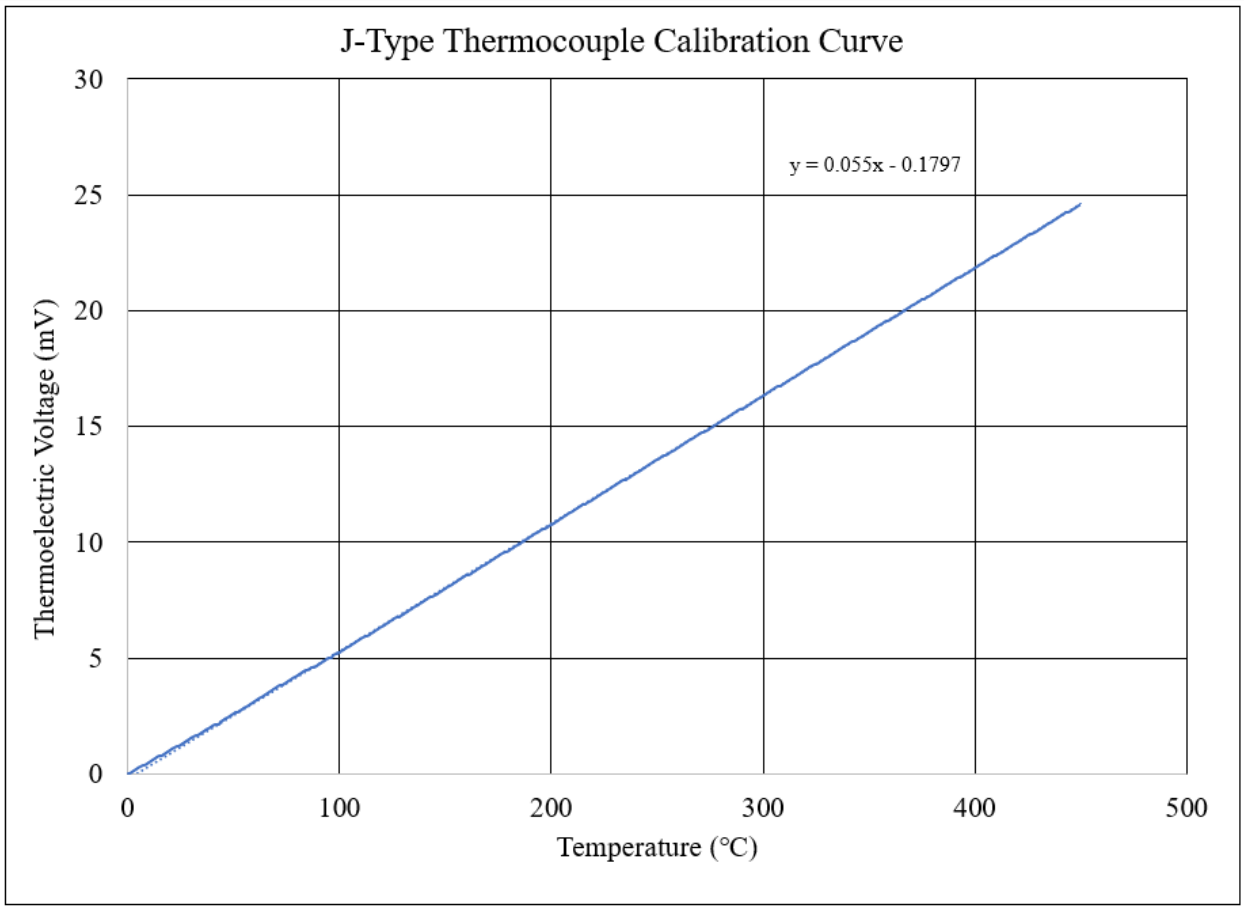


Figure 123: J-Type Thermocouple Calibration Curve Using NIST Data

# APPENDIX B: BRINE CONDUCTIVITY

The data shown in the calibration curve in Figure 124 was determined experimentally by mixing NaCl and DI water in a beaker.

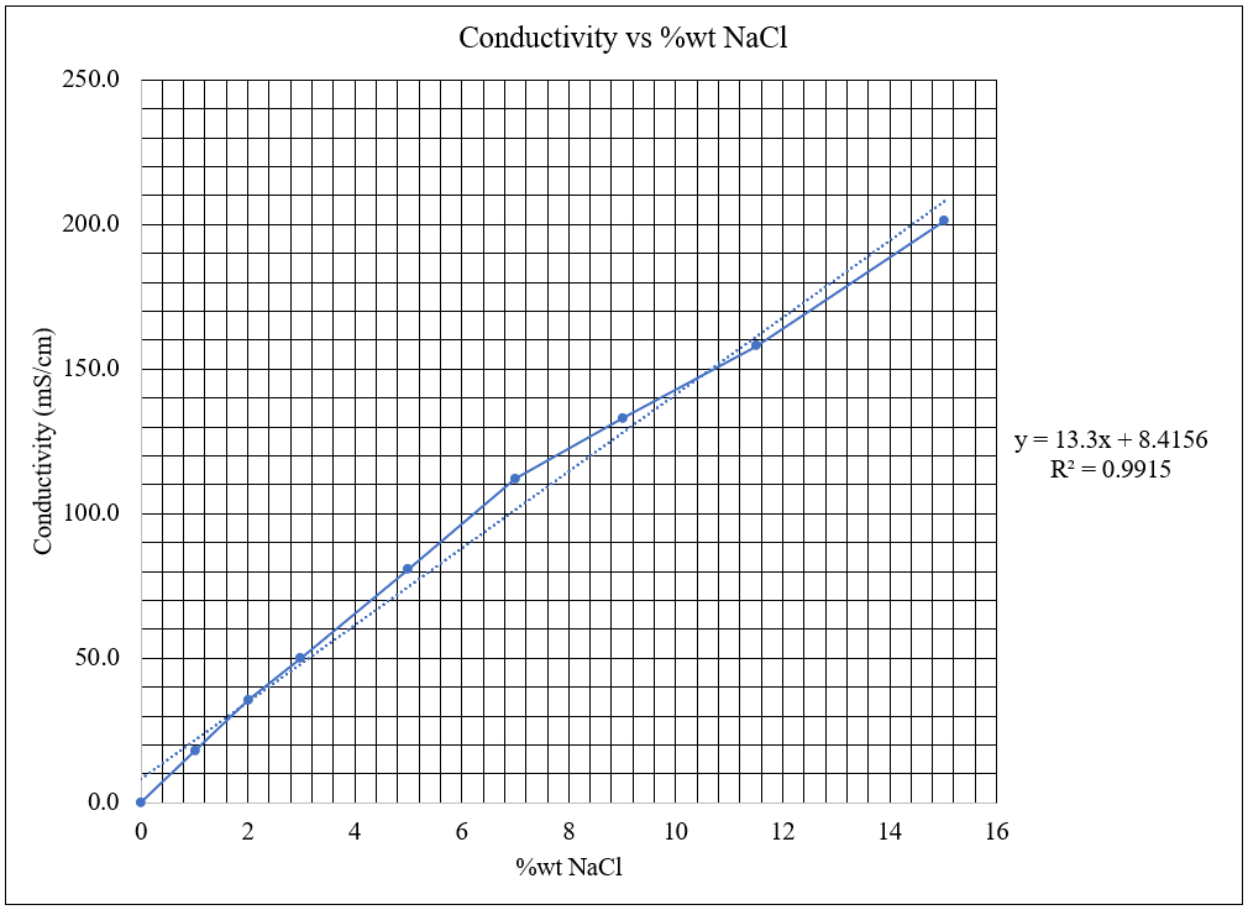


Figure 124: Conductivity dependent on salinity of NaCl by % weight.

# APPENDIX C: MATLAB CODE

The MATLAB code provided only import data from a spread sheet and plots it. There are very few calculations taking place within the MATLAB program.

# APPENDIX D: DATA

Contact the author or institution for data collected during this study. It is too large and ungainly to show in an appendix.

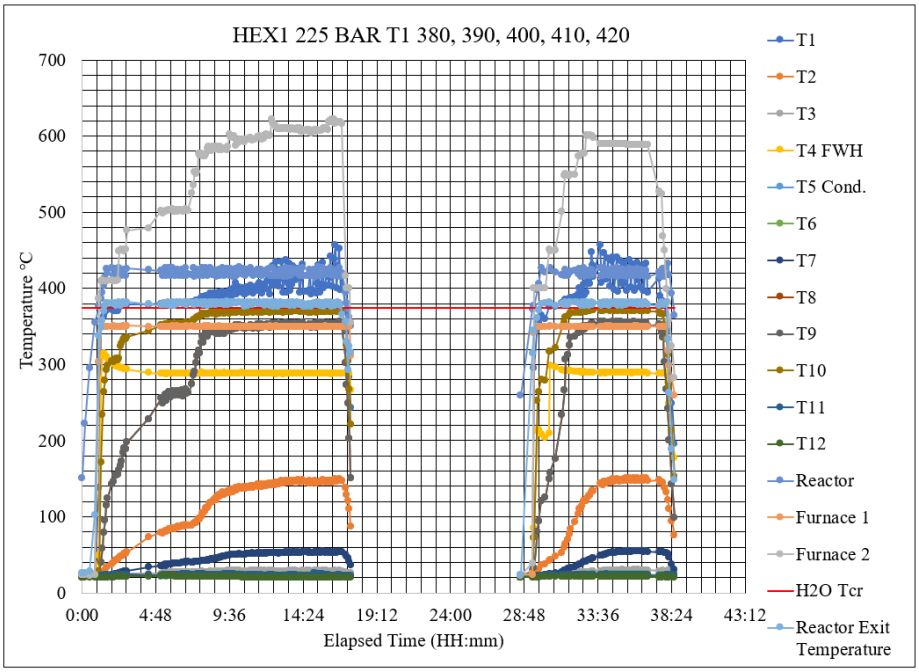


Figure 125: HEX1 at 225 BAR with hot inlet temperatures T1 of 380, 390, 400, 410 420

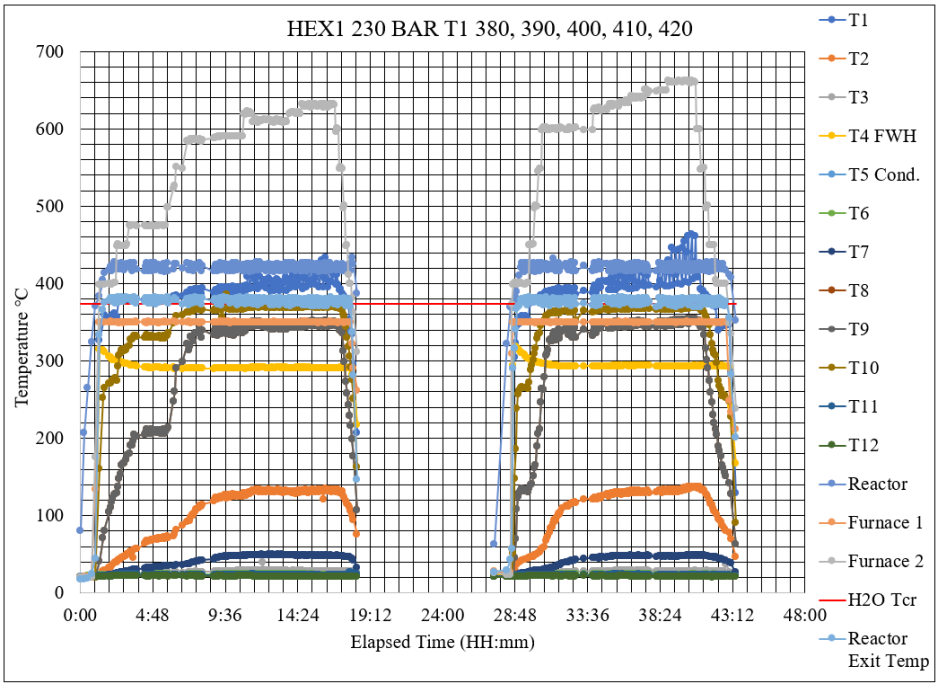


Figure 126: HEX1 at 230 BAR with hot inlet temperatures T1 of 380, 390, 400, 410 420

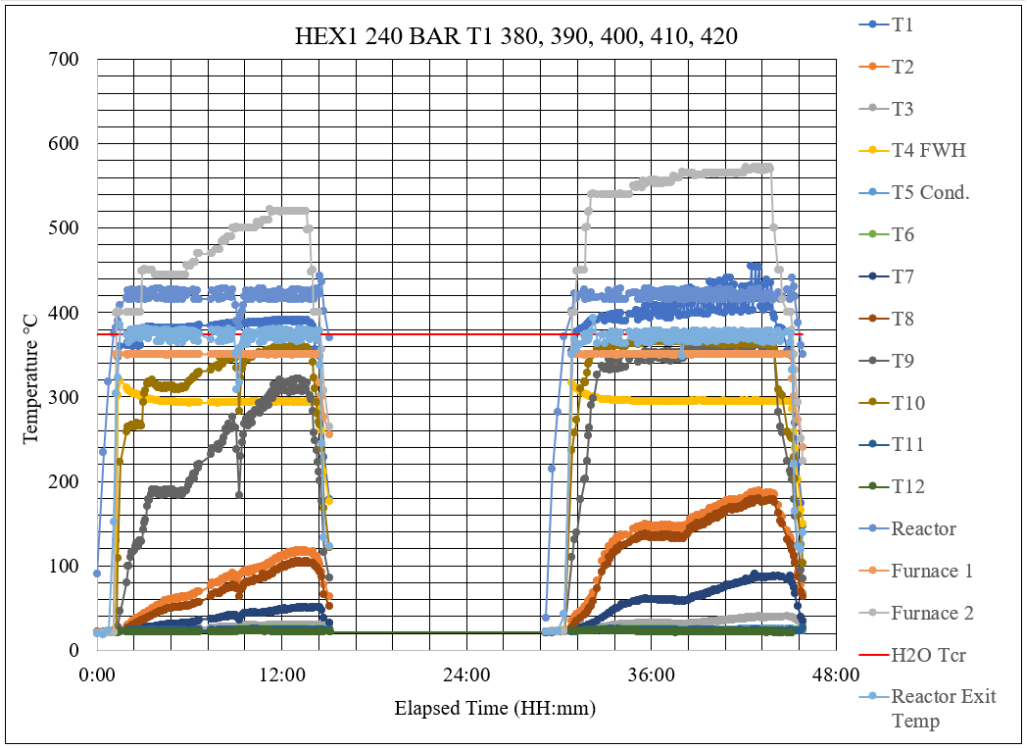

Figure 127: HEX1 at 240 BAR with hot inlet temperatures T1 of 380, 390, 400, 410 420

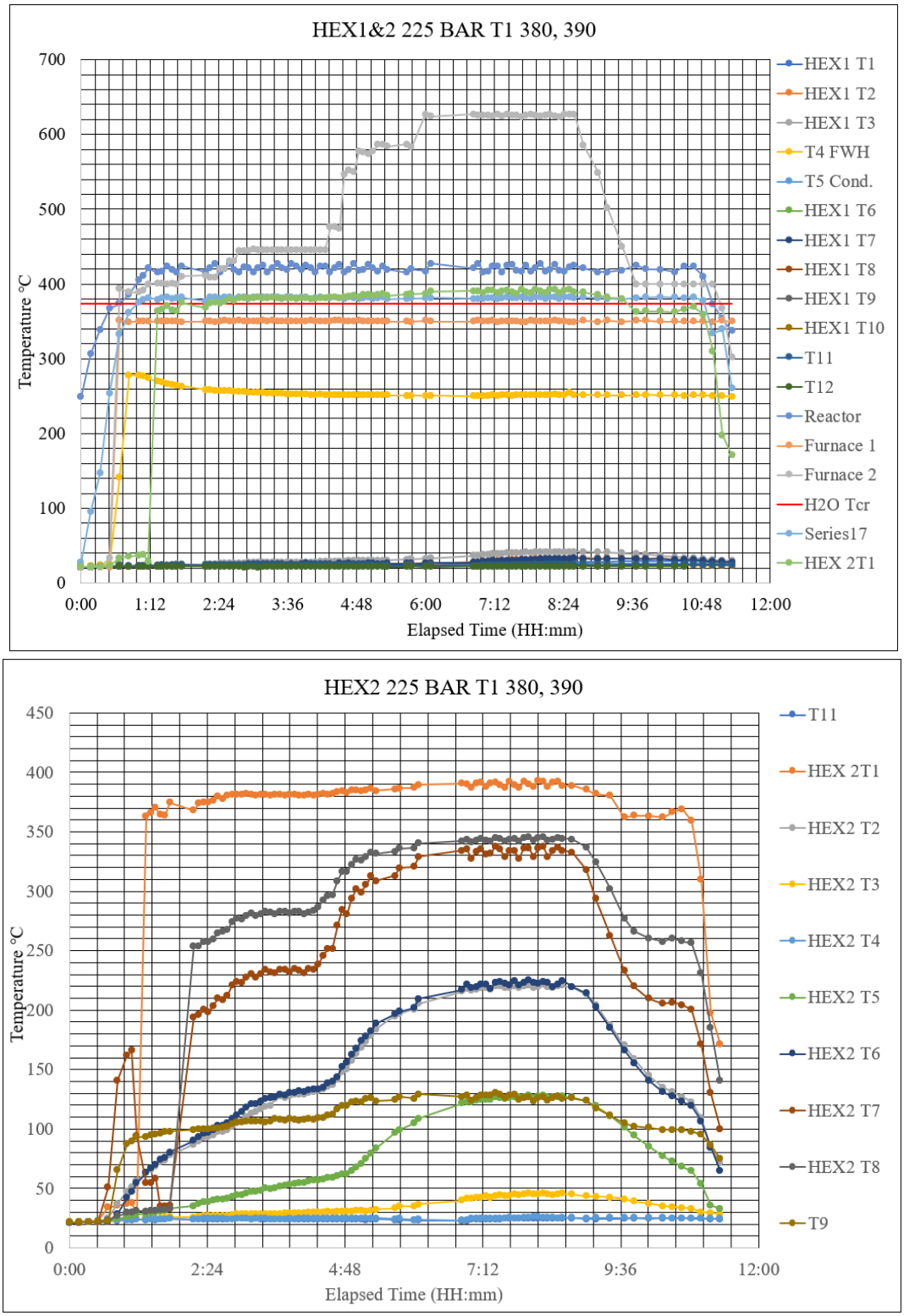


Figure 128: HEX1 & HEX2 at 225 BAR with T1 of 380 and 390

The graphs that are in similar format to Figure # are linked as one figure because the data was recorded for the same experiment at the same time.

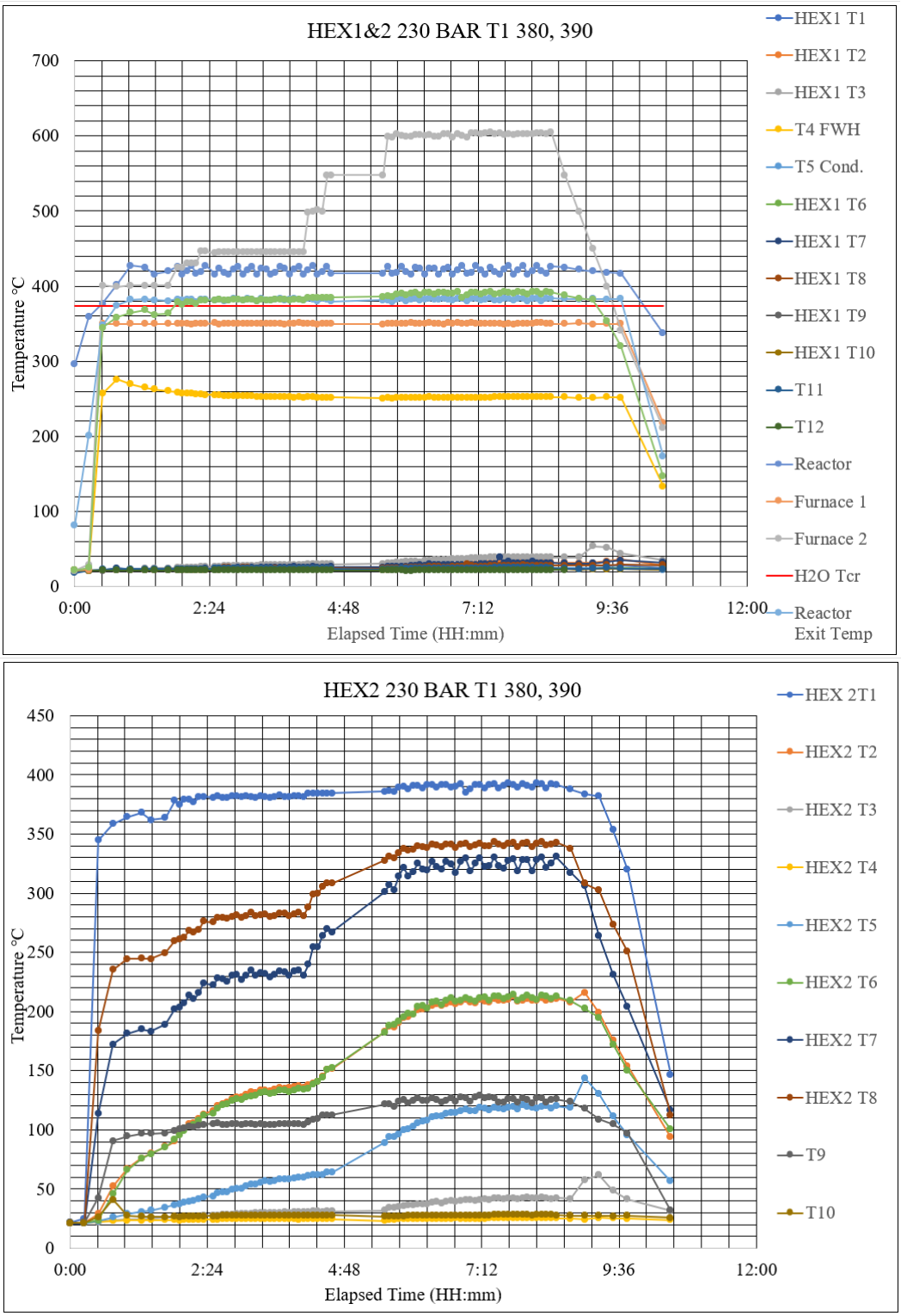


Figure 129: HEX1 & HEX2 at 230 BAR with T1 of 380 and 390

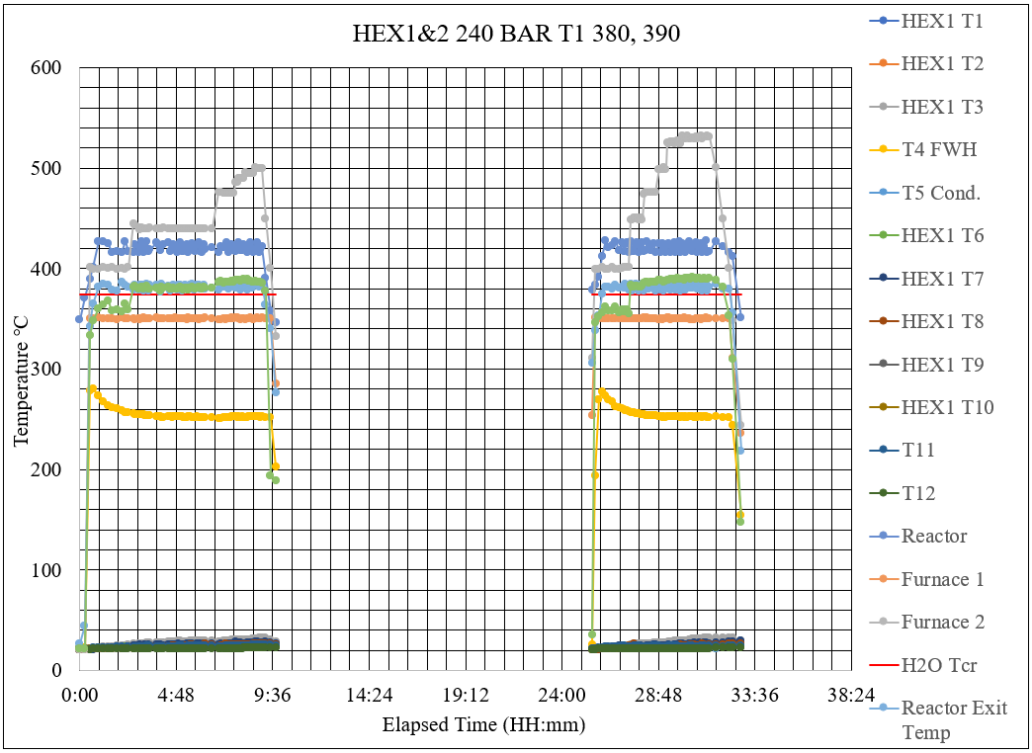


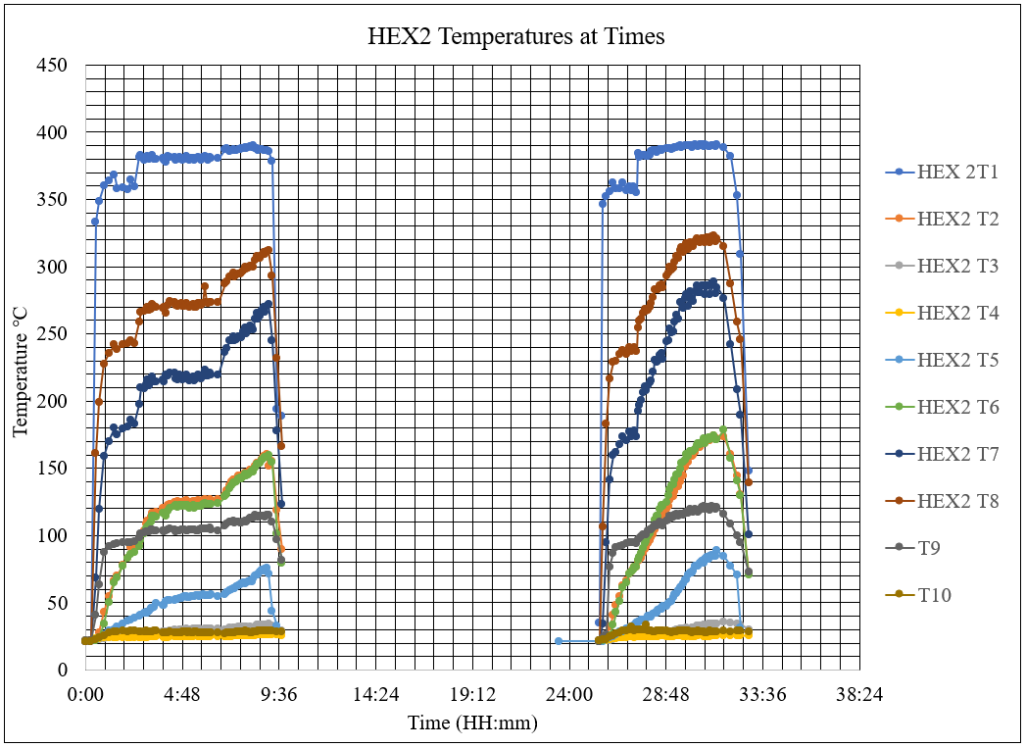


Figure 130: HEX1 & HEX2 at 240 BAR with T1 of 380 and 390

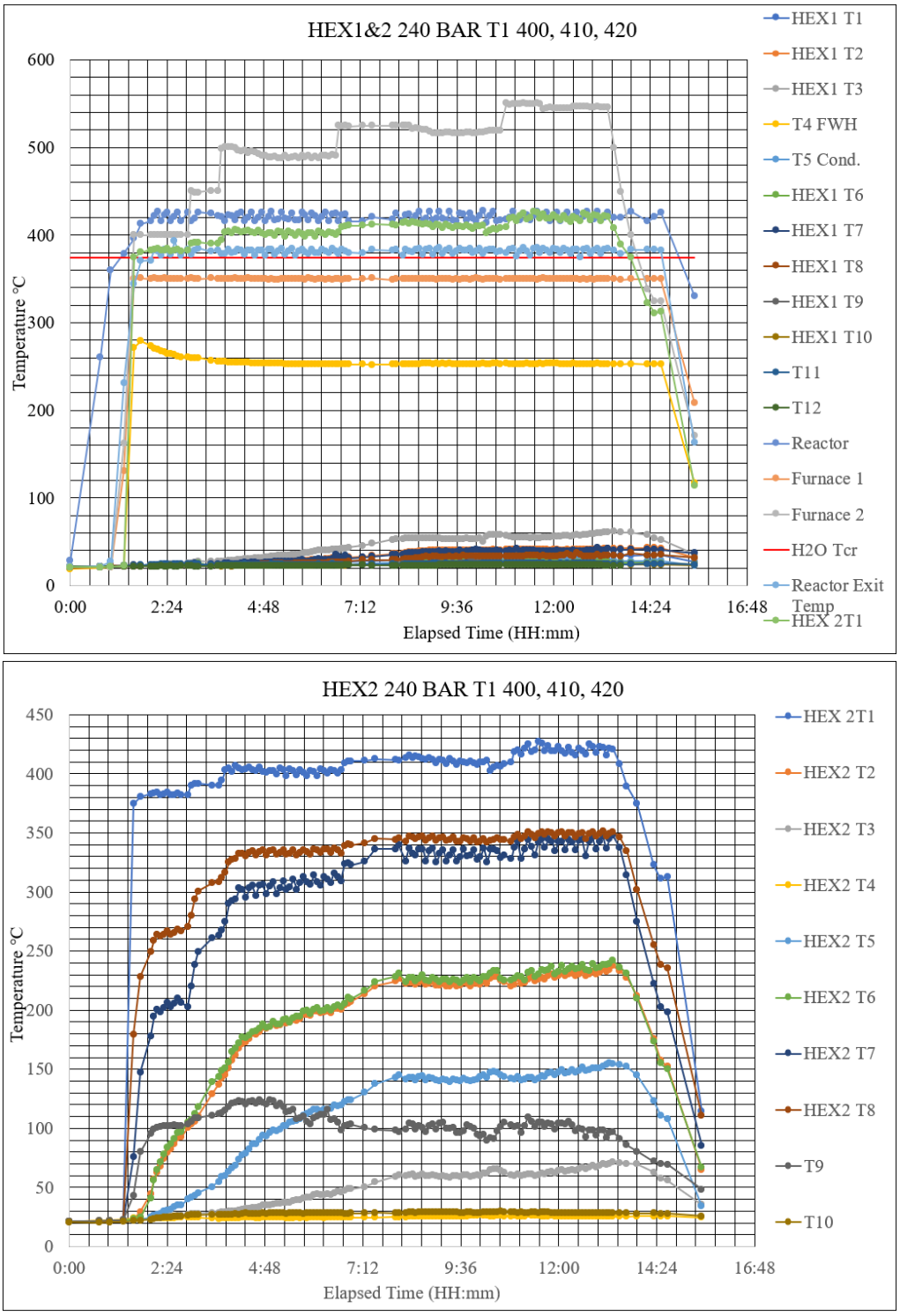


Figure 131: HEX1 & HEX2 at 240 BAR with T1 of 400, 410 and 420

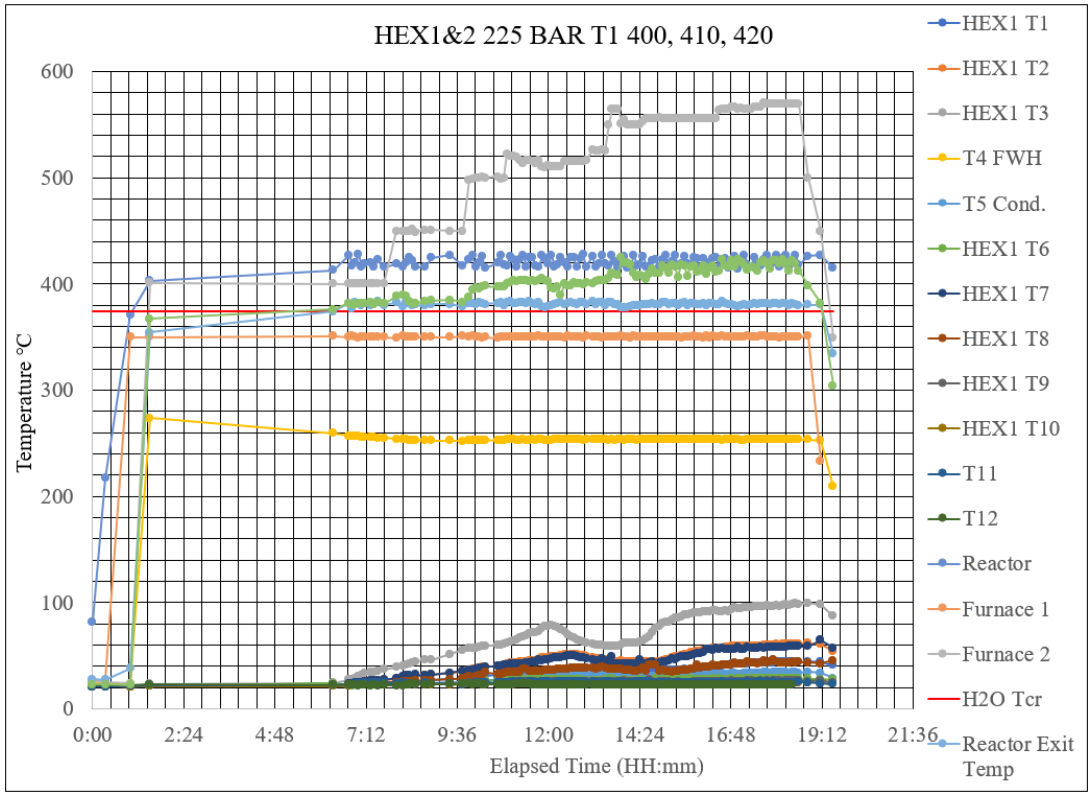


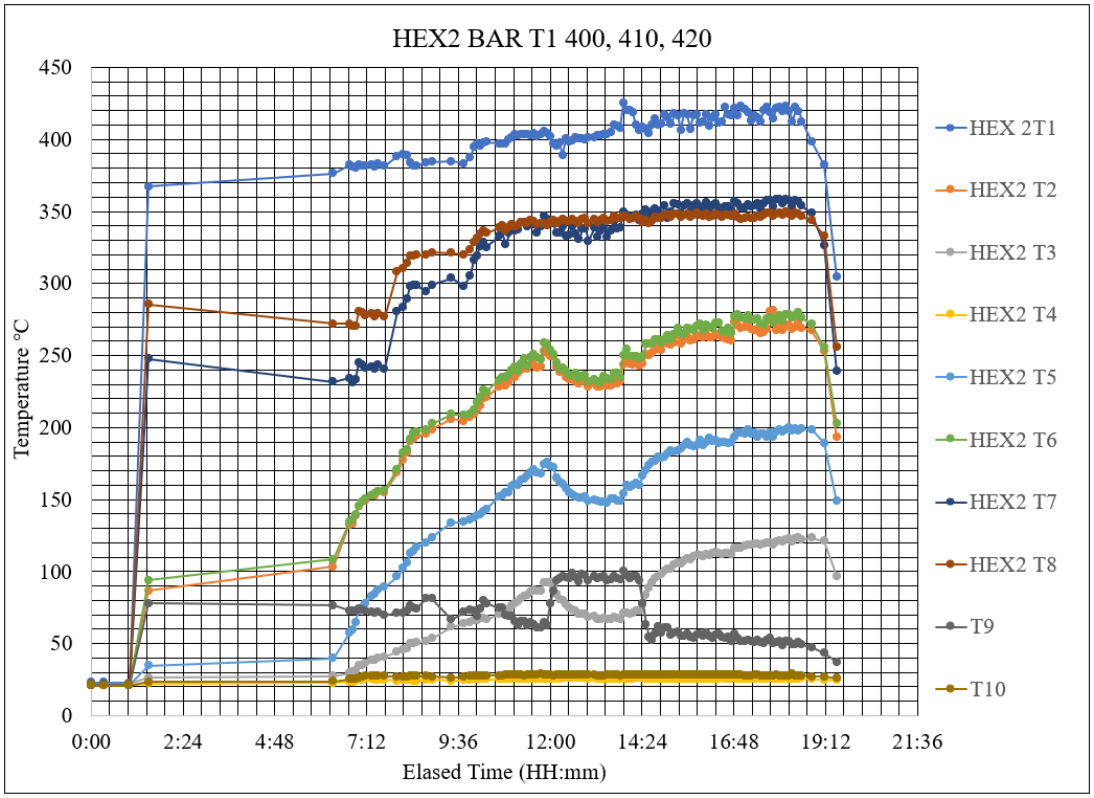


Figure 132: HEX1 & HEX2 at 240 BAR with T1 of 400, 410 and 420

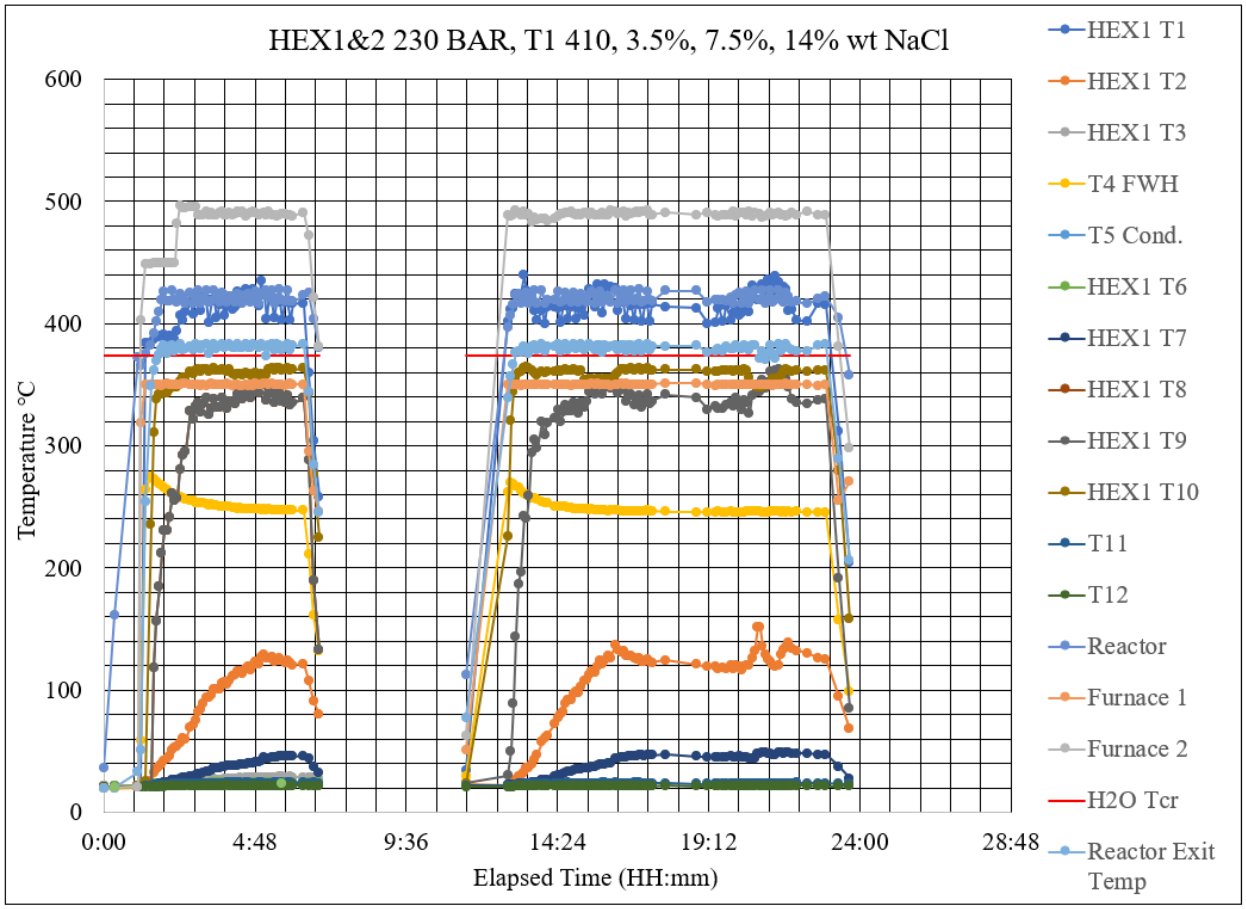


Figure 133: HEX1 at 230 Bar with T1 of 410 with 3.5wt%, 7.5wt% and 14wt% NaCl

# APPENDIX E: MECHANICAL DRAWINGS

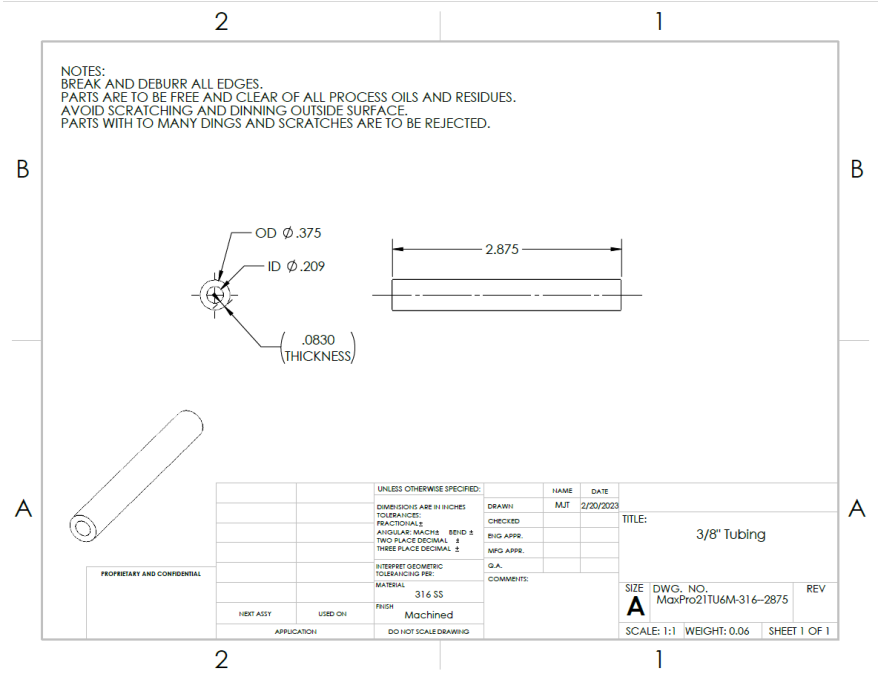


Figure 134: 3/8” Tubing 2.875” long

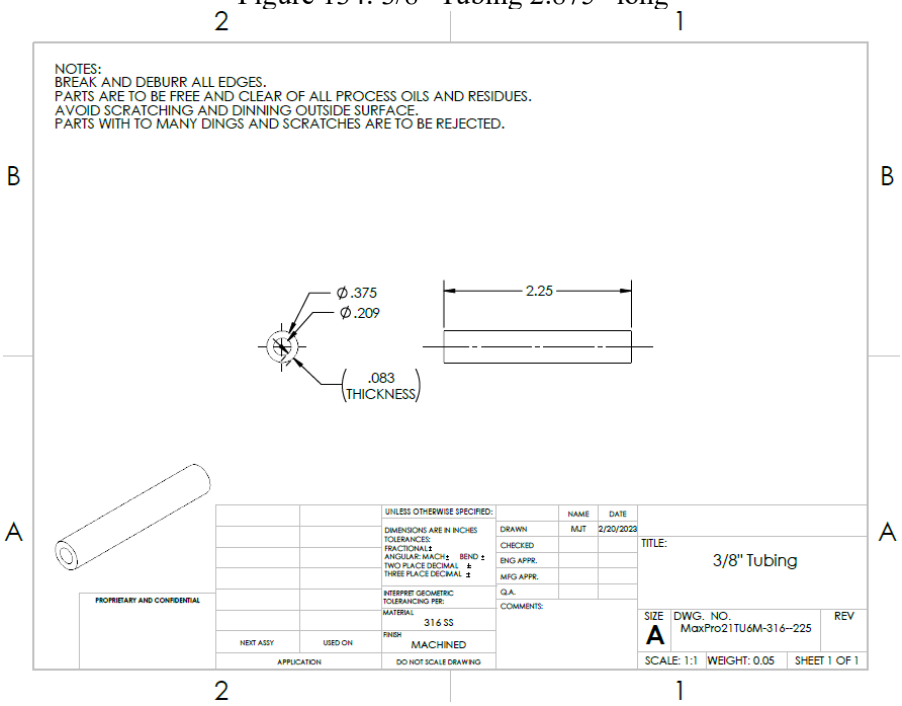


Figure 135: 3/8” Tubing 2.25” long

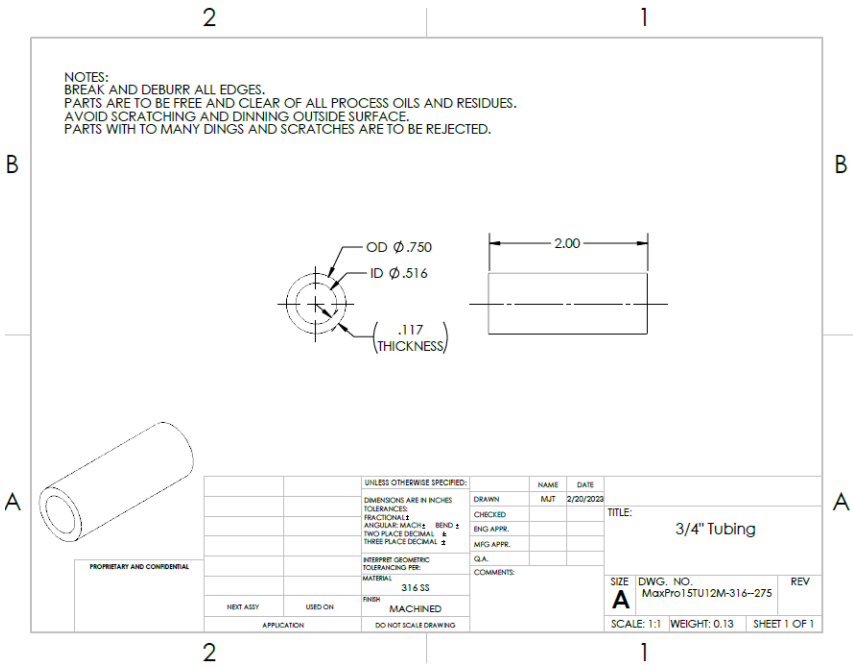


Figure 136: ¾" Tubing 2" long

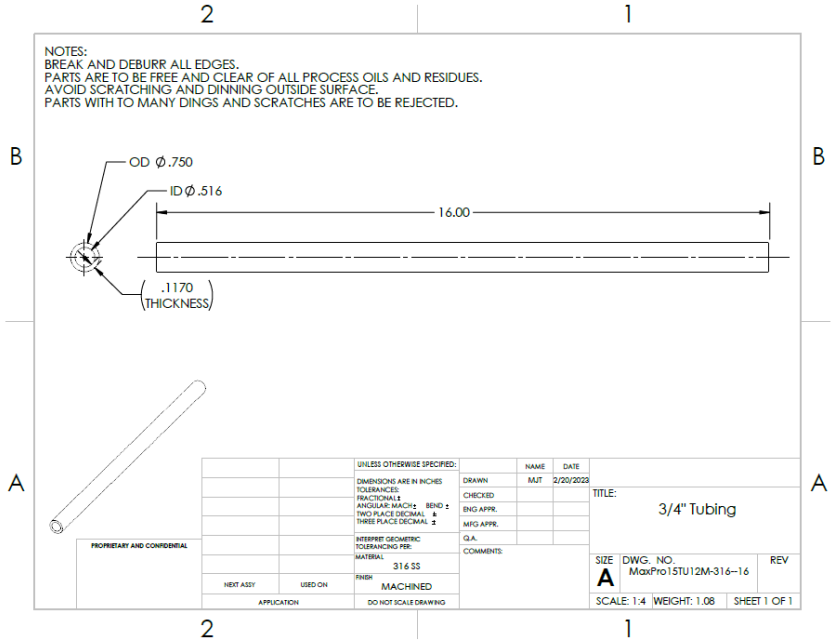


Figure 137: ¾" Tubing 2" long

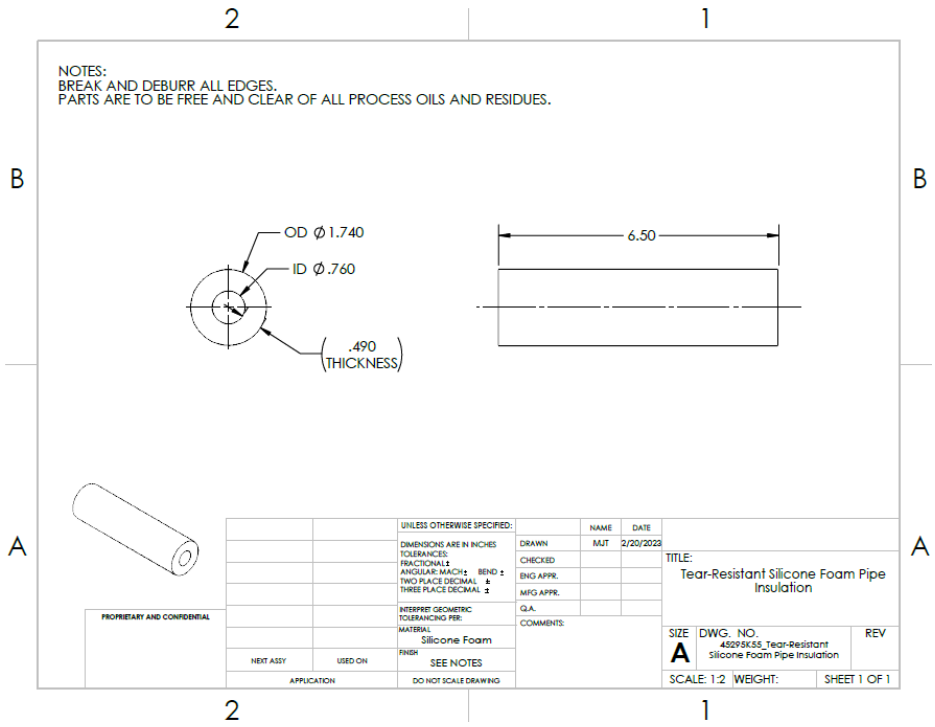


Figure 138: Insulation

| ITEM NO. | PartNo | DESCRIPTION | Vendor | QTY. |
|---|---|---|---|---|
| 1 | 15TU12M-316 | 3/4" Tubing | MaxPro | 12 |
| 2 | 15TU12M-316 | 3/4" Tubing | MaxPro | 4 |
| 3 | 21TU6M-316 | 3/8" Tubing | MaxPro | 13 |
| 4 | 21TU6M-316 | 3/8" Tubing | MaxPro | 2 |
| 5 | 21TU6M-316 | 3/8" Tubing | MaxPro | 2 |
| 6 | SS-1210-6-6 | 3/4" to 3/8" Reducer Union | Swagelok Company | 2 |
| 7 | SS-600-6-4 | 3/8" to 1/4" Reducer Union | Swagelok Company | 3 |
| 8 | SS-600-9 | 3/8" 90 Degree Elbow | Swagelok Company | 4 |
| 9 | SS-1210-6-4BT | 3/4" to 1/4" Bored Through Reducer | Swagelok Company | 4 |
| 10 | SS-1210-6-6BT | 3/4" to 3/8" Bored Through Reducer | Swagelok Company | 4 |
| 11 | SS-400-1-4BT | 1/4" to 1/4" NPT Bored Through | Swagelok Company | 5 |
| 12 | SS-600-3TTF | 3/8" Tee Fitting to 1/4" NPT | Swagelok Company | 10 |
| 13 | SS-1210-3 | 3/4" Tee Fitting | Swagelok Company | 8 |
| 14 | 9891T202 | Extreme-Temperature Pressure Gauge | McMaster-Carr Supply Company | 4 |
| 15 | 45295K55 | Tear-Resistant Silicone Foam Pipe Insulation | McMaster-Carr Supply Company | 8 |
| 16 | 3856K27 | Bendable Thermocouple Probe for Liquid and Gas | McMaster-Carr Supply Company | 9 |
| 17 | 3869K69 | Type J Thermocouple Adapter | McMaster-Carr Supply Company | 9 |
| 18 | 3126T364 | Aluminum Railing Clamp | McMaster-Carr Supply Company | 4 |
| 19 | 9633T15 | Clamping Two-Piece Shaft Collar | McMaster-Carr Supply Company | 4 |
| 23 | 5556K711 | Steam-Resistant High-Temperature Fiberglass Insulation | McMaster-Carr Supply Company | 4 |
| 24 | 5556K731 | Steam-Resistant High-Temperature Fiberglass Insulation | McMaster-Carr Supply Company | 9 |
| 25 | 5556K733 | Steam-Resistant High-Temperature Fiberglass Insulation | McMaster-Carr Supply Company | 6 |
| 26 | ST1 | Rupture Disc Holder | Zook | 1 |
| 27 | 9364K51 | Mineral Wool Pipe Insulation 2-7/8" Thick 10" Long | McMaster-Carr Supply Company | 4 |
| 28 | 9364K51 | Mineral Wool Pipe Insulation 2-7/8" Thick 16" Long | McMaster-Carr Supply Company | 2 |
| 29 | 9364K51 | Mineral Wool Pipe Insulation 2-7/8" Thick 11" Long | McMaster-Carr Supply Company | 2 |

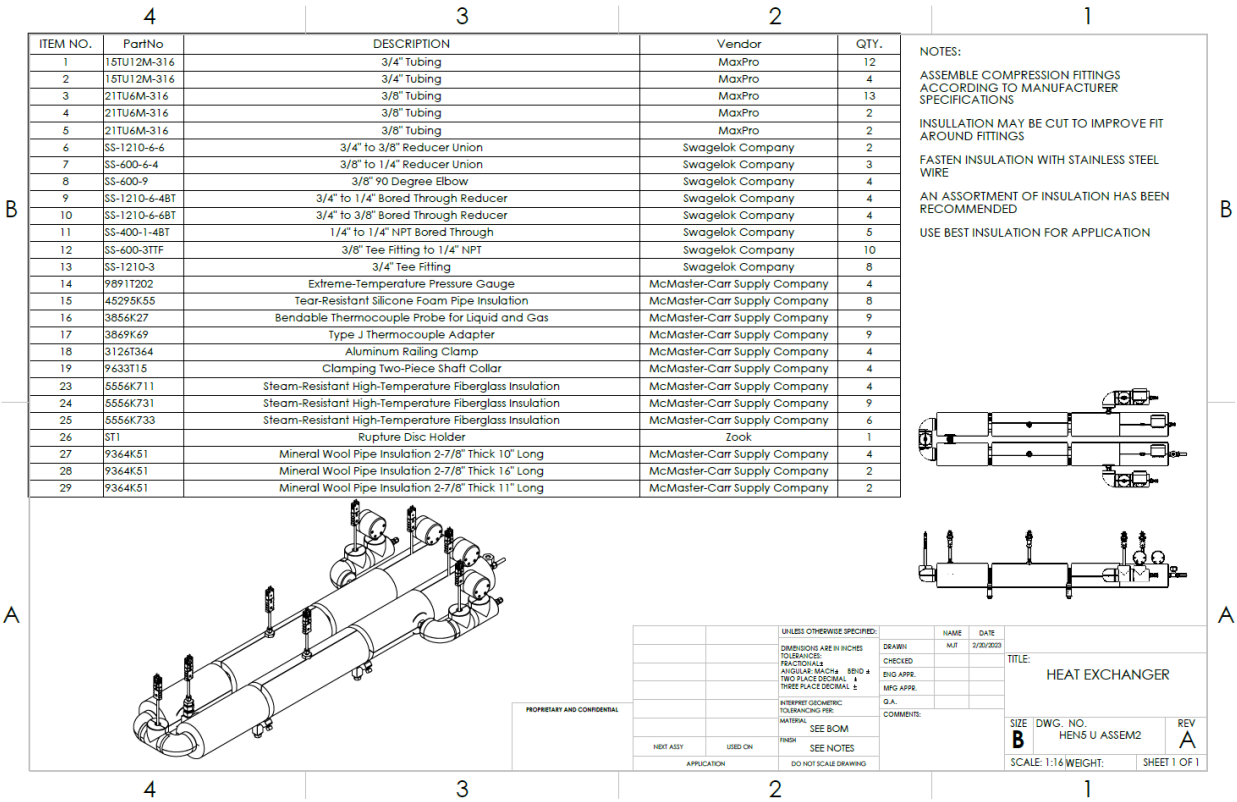


Figure 139: Bill of Materials for HEX design

# APPENDIX F: PROBE ADAPTER AND MOUNTING

The probe adapter and mounting method shown in this appendix can be used to collect temperature and pressure data from a single probe point without the problem of spacing the temperature and pressure measuring probes a distance apart.

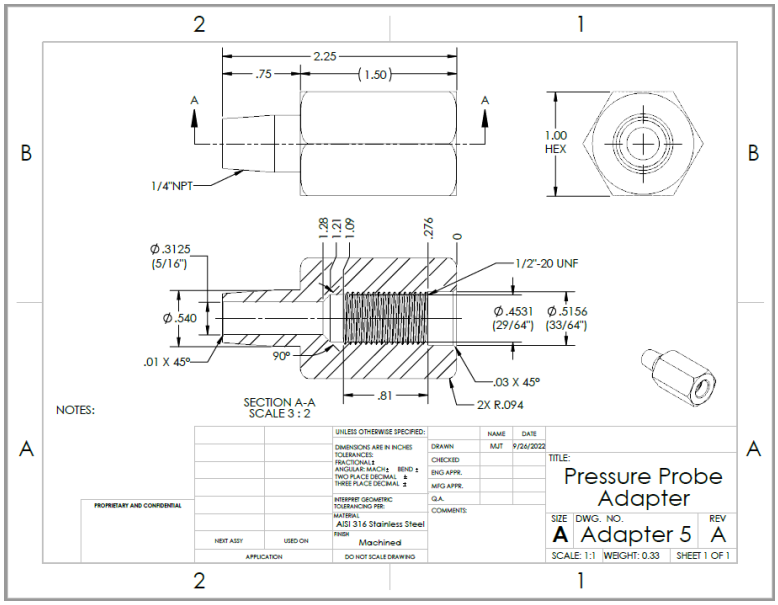


Figure 140: Pressure Probe Adapter Drawing

The pressure temperature combination probe shown is similar geometry to a burst plug. A stainless-steel adapter was designed and machined to connect the probe to a ¼" NPT (National Pipe Thread) Swagelok tee-fitting. The thread on the probe end is a ½-20 TPI (Threads Per Inch) thread. The probe seals with matching tapers like an AN (ARMY-NAVY) fitting, which are commonly used on hydraulic applications. The steel adapter was machined from 1 in stock with a hexagon cross-section. Unions are not considered dead volume unions.

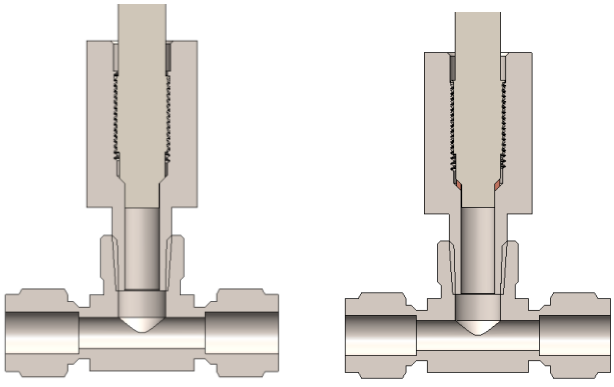

Figure 141: Pressure temperature probe with copper crush washer and without copper crush washer

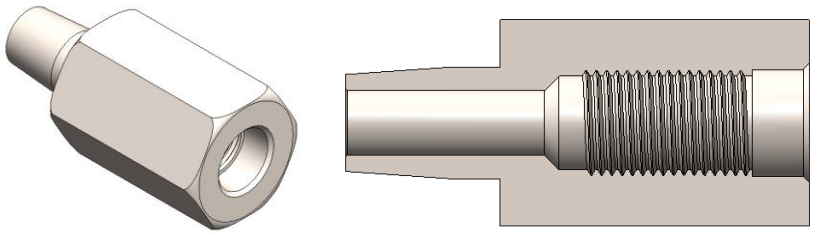

Figure 142: Pressure Temperature Probe section (NPT is not shown)

½-20 thread appears is burst plug thread pattern with a 90° taper at the base of the hole. The 90° taper allows the probe to seal against the adapter. Mechanical taper seals are common on brake lines, hydraulic lines and -AN fittings. A copper crush washer can be added between the adapter and the probe to aid in sealing at high pressure. Copper and aluminum crush washers are common for taper seal applications, stainless steel crush washers a used for extreme high-pressure conditions.

Figure 143: Machined Probe Adapters as received.

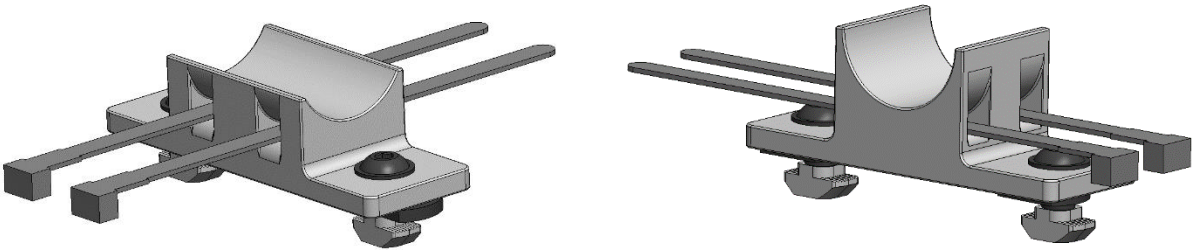

Figure 144: 3D printed Pressure Temperature Probe mount.

The temperature probe used in this application comes with an umbilical line that leads to an enclosure that needs to be tied down.

Figure 145: 3D printed bracket with mounted pressure sensor support electronics enclosure on the 100mL/min desalination system.

A bracket was 3D printed to support the pressure probe electronics housing.

# APPENDIX G: SEA SALTS

Table 49 contains a list of substances found in sea water that could be fed into the SCWD. Solubility in decreasing order KCL> NaCl>$CaCl_2$>$Na_2SO_4$>$Na_2CO_3$

Table 49: Salts and substances found in sea water.

| Sodium Chloride | NaCl | n | Atomic Mass | 58.443 | Mole Fraction |
|---|---|---|---|---|---|
| | Na | 1 | 22.990 | 22.989769 | 0.393 |
| | Cl | 1 | 35.453 | 35.453 | 0.607 |

| Potassium Chloride | KCl | n | Atomic Mass | 58.443 | Mole Fraction |
|---|---|---|---|---|---|
| | K | 1 | 22.990 | 22.989769 | 0.393 |
| | Cl | 1 | 35.453 | 35.453 | 0.607 |

| Calcium Chloride | CaCl2 | n | Atomic Mass | 110.984 | Mole Fraction |
|---|---|---|---|---|---|
| | Ca | 1 | 40.078 | 40.078 | 0.361 |
| | Cl | 2 | 35.453 | 70.906 | 0.639 |

| Magnesium Hydroxide | Mg(OH)2 | n | Atomic Mass | 58.319 | Mole Fraction |
|---|---|---|---|---|---|
| | Mg | 1 | 24.305 | 24.305 | 0.417 |
| | O | 2 | 15.999 | 31.998 | 0.549 |
| | H | 2 | 1.008 | 2.01568 | 0.035 |

| Calcium Carbonate | CaCO3 | n | Atomic Mass | 116.085 | Mole Fraction |
|---|---|---|---|---|---|
| | Ca | 1 | 40.078 | 40.078 | 0.345 |
| | C | 1 | 12.011 | 12.011 | 0.103 |
| | O | 4 | 15.999 | 63.996 | 0.551 |

| Strontium Sulfate | SrSO4 | n | Atomic Mass | 183.682 | Mole Fraction |
|---|---|---|---|---|---|
| | Sr | 1 | 87.620 | 87.62 | 0.477 |
| | S | 1 | 32.066 | 32.066 | 0.175 |
| | O | 4 | 15.999 | 63.996 | 0.348 |

| Sodium Sulfate | Na2SO4 | n | Atomic Mass | 142.042 | Mole Fraction |
|---|---|---|---|---|---|
| | Na | 2 | 22.990 | 45.979538 | 0.324 |
| | S | 1 | 32.066 | 32.066 | 0.226 |
| | O | 4 | 15.999 | 63.996 | 0.451 |

| Sodium Carbonate | Na2CO3 | n | Atomic Mass | 105.988 | Mole Fraction |
|---|---|---|---|---|---|
| | Na | 2 | 22.990 | 45.979538 | 0.434 |
| | C | 1 | 12.011 | 12.011 | 0.113 |
| | O | 3 | 15.999 | 47.997 | 0.453 |

| Sulfuric Acid | H2SO4 | n | Atomic Mass | 98.078 | Mole Fraction |
|---|---|---|---|---|---|
| | H | 2 | 1.008 | 2.01568 | 0.021 |
| | S | 1 | 32.066 | 32.066 | 0.327 |
| | O | 4 | 15.999 | 63.996 | 0.653 |

| Water | H2O | n | Atomic Mass | 18.015 | Mole Fraction |
|---|---|---|---|---|---|
| | H | 2 | 1.008 | 2.016 | 0.112 |
| | O | 1 | 15.999 | 15.999 | 0.888 |

| Carbon Dioxide | CO2 | n | Atomic Mass | 33.006 | Mole Fraction |
|---|---|---|---|---|---|
| | C | 1 | 1.008 | 1.008 | 0.031 |
| | O | 2 | 15.999 | 31.998 | 0.969 |

| Carbon Monoxide | CO | n | Atomic Mass | 17.007 | Mole Fraction |
|---|---|---|---|---|---|
| | C | 1 | 1.008 | 1.008 | 0.059 |
| | O | 1 | 15.999 | 15.999 | 0.941 |

| Nitrogen Gas | N2 | n | Atomic Mass | 28.014 | Mole Fraction |
|---|---|---|---|---|---|
| | N | 2 | 14.007 | 28.014 | 1 |

# APPENDIX H: ELEMENT TABLE, MASS FRACTION, and GAS CONSTANT

Table 50: Element Table

| Element | Proton | Neutron | Electron | Atomic Number | Atomic Mass |
|---|---|---|---|---|---|
| Hydrogen | 1 | 0 | 1 | 1 | 1.00784 |
| Oxygen | 8 | 8 | 8 | 8 | 15.999 |
| Sodium | 11 | 12 | 11 | 11 | 22.989769 |
| Chlorine | 17 | 18 | 17 | 17 | 35.453 |

Table 51: Mass Fraction and Gas Constant

| Fluid | Chemical Formula | Pressure (Bar) | Pressure (%) | Atomic mass | | | Molecular Mass (kg/mol) | Mass of Mole Fraction | Mass Fraction |
|---|---|---|---|---|---|---|---|---|---|
| | | | | H | N | O | | | |
| | | | | 1 | 14 | 16 | | | |
| Water | H2O | 100 | 40% | 2 | 0 | 1 | 18 | 7.2 | 30% |
| Nitrogen | N2 | 150 | 60% | 0 | 2 | 0 | 28 | 16.8 | 70% |
| | Totals | 250 | 100% | | | | 46 | 24 | 100% |

| Ci | Ri | CiRi | Cp | CiCpi | |
|---|---|---|---|---|---|
| 30% | 0.4615 | 0.1385 | 1.872 | 0.5616 | |
| 70% | 0.2968 | 0.2078 | 1.042 | 0.7294 | |
| | ΣRmax | 0.3462 | ΣCiPi | 1.291 | kJ/kg-K |

# APPENDIX I: LAB FORMED SALT CRYSTALS

Figure 146 shows a Face Center Cubic (FCC) matrix pattern. The salt crystals shown are from brine that was left in the lab and allowed to evaporate. The salt crystallization that occurs within the reactor does not take this shape.

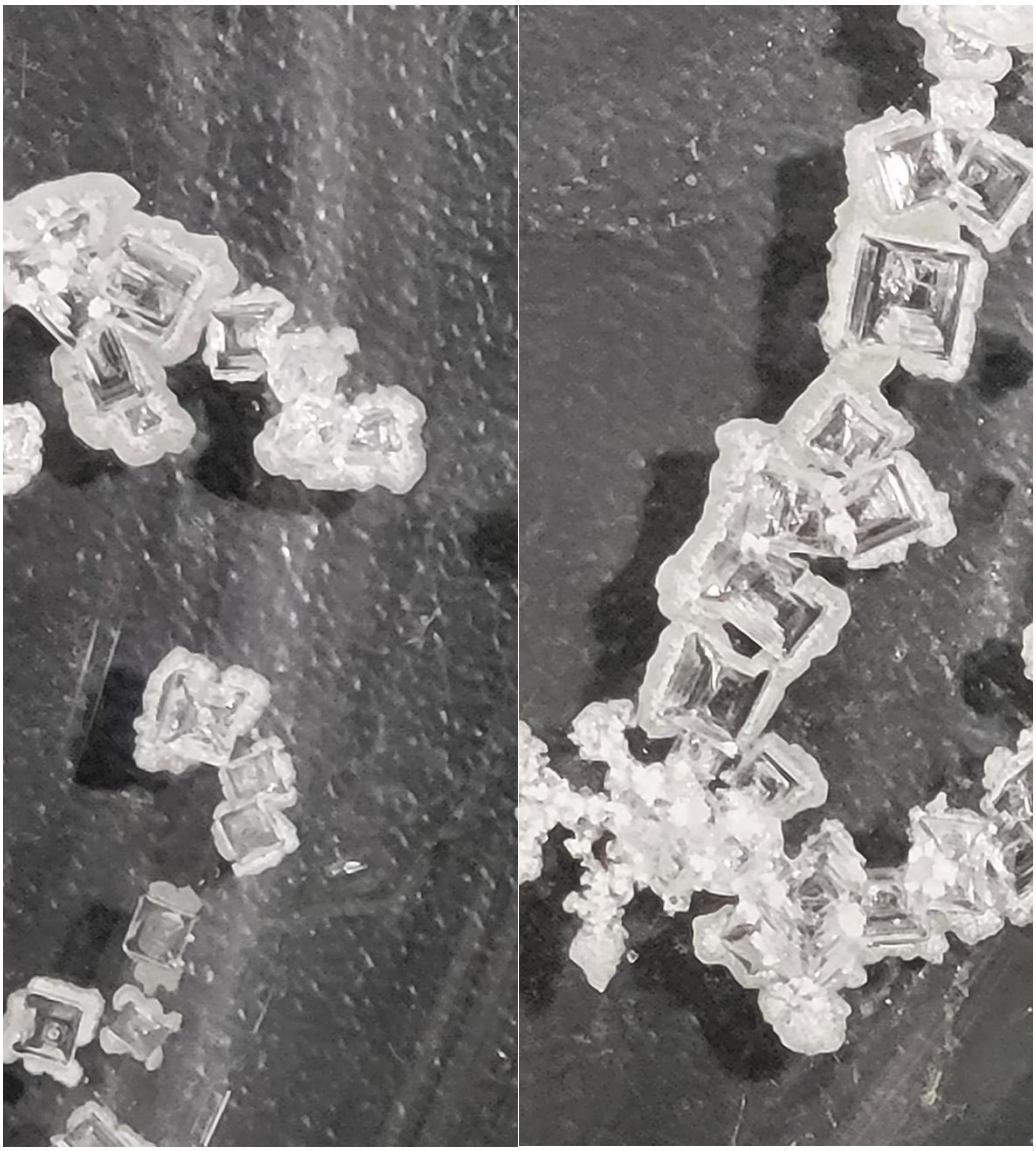

Figure 146: Crystalized NaCl at room temperature and atmospheric pressure